THE UNIVERSITY
of EDINBURGH

Characterization of the Developing Haematopoietic Stem Cell Niche using a Novel Immortalization System

THE UNIVERSITY *of* EDINBURGH

Yiding Zhao

Thesis presented for the degree of Doctor of Philosophy
Institute for Stem Cell Research, Centre for Regenerative Medicine
University of Edinburgh
2015

Declaration

I declare that:

(a) that the thesis has been composed by the candidate, and

(b) either that the work is the candidate's own, or, if the candidate has been a member of a research group, that the candidate has made a substantial contribution to the work, such contribution being clearly indicated, and

(c) that the work has not been submitted for any other degree or professional qualification except as specified

Yiding Zhao

_____ _____

Signature Date

Version 13.055.9 Date: 2015-09-30

To my grandpa, finally I contributed something to science…

Acknowledgements

First, I would like to thank my supervisor, Prof. Alexander Medvinsky. He is an insightful man, who guides me through this complex project. His rigorousness and thirst to excellence elevated this project to a new level. His full devotion of science is simply illuminating. By working under guidance of him, I had a taste of intensive academic research in top tier institution. Such experience imprinted a heavy mark on my life. Then I would like to thank Dr. David Hills, he kindly educated me on all works with molecular cloning and helped me with my constructs. And he kindly proofread my thesis. I want to thank Dr. Stanislav Rybtsov for tirelessly teaching me about aggregation culture system and done transplantation with me. I also want to thank Dr. Sabrina Gordon-Keylock and Dr. Kumiko Iwabuchi for advice on real-time PCR. Sabrina also tirelessly proofread my thesis (until 2am in the morning…) and gave a lot valuable inputs. Her kindness deeply moved me. I also want to thanks Ms. Alison McGarvey, Dr. Celine Souilhol and Dr. Jordi Senserrich for helps of experiment. And I want to thanks Mrs. Suling Zhao for teaching me various techniques and provided logistics for my research. This research will not come to fruit without kind help from Audrey Wright, Euan McPherson, Robbie MacCaig, Helen Henderson, Marilyn Thomson. They kindly provided all related reagents, glass ware and TC solutions. Mrs. Carolyn Manson and BRF staffs helped taken care of my animals. Mr. Simon Monard and Ms. Olivia Rodrigues helped on flow cytometry and FACS sorting. I also want to thanks Dr. Xin Jin, Dr. Rui Ma, Dr. Zhe Liu, Ms. Heather Wilson, Dr. Fiona Murphy, Dr. Niamh Fanning, Dr. Andrejs Ivanovs, Ms. Anahi Minagui-Casas, Ms. Antoniana Batsivari, Ms. Daria Paruzina, Mr. Javier Gonzalez, Dr. Jennifer Easterbrook, Ms. Kateryna Bilotkach, Ms. Sara Tamagno, Dr. Vincent Frontera, Dr. Boni Afouda for help with experiment and

insightful scientific discussions. They also tirelessly attempted to cheer me up in the ultra-demanding research environment.

I want to thank my dad and mom for nurturing me and educating me about science and life. And I would like to thank my wife Mrs. Jiexin Xie for supporting me in such difficult time. She pulled me from the dark hole of depressive thoughts. Without her, I probably cannot finish this thesis, or even worse, probably already finished my life. Her importance to me is beyond measurement. I would like to thank members of Southern Edinburgh Psychiatric Team and Dr. Alex McKain and Dr. Howard Morley for treating my depression. And I would like to thank J Sainsbury Plc for orange juice and Burger King Corp. for Chicken Tender Crisp Burger, they are my favorite.

I would like to thank Prof. Xicai Yang, Ms. Hong Wang for introducing me into the world of biomedical research. Thank Prof. Yuanqu Lin and Dr. Rui Wang for teaching about basic mathematical concepts used in this thesis. Thank Prof. Guo Lu for teaching about wave and vector field. Prof. Ge Gao for teaching about cellular automaton and Markov Models. Thanks Prof. Hongkui Deng and Dr. Chengyan Wang for introduction of cell biology and hematology.

At last, I would thank my grandpa, a retired dean of a small college. Before I came to UK, he told me in the phone: “I am too old to read and understand new literatures, you are still young, and you can do something to contribute to science.” Shortly after I came to UK, he went into coma and passed away. That was the last time he talked to me. And sadly because extensive work loads, I didn’t have a chance to attend his funeral. Taking his word in heart, in the past five years I pushed myself beyond limit, trying to contribute something as he told me. Many times in work, I feel it is too hard and thought to give up. It is his last word encouraged me to push on. Here I dedicate my thesis to him; finally, I contributed something to science and fulfilled his last wish.

Lay Summary of Thesis

Blood cells provide nutrition to different parts of body, immune cell helps us to fight bugs inside our body. They all come from cells called haematopoietic stem cells (HSC). HSC are adult stem cells that reside in our bone marrow. Sometimes, these stem cells become faulty, then patients got leukemia. A lot effort is made to discover means of replace those faulty cells and return patients a normal life.

In 2006, one method to derive pluripotent stem cell from skin cells was discovered. Such method provides a source of cells that have potential to become all kinds of cells in our body. To unleash such potential, right environment signal must exists to "educate" that pluripotent cells to become HSC. This study is aimed at discovering signals that is critical for maturation of HSC in a critical stage of embryonic development. It is hoped eventually we could translate such discovery into protocol to generate HSC for every leukemia patients.

Abstract

Embryonic haematopoiesis is a complex process under intensive research. Murine definitive Haematopoietic Stem Cells (HSCs) originates from the Aorta-Gonad-Mesonephros (AGM) region of E10.5 embryo. It is thought that definitive HSCs arise from endothelial lining of dorsal aorta. However, detail of HSC specification in the developing embryo remains elusive. One way to deciphering events occurred during HSC specification is to derive cell lines from the developing HSC niche. Previous work by Oostendorp *et al.* showed the AGM and fetal liver derived lines could maintain HSCs *in vitro* (Oostendorp, Harvey et al. 2002). In this study, I established a more robust immortalization system using normal SV40 large T antigen delivered via Neon™ electroporation system. The new immortalization system achieved direct immortalization without going through crisis. And it is compatible with small number of primary cells dissected from different haematopoietic niches. With my new system, multiple cell lines from different haematopoietic sites at different developmental points are derived. Moreover, some of these lines demonstrated ability to mature precursors from E9.5 embryo (pro-HSCs) to definitive HSC without help of growth factors. This result is better compared to OP9 stromal lines. Such data proved usefulness of using stromal cell lines to study haematopoietic specification.

List of abbreviations

7-AAD	7-aminoactinomycin D
AGM	Aorta Gonad Mesonephros
AoV	Dorsal Aorta, Ventral Domain
CER	Cerulean fluorescence protein
CFU-C	Colony Forming Unit-Culture
CLP	Common Lymphoid Progenitor
DLP	Dorsal Lateral Plate (mesoderm)
EC	Endothelial Cell
ES	Embryonic Stem (Cells)
EHT	Endothelial to Haematopoietic Transition
ENU	1-ethyl-1-nitrosourea
FMO	Fluorescence Minus One (controls)
GEMM	Granulocyte, Erythrocyte, Monocyte, Megakaryocyte (Colonies)
HESC	Human Embryonic Stem Cell
HLA	Human Leukocyte Antigen
HPC	Haematopoietic Progenitor Cell
HSC	Haematopoietic Stem Cell
ICM	Inner Cell Mass
ITR	Inverted Terminal Repeat sequences
iPS	Induced Pluripotent Stem (Cell)
LMPP	Lymphoid-Primed Multipotent Progenitors
LT-HSC	Long Term Haematopoietic Stem Cells
MEP	Megakaryocyte-Erythroid Progenitor

PCR	Polymerase Chain Reaction
p-SP	Para-aortic Splanchnopleura
SNS	Sympathetic Nervous System
ST-HRC	Short Term Haematopoietic Repopulating Cells
SV40T	Large T antigen from SV40 virus
VBI	Ventral Blood Island
VMZ	Ventral Marginal Zone

Table of Content

1. Chapter 1: Introduction

Haematopoietic Stem Cells (HSCs) were cells that replenish cells of all blood lineage (Osawa, Hanada et al. 1996). To do this throughout the life span of the organism, HSCs must be able to self-renew and differentiate. Self-renewal assured that a stable pool of HSC was maintained during entire life span of the organism. Previously, it was though that the majority of HSCs reside near osteoblasts that formed boundary between bone and marrow at trabecular bone (Wilson and Trumpp 2006, Kiel and Morrison 2008). However, recently S. Morrison's group published two elegant studies demonstrating HSCs were more related to perivascular niche formed by endothelial and mesenchymal stromal cells. Usually these cells were located near sinusoids or other blood vessels presented in bone marrow. The osteoblast niche was more related to downstream progenitors (Ding, Saunders et al. 2012, Ding and Morrison 2013). Perivascular niche regulated HSC with secreted molecules (e.g. CXCL12) (Lo Celso, Fleming et al. 2009) and direct cell to cell interactions (e.g. Notch/Jagged signalling). Environmental conditioning like hypoxia also might contributed to HSC maintenance and regulation (Takubo, Goda et al. 2010). The HSCs travelled between bone marrow and extramedullary sites, allowed efficient response to external environmental signals, including stress. Recent research suggested HSC pool was a heterogeneous population, with slow cycling latent long-term HSC (LT-HSC) and more active short-term Haematopoietic Stem Cells (ST-HSC). ST-HSCs gave rise to more proliferative progenitors that differentiated into all myeloid and lymphoid cell types. Several paradigms of HSC differentiation had been proposed, the most commonly accepted paradigm suggested that HSC first differentiate into a multipotent progenitor (MPP) than differentiate into distinct common myeloid progenitor (CMP) and common lymphoid progenitor (CLP) (Kondo, Weissman et al. 1997, Akashi, Traver et al. 2000). The recent discovery of other types of progenitors added new element to paradigm of HSC

differentiation. In new paradigm, HSC differentiated into megakaryocyte and erythrocyte progenitor (MEP) and lymphoid primed multipotent progenitors (LMPP) (Adolfsson, Månsson et al. 2005). Progress had been made to characterize and enrich HSCs from adult bone marrow. It was discovered that murine adult HSCs were enriched in Lineage$^-$Sca1$^+$c-Kit$^+$ population (Spangrude, Heimfeld et al. 1988, Ogawa, Matsuzaki et al. 1991). Later studies showed that Lin$^-$CD41$^-$CD48$^-$CD150$^+$ (signalling lymphocyte activation, SLAM) marker could provide better enrichment of HSC from adult bone marrow (Kiel, Yilmaz et al. 2005).

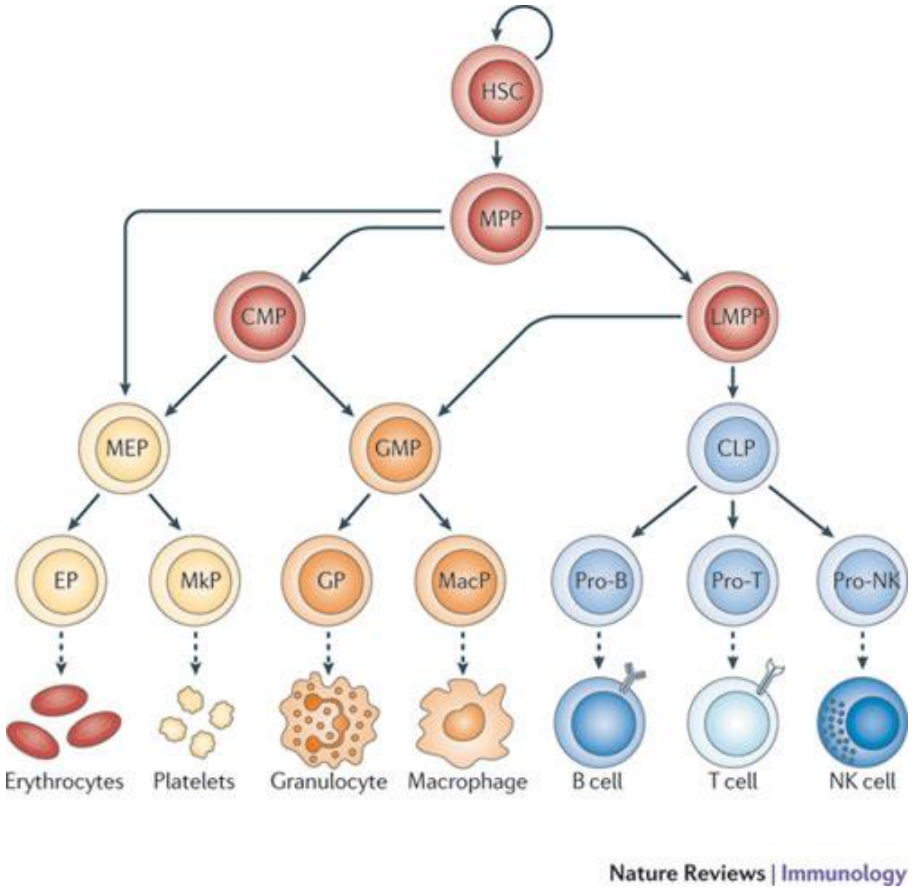

Figure 1-1. Differentiation of Haematopoietic Stem Cell (HSC). Differentiation of HSC was stepwise, involved external signalling and internal decision making. This figure was reproduced from Cedar and Bergman (2011) with permission.

If HSCs or their progenies became oncogenic, the organism would experience a wide variety of haematopoietic disorders. It was determined that leukaemia is the

most prevailing childhood cancer in most parts of world, except Africa (2011). To treat leukaemia and other haematopoietic disorders, bone marrow transplantation is often required. Current difficulties of finding Human Leukocyte Antigen (HLA) matched donors and expanding HSCs *in vitro* limit the number of patient receiving bone marrow each year. To resolve this issue, researchers started to look for ways of generating patient specific HSC *in vitro*. Several groups attempted to differentiate embryonic stem cell (ES) into adult HSCs either using a co-culture system with stromal cells (Ledran, Krassowska et al. 2008) or by adding haematopoietic cytokines (Wang, Li et al. 2004). After generation of iPS cells, attempts have been made to generate HSC from iPS cell generated teratoma (Suzuki, Yamazaki et al. 2013) or by direct re-programming of differentiated haematopoietic cells (Riddell, Gazit et al. 2014).

Limited success of generating adult HSC *in vitro* from ground pluripotent state indicates there is something missing in our understanding about haematopoiesis in general. To work around that problem, researchers start to look into embryonic haematopoietic development. It is thought that adult HSC can be generated *ex vivo* by mimicking *in vivo* developing processes.

1.1. Overview of embryonic haematopoiesis

Haematopoiesis during embryonic development is somewhat different with adult haematopoiesis described above. Adult haematopoiesis generates cells of blood, myeloid and lymphoid lineages while maintaining a stable pool of HSCs. But in embryonic haematopoiesis, developing haematopoietic system need to provide pools of haematopoietic cells serving other embryonic systems while generating HSC pool for adult life hood. Haematopoietic system was a conserved feature of different species in the animal kingdom. In acoelomates, free moving cells with digestive or other functions had been observed. In more advanced coelomates, free flowing haemocytes were present in coelom cavity or vascular system (Hartenstein 2006).

Such conservation was useful to use animal models to study embryonic haematopoiesis in general. Historically, several animal models had been of much interest, including amphibian, avian, fish and mouse. With the discovery of ES and iPS cells, they had also been used to model embryonic haematopoiesis.

1.1.1. Embryonic haematopoiesis in amphibian model

Research in amphibian models initially concentrated on ventral blood island (VBI), because removing VBI at tail bud stage of embryonic development reduced the number of circulating erythrocytes (Goss 1928). In amphibian embryos, cells in marginal zones were specified with a mesodermal fate by secreted factors like BMP-4, members of FGF family or Noggin (Jones, Dale et al. 1996). After extensive reorganization, cells at the ventral tip of marginal zone (Ventral Marginal Zone, VMZ), opposite to Spemann Organizer, were induced by local mesodermal signals to form ventral blood island (Kumano, Belluzzi et al. 1999, Hartenstein 2006). Later in development, VBI cell formed progenitors that gave rise to haematopoietic cells that enter circulation. However, later experiments showed that the reduction of erythrocytes was temporary. By grafting *Xenopus* embryos from different species Maeno *et al.* showed that haematopoietic cells *Xenopus* late larva and adult stage are also from dorsal lateral plate (DLP) mesoderm (MaÉNo, Todate et al. 1985). Combined with other data, it was concluded that there are two distinct waves of haematopoietic cell generation in amphibian embryonic development (Turpen 1998). The first wave of primitive haematopoietic cells originated from VBI while the second wave of more definitive haematopoietic cells originated from DLP.

1.1.2. Embryonic haematopoiesis in avian model

Initial research about haematopoiesis in the avian model is also concentrated in yolk sac, the avian equivalent of VBI. A key enabling technology for haematopoietic research is the chicken/quail labelling system. By making chick/quail chimera of various compositions, decedents of different region of primitive embryo are studied (Francoise-Lievre 2005). Moore and Owen proved that haematopoietic cells

massively circulate in developing embryos before seeding bone marrow and spleen by parabiosis (Moore and Owen 1965), later they proposed origin of such circulating HSC to yolk sac (Moore and Owen 1967). However, Dieterlen-Lievre *et al*. generated quail embryo body-chick yolk sac chimeric embryo to show that yolk sac originated cells are only transient while definitive HSCs arise from intra-embryonic sites (Dieterlen-Lievre 1975). Later, her group proposed that the ventral wall of aorta is the likely source of adult haematopoietic stem cells in the avian embryo (Dieterlen-Lievre and Martin 1981). Their work suggested that there are at least two waves of haematopoiesis in avian embryonic development, one extra-embryonic wave which provide primitive haematopoietic cells and one intra-embryonic wave which provides adult (definitive) haematopoietic cells. Their group also used chick quail chimera experiments to demonstrate that that allantois in avian embryo can produce haematopoietic cells (Caprioli, Jaffredo et al. 1998).

1.1.3. Embryonic haematopoiesis in zebrafish model

Another commonly used model organism in embryonic haematopoietic development was zebrafish. Zebrafish had several advantages for haematopoietic studies. Its embryo was transparent, made real time non-invasive observation possible. A large quantity of zebrafish embryos could be easily generated, plus robust forward (using 1-ethyl-1-nitrosourea, ENU) and reverse (using morpholino) genetic tools were available. These properties allowed massive parallel genetic screening to be conducted. In zebrafish, there were also two waves of haematopoiesis. The primitive wave was also developed from ventral mesoderm like other organisms. However, primitive haematopoietic precursors did not migrate to extra embryonic sites, instead they moved to intermediate cell mass (Detrich, Kieran et al. 1995). Subsequently, definitive HSCs started to bud off from endothelium at ventral wall of dorsal aorta (Bertrand, Chi et al. 2010). Such observation strongly supported the notion that HSC had an endothelial origin and highlighted importance of Endothelial to haematopoietic transition (EHT) (Kissa and Herbomel 2010). After HSCs entered

circulation, they moved into caudal haematopoietic tissue (CHT). The CHT was located near tail of embryo. Later, at around 4 days post fertilization, definitive HSCs seeded into kidney marrow, the zebrafish equivalent of bone marrow (Paik and Zon 2010).

1.1.4. Embryonic haematopoiesis in rodent model

Mus musculus was another heavily studied model organism. Researchers favoured it because of its similarity with *Homo sapiens*. In *Mus musculus*, germ layer differentiation usually started around the early streak stage (Embryonic Days 6.5, E6.5). Later, some cell from the distal proximal region of the primitive streak migrated to extra-embryonic mesoderm and becomes yolk sac primitive haematopoietic cells. Then at the late streak stage, lateral mesoderm developed. Some cells appear at dorsal lateral plate mesoderm. They were destined to become AGM cells. At neural plate stage (E7.25 to E7.5), yolk sac blood island appeared, it contains primitive haematopoietic cells (Ueno and Weissman 2010). Yolk Sac Blood Island produced primitive haematopoietic cells, mainly nucleated erythrocytes. At around E8.25 circulation between yolk sac and embryo proper is established.

Definitive haematopoiesis in mouse embryonic development appeared within the embryo proper (Medvinsky and Dzierzak 1996). Some cells with the potential to become definitive HSCs appeared in para-aortic splanchnopleura around E8.5 (Cumano, Ferraz et al. 2001). HSCs that could be transplanted into irradiated recipients and maintain long term engraftments first appeared in AGM region at around E10.5 (Muller, Medvinsky et al. 1994). Later definitive HSCs generated in AGM region circulated to foetal liver at around E12.5 and expanded rapidly in there (Morrison, Hemmati et al. 1995). At last, adult HSCs seeded their final destination, bone marrow, shortly before birth (Christensen, Wright et al. 2004, Mikkola and Orkin 2006, Ueno and Weissman 2010).

The origin of definitive HSCs during mouse development was a debated question. Several organs had been found containing HSC at various stages during embryonic development, included placenta (Ottersbach and Dzierzak 2010) and later umbilical cord (de Bruijn, Speck et al. 2000, Dieterlen-Lievre, Corbel et al. 2010, Gordon-Keylock, Sobiesiak et al. 2013). Even the embryonic head was considered to have some haematopoietic potential (Li, Lan et al. 2012). But the main research is still focused on AGM and yolk sac.

Yolk sac blood "islands" were the first haematopoietic related structure which appear during embryonic development (Palis, McGrath et al. 1995). In embryo sections, yolk sac blood islands usually appeared as two clusters of primitive haematopoietic cells with endothelial cells surrounding them. However, whole mount staining showed that primitive haematopoietic cells forms a band like structure; the two "classical" islands are formed by slicing the "blood band" (Ferkowicz and Yoder 2005). Contrasting previous theories, chimera experiments showed that cells forming the blood band are not monoclonal, but from multiple progenitors (Ueno and Weissman 2006). Functional *in vitro* assays showed that erythroid colony forming (EryP-CFC) or macrophage colony forming (Mac-CFC) cells could be detected as early as in mid-primitive steak stage (E7.0-E7.25) at presumptive extra-embryonic tissue. At E7.5 nucleated primitive erythrocytes appeared in the yolk sac blood belt. Such wave of primitive progenitors was transient. Primitive haematopoietic cells quickly disappeared at around the 20sp (somite pair) stage (around E9.0) (Palis, Robertson et al. 1999). Because definitive HSCs appeared in developing embryos after the yolk sac was connected to embryo proper, extensive research was focused on the potential of early yolk sac cells to contribute to definitive haematopoiesis after education by various niches. It was shown that E8.0 yolk sac cells (and p-SP cells) can generate definitive HSC after 4 days of co-culture with E10.5 AGM derived cell line AGM-S3 for 4 days (Matsuoka, Tsuji et al. 2001). However, this study was not repeated. To provide the necessary

maturation environment of yolk sac haematopoietic cells, Yoder's group transplanted E9 (Yoder, Hiatt et al. 1997) and E10 (Yoder and Hiatt 1997) yolk sac cells into irradiated neonatal recipients which resulted in long-term engraftment.

The view point that the mammalian AGM region was the source of true definitive HSC was uphold by many researchers. In the early 90s, Medvinsky *et al.* found high CFU-S (colony forming unit-spleen) numbers at E10 AGM region (Medvinsky, Samoylina et al. 1993). Later, they demonstrated that the E10 AGM region could generate definitive HSCs in organ explant culture while yolk sac cells at similar stage failed to do so (Medvinsky and Dzierzak 1996). Definitive HSCs from E10 AGM were c-kit^{+}, and mainly CD34^{+}. Mac-1 did not significantly enrich AGM derived definitive HSC (Sanchez, Holmes et al. 1996), this was different compared to the case in foetal liver (Morrison, Hemmati et al. 1995). In 2000, Marella de Bruijn *et al.* demonstrated that definitive HSCs first appeared in the dorsal aorta and later appeared in urogenital ridges (UGR) by transplanting sub-dissected AGM tissues (de Bruijn, Speck et al. 2000). Two years later Medvinsky *et al.* demonstrated with serial dilution assay that around E11, AGM, yolk sac or foetal liver each possessed around 1 definitive HSC (Kumaravelu, Hook et al. 2002). The pool of definitive HSCs was drastically expanded between E11 to E13. The capacity of definitive HSC generation was high on E11 while yolk sac harboured definitive HSC only on E12. Cells generated in AGM and yolk sac colonized foetal liver on about the same day. Dzierzak and colleague showed that the *Sca*-1-GFP marker could be used to label HSCs in the AGM region. *Sca*-1-GFP positive cells were localized to the endothelial aorta wall of the E11 AGM (de Bruijn, Ma et al. 2002). This finding implied that emerging HSCs had close relationships with endothelial cells (Yokomizo and Dzierzak 2010). Recent advances in *in vivo* imaging showed that in unfixed slices of the aorta, HSC might bud off from the aortic endothelium (Boisset, van Cappellen et al. 2010), supported the notion that HSCs go through Endothelial to Haematopoietic Transition (EHT) during maturation. Another strong

support of endothelial origin of HSC came from characterization of its immediate precursor, named as pre-HSC. In one study, the Medvinsky group developed a 3D liquid-air interface aggregation culture system which allowed maturation of definitive HSC from pre-HSCs. By aggregating cells with different markers from GFP AGM with native ($CD45^-$) counterparts, they determined those pre-HSC bear VE-Cadherin marker (Taoudi, Gonneau et al. 2008). Later they discovered that two types of pre-HSCs appeared sequentially with distinct markers: pre-HSC I with $VE\text{-}Cad^+CD45^-CD41^+$ marker appeared first, later they matured into the $VE\text{-}Cad^+CD45^+$ pre-HSC II phenotype. Pre-HSC II cells later matured into definitive HSC and migrated out of the AGM region at E11.5 or earlier (Rybtsov, Sobiesiak et al. 2011).

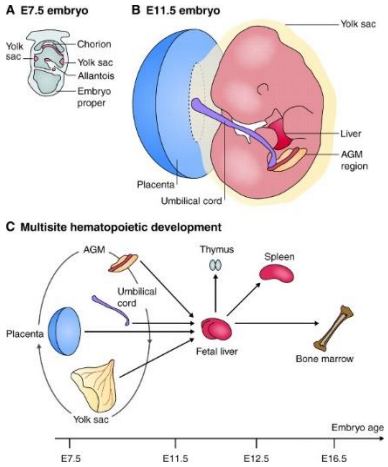

Figure 1.1.4-1. Embryonic haematopoiesis in rodents. A) Primitive haematopoietic cell originated from extra-embryonic structures. Yolk sac was the most prolific haematopoietic structure at that time. However, chorion and allantois were also implied in embryonic haematopoiesis. B) In E11.5 embryo, multiple tissues contained HSC, including placenta, yolk sac, umbilical cord and AGM region. HSCs also started to colonize foetal liver. These sites were linked by blood vessel. C) A schematic representation of haematopoietic development sequence. From E7.5 to E11.5, haematopoietic cells appeared in yolk sac, placenta, Umbilical cord and AGM, After E11.5, these HSCs started to colonize foetal liver and rapidly expand there. Later, they colonized thymus, spleen and bone marrow. This figure was reproduced from (Medvinsky, Rybtsov et al. 2011) with permission.

Based on the close relationship between endothelial and haematopoietic lineages, some researchers suggest that they shared a common ancestor-the haemangioblast. By definition, haemangioblast cells should have a mesodermal origin and could only generate endothelial and haematopoietic lineages. This notion was first proposed because in early 20th century because of morphological observations of endothelial cells specified near blood cells in Yolk Sac Blood Island. But later observations suggested that yolk sac blood "islands" were not islands and they were not monoclonal (Ferkowicz and Yoder 2005, Ueno and Weissman 2006). Haemangioblasts had been demonstrated in an ES differentiation system (Choi, Kennedy et al. 1998, Nishikawa, Nishikawa et al. 1998), but cells isolated from developing embryos displayed potential to also differentiate into smooth muscle cells (Huber, Kouskoff et al. 2004). Such observation caused the alternative theory of haemogenic endothelium to gain momentum (Hirschi 2012). The haemogenic endothelium was defined as a special kind of endothelium with haematopoietic potential. Haemogenic endothelium was first observed in chicken embryo almost 100 years ago (Reprinted in Sabin (2002)). Given all evidence about haematopoietic budding in embryonic aorta mentioned before, it seemed that definitive haematopoietic cells were generated from endothelial cells of the dorsal aorta. The process of budding involved endothelial to haematopoietic transition (EHT). Cellular signals controlling the EHT would be discussed in later sections.

1.1.5. Embryonic haematopoiesis in human

Studies of human embryonic haematopoiesis were constrained by the lack of available tissues and experimental limitations. Early observations of human embryos focused on primitive haematopoiesis at the yolk sac. Functional studies detected CFU (colony forming unit) activity in the yolk sac at 4.5 weeks after conception (Migliaccio, Migliaccio et al. 1986). Blood circulation between yolk sac and embryo proper might happen as early as 21 days after conception, manifested by presence of Gly-A expressing erythroblasts in the cardiac cavity (Tavian, Hallais et al. 1999).

However, yolk sac haematopoiesis in human was transient, haematopoietic progenitors disappeared in yolk sac after 6 weeks of gestation (Tavian and Peault 2005). Definitive HSCs in the human embryo emerged from the AGM region. Similar to mouse, haematopoietic cells attached to aortic endothelium were also observed in 27 day post conception (dpc) inhuman embryos (Tavian, Coulombel et al. 1996). Such cell cluster formation gradually extended into the umbilical cord region and the vitelline artery until about 35 days post conception. They disappeared at around 40 days post conception (Tavian, Hallais et al. 1999). Functionally, highly proliferative definitive HSCs appeared in the human AGM region at Carnegie Stage 14-15 (around 38 to 48 dpc), sub-dissection of AGM region pinpointed its source to be the dorsal aorta (Ivanovs, Rybtsov et al. 2011). Further experiments showed that the ventral wall of dorsal aorta was the source of definitive HSCs. These definitive HSCs were $CD34^{+}$VE-$Cadherin^{+}CD45^{+}$C-$KIT^{+}THY\text{-}1^{+}RUNX1^{+}CD38^{-/lo}CD45RA^{+}$ (Ivanovs, Rybtsov et al. 2014).

1.2.Regulation of embryonic definitive haematopoiesis

The development of definitive HSCs was a highly dynamic process. Various intrinsic and extrinsic factors acted in a coordinated manner to determine HSC identity. The development of HSC occurred in different niches. Cells with the potential to become HSC appeared in mesoderm, then developed within the endothelial lining of the dorsal aorta. In the dorsal aorta, these cells initiated the haematopoietic program and some of them became definitive HSC. Later they migrated to the foetal liver and finally colonized the bone marrow, the HSC maintenance niche throughout the animal's life span.

In ventral wall of dorsal aorta, initially all endothelial cells are of similar origin and identity, but after extensive cell to cell interactions and internal decision making, a small fraction of endothelial cells acquired the haemogenic endothelium fate. They formed specialized cluster-like patterns. Capacity to facilitate *de novo* specification of definitive HSC was what made aortic niches different with perivascular niches in

bone marrow. To figure out how HSCs acquired stem cell identity during specification, researchers must identify all intermediate cell state between totipotent ICM (Inner Cell Mass) cell and HSC, and work out rules governing each transition. Such rules included extrinsic factors and internal gene regulatory networks involved in major cell states transitions (Swiers, Patient et al. 2006). So far, several major steps of stem cell specification had been identified. A totipotent ICM cell went through mesodermal specification, acquired endothelial fate, acquired haemogenic potential, became a pro-HSC, then pre-HSC and finally matured with a definitive HSC phenotype. Both intermediate cell states and transition from one to the next would be discussed in following section.

1.2.1. Endothelial specification

The first step of definitive HSC specification was the induction of the primitive streak. After induction of primitive streak, some posterior primitive streak cells became *Flk*1 positive (also known as KDR, VEGFR2), a sign of haematopoietic mesoderm commitment. Next, precursors of HSC further acquired endothelial fate. The *Wnt* pathway was critical for early specification of primitive streak cells. Disruption of *Wnt* signalling had profound negative effects on endothelial specification in embryonic development (Bigas, Guiu et al. 2013). Suppression of the *Wnt* pathway by deletion of β catenin caused alteration of vascular patterning and formation of lacunae at bifurcations and haemorrhages (Cattelino, Liebner et al. 2003). Similarly, disruption of the *Wnt* pathway by disruption of *Frizzled*-5 (*Fzd*5, one of the *Wnt* receptor) leaded to defect in angiogenesis (Ishikawa, Tamai et al. 2001). Work with pluripotent stem cells demonstrated that *Wnt* had distinct functions at different stage of haematopoietic specification. *Wnt* was also critical for induction of primitive streak like cells in ES cultures (Jackson, Schiesser et al. 2010).

Another well studied mesodermal fate inducer was BMP4, a member of TGF-β family. It activated the SMAD pathway (Larsson and Karlsson 2005). BMP4

signalling was related to generation of both the Ventral Blood Island (VBI, associated with primitive haematopoiesis) and dorsal lateral plate mesoderm (DLP, associated with definitive haematopoiesis) in *Xenopus* embryos (Sadlon, Lewis et al. 2004). Mouse embryos with disrupted BMP function had reduced mesoderm development and died early. On a few special genetic backgrounds, BMP4 null embryos could survive a little longer, but had abnormal yolk sac and reduced primitive haematopoietic cells (Winnier, Blessing et al. 1995). Work on pluripotent stem cells indicated that BMP4 induces ventral posterior mesodermal fate by upregulating *Wnt3a* and *Cdx-Hox* genes (Lengerke, Schmitt et al. 2008). Further studies demonstrated an importance of orchestrated signalling of BMP4 and other molecules like *Activin/Nodal* or *Wnt* in the induction of primitive streak like cells (Kennedy, Awong et al. 2012) and haematopoietic mesoderm (Sumi, Tsuneyoshi et al. 2008, Jackson, Schiesser et al. 2010). Besides Brachyury, BMP induced primitive streak cells primarily expressed *HoxB1* and *MesP1* (Saga, Hata et al. 1996). Expression of *FoxA2* was low to negative in BMP induced primitive streak cells. BMP4 positive cells were restrained to posterior part (Saga, Hata et al. 1996, Nostro, Cheng et al. 2008).

Another important factor of TGF-β family, *Nodal*, was involved in mesodermal formation and body axis speciation of vertebrate development. In early embryonic development, sometimes effects of *Nodal* were similar to *Activin*, and were usually referred to as *Activin/Nodal* pathways (Shen 2007). *Activin/Nodal* signalling was required for induction of primitive streak like cells in ES culture. Such cells were marked with expression of *Brachyury* (Gadue, Huber et al. 2006, Nostro, Cheng et al. 2008). Inhibition of *Nodal* or *Wnt* signalling completely blocked formation of *Brachyury* cells induced by BMP signalling. Addition of ACTIVIN A and WNT3A induced primitive streak cell like phenotypes, but not all of them expressed posterior markers which were haematopoiesis related, some of induced cells expressed high

level of *FoxA2*, suggested anterior primitive streak identity (Nostro, Cheng et al. 2008).

Flk1, a receptor for *VEGF* signalling, was generally accepted as a marker for cells committed to mesodermal fate. Expression of *Flk1* was critical to normal endothelial development and haematopoiesis (Vieira, Ruhrberg et al. 2010). *Flk1* knockout ES cells could not contribute to the endothelial lineage. In chimera experiments, $Flk1^{-/-}$ ES cells did not contribute to yolk sac primitive haematopoiesis. Definitive haematopoietic cells of adult chimeras were derived only from $Flk^{+/+}$ wild type cells (Shalaby, Ho et al. 1997). Experiments with $Flk1^{+/Cre}$, Rosa26R-LacZ embryos showed extensive staining of endothelial and haematopoietic cells at dorsal aorta and yolk sac. Analysis of bone marrow of adult $Flk1^{+/Cre}$, Rosa26R-EYFP mice showed that almost all myeloid, T cell, B cells and haematopoietic cells are labelled by EYFP, suggesting they came from *Flk1* expressing cells (Lugus 2008).

The emergence of $Flk1^{+}$ cells in pluripotent differentiation cultures could be efficiently induced by BMP signalling prior to *Brachyury* expression. However, BMP added to $Brachyury^{+}Flk1^{-}$ population did not induce *Flk1* expression as robust as *Activin A* (Nostro, Cheng et al. 2008).

One critical downstream factor of coordinated BMP, WNT and NOTCH induction of *Flk1* was ER71 (*Etv2*). In ES culture systems, forced expression of ER71 rescued $Flk1^{+}$ expression from BMP, *Notch* and *Wnt* inhibition. Such observations suggested existence of *Flk1*-ER71 auto-regulatory loop. And ER71 deficient mice displayed phenotype highly resembled *Flk1* deficient mice (Lee, Park et al. 2008). Additional research showed that ER71 expression was only restricted to a subset of $Flk1^{+}$ cells at primitive streak stages, and ER71 expression was significantly reduced in *Flk1* deficient embryos while *Flk1* expression was only modestly affected in ER71 deficient embryos (Rasmussen, Shi et al. 2012). ER71 regulate *Wnt* downstream factors in $Flk1^{+}$ mesoderm induction was observed (Liu, Kang et al. 2012). Work on embryonic stem cells by Gordon Keller *et al.* demonstrated that *Wnt* signalling

promoted the generation of haematopoietic colonies after *Flk1*$^{+}$ mesoderm induction (Nostro, Cheng et al. 2008). Above works suggested complex context dependent effects of different signals at different stage of *Flk1*$^{+}$ mesoderm specification.

Scl was a transcription factors that was highly critical for normal haematopoietic development (Bloor, Sanchez et al. 2002). This could be demonstrated by the fact that *Scl* knockout mice died at E9.5 due to lack of primitive haematopoietic cells (Robb, Elwood et al. 1996). *Scl* knockout ES cells failed to produce haematopoietic colonies upon haematopoietic differentiation; this could be rescued by *Scl* cDNA expression (Porcher, Swat et al. 1996). Studies had shown that *Scl* had complex-context dependent functions during haematopoiesis. *Scl* expression initiated a transition from mesodermal to endothelial identity (L écuyer and Hoang 2004). *Scl* expression was required for definitive haematopoiesis prior to VE-Cadherin expression (Endoh 2002). Furthermore, chimeras with normal and Scl$^{-/-}$ ES cells demonstrated that Scl was required for vascular remodelling (Visvader, Fujiwara et al. 1998).

After induction of endothelial cells during development, VEGF signalling was responsible for its maintenance and expansion. Deletion of one VEGF allele resulted in abnormalities in blood vessel formation and premature death of embryos (Carmeliet, Ferreira et al. 1996, Ferrara, Carver-Moore et al. 1996). VEGF signalling was also critical to establishing arterial identity by inducing arterial markers like *EphrinB2* (Mukouyama, Gerber et al. 2005).

1.2.2. Endothelial to Haematopoietic transition (EHT)

One of major milestones of haematopoietic specification was the initiation of the haematopoietic program. Endothelial cells with haematopoietic potential were called the haemogenic endothelium. It was specified from endothelial cells via a process called Endothelial to Haematopoietic Transition (EHT). With advanced *in vitro* imaging, EHT had been visualized in real-time in development (Kissa and Herbomel 2010) (Bertrand, Chi et al. 2010) (Boisset, van Cappellen et al. 2010). A fate tracing

experiment involved VE-Cadherin-Cre mediated selective labelling of endothelial compartment during development showed that HSC had endothelial origin (Zovein, Hofmann et al. 2008, Chen, Yokomizo et al. 2009).

Specification of haemogenic endothelium involved multiple pathways. The *Notch* pathway was critical for normal specification of haematopoietic stem cells (Chen, Yokomizo et al. 2009). Kumano *et al.* demonstrated that knocking out of *Notch1* in mouse embryos severely impaired definitive haematopoiesis while knocking out *Notch2* had no profound effect to haematopoiesis (Kumano, Chiba et al. 2003). *Notch* signalling regulated expression of a wide variety of haematopoietic related genes, included *Runx1*, *Gata2* and *Scl* (Robert-Moreno, Espinosa et al. 2005). Work in zebrafish suggested that Notch-dependent expansion of haematopoietic cells could be inhibited by knocking out *runx1* (Burns, Traver et al. 2005), thus suggested *Runx1* was a downstream target of *Notch* signalling. This was further confirmed by the fact that the haematopoietic function of cells from *Notch1*$^{-/-}$ embryos was partially rescued after retroviral expression of *Runx1* (Nakagawa, Ichikawa et al. 2006).

Runx1 was a critical haematopoietic transcriptional factor. *Runx1*$^{-/-}$ embryos died early during embryonic development with no definitive haematopoietic progenitors present in the foetal liver(de Bruijn and Speck 2004). It had two promoters, one proximal (P2) and one distal (P1). Experimental data suggested that the proximal promoter was related to primitive haematopoiesis while distal promoter was related to definitive haematopoiesis (Sroczynska 2009). It had been noticed that Runx1 was required in VE-Cadherin positive stage of HSX specification but not in later Vav1 positive stage (Chen, Yokomizo et al. 2009). This finding suggested that Runx1 was critical for the haematopoietic development before the EHT.

Several important transcription factors were regulated by Runx1, one of them was PU.1 (Huang, Zhang et al. 2008). PU.1 regulated Common Myeloid Progenitor (CMP) fate decision and affected macrophage differentiation by modulating

expression of receptor of Colony-stimulating factor 1 (Csf1r) (Tagoh, Himes et al. 2002, Hoogenkamp, Krysinska et al. 2007). During haematopoietic specification, PU.1 interacted with other haematopoietic transcription factors like Gata1. Both Gata1 and PU.1 gene had auto regulatory loops and they directly suppressed each other. Such gene regulatory network structure allowed efficient bi-state switch of erythroid and myeloid lineages (Chickarmane, Enver et al. 2009). Recent advances in Gata1/PU.1 research suggested that additional factors were present in Gata1/PU.1 gene regulatory network that affect lineage selection (Monteiro, Pouget et al. 2011).

Gata1 and *Gata2* were critical transcription factors involved in the specification of the haematopoietic program. *Gata1* knock out cells could not develop into red blood cells in chimeric mice (Pevny, Lin et al. 1995) and Gata1 null mouse embryos died around E10.5 due to anaemia (Fujiwara, Browne et al. 1996). *Gata1* could bind to its own promoter and up regulated its own expression (Tsai, Strauss et al. 1991). Such auto-regulatory loop was critical to the initiation of downstream gene regulatory networks. *Gata1* expression was high in primitive erythrocytes, but in definitive haematopoiesis, expression of *Gata1* was gradually replaced with *Gata2*. *Gata1* expression was regained at the later stages of erythropoiesis (Moriguchi and Yamamoto 2014).

Gata2 was expressed in the p-SP and AGM region of the developing mouse embryo (Minegishi, Ohta et al. 1999). *Gata2* expression marked of definitive haematopoiesis. Early work on *Gata2* knock out ES and chimeric embryos showed its critical function in definitive haematopoiesis (Tsai, Keller et al. 1994). Even knocking out just one *Gata2* allele in embryo caused significant reduction of HSC activity in the AGM region and reduced HSC quality (Ling, Ottersbach et al. 2004). *Gata2* also auto regulated its own promoter (Swiers, Patient et al. 2006). Such auto-regulation might be important for *Gata2* to quickly initiate its expression and replace *Gata1* in the switch from primitive haematopoiesis to definitive haematopoiesis.

Scl had multiple roles in haematopoiesis besides regulating haematopoietic mesoderm specification (Mead, Kelley et al. 1998). Sanchez *et al.* demonstrated that haematopoietic defect of *Scl* knockout could be rescued by expression of *Scl* in a haematopoietic stem and progenitor cell population (Sánchez, Bockamp et al. 2001). In ES culture systems, *Scl* over-expression could rescue haematopoietic defects induced by blocking *Hedgehog* and *Notch* pathways during the EHT (Kim, Albacker et al. 2013). These finding highlighted that function of *Scl* was context dependent and affects multiple stages during of haematopoiesis.

Besides important function in the specification of the primitive streak, *Wnt* signalling also regulated haematopoiesis after expression of *Flk1*. It was observed that some non-haematopoietic cells in AGM region were active in *Wnt/β-Catenin* signalling and such signalling from developmental HSC niche was indispensable (Ruiz-Herguido, Guiu et al. 2012). Another example of context dependent signalling was BMP signalling. Besides played a critical role of haematopoietic mesodermal specification, BMP was also required in zebra fish for Runx1 expression in the ventral wall of dorsal aorta (Wilkinson, Pouget et al. 2009). Similarly, inhibiting BMP activity in mouse AGM explant cultures abolished HSC generation (Durand, Robin et al. 2007). Polarized BMP4 expression had also been discovered in human AGM region (Marshall, Kinnon et al. 2000), suggesting it was a conserved mechanism.

1.2.3. Maturation of pre-HSCs to definitive HSC

After initiation of definitive haematopoietic program, precursors of HSC were specified in endothelial lining of dorsal aorta of AGM region. HSC emergence was polarized and localized to the ventral wall of dorsal aorta, suggested that HSC maturation was heavily influenced by external signalling.

Besides BMP4 signalling mentioned in the last section, emergence of HSC in the AGM region depended on several factors from adjacent tissues. Ventral embryonic tissue support HSC emergence by providing *Hedgehog* (*Hh*) signalling, which was

demonstrated by the fact that addition of *Indian hedgehog* (*Ihh*) or *Desert hedgehog* (*Dhh*) enhanced HSC production in AGM explant while addition of anti-*Hh* antibody blocked HSC generation (Peeters, Ottersbach et al. 2009). Research also showed that Sympathetic Nervous System (SNS) was critical for HSC emergence. Gata3 regulated SNS formation by controlling biosynthesis of catecholamine. Loss of SNS formation reduced HSC content in AGM region (Fitch, Kimber et al. 2012).

One novel signalling involved in this stage of haematopoietic specification was biomechanical force. Initially, Yoder *et al.* established an *Ncx1*$^{-/-}$ mouse model that did not initiate heartbeat. In that model, no haematopoietic progenitor activity was detected in AGM region, thus suggested the significance of blood flow in HSC maturation (Lux, Yoshimoto et al. 2008). Later, Leonard I. Zon *et al.* demonstrated that HSC maturation was regulated by blood flow through NO (nitric oxide) signalling in zebrafish (North, Goessling et al. 2009). Daley *et al.* further demonstrated that biomechanical force was critical to haematopoiesis in mouse embryo (Adamo, Naveiras et al. 2009). Expression of *Runx1* and CFU activity in cells from *Ncx1*$^{-/-}$ embryo could be restored by artificially induced shear stress. Several receptors could sense biomechanics force and activated signalling affecting haematopoiesis (reviewed in Lee, Li et al. (2013)).

Mll (*Kmt2a*) was another factor involved in HSC emergence. Knocking out *Mll* resulted in ablation of AGM HSC activity although progenitor activity of HSC was maintained (Ernst, Fisher et al. 2004). *Sox17* was a recently identified transcription factor required for HSC emergence, it was critical for maintenance of aortic clusters (Nobuhisa, Osawa et al. 2014).

At last, it was worth mentioning that some commonly used haematopoietic cytokines in AGM cultures. SCF was implicated in embryonic haematopoiesis, with naturally occurring SCF mutant Sl did not survive to birth due to haematopoietic defects. Nobushisa *et al*. demonstrated Lnk adaptor protein could inhibit HSC

formation in AGM region by inhibition of SCF/kit signalling (Nobuhisa, Takizawa et al. 2003). SCF was also shown to regulate haematopoietic clusters in the placental niche (Sasaki, Mizuochi et al. 2010). Il3 was another cytokine that had critical function in haematopoiesis. Robin *et al.* demonstrated Il3 could dramatically expand pool of HSC in a Runx1$^{+/-}$ background (Robin, Ottersbach et al. 2006). Flt3l was another commonly used haematopoietic cytokine that had positive effect on haematopoiesis. Flt3l was beneficial for *in vitro* expansion of haematopoietic cultures (Tsapogas, Swee et al. 2014). However, yet no report was published describing its detailed function in AGM region.

1.2.4. Seeding foetal liver and bone marrow niche

After specification in the AGM region, HSC migrated to foetal liver. Expansion of HSC in mouse embryo occurred at E11-12 and peaked at E13-14 (Sasaki and Sonoda 2000). Foetal liver haematopoiesis went down at E19 (Sasaki and Sonoda 2000) but continued even in new-born mice (Masaki Takeuchi 2000). Murine foetal liver HSCs expressed AA4.1 and Mac1, which was not expressed in adult bone marrow HSC (Jordan, McKearn et al. 1990). A portion of definitive HSCs expanded in foetal liver was constantly circulating in blood, and migrated to foetal spleen and thymus. Chemotaxis of foetal liver HSC was regulated by SDF-1 and SCF (Christensen, Wright et al. 2004). Eventually, definitive HSC colonized bone marrow niche and stayed there for the rest of organism's life (Suárez-Álvarez, López-Vázquez et al. 2012).

In summary, embryonic development of HSC was a dynamic process with different stages (Medvinsky, Rybtsov et al. 2011). Major milestones of HSC emergence included specification of primitive streak, induction of mesoderm with haematopoietic potential, endothelial specification, endothelial to haematopoietic transition (EHT) and maturation of definitive HSC. Then definitive HSC migrated into foetal liver and finally, the adult bone marrow niche. Intrinsic and extrinsic

factors modulating above steps were discussed. Some factors had context dependent effect on embryonic development.

1.3.Dissection of HSC specification niche using *in vitro* models

Beside animal models, *in vitro* models also played a critical role in studying embryonic definitive haematopoiesis. Pluripotent stem cells differentiation models were used to model *in vivo* HSC specification process. EB formation was a common method for early stage differentiation. Cytokines, feeder cells and conditioned medium/trans-wells could be used to alter property of haematopoietic populations derived from pluripotent stem cells. To remove interference from unwanted populations, population of interest could be sorted out from culture. To promote production of haematopoietic cells from pluripotent stem cells, a combination of these methods was usually employed.

1.3.1. Utilizing ES differentiation system to study specification of haematopoietic cells

It was very convenient to use ES/iPS differentiation system to examine effect of various cytokines on haematopoietic differentiation. In one elegant study, Pick *et al.* investigated effects of BMP4, VEGF, SCF and FGF2 on haematopoietic differentiation (Pick, Azzola et al. 2007). Gordon Keller's group investigated staged regulation of haematopoietic differentiation by *Wnt*, Activin A and BMP (Nostro, Cheng et al. 2008). Later, they demonstrated that *Wnt* signalling was critical to switch between primitive and definitive haematopoietic differentiation programs (Sturgeon, Ditadi et al. 2014).

ES differentiation models also helped to identify critical populations during haematopoietic differentiation. The onset of haematopoietic differentiation of ES cells was marked by appearance of *Brachyury* positive cells. *Brachyury* was a commonly accepted marker for primitive steak/mesodermal fate, its expression usually turned on around day 4 during differentiation (Purpura, Morin et al. 2008).

Shortly after, *Brachyury* expression was down regulated. It was replaced by *Flk1* expression. In both *in vivo* development (Lugus, Park et al. 2009) and ES differentiation (Irion, Clarke et al. 2010), haematopoietic cells developed from *Flk1* positive ancestors. Interestingly, Keller's group discovered there were two waves of *Flk1* expression in ES differentiation system. The first wave of $Flk1^+$ cells was related to primitive haematopoiesis while a second wave of $Flk1^+$ cells arises from $Brachyury^+Flk^-$ population. Those secondary were related to definitive haematopoiesis (Irion, Clarke et al. 2010). First wave of $Flk1^+$ cells were also $CD235a^+$, a marker for erythroid fate. After a day or two, primary $Flk1^+$ cells became $CD34^+$, an indication of haematopoietic fate. Later, they differentiated into primitive erythroid, myeloid and NK cells. On the other hand, the more definitive Flk^+CD235^- populations would also become $CD34^+$ later. They became progenitor cells that could not only produce erythroid, myeloid and NK cells, but also produce T lymphoid cells (Sturgeon, Ditadi et al. 2014).

One critical contribution of ES differentiation system toward study of embryonic haematopoiesis was *in vitro* induction of haemangioblast. In a landmark study published in 1998, Keller *et al.* identified a unique blast-colony-forming cell that could generate both haematopoietic and endothelial progenies (Choi, Kennedy et al. 1998). This was the first experimental evidence such cells exist, at least in culture. Later studies showed that haematopoietic cells were generated from haemogenic endothelium derived from haemangioblast (Eilken, Nishikawa et al. 2009, Lancrin, Sroczynska et al. 2009).

Thus later research focused on how to generate haemogenic endothelium in ES differentiation cultures. Rafii and colleagues generated cell lines from human primary endothelial cell (EC) and used such cell lines to promote hESC differentiation (Rafii, Kloss et al. 2012). They used VE-Cadherin and CD41 promoters to drive fluorescence protein to track differentiating hESCs. They

observed a switch between VE-Cadherin expressing endothelial fate cell and CD41 expressing haematopoietic cells.

After multiple factors regulating haematopoietic development were identified, it was natural to think about designing chemical defined differentiation system. Bhatia *et al.* developed a chemically defined differentiation system that had a profound impact on related research. They made EB from hESCs with presence of SCF, Flt3l, Il-3,Il-6, and BMP4 (Chadwick, Wang et al. 2003). Within such EBs, they isolated a $CD45^{-}PECAM\text{-}1^{+}Flk1^{+}VE\text{-}Cadherin^{+}$ (Cd45negPFV) population with both endothelial and haematopoietic potential (Wang, Li et al. 2004). This system generated progenitors with good CFU-C activity, but no transplantable HSCs were generated. To enhance differentiation, a staged differentiation system was used. Keller *et al.* developed a two stages system for human pluripotent stem cell differentiation (Kennedy, Awong et al. 2012). First induction and specification stage involves timed addition of BMP4, bFGF, Activin A or small molecule SB-431542, VEGF, DKK, IL-6, IL-11, IGF-1, SCF, EPO, TPO, FLT-3, IL-3. Second stage of maturation and expansion had a few days of overlap with first stage, with addition of bFGF, VEGF, DKK, IL-6, IL-11, IGF-1, SCF, EPO, TPO, FLT-3 and IL-3. Then differentiated ES cells were either co-cultured with OP9 cells with presence of serum or had DKK withdrawn. One major advantage of such differentiation system was that cells generated by it have lymphoid potential. Such potential was demonstrated by commonly used OP9-Dll4 co-culture assay. Successful generation of T cells is a major step toward generation of HSCs with the capacity to differentiate into all haematopoietic, myeloid and lymphoid lineages.

To better study the intrinsic genetic network regulated haematopoietic differentiation, ES cells or their differentiated progenies were modified. Initial modifications were more concentrated on altering expression of transcriptional factors related to haematopoietic development. Kitajima *et al.* used Gata1 knockout ES to demonstrate that *Gata1* was indispensable for erythroid differentiation,

without *Gata1*, cells had difficulty maintaining erythroid identity. (Kitajima, Zheng et al. 2006). Liu *et al.* used knockout ES cell lines to demonstrate that critical role of ER71 in haematopoietic specification of *Flk1*$^{+}$ mesoderm by inhibiting cardiac fate (Liu, Kang et al. 2012). *Gata2* was another critical transcriptional factor related to haematopoietic differentiation. Several groups manipulated *Gata2* expression in ES cells to determine its function in haematopoietic differentiation. Orkin *et al.* used *Gata2* knocked out ES to demonstrate *Gata2* was important for maintenance of multipotent progenitors (Tsai and Orkin 1997). Later, Kitajima *et al.* used conditional expression *Gata2* ES system to investigate function of *Gata2* at each stage of *in vitro* haematopoietic differentiation. This study revealed complex regulatory wiring between *Gata2* and PU.1, suggesting *Gata2*-PU.1 formed a critical node in gene regulatory network related to haematopoiesis (Kitajima, Tanaka et al. 2005). Knockout/conditional expression system was not restricted to master transcription factors, other genes had been knocked out in ES cells for haematopoiesis research, including ALL-1 (Fidanza, Melotti et al. 1996), *Stat5* (Kyba, Perlingeiro et al. 2003), and *Men1* (Novotny, Compton et al. 2009). Knockout or conditional expression in ES system would remain a versatile tool to study haematopoietic specification in the future. The function of *Runx1* was also extensively studied with ES model. Lacaud *et al.* tested haematopoietic differentiation capacity of *Runx1* knock-out ES cell line. They observed alteration of gene expression pattern and marked reduction of BL-CFC potential (Lacaud, Gore et al. 2002), such deficiency could be rescued by retroviral-introduced *Runx1*. It was also observed that Runx1 deletion did not affect primitive haematopoiesis. Differentiation of primitive erythroid lineages was not altered. Later Medvinsky's group generated a reactivable *Runx1* allele (Samokhvalov, Thomson et al. 2006). They also observed a specific blockage of myeloid/mix lineage differentiation *Runx1* knockouts while more primitive erythroid differentiation was not completely blocked. Such blockage could be partially rescued with reactivation of *Runx1* allele

(Samokhvalov, Thomson et al. 2006). These observations reinforced the idea that Runx1 was pivotal for definitive haematopoiesis while not indispensable for primitive haematopoiesis.

Not only ES cells themselves could be engineered, their differentiated progenies were also good targets for manipulation. For example, Nakajima-Takagi *et al.* screened a panel of transcription factors in ES derived endothelial cells and found that Sox17 was an important haematopoietic stimulator. Sox17 primed early endothelial cells to haematopoietic fates (Nakajima-Takagi, Osawa et al. 2012). This approach was very interesting. ES differentiation system was a very complex culture. It contained different populations interacted with each other. Such kind of in-culture screening might reveal factors that mediated interactions between different cell populations in ES differentiation culture.

One aspect of haematopoietic differentiation of pluripotent cell research was focused on generation of red blood cells. Mature red blood cells had a short life span; some patients with haematopoietic disorder required constant infusion of freshly made red blood cells. Mature red blood cells did not had a nucleus, thus were devoid of genetic materials that might cause problem in other cell types. Such unique properties made red blood cell an ideal cell type for cell therapy. Oliver *et al.* used hESC derived $CD34^+$ cells to generate red blood cells (Olivier, Qiu et al. 2012). This protocol achieved generation of high percentage of enucleated red blood cells but hESC derived red blood cells still had haemoglobin profile similar to their foetal counterparts. More disappointing, their protocol used foetal liver cell line to promote generation of $CD34^+$ cells and murine enucleate red blood cells. Those foetal cell lines were difficult to meet Good Manufacture Practice (GMP) requirement. Lu *et al.* developed a chemical based method to generate red blood cells from hESC (Lu, Feng et al. 2010). Their protocol was more GMP friendly compared to cell line based method, but only about 10-30% of red blood cells generated were enucleated and switch to adult haemoglobin was not complete.

After successful derivation of iPS cells in 2006 (Takahashi and Yamanaka 2006), a lot of interest was devoted to apply iPS cells or its screening technology to haematology research. One brutal but interesting approach involved transplanting iPS into immuno-compromised mice and harvested HSC from teratoma and bone marrow of iPS recipients (Suzuki, Yamazaki et al. 2013). To facilitate haematopoietic development inside teratoma, they co-transplanted OP9 cell and a mini-pump to provide haematopoietic cytokines. They used a gamma-c corrected murine iPS cell line to form teratoma in X-SCID mouse model. HSC derived from teratoma generated normal T cells and trace amount of B cells. This experiment demonstrated the principle of gene correction using iPS formed teratoma. Similar approach with human iPS and NSG mouse model yielded detectable amount of $hCD45^{+}mCD45^{-}$ cells in teratoma bearing NSG mice, and human originated multilineage engraftment was observed. Considering the fact that Japanese researchers were rapidly moving on to test human-pig chimera for generating human organs (Matsunari, Nagashima et al. 2013) (Normile 2013), it was possible that pigs could be used to house patient specific teratoma. Enough human HSCs for transplantation might be harvested from the pig.

A more delicate approach was to screen transcription factors that allowed a direct change to HSC identity. In 2010, Bhatia and colleague reported conversion of fibroblast to multilineage blood progenitors by forced expression of Oct4 (Szabo, Rampalli et al. 2010). These converted cells expressed CD45 and had some myeloid potential when stimulated with haematopoietic cytokines. However, human Oct reprogrammed $CD45^{+}$ fibroblasts generated only trace amount of engraftment when transplanted into NSG mice model, and the ability to homing into bone marrow niche was not tested with tail vein injection. In 2014, Riddell *et al.* reported generation of induced HSC from committed myeloid cells by forced expression of *Runx1t1, Hlf, Lmo2, Pbx1, Zfp37 and Prdm5* (Riddell, Gazit et al. 2014). They also reported increase of reprogramming efficiency by additional expression of *Meis1*

and *MycN*. They generated relatively high level of engraftment, a marked improvement compared to previous studies. The iHSC generated with their system was capable of secondary transplantation. However, such results still awaited independent replication. If replicated, above experiments would be considered as major breakthrough in HSC biology.

1.3.2. Utilizing cell co-culture system to study specification of HSC

Cell co-culture system was also a frequently used system to study haematopoietic specification. Two kinds of co-culture studies were common. One kind was to co-culture of ES or iPS cells with haematopoietic feeder lines. This kind of studies mainly focused on how surrounding cells interacts with precursors of HSC. The other kind was to co-culture primary embryonic cells with feeder lines and investigate their maturation toward HSC. Such study was primarily focused on studying developmental potential and transcriptional regulation of embryonic primary cells that are destined to become HSC.

1.3.2.1. Studying HSC specification using pluripotent stem cells and their progeny

It was thought that cell lines were a better source of feeder cells than primary cells in co-culture experiments. Cell lines were culture of immortalized primary cells. These cells passed senescence and crisis. They could grow indefinitely. They were more stable compared to primary cells. To increase chance that cultured cells overcoming growth senescence and crisis, external immortalization factors were usually introduced. Immortalization factors usually interacted with multiple cellular factors, mainly tumour suppressors (Ahuja, Saenz-Robles et al. 2005).

As early as 1987, Collins and Dorshkind established S17 cell line from long term bone marrow culture. That cell line could support B lymphopoiesis and myelopoiesis (Collins and Dorshkind 1987). Later in 1994, Nakano *et al.* reported establishment of cell line OP9 from bone marrow of M-CSF mutated op/op mice

(Nakano, Kodama et al. 1994). They demonstrated that OP9 cell line could differentiate ES cells toward lymphoid lineages. Later, OP9 had become one of most used cell lines in co-culture studies about developmental haematopoiesis, although it was derived from adult bone marrow, not embryonic haematopoietic sites. Slukvin *et al.* developed a chemically defined protocol to differentiate human PSCs on over-confluent OP9 layers (Choi, Vodyanik et al. 2012). Their system could generate CFU colonies.

Oostendorp and colleagues generated cell lines from mouse embryonic AGM region. Details of cell lines generated were discussed in the next section (Oostendorp, Harvey et al. 2002, Oostendorp, Medvinsky et al. 2002, Oostendorp, Harvey et al. 2005). Other researchers tested Oostendorp's stromal cell lines' ability to promote haematopoietic differentiation in mouse ES differentiation systems (Krassowska, Gordon-Keylock et al. 2006). In 2008, Lako and colleagues co-cultured these cell lines with human ES cell and yielded up to 16% engraftment in blood, but only modest engraftment in bone marrow was detected (Ledran, Krassowska et al. 2008).They found that haematopoietic maturation signals was not completely secreted or reside within extracellular matrix. However, this important study often met scepticism and had not been reproduced by others.

Malcolm Moore of Memorial Sloan-Kettering Cancer Center had his fellow researchers derived 106 cell lines from E10.5 AGM region. After derivation, they did similar screening of stromal lines capacity to support mouse bone marrow cells and human cord blood $CD34^+$ cells. Furthermore, they tested derived line's capacity to differentiate mouse ES cells. They profiled expression of surface marker and cytokines of those lines, select lines were analyzed with microarray (Weisel and Moore 2005). Interestingly, they discovered that some cell lines gradually lost haematopoietic supportive function as they get passaged, with AGM-S26 line lost 9 fold CFC generation capacity as they grow from passage 5 to passage 19 (Weisel, Gao et al. 2006).

Beside AGM derived cell line, aforementioned work with Rafii (Rafii, Kloss et al. 2012) utilized primary endothelial cell lines derived from ES cells as feeder to promote haematopoietic differentiation.

In summary, research used derivation of haematopoietic supporting or maturing cell lines had been significantly advanced. Initial works with S17 and OP9 were derived from adult haematopoietic maintenance niche in bone marrow. Their capacity to promote haematopoietic differentiation of pluripotent cells was limited. Later work by Oostendorp *et al.* started to derive lines from embryonic haematopoiesis niche like AGM and foetal liver (Oostendorp, Harvey et al. 2002). By doing this, researches were done with stromal lines that closely resemble the microenvironment of embryonic haematopoiesis. Their capacity to promote haematopoietic differentiation of pluripotent cells was batter compared to previous lines. On the other hand, Rafii *et al*. tried to re-create necessary microenvironment by used ES derived cells as feeder cells (Rafii, Kloss et al. 2012).

1.3.2.2. Studying HSC specification using haematopoiesis related primary cells

The other commonly used paradigm was to co-culture primary haematopoietic precursor cells with already derived cell lines. As early as 1980, Gartner and Kaplan reported that human bone marrow derived adherent cells could support long-term human CFU production (Gartner and Kaplan 1980). Later, a series of haematopoietic related stromal lines was developed. And derived cell lines were tested for their ability to maintain and expand haematopoietic stem cell or progenitors (Issaad, Croisille et al. 1993, Nakano, Kodama et al. 1994, Wineman, Moore et al. 1996). Soon stromal cell lines were generated from embryonic AGM tissues (Ohneda, Fennie et al. 1998, Oostendorp, Harvey et al. 2002).

At about the same time, some researchers expanded into new direction of studying dynamic of haematopoietic specification of early embryonic cells. In 1998, Xu *et al.*

established stromal cell lines from mouse AGM region. They derived three cell lines from AGM region of mouse E10.5 embryos and denoted them as AGM-S1, AGM-S2 and AGM-S3 (Xu, Tsuji et al. 1998). They tested these lines for their capacity to support mouse bone marrow progenitor by cobblestone-like colony and CFU-C counting assay. Subsequently, they plated LSK cells ($Lin^{-}Sca1^{+}c\text{-}Kit^{+}$) from mouse bone marrow onto AGM-S3 line and detected CFU-C and CFU-S colonies. Next they tested their cell line's capacity to support human $CD34^{+}CD38^{+}$ cells. The best performing cell line, AGM-S3, was demonstrated to support human HSC in culture. Finally, they profiled surface marker and cytokine expression of AGM-S3.

Early in 2001, Matsuoka *et al.* applied Xu *et al.*'s cell line to a human stromal line co-culture system they developed. They co-cultured their best performing AGM-S3 line with primary E8.5 p-SP and yolk sac cells. They claimed that they detected CFU-C activity and production of macrophage after 7 days of culture. After 6 day of co-culture, CFU-S activity and generation of definitive HSCs were also detected from AGM-S3 co-cultured primary E8.5 p-SP and yolk sac cells. Engraftment could be detected in B cell, T cell and Myeloid cell linages up to 6 months. They also generated definitive erythrocytes from that culture. Similar culture with E8.0 p-SP and yolk sac cell also generated engraftment of definitive HSC (Matsuoka, Tsuji et al. 2001). 7 years later, another group abandoned the system involved co-culture with E8.0 primary cells and reverted back to testing capacity of supporting LSK cells. They sub-cloned AGM-S3 to 13 sublines and tested each clone's capacity to support bone marrow LSK cells and profiled gene expression of non-supportive cell (AGM-S3-A7) alongside with supportive lines (AGM-S3-A9 and OP9) (Nagao, Ohta et al. 2008). However, there was no further replication about cell line AGM-S3's capacity to mature precursor of HSCs from E8.5 or E8 embryos. It would be highly beneficial for Nakahata's group to repeat this study and try to derive more cell lines to confirm these line's capacity to mature precursors of HSC.

In 2002, Oostendorp *et al.* generated more than 100 stromal lines from E11.5 mouse embryo using transgenic mice expressing an immortalization factor (Oostendorp, Harvey et al. 2002, Oostendorp, Medvinsky et al. 2002, Oostendorp, Harvey et al. 2005). These cell lines came from different parts of the AGM region or foetal liver. Oostendorp *et al.* faced problems to deliver immortalization factor into small number of cells. To deal with that problem, they decided to knock in an immortalization factor into PGK or beta-actin allele and express it in a constitutive manner. Constitutive expression of immortalization required a delicate balance between increase powers of immortalization and avoid spontaneous tumour formation. Thus the tsA58, a relatively weak immortalization factors was selected to minimize tumour formation. It was a temperature sensitive version of SV40 large T antigen. Such weak immortalization vector required several months for cells passing through crisis and achieve full immortalization. Before immortalization, cultured primary cells would stop growing after a few passages. That was called replicative senescence (M1 stage of aging). After a few culture, cells reached crisis (M2 stage) with marked increase of cell death and chromosomal abnormalities (Lustig 1999). It was suggested cells had extensive transcriptome alteration as they go through crisis. Thus the cell lines derived in Oostendorp's study might not preserve all haematopoietic specification related transcription program.

They did a comprehensive characterization of their cell lines. They checked growth rate of various clones and established that the tsA58 was beneficial for cell growth. They co-cultured lines derived with bone marrow cells and detected progenitor (via CFC) or HSC content (via transplantation). The results showed some clones can support and expand haematopoietic progenitor, bone marrow HSC and HSC from E11.5 AGM (Oostendorp, Harvey et al. 2002, Oostendorp, Medvinsky et al. 2002).

They also conducted a wide survey about surface marker expression of cell lines they derived, and discovered that most cell line derived bear mesenchymal marker, not endothelial nor haematopoietic marker, some lines demonstrated high level

expression of haematopoietic promoting factors (Charbord, Oostendorp et al. 2002). Later, it was demonstrated that Wnt5a played a critical role in the capacity of haematopoietic promotion of these cell lines (Buckley, Ulloa-Montoya et al. 2011).

They tested these line's capacity to support haematopoietic progenitors in human cord blood. Some lines even could support human progenitors and HSC in *in vitro* co-culture condition (Kusadasi, Oostendorp et al. 2002). Experiments with these lines using Transwell showed that long term maintenance of HSC did not depend on contact between HSC and stromal cells (Oostendorp, Robin et al. 2005).

Later Professor Medvinsky's group developed 3D aggregation culture system that float on the interface between air and medium (Taoudi, Gonneau et al. 2008). Such system was improved from organ-explant culture system described in (Kumaravelu, Hook et al. (2002), Medvinsky, Taoudi et al. (2008)). Unlike explant culture system, it allowed study of development of independent subpopulation isolated from primary tissues. Using aggregation system, they isolated two precursor populations of HSC-pre-HSC I and pre-HSC II (Rybtsov, Sobiesiak et al. 2011). Pre-HSC I population bear the marker of VE-Cad^{+}CD45^{-}CD41^{+}, they developed into pre-HSC II bear the marker of VE-Cad^{+}CD45^{+}CD41^{+}. Later, pre-HSC II further matured into definitive HSC. However, because inconsistent results were acquired from aggregation experiments with primary cells only, OP9 cells were used to provide niche signal necessary for haematopoietic maturation.

1.4. Introduction to *piggyBac* transposon based immortalization system

In previous studies, two approaches of deriving cell lines from haematopoietic sites were used. The first way was to harvest cells from transgenic mouse strain that contains immortalization factor or wild type mouse and culture them to allow spontaneous cell line formation as described previously (Xu, Tsuji et al. 1998, Kusadasi, Oostendorp et al. 2002, Oostendorp, Harvey et al. 2002, Weisel and

Moore 2005). Another kind of study used viral vector to deliver immortalization factors into target cell populations directly (Seandel, Butler et al. 2008, Rafii, Kloss et al. 2012). This method assured strength of immortalization, but preparing viral particle was a demanding work, and using viral particles on certain cell types might pose regulatory difficulty.

In this study, a *piggyBac* transposon based immortalization system was used. The *piggyBac* transposon was one class II mobile element that was discovered from baculoviruses that infected certain insects (Fraser 2002). Some mutant baculoviruses were seen with a phenotype of generating few polyhedral occlusion bodies (FP), and such phenotype was a function of the host. This phenomenon was now known to be caused by FP locus being a preferred site for host transposable element. Several transposable elements were isolated from that locus. One of them, IFP2 (Insertion in FP mutant 2) from *Trichoplusia ni* was considered as the most interesting (Cary, Goebel et al. 1989). It was later renamed as *piggyBac*. Follow up research showed *piggyBac* transposon contained an ORF that encode a transposase (Fraser, Cary et al. 1995) and was TTAA specific (Cary, Goebel et al. 1989). Based on this property, *piggyBac* transposon was developed as a gene delivery vector. It was used in Drosophila (Horn and Wimmer 2000), and mammalian cells (Li, Michael et al. 2013).

1.5.Strategy and aims

Previous studies with haematopoietic promoting cell lines revealed their potentials in maintaining early haematopoietic cells in developing embryo. Several studies derived cell lines from embryonic AGM and FL tissues, but no cell line was established based on surface marker expression profile of its primary cell ancestors (Xu, Tsuji et al. 1998, Oostendorp, Harvey et al. 2002). Osamu *et al.* isolated primary cells from mouse AGM, stimulated expansion of endothelial population with endothelial cell-growth supplement, sorted out $CD34^+$ population from culture

and established cell lines from them (Ohneda, Fennie et al. 1998). Rybtsov *et al.* (Rybtsov, Batsivari et al. 2014) used aggregation system to mature pro-HSC from E9.5 embryo to definitive HSC. In this study, I combined advantages of these studies to derived cell lines from primary cells isolated from AGM region and haematopoietic related sites of early embryos. Some cell lines were derived from primary cells bear different surface markers. Their capacity to maintain HPCs and mature pro-HSCs were tested. The experimental protocols involved were described in chapter 2.

In chapter 3, the pB-PGK-TAG-CER immortalization vector constructed for this study was described. This vector employed *piggyBac* transposon as genomic delivery vehicle, which was better than viral vectors because it was removable. Immortalization was achieved through expression of SV40 large T antigen. It was better compared to temperature sensitive version of SV40T because it could achieve direct immortalization of murine cell without going through crisis.

In chapter 4, the derivation of stromal line was discussed. In this study, I chose electroporation as the mean to deliver DNA into target cells. The Neon™ capillary electroporation system was optimized to work with sorted embryonic AGM cells. Afterward, cell lines were derived from sorted E11.5 AGM primary cells and from primary cells isolated from haematopoietic sites of earlier embryos.

In chapter 5, the results of 4 days HPC production assay and pro-HSC maturation assay were discussed. Such two assays were aimed at evaluate derived stromal line's capacity to promote haematopoietic maturation. It was discovered that cell lines derived in this study could match or even outperform the commonly used OP9 in capacity to promote haematopoietic maturation.

In chapter 6, discussion was focused on gene expression profiling of some stromal lines. To accurately measure gene expression, a reliable qPCR platform was

established, then a panel of derived cell lines were analysed alongside with OP9 control. The gene expression profiling results were analysed.

In the last chapter, chapter 7, this study was compared with several studies done previously. The advantages of this study were discussed and directions for further improvements were mentioned. At last, result gathered in this study was interpreted using Multi-ordered Markov Random Field model. This model could better explain the stochastic nature of pro-HSC maturation discovered in this study.

2. Chapter 2: Material and Methods

This project was aimed at deriving cell lines from different haematopoietic related primary cell populations. That included different subpopulations of E11.5 AGMs and earlier E8-E10 embryos. To achieve this, a *piggyBac* based immortalization vector was constructed. A protocol to electroporate vectors into primary cells derived from haematopoietic developmental sites was developed. Cell lines were established from different haematopoietic developmental sites and/or from primary cells bear different surface markers. Some of these cell lines were subjected to aggregation assays that were developed in our lab. Two assays were employed: E11.5 haematopoietic progenitor assay and E9.5 pro-HSC maturation assay. A quantitative Polymerase Chain Reaction (qPCR) protocol was established to determine expression of haematopoiesis related genes.

2.1. Construction of pB-PGK-TAG-CER and pB-PGK-CER vector

Briefly, to make the pB-PGK-TAG-CER immortalization vector, a PGK fragment was amplified using Polymerase Chain Reaction (PCR) and inserted in to pCR-BluntII intermediate vectors (Life Technologies). PCR primers used in this section are listed in table 2.1-1. Dr. David Hills designed first 11 primers listed in that table. Reaction is carried out using Platinum *Pfx* DNA polymerase (Lift Technologies). After verification PGK fragment was inserted into pB-CAG *piggyBac* backbone to replace CAG promoter. The new vector was named as pB-PGK vector. Then Dr David Hills helped to introduce additional enzymatic sites into pB-PGK backbone using PCR, made it pB-PGK-M (M stand for “modified”) vector. Next, SV40T and 2A-CER fragments were generated via PCR and inserted into pCR-BluntII intermediate vectors respectively. After verification, both fragments were cut from intermediate vectors and ligated with digested pB-PGK-M backbone in a triple ligation reaction (recipes in appendix table 8.1.1-1). To verify the pB-PGK-TAG-CER vector, clones from previous experiment were screened by

HindIII digestion (NEB). Positive clones were sequenced using primers PGK-NheI-For, SV40-Tag-F, SV40 Primer1, SV40 Primer2, SV40 Primer3, SV40-TAg-2A-R and CER-R (listed in Table 2.1-1).

Primer Name	Sequence (5'to 3')	Length (nt)	Tm (°C)	GC (%)
PGK-NheI-For	CCC GCT AGC GAA ATT CTA CCG GGT AGG GGA	30	67	60
PGK-SacII Rev	TTT CCG CGG CAC GTG CAG CTT GAT GAT CA	29	67.3	55.1
pB-PGK-A	AAG CGG CCG CCA TGG TGA TAA CCT GCA GGA TCC GG	35	71.8	62.9
pB-PGK-B	AAG CGG CCG CCA TGG GCT CCC TTA TAC ACA GCC A	34	72	61.8
E2A-SV40tail-For	TGA ACC TGA AAC AGC CCG GGG AGG GCA GA	29	69.6	62
SV40-E2A-Tail-R	TCT GCC CTC CCC GGT GTT TCA GGT TCA GGG GGA	33	71.8	63.6
SV40-SacII-F	TCC GGA CCG CGG ACC ATG GAT AAA GTT TTA AAC	33	64.3	48.4
2A-F	CCC GGG GAG GGC AGA GGA A	19	64.6	73.7
2A-R	TGG GCC AGG ATT CTC CTC G	19	59.3	63.2
2CER-F	A GGA GAA TCC TGG CCC AAT GGT GAG CAA GGG CGA C	39	71.9	61.5
CER-R	GCG GCC GCT CGA GAC TTT ACT TGT ACA GCT CGT CC	35	68.6	60
SV40 Primer1	CAA CTG AGA TTC CAA CCT AT	20	49.3	40
SV40 Primer2	GTT TGC CAG GTG GGT TAA AG	20	54.3	50
SV40 Primer3	GGT GTA CAA CAT TCC TAA AA	20	47.7	35
SV40 Primer4R	CGT TAA CAA CAA CAA TTG CA	20	49.8	35

Table 2.1-1. Primers used to generate and sequence pB-PGK-TAG-CER construct. Primers for PGK-NheI-For and Rev were used to generate PGK fragment for pB-PGK vector. pB-PGK-A and B were used to modify pB-PGK vector. SV40-SacII-F and SV40-T2A-Tail-R were used to generate SV40T Fragment. 2A-F, 2A-R, 2CER-F, CER-R were sued to generate 2A-CER fragment by overlapping PCR. SV40 primer 1 through 4R were used to sequence SV40T region. All primers were synthesized at Integrated DNA Technologies, Inc.

DNA from clones with correct TAG-2A-CER cassette was maxipreped, electroporated into OP9 or 293T cells. Expression of Cerulean fluorescence protein was confirmed using flow cytometry, confocal microscopy and immuno-histological staining. Expression of SV40T antigen was also confirmed using immuno-histological staining. After pB-PGK-TAG-CER transfected cells recovered from electroporation, they were seeded onto gelatin coated wells with autoclaved cover slips and used next day. On the next day, 10X TBS stock solution was prepared by adding 14.8g of $Na_2HPO4•2H_2O$, 4.3g of KH_2PO4, 70g NaCl, 50g Tris and 2g NaN_3 into 1L ddH_2O and mixed well. Then 4% paraformaldehyde (PFA) solution was made from PFA powder. To help PFA dissolve, 18MΩ water was heated and some NaOH were added. Cell culture medium was aspirated and cells were washed twice with TBS, then they were fixed in 4% PFA solution for 10

minute at room temperature. Fixed cells were treated with TBST (1X TBS solution with 3% Triton X-100) for two washes of 5 minute each. After TBST wash, cells were blocked by blocking solution made by adding 1% BSA and 3% goat serum to TBST solution, incubated for 15 minute at room temperature. Then cells were incubated with SV40T primary antibody (BD Pharmingen, catalogue number:554149, isotype: mouse IgG2a) at 1:200 concentration and Alexa 488-conjugated GFP antibody at 1:200, which also recognize Cerulean (Voges, Bachmann et al. 2010) (Life Technologies, catalogue number: A21311) at 4℃ overnight. Next day, the cells were washed three times with TBST for 10min at room temperature. Then they were incubated with Alexa 568 goat-anti-mice secondary antibody (Life Technologies catalogue number: A11004) at 1:750 for 1 hour. After that cells were stained with DAPI for 5min and washed three times for 10min in 1X TBS. At last, the cover slip was coated with ProLong antifade reagent (Life Technologies, catalogue number: 36930) and placed on a slide. Pictures were taken with an Olympus IX50 inverted microscope and a QImaging Retiga 2000 camera.

Functionality of SV40T large T antigen was confirmed by growth curves. Growth curves were established by transfecting pB-PGK-TAG-CER vector and pB-PGK-CER control vector into separate but identical AGM primary cell sample and counting both samples during each passage. Functionality of CER was confirmed by confocal microscopy. Transfected cells were seeded in sterile coverslips placed in 6 well-plate wells and cultured as normal. Untransfected cells derived from head tissues of E11.5 BL6 were used as negative control. On the day of analysis, coverslips with cell were picked up from well using forceps, briefly stained with propidium iodide (PI, provided by SCRM flow cytometry core) and carefully dried, then mounted to slides and observed under a Leica SP5C confocal microscope at Confocal and Advanced Light Microscopy Facility (CALM) in QMRI, UoE. Following parameters were used: excitation: 458nm, laser power 27%;

collection filter: 465-600nm, PMT amplification voltage: 1081V scan speed is 400Hz, 2,5ms. Pictures were taken with 40X projective lens.

A pB-PGK-CER control vector was also constructed that lacks SV40T. Primers used to make this construct were listed in table 2.1-2. Both primers were designed based on CER sequence from pCR-Blunt-CER1 vector. SacII-Ko-ATG-F primer had protective bases, SacII site, Kozak sequence and ATG added before CER sequence, SalI-R primer had SalI site and protective bases added after CER sequences. Briefly, Ko-ATG-CER cassette was generated by PCR and inserted into pCR-BluntII vector. After sequencing, correct clone was cut by SacII and SalI to release the Ko-ATG-CER cassette. Digested Ko-ATG-CER fragment was ligated with digested pB-PGK-M vector. Resulting clones were screened using enzymatic digestion and sequencing. The pB-PGK-CER control vector was electroporated into destination primary cells alongside with pCyL043 helper plasmid. Expression of Cerulean was confirmed by flow cytometry.

Primer Name	Sequence (5'to 3')	Length (nt)	Tm (°C)	GC (%)
SacII-Ko-ATG-F	GAATTCCGCGGGCCACCATGGAGGAGAATCCTGGCCCA	38	72.8	63.2
SalI-R	GGCCGTCGACTTACTTGTACAGCTCGTCCA	30	65.7	56.7

Table 2.1-2. Primers used to generate and sequence pB-PGK-CER control vector.

2.2. Establishing electroporation parameters for AGM primary cells

To establish the optimal parameters for primary AGM cell transfection, a set of pilot experiments were carried out. All experiments were conducted with identical experimental templates to allow comparison between them. AGM dissection methods were described in Medvinsky, Taoudi et al. (2008). Electroporation was carried out using Neon™ Transfection System and its proprietary buffer R (Life Technologies, catalogue number: MPK5000)

Experiments were aimed to find an optimal electroporation parameters combination. Parameter being optimized were: pulse voltage (V), pulse width (ms), pulse number (n). An initial survey of different parameter combinations with E11.5 AGM cells

was conducted. Then an envelope expansion experiment near rich spots discovered previously was done. Later, transfected cells were analysed with a refined set of marker to detect potential bias in electroporation efficiency.

2.2.1. Electroporation of murine AGM cells

In a typical experiment, mice were mated at 16:00 afternoon. In the next morning, females with detectable vaginal plug were pooled together and designated as embryonic day 0.5 (E0.5). At pre-determined time of dissection, pregnant mice were culled by cervical dislocation and had their uterus taken out with scissors. These uterus were kept in dissection buffer (7% FCS in PBS with Ca2+ Mg2+ from Gibco, catalogue number: 14040-083). Each uterus was carefully opened with a pair of forceps and had its embryos collected in a new petri dish soaked in dissection buffer. After all embryos were collected, they were dissected using a pair of Tungsten needles under dissection scope, detailed dissection technique was explained in (Medvinsky, Taoudi et al. 2008). Harvested tissues were collected in a FACS tube (5mL polystyrene round bottom tube, BD Biosciences catalogue number 352054) with about 900μL dissection buffer. After dissection, 10X concentrated collagenase/dispase (made from powder, Roche Applied Science, catalogue number: 11097113001, stock solution concentration: 10mg/mL) were added to the tube to a final concentration of 1X and cells were incubated on 37℃ rotating water bath for 35-40 minutes. To stop reaction, about 4mL FACS buffer (PBS without Ca^{2+} and Mg^{2+} from Sigma, catalogue number: D8537 with 7% FCS) were added. Cells were centrifuged at 1350 rpm for 5 minutes and resuspended in 1mL FACS buffer. Then cells were counted with Fast-Read 102 dispensable hemocytometer (Immune System Ltd). Then cell suspension was transfer to a 1.5mL screw cap tube (Sarstedt, catalogue number 72.692.005) that was electrical neutral. Cells were centrifuged at 1350 rpm for 5 minutes and resuspended in electroporation solution (containing DNA and Buffer R). Every optimization sample contained 10e5 or 30e5 cells, 500ng of maxipreped pEGFP-N1 DNA. They were resuspended in 12μL Buffer R and was

electroporated with respected parameters. Real samples were transfected with pB-PGK-TAG-CER and pCyL043 vectors with the following parameters: 1350V, 20ms, single pulse. After electroporation, each sample was placed separately in 96 well plates, each well contained 200μL electroporation medium (50mL IMDM medium from Life Technologies, catalogue number: 21980-065 with 600μL Glutamine from SCRM tissue culture core lab). Tips were changed every two electroporations. Pen/Strep solution (Penicillin-Streptomycin, Life Technologies, catalogue number: 15140-122, final concentration: 100U/mL made by SCRM tissue culture core lab) was added 24 hours after electroporation.

2.2.2. Flow cytometry analysis of transfected cells.

48 hours post transfection, cells were harvested by 4X TVP treatment. Medium in the wells were aspirated and 200μL of PBS without Ca^{2+} and Mg^{2+} (Sigma, catalogue number: D8537) was added to each 96 well-plate well to wash cells. After aspirating PBS, 200μL 4X TVP (made by SCRM TC, PBS solution with 0.1% TVP, 1% Chicken Serum, 0.04% EDTA. Used 2.5% Trypsin from Life Technologies, catalogue number: 15090046; Chicken serum from Sigma-Aldrich, catalogue number C5405; EDTA from BDH, catalogue number: 104245-S; PBS from Sigma-Aldrich, catalogue number: D8537) was added to each well. After 5 minute incubation at room temperature, reaction was quenched using 50μL Foetal Calf Serum (FCS, from Life Technologies, catalogue number: 10270106). 5μL well shaken Microbeads solution from Cytognos (catalogue number: CYT-PCM-100) was added to each well to accurately count cells using flow cytometry. Later cells were centrifuged at 1350 rpm for 5 minute, resuspended in 50μL FACS buffer containing antibodies listed in table 2.2.2-1. Note each transfection condition had two samples, one was stained with “endothelial” set of staining solution while the other one was stained with “mesenchymal” set of staining solutions. These two samples were used to detect transfected (GFP^+) cells in different sub-populations. All samples were stained in dark on ice for 30 minute. At same time, isotype

controls were made from spare untransfected primary cells that were kindly provided by colleagues. Beads control for V450, FITC, PE and APC were also made. After first staining, reaction was stopped by adding 200 µL FACS buffer. Cells were pelleted by centrifuging at 1400rpm (357g on Beckman GS-6R centrifuge with GH3.8 rotor) for 5 minutes. Then they were resuspended in 50 µL FACS buffer containing Streptavidin-PE for 30 minute. During both incubations, samples were kept on ice in the dark. After second staining, cells were washed with 200 µL FACS buffer, and were resuspended in 50 µL 7AAD viability staining solution (concentration 1:40, eBioscience catalogue No 00-6993-50) and analysed using LSRFortessa™ (BD bioscience) flow cytometer. Data were analysed using FlowJo7 (FlowJo, LLC).

Staining	Antibody	Concentration	Manufacturer	Catalogue number
Both	Anti-mouse CD16/32 antibody (Fc block)	1:200	eBioscience	16-0161-86
Both	Biotin rat anti-mouse CD45	1:10	BD Bioscience	553078
Both	Anti-mouse CD41 biotin	1:300	eBioscience	13-0411-82
Both	Rat anti-mouse TER-119/Erythroid cells	1:30	BD Bioscience	553672
Both	Anti-Mouse CD11b biotin	1:50	eBioscience	13-0112-82
Both	Biotin Rat antt-mouse Ly-6G and Ly-6c	1:50	BD Bioscience	553125
Both	PE Streptavidin	1:500	BD Bioscience	554061
Endothelial	Anti-Mouse CD123 PE	1:100	eBioscience	12-1231-81
Endothelial	Anti-mouse CD144 Alexa Fluor® 647	1:50	eBioscience	51-1441-82
Mesenchymal	Anti-mosue CD51 PE	1:200	eBioscience	12-0512-82
Mesenchymal	APC anti-mouse CD105 antibody	1:100	Biolegend	120414

Table 2.2.2-1. Antibodies used to analyse pEGFP-N1 transfected cells. Antibodies labelled as "both" were used in both mesenchymal staining and endothelial staining. Antibodies labelled as "Endothelial" or "Mesenchymal" were used to make respective solutions. Concentration column states final concentration of antibodies in staining solution.

2.3. Establishing feeder cell lines from mouse embryos

To derive cell lines from murine embryos, pregnant females were generated in same the way as described in section 2.2.1. Dissection protocol was similar to section 2.2.1. All embryos were screened visually to make sure they were at correct developmental stage before dissection. To generate cell lines from E8 pre-somatic embryos, one E8 embryo was dissected. To generate cell lines from E9 embryos, caudal half of embryos were harvested by cutting between heart and forelimbs. For

E10 embryos, AGMs were dissected out. Then cells were dissociated and electroporated as described in section 2.2.1.

In different experiments, either AGM, aorta or dorsal part of aorta of E11.5 embryos were dissected and collected. Cell suspensions were passed through a cell strainer to remove clumps (BD Biosciences, catalogue number 352235). Then E11.5 samples were stained with marker of interest (table 2.3-1) as described earlier in section 2.2.2. Staining volume was 100 µL. In different experiments, different surface marker combinations were experimented, they were listed in table 2.3-2. After staining, primary cells were sorted on BD FACSAria™ II flow cytometry sorter. Large populations (e.g. $CD123^{-}CD106^{-}$) were collected in FACS tube with 1mL electroporation medium (the one with IMDM, not electroporation solution), while smaller population (e.g. $CD123^{+}CD106^{+}$) were collected in 1.5mL tubes with screw cap (Sarstedt, catalogue number 72.692.005). After sorting, cells were collected and electroporated. Master-mixes of buffer R and two plasmids were made for all samples. For samples with more than 10,000 cells, each sample received 0.5 µg of pB-PGK-TAG-CER immortalization vector and 0.5 µg of pCyL043 helper plasmid. Samples with less than 10,000 cells received 0.25 µg immortalization vector and 0.25 µg helper plasmid. Then each sample was resuspended in 10 µL corresponding master-mix and electroporated with a single 1350V 20ms pulse.

Staining	Antibody	Concentration	Manufacturer	Catalogue number
Common	Anti-mouse CD16/32 antibody (Fc block)	1:200	eBioscience	16-0161-86
Common	FITC Rat anti-mouse CD45	1:100	BD Biosciences	553080
Common	FITC Rat anti-mouse CD41	1:100	BD Biosciences	553848
Common	Anti-mouse TER119 FITC	1:200	eBioscience	11-5921-85
Common	FITC Rat anti-mouse CD45R/B220	1:200	BD Biosciences	553088
Common	FITC Rat anti-mouse CD11b (Mac-1)	1:200	BD Biosciences	553310
Common	²ITC Rat anti-mouse Ly-6G and Ly-6C (Gr-1	1:200	BD Biosciences	553127
CD123	Anti-mouse CD123 PE	1:100	eBioscience	12-1231-82
CD106	Alexa Fluor 647 anti-mouse CD106 antibody	1:100	Biolegend	105712
mSCF	in house biotinlayted mouse SCF Mab	1:50	R&D System	MAB455
mSCF	APC streptavidin	1:500	BD Biosciences	554067
VE-Cadherin	Anti-mouse CD144 Alexa Fluor® 647	1:50	eBioscience	51-1441-82
mSCF	PE Streptavidin	1:2000	BD Bioscience	554061
Flt3	Anti-mouse CD135 (Flt3) PE	1:100	eBioscience	12-1351-82

Table 2.3-1. Antibodies used to stain primary AGM cells to derive cell lines from different sub-populations. Note unconjugated antibodies against SCF was from R&D system and biotinlayted by our lab members using biotinylation kit from Life Technologies. Clones used

were CD123: 5B11; CD106: 429 MVCAM.A; SCF: 40215; VE-Cadherin: BV13; Flt3: A2F10.

Experiment Number	Marker tested	Cell source	Number of embryos used
1	CD123 CD106	Ventral arota	24
2	CD123 CD106	Ventral arota	24
3	CD123 SCF	Arota	24
4	VE-Cad SCF	Ventral arota	26
5	Flt3 SCF	Ventral arota	28
6	VE-Cad Flt3	Ventral arota	22

Table 2.3-2. List of cell line derivation experiments with E11.5 AGM cells. All experiments were conducted using BL6 embryos.

After electroporation, cells from each population were distributed to 24 wells. Four of them each had roughly one fourth of total population, they were denoted as “bulk culture” wells. 20 wells each had 2-50 cells seeded (assuming 90% electroporation efficiency and 10% cell survival), they were denoted as “low density” wells. 48 hours post electroporation, Pen/Strep was added to each well. Cells were fed with 50% fresh OP9 medium and 50% AGM-line-conditioned OP9 medium every week. OP9 medium was made by adding 50mL of FCS, 2.4mL Glutamine, 2.4mL Pen/Strep, 200 µL 2-Mercaptoethanol (2ME, diluted in UHP water, final concentration 0.1M) to 200mL IMDM medium. Conditioning time was usually 2-3 days. Wells were observed for up to three months, those with cell outgrowth were harvested using 4X TVP treatment described earlier. Cultures were gradually expanded and frozen down to two tubes in liquid nitrogen at passage 4 (cultured in T75 flasks).

To sub-clone bulk cultured populations, transfected primary cells were harvested when they reach confluence in 96 wells, cells were lifted using 4X TVP treatment and counted with haemocytometer, then samples were diluted and were deposited to gelatine coated 96 well plate wells in a concentration of 1 or 2 cells per well. Sub-clones were passaged once they reached confluence and treated the same way as other lines.

2.4. Characterization of Derived Cell lines

Several assays were used to characterize the cell lines. First, the cell lines were aggregated with E11.5 AGM primary cells and cultured at the air liquid interface for

4 days. And the haematopoietic colony formation potential of cells in aggregates was determined by methylcellulose CFU-C assay using MethoCult GF M3434 (Stem Cell Technology). After 7 days, haematopoietic colonies in methylcellulose dishes were categorised and counted. Selected cell lines were aggregated with E9.5 caudal part cells and tested for their ability to mature E9.5 pro-HSC into definitive HSCs by a combination of CFC, flow cytometry and transplantation assays. .

2.4.1. E11.5 haematopoietic progenitor assay

Immortalized cell lines were passaged every 3-5 days. Before aggregation, they were maintained in T75 flasks (Corning) until confluent. To maximize cell recovery, in the first experiment of given batch, cultures were generally given more cells to allow them stay in over confluence before experiment. On the day of aggregation, immortalized cells were harvested using 4X TVP treatment described before and counted. Primary cells from E11.5 BL6 mouse embryo were harvested using method described earlier. Harvested cells were stored in FACS buffer and kept on ice. After harvest, primary and immortalized cells were mixed and made into aggregates using methods described in Medvinsky, Taoudi et al. (2008) and section 2.4.1.1. Four days after culture, aggregates were harvested and subjected to CFU-C assay as described in section 2.4.1.2.

2.4.1.1. Setting up 3D aggregation culture

The protocol used in this experiment was similar to one described in (Medvinsky, Taoudi et al. 2008). For aggregation experiments in E11.5 haematopoietic progenitor assay, each cell line was tested in three conditions: one with AGM primary cells and growth factors (Flt3l, SCF, Il3, referred as “+GF” conditions); one with AGM primary cells but without growth factors (“-GF” conditions) and one without AGM cells (immortalized cells only) but with growth factor (referred as “blank” conditions). Before harvesting cells, media for aggregation culture were prepared. Volume of basal media (without growth factor) and with growth factor (+GF) media were calculated. To make 10mL basal media, 7.8mL IMDM medium,

2mL aggregation “gold” serum (Foetal Bovine Serum “Gold”, EU approved, PAA, catalogue number: A15-151), 100µL freshly defrosted glutamine, 100µL Pen/Strep were added together and mixed well. +GF media were made by adding 100µL of Flt3L, SCF and Il3 IMDM solution to 10mL basal media. These stock cytokine solutions had a concentration of 10µg/mL (Flt3l, PeproTech, catalogue number: 250-31L; SCF PeproTech, catalogue number: 250-03; Il3 PeproTech, catalogue number: 213-13). This made the final concentration of each cytokine in “+GF” media was 100ng/mL. After preparation, medium were kept on ice. Once defrozen aggregations serum could be kept in 4℃ for up to 3 days.

At same time membranes used to hold aggregates on air-medium interface were also prepared. In every experiment, each condition used one membrane, so each cell line used 3 membranes. A few spare membranes were prepared. 0.8µm nitrocellulose filter membranes from Millipore (catalogue number: AAWP02500) were washed four times in sterilized 10MΩ Millipore water. Each wash was 15 minute long. After wash membranes were dried on top of yellow tips in an open tip box in sterile hood. A visual examination of membranes was conducted to make sure no greyish humid spot existed on them. Membranes must be completely white or they will sunk into liquid surface once deployed. Washed membranes could be stored for several months.

Aggregation tips were also made before experiment. One square “section” of parafilm M (Bemis Company Inc., catalogue number: P7668-1EA) was cut into four equal smaller square pieces. Then each piece was folded twice along centreline, forming a small square that was one sixteenth of original “section” size. To make aggregation tip, an autoclaved 200µL yellow tip was used to half penetrate the parafilm right in the centre. After that the rest of small “square” was squeezed around the tip to form a tight seal.

On the day of aggregation, primary E11.5 AGMs were dissected and dissociated into single cells as described earlier. Clumps in primary cells were removed using

strainer. Next immortalized cells were harvested using 4X TVP treatment. Appropriate number of both primary and immortalized stromal cells were mixed together in a clean FACS tube prepared for every condition tested. After centrifugation, they were resuspended in basal medium. 20μL of basal medium were used for one aggregate. Each membrane had 5 aggregates, each aggregate contained $10e^5$ stromal cells and 0.2ee (embryo equivalent) primary AGM cells. Each aggregation tip loaded with solutions contained cells was transferred to a sterile FACS tube and all tubes were centrifuged at 4℃ at 350g for 12 minute. At the same time, 5mL of aggregation medium was put into each well of 6-well plate. All bubbles on surface of medium were pierced using a yellow tip. Then dried membranes were carefully floated on top of the medium, a visual examination was conducted to make sure edge of membranes was not below the media surface, which would cause the membranes to sink to bottom of wells during culture.

After centrifugation, parafilm seal tied to the tip of yellow tube was carefully removed without disrupting aggregates inside. Then aggregate was carefully expelled from tip onto filter membrane floating on medium by squeezing from the open end of tip with thumb. Each condition had 3-5 aggregates on one membrane with 5mL aggregation medium, all aggregates shared same cell sources. After all aggregates were placed onto membrane, the plate was incubated at 37℃ 5% CO_2. Special care was exercised to prevent membrane held aggregates to sink into medium due to shaking.

At end of culture, aggregates were harvested. In E11.5 haematopoietic progenitor assay, aggregation culture was 4 days long and in E9.5 pro-HSC maturation assay aggregation culture time was 7 days. For each condition, one FACS tube with 1.2mL dissection buffer was prepared. Membranes with aggregates were picked up with forceps, the edge of the membrane without cells was cut away and the remaining part was quickly submerged in dissection medium. After all membranes were picked up, they were treated with 1.5mL of 1x collagenase/dispase solution in 37℃ rotating

water bath for 35-40 minutes. Reaction was stopped by topping up the tube to 4.5mL with FACS buffer and centrifuging for 5 minutes. Then supernatant was removed without exposing the membrane to air. Afterwards, membranes were washed again with FACS buffer to remove residue collagenase/dispase. Next cells attached to membrane were washed away by pipetting. To pick up and check membrane at bottom of FACS tube, a yellow tip was inserted on top of a blue tip and bended. Such assembly was used as a hook. Once all cells were washed away from membranes, waste membranes were removed from FACS tube and cells were collected by brief centrifugation and resuspended in 1mL FACS buffer. For conditions with growth factors (+GF conditions), 0.01ee cells were taken for CFC assays. For conditions without growth factors (-GF conditions), 0.1ee cells were taken. For blank aggregate without primary cells, half of all cells (equivalent to 250K input cells) were taken.

2.4.1.2. Colony Forming Unit assay

Colony Forming Unit-Culture (CFU-C) assays were aimed to detect haematopoietic progenitor cells presented in samples. For all sample dishes observed, clusters of feeder cells were excluded based on their tight sphere shaped morphology. Granulocytes and Macrophages were distinguished by size of cell and compactness of the colonies. Granulocyte-Macrophage colonies were identified by presence of two cell size in one colony. Mast colonies were identified by their ultra-small size and “radiating” feature. Erythrocyte colonies were identified by their red colour. GEMM colonies were identified by the presence of both red and white cells and at least two different cell sizes should be observed in same colony. For examples of colonies observed, see figure 6.1-1.

After harvest, cells from each condition were placed in respective tubes containing 2mL mouse methylcellulose (MethoCult GF M3434, Stem Cell Technology, catalogue number: 03434). The contents inside the tubes were briefly mixed on vortex shaker and distributed to two different uncoated 30mm plastic dishes. Dishes

contained methylcellulose were incubated in 37℃ incubator with a dish of sterile water to keep the area humid. After 7-8 days, dishes were observed under microscope (Motic AE2000) with 100X magnification. Colonies were classified and counted. Dishes contained blank aggregates were also observed to train to distinguish clumps of stromal cells with real haematopoietic colonies. All readings were inputted into Microsoft® Excel and processed.

2.4.2. E9.5 pro-HSC maturation assay

Each cell line was tested with +GF (supplemented with growth factors Flt3l, SCF, Il3, final concentration 100ng/mL, Peprotech) and –GF (without growth factors) conditions. Membranes and medium were prepared in the same way as described in section 2.4.1.1. Feeder cells were harvested as described in section 2.4.1.1. Special care was taken to identify developmental stage of E9.5 embryos, only embryos within 24-28 somatic pair stage were used. They were staged by counting somite pairs, staging was confirmed Dr Stanislav Rybtsov. Caudal part of corrected staged E9.5 embryos were processed with method described in section 2.3.

Each condition had three aggregates shared the same membrane and medium. Each aggregate had 10^5 immortalized cells and about 1 embryo-equivalent primary cells. For E9.5 HSC maturation assays, only 2mL medium were added into each well in the first day. After 1 day of incubation, medium in wells were carefully removed and 5mL of fresh aggregation medium were carefully added back into each well. It was very important to avoid membranes broke the surface of the medium, to sink or rotate during this process. Six days later, membranes were harvested as described in section 2.4.1.1. This made total culture length 7 days. 0.01ee (+GF conditions) or 0.2ee (-GF conditions) aggregates cells were used in CFU-C assay as described in section 2.4.1.2; about 0.1 to 0.3ee cells were used for flow cytometry analysis with CD45, VE-Cadherin and CD41. Antibodies used was listed in table 2.4.2-1.

Antibody	Concentration	Manufacturer	Catalogue number
FITC Rat Anti-mouse CD45	1:100	BD Biosciences	553080
PE Rat Anti mouse CD41	1:100	BD Biosciences	558040
Anti-mouse CD144 Alexa Fluor® 647	1:50	eBioscience	51-1441-82
Anti-mouse CD16/32 antibody (Fc block)	1:200	eBioscience	16-0161-86

Table 2.4.2-1. Antibodies used to analyse harvested aggregates with flow cytometry. Clones of antibody used were: CD45: 30-F11; CD41: MWReg30; CD144: BV13; CD16/32: 93.

2.4.2.1. Transplantation of aggregated cells into irradiated recipients

The remaining cells, about 3ee, were used for transplantation into irradiated mouse recipients. Each condition had three recipient mice, each of them received cells from 1 aggregate contains CD45.2 homozygous primary cells and 10e5 carrier cells from bone marrow of CD45.1 homozygous mice. Cells were resuspended in 300 µL transplantation buffer (PBS without Ca^{2+} and Mg^{2+} with 3% FCS) and kept on ice. BL6-ly5.1/ly5.2 heterozygous recipient mice were gamma irradiated for two doses of 10 minute and 7 minute 48 seconds (9.5Gy) with at least 3 hours in between. Then mice were left to recover for 4-5 hours before transplantation. Next cell suspensions were injected into tail vein of irradiated mouse using 30G needle (BD Microlance™ 3, catalogue number 30400). After injection, mice were kept on sterile water with antibiotics for a month.

Peripheral blood samples were taken from recipients 6 weeks after transplantation. Approximately 50 µL of tail blood was taken from the tail vein by venesection and collected into 500 µL bleeding buffer (FACS buffer with 10 µM EDTA). Two spare blood samples were taken for single staining controls. After bleeding, all cells were centrifuged briefly and resuspended in 1x BD Pharm Lyse RBC lysis solution (BD Bioscience, catalogue number 555899). Lysis was completed with 5-7 minutes incubation at room temperature. After lysis, white cells were collected by centrifugation and stained with CD45.1-APC (eBioscience, catalogue number: 17-0453-82, clone A20) and CD45.2-PE (eBioscience, catalogue number: 12-0454-83 clone 104) antibodies. Donor (CD45.2 homozygous) engraftment was

determined by flow cytometry using BD FACSCalibur™ flow cytometer. Gating was set based on CD45.1 APC and CD45.2 PE single stain sample.

6 months post transplantation, mice with significant (>10%) engraftment in peripheral blood were subjected to multilineage analysis. Blood samples were taken and lysed as described above. They were analysed with LSRFortessa™ flow cytometer with antibodies listed in table 2.4.2.1-1.

Antibody	Concentration	Manufacturer	Catalogue number
V450 Mouse anti-mouse CD45.1	1:200	BD Biosciences	560520
V500 Rat anti-mouse Ter119/Erythroid cells	1:100	BD Biosciences	562120
ITC Rat anti-mouse Ly-6G and Ly-6C (Gr-1	1:600	BD Biosciences	553127
Anti-mouse CD11b PE (Mac-1)	1:600	eBioscience	12-0112-82
PE-Cy™7 rat anti-mouse CD45R/B220	1:200	BD Biosciences	552772
Anti-mouse CD3e APC	1:200	eBioscience	17-0031-82
Anti-mouse CD16/32 antibody (Fc block)	1:200	eBioscience	16-0161-86

Table 2.4.2.1-1. Antibodies used for flow cytometry analysis of blood/ spleen/bone marrow samples to detect multilineage engraftment. CD45.1 antibody was used to exclude carrier and recipient originated cells. Ter119 antibody was used to exclude erythrocytes. Gr-1 antibody was used to label granulocytes. Mac-1 antibody was used to label Macrophage. B220 antibody was used to label B cells, CD3e was used to label T cells. Fc block was used to prevent unspecific staining.

After multilineage analysis of blood sample, select mice were culled. Blood sample of these mice were taken as described before. Thymus and spleen were dissected, and placed in dissection buffer. Spleens were further cut into pieces with a pair of scissors. Bone marrow cells were flushed from both femurs of mice using FACS buffer and a 25G needle. Then thymus and spleen were crushed using piston from 1mL syringes against cell strainer. Cells were collected by washing crushed tissues using FACS buffer. Blood, bone marrow and filtered spleen cells were stained in 100 µL staining solution (table 2.4.2.1-1) with the method described in section 2.2.2. Antibodies used was listed in table 2.4.2-1. Thymus samples were stained using antibodies listed in table 2.4.2.1-2. Fluorescence minus one (FMO) controls were made from spare bone marrow cells. FMO controls were set against following channels V450, V500, APC, FITC, PE and PE-Cy7. Beads staining controls were

also made. Extra buffer was added to the spleen samples because they could be very sticky. Then samples were analysed on LSRFortessa™. Data were processed with FlowJo™. Because some samples were very sticky, and might affect florescence readings as cytometer running time accumulate, a time gating was applied to gate out events with altered florescence strength signals.

Antibody	Concentration	Manufacturer	Catalogue number
V450 Mouse anti-mouse CD45.1	1:200	BD Biosciences	560520
V500 Rat anti-mouse Ter119/Erythroid cells	1:100	BD Biosciences	562120
Anti-mouse CD8a FITC	1:600	eBioscience	11-0081-85
PE hamster anti-mouse TCR beta chain	1:100	BD Biosciences	553172
Anti-mouse CD127 PE-Cyanine7	1:200	eBioscience	25-1271-82
Anti-mouse CD4 APC	1:200	eBioscience	17-0041-83
Anti-mouse CD16/32 antibody (Fc block)	1:200	eBioscience	16-0161-86

Table 2.4.2.1-2. Antibodies used for flow cytometry analysis of thymus samples to detect multilineage engraftment in thymus samples. CD45.1 antibody was used to exclude carrier and recipient originated cells. Ter119 antibody was used to exclude erythrocytes. CD4 and CD8 antibodies were used collectively to determine stage of thymocyte development. TCR beta and CD127 were also used to label stage specific development of T cells.

Later, one highly engrafted mouse was culled, and its bone marrow cells are harvested from its femur and i.v. transplanted into two secondary recipients. Each recipient receives cell amount that equivalent of one third of a femur. 7 weeks post transplantation, peripheral blood of secondary recipients was analysed for $CD45.2^{+/+}$ secondary engraftment as described before.

At last, a preliminary experiment to detect transfected cells in engraftment recipient was carried out. One mouse from experiment SRYZH6 and two mice from SRYZH9 were tail bled 6 months after transplantation. Genomic DNA was isolated using Puregene Blood core Kit C (Qiagen, catalogue number: 158389). Isolated gDNA was amplified using Taq DNA polymerase kit (Qiagen, catalogue number 201205). PCR parameters were listed in appendix table 8.3-1 a. Primer 2A-F and CER-R were used to detect gDNA from transfected cells (table 2.1-1), while primer Myo-1 and Myo-2 were used as internal control. Sequence for primer Myo1 was: TTA CTG

CCA TCG TGG ACA GC, sequence for primer Myo2 was: TGG GCT GGG TGT TAG TCT TA. Reaction system was listed in appendix table 8.3-1 b. PCR product was ran on agarose gel and visualized with UV illuminator.

2.5. Reverse transcription quantitative-PCR

All RT-qPCR experiments were performed using LightCycler® 480 II instrument (384 wells version. Roche, product no: 05015243001, serial no: 5335). UPL probes and LightCycler® 480 probe master (Roche, product No 04887301001) were used. All reactions used UPL probe had 10 µL volume. Each sample well contained 4 µL of cDNA (1ng/µL assuming 100% RT efficiency), 1 µL of primer-probe mix (table 2.5-1), and 5 µL of LightCycler® 480 probe master (Roche, product No 04887301001).

Item	Concentration	Volume (µL)
PCR grade water	n/a	81
Forward (5') primer	100nM	4.5
Reverse (3') primer	100nM	4.5
Corresponding UPL probe	10µM	10
Total		100

Table 2.5-1. Composition of Primer-Probe Mix (PPM) for qPCR reactions used UPL technology. To ensure reproducibility, PPMs were made as 100µL master mixes. They could stay in freezer for about a month.

A candidate pool of 64 genes was selected based on educated guess. All genes were checked against mouse reference genomic assembly version GRCm38 C57/Bl6J hosted on NCBI (http://www.ncbi.nlm.nih.gov/assembly/GCF_000001635.20/). For loci with only one transcript, the transcript was designates as the target transcript of that locus. For loci with multiple transcripts, its locus structure was studied and a literature survey was conducted to determine the transcript with desired biological function. If no previous literature available, I tried my best to pick a most representative transcript as target transcript. Loci without a clear representative transcript were excluded from study. All target transcripts were loaded into UPL assay design centre with Organism set to *Mus musculus* and feature “automatically select an intron spanning assay” set to on (Roche, qpcr.probefinder.com). For every

target transcript, the best scoring pair of primers was selected. If no intron spanning assay was available, the best pair of intra exon primers was selected. If the primary pair failed in verification experiment, I tried my best to design the second pair of primers so they spanned another intron or at least had different primer binding sites spanning the same intron.

As a result, target transcripts for 46 genes are identified by a combination of bioinformatical analysis and literature search. A total of 96 pairs of primers (appendix table 8.4-2) were designed against those 46 target transcripts. 15 out of 96 pairs were kindly designed by Ms. Alison McGarvey. For gene Igfbp2 and Fgf9, Roche's database did not contain newest transcript listed in GRCm38 (NM_013518.4 and NM_008342.3), thus the newest version in Roche database (NM_013518.3 and NM_008342.2) were designated as target transcript

Primer pairs were named by their MGI symbol followed by exons they bind with. For example, "Angpt2 E5/6" was the name of a pair of primers targeting Angpt2 gene spanning exon 5 and 6. If multiple primer pairs were designed spanning same exon junctions, a suffix was added, like "Bmp4 E3/4b" indicated the second pair of primers designed targeting exon junction 3/4 of Bmp4 gene. Primers within a pair were distinguished by suffix, e. g. "Bmp4 E3/4b 5' " and "Bmp4 E3/4b 3' ". They were all synthesized by Integrated DNA Technologies, Inc.

Total RNA from cell lines were harvested using RNeasy Plus Mini Kit (Qiagen, catalogue number: 74134) in according to manufacturer's instructions. Isolated RNA was reverse transcribed using M-MLV Reverse Transcription system (Life Technologies, Catalogue No: 20825-013) with Random hexamer (Thermo Scientific, Catalogue No: AB-1297/B). RNaseOUT™ Recombinant Ribonuclease Inhibitor (Life Technologies, Catalogue No 10777-019) was used in reverse transcription to prevent RNA degradation. Every pair of primers and its corresponding probe was tested with different cDNA sample. In every run, a standard curve with 4 data points was included. Their cDNA concentration were: 20ng/rxn, 2ng/rxn, 0.2ng/rxn and

0.02ng/rxn. Three identical wells with 4ng cDNA pre reaction were also included for every primer pair. qPCR program was listed in table 2.5-2.

Program	Cycles	Analysis mode	Target Temp (°C)	Acquisition mode	Hold time	Ramp rate (°C/s)
Preincubation	1	None	95	none	5:00	4.8
Amplification	45	quantification	95	none	0:10	4.8
			60	single	0:17	2.5
Extension	1	None	60	none	10:01	4.8

Table 2.5-2. qPCR program used to evaluate primers. Amplification time was slightly increased to 17 sec to maximize template extension.

A pair of primer was considered good when in two consecutive runs, amplification efficiency calculated from standard curve was between 1.75 and 2.1 and amplification error of both standard curve and repetitive wells was smaller than 0.2. If one of two repeats had results that were slightly out of boundary, verification of the cDNA-primer/probe pair was repeated until two consecutive good runs were achieved.

The primers passed first round of evaluation was subjected to a SYBR green melting curve screen to detect unspecific product. qPCR experiments with SYBR Green was carried out using LightCycler® 480 SYBR I green master (Roche, product No 04707516001). In SYBR Green experiments, total volume was 10 µL. Concentration of cDNA and primers was the same as UPL experiments. In SYBR green experiments, SYBR I green master (Roche, product No 04707516001) was used and no UPL probe was added to reaction. Parameters for SYBR green qPCR and melting curve experiment were listed in table 2.5-3. I used E11.5 caudal parts cDNA generated by Alison McGarvey and Dr. Stanislav Rybtsov from our group. cDNA concentration was 125ng/µL. Concentration for standard curve wells were 40ng/rxn, 4ng/rxn, 0.4ng/rxn, and 0.04ng/rxn. And all of the three sample wells had a concentration of 4ng/rxn. A primer was considered good if at least two of three replicates showed single peak in melting curve analysis (appendix figure 8.4-1). All primer pairs tested passed melting curve analysis.

Program	Cycles	Analysis mode	Target Temp (°C)	Acquisition mode	Hold time	Ramp rate (°C/s)
Preincubation	1	None	95	none	5:00	4.8
Amplification	45	Quantification	95	none	0:10	4.8
			60	none	0:10	2.5
			72	single	0:18	4.8
Melting curve	1	Melting Curve	95	none	1:00	4.8
			65	none	1:00	2.5
			97	continuous (10 per second)		0.06
			40	none	0:10	2.5

Table 2.5-2. qPCR program used to determine melting curve of selected primers. Amplification time was slightly increased to 18 sec to maximize possibility to detect unspecific products.

15 pairs of primers passed the primer verification test. Two redundant sets of primers that preformed less well were removed. Their sequence was listed in table 6.1-1. RT-qPCR was carried out with 9 stromal lines plus the OP9 positive control. RNA extraction and reverse transcription were done as described previously. qPCR program was listed in table 2.5-4. Crossing points for each well was determined automatically by LightCycler® 480 Software release 1.5.1.62 (Roche, product No 04994884001) using secondary derivate max method in high confidence mode. Then data were extracted to Excel 2010 and all graphs are drawn using it.

Program	Cycles	Analysis mode	Target Temp (°C)	Acquisition mode	Hold time	Ramp rate (°C/s)
Preincubation	1	None	95	none	5:00	4.8
Amplification	50	Quantification	95	none	0:10	4.8
			60	single	0:18	2.5
Extension	1	None	60	none	10:01	4.8

Table 2.5-4. qPCR program used to get expression data for haematopoietic genes. Note the format of holding time was mm:ss, thus 05:00 indicated 5 minutes

3. Chapter 3: Generation of a piggyBac transposon based immortalization vector system

In this study, a novel immortalization system was established. It surpassed previous systems because it can immortalize primary cells based on their surface marker expression, and immortalized cells did not went through crisis. In order to meet such requirements, immortalization vector was designed and constructed with following properties:

- The vector should contain the *piggyback* Inverted Terminal Repeat (ITR) to facilitate translocation of immortalization cassette to genomic DNA
- The vector should have a normal SV40T gene, stronger than previously used tsA58 factor. It should allow direct immortalization of transfected cells without going through crisis.
- The vector should have a fluorescent protein tag to label immortalized cells. its expression level correlates with SV40T expression

A vector contained SV40T and Cerulean protein linked together by T2A self-cleaving polypeptide was constructed (Kim, Lee et al. 2011). It was named as pB-PGK-TAG-CER. To determine its functionality, a pB-PGK-CER vector lacked SV40T immortalization factor was made as a control. The pB-PGK-TAG-CER vector went through following tests:

- Enzymatic test and sequencing to confirm vector's structure and sequence of SV40T-2A-CER cassette.
- Immunohistochemistry staining of transfected cells to detect expression of both SV40T and CER.
- Flow cytometry and confocal microscopy assay to prove the functionality of Cerulean fragment.
- Side-by-side comparison of immortalization vector transfected culture and control vector transfected culture, to establish a growth curve that demonstrated functionality of SV40T immortalization factor.

In this chapter, I discussed results related to generation and verification of pB-PGK-TAG-CER vector. These results indicated that clone M20 of pB-PGK-TAG-CER vector could express functional SV40T and CER protein. The expression level of SV40T was strongly enough to immortalize primary cells.

However, fluorescence generated by Cerulean protein was not strong enough to label all transfected cells.

3.1.Construction of pB-PGK-TAG-CER and pB-PGK-CER vectors

The *piggyBac* based immortalization system used in this project utilised two vectors. One was the pCyL043 helper plasmid described in Wang, Lin et al. (2008). The pCyL043 vector encoded a *piggyBac* transposase (IFP2) driven by CAG promoter and a PGK driven puromycin selection gene (Wang, Lin et al. 2008). The other was the pB-PGK-TAG-CER immortalization vector, which was constructed in this project.

A pB-PGK-CER control vector was constructed to demonstrate that unrestricted growth of transfected primary cells was promoted by SV40 large T antigen, not due to genomic integrations disrupting tumour-suppressor genes, or some other elements on the *piggyBac* backbone. The control vector was based on pB-PGK-M9 backbone same as immortalization vector, but Cerulean protein expression was initiated directly from its start codon in a strong Kozak context (Kozak 1987). This vector lacks both SV40 T antigen and 2A coding sequence (see figure 3.1-1, b).

a) b)

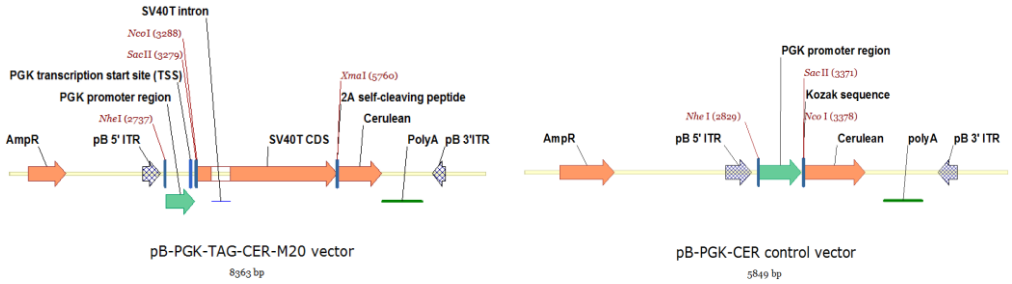

Figure 3.1-1. Maps of pB-PGK-TAG-CER vector (a) and pB-PGK-CER control vector (b). (a) The pB-PGK-TAG-CER vector clone M20 had SV40T and Cerulean fused with T2A polypeptide. The SV40T-2A-CER fusion was driven by PGK promoter. Note the XhoI site was destroyed after triple ligation. (b) pB-PGK-CER control vector had a Cerulean fragment downstream of PGK with Kozak sequence. The polyA sequence of both vectors was obtained from rabbit beta-globin gene.

The CAG promoter of pB-CAG vector was replaced with PGK promoter, and additional enzymatic sites were introduced to pB-PGK backbone. DNA fragments encoding SV40 T antigen and Cerulean were cloned into pCR-BluntII intermediate vector respectively. A triple ligation of the three was conducted taking advantage of the fact that SalI and XhoI were isocaudomers (Figure 3.1.2a). Two clones, M20 and D5, passed preliminary digestion tests and were subjected to further verification.

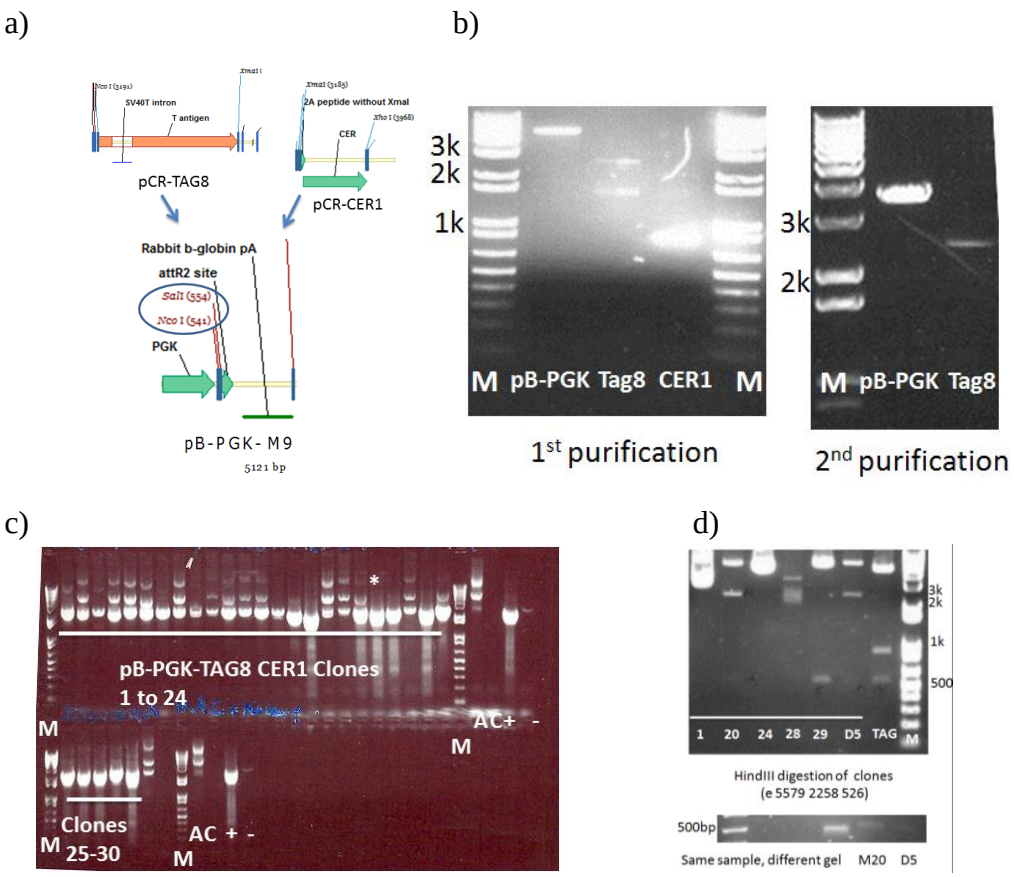

Figure 3.1-2. pB-PGK-TAG-CER vector was generated by a triple ligation reaction. a) Schematic representation of triple ligation reaction. b) Digested and recovered piggyback backbone (5108bp), T antigen (2470bp) and 2A-CER (783bp) DNA fragments. Upper band of Tag8 in 1st recovery was re-purified and shown in right panel. c) Screening of pB-PGK-TAG8-CER1 clone 1 to 30 used PCR targeted to T antigen. Clone number 20 was marked with a *. Lane A was negative control reaction with pB-PGK M9 backbone only, Lane C was negative control reaction with pB-PGK M9 and pCR-BluntII-CER1 plasmid. (See table 8.1.1-1 in appendix) Lane "+" were positive control with TAG8 plasmid, and lane "–" were no template control. Lane M was 1kb+ ladder from Life Technologies d) *Hind*III digestion of selected clones. Clone 1, 20, 24, 28 and 29 shown here were from T antigen PCR screen, D5 was from Dr David Hills. Lane TAG was a positive control digestion contained 526bp target band. (This experiment was conducted once, n=1)

To construct pB-PGK-CER control vector without T antigen, a pair of primers that introduced the Kozak translational initiation sequence at the start codon of CER was designed (Table 2.1-3). The SacII-Ko-ATG-CER-SalI fragment was generated by PCR and recovered. Both vector and insert were sequentially digested with SalI and

SacII (figure 3.1.3a). Digestion products were recovered and ligated together using T4 DNA ligase. DNA from transformed clones was prepared and digested with NheI and PstI. Correct clones should have bands of 3875bp and 1974bp. Clone number 2 had expected bands (figure 3.1.3b) and was confirmed by sequencing. Original chromatograms, sequence and annotation of pCR-BluntII-CER1 plasmid could be accessed in electronic supplementary files.

a) b)

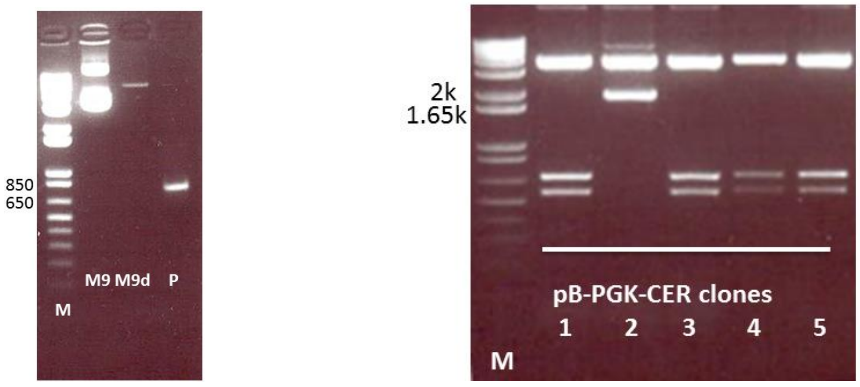

Figure 3.1.3. pB-PGK-CER control vector was generated with ligation of pB-PGK M9 backbone and SacII-Ko-ATG-CER-SalI PCR product. a) Digestion of pB-PGK-M9 and SacII-Ko-ATG-CER-SalI PCR product. Lane M was 1kb+ DNA ladder from Life Technologies. Lane M9 was circular M9 plasmid, Lane M9d was pB-PGK-M9 after SalI and SacII digestion (5099bp). Lane P was PCR product digested with SalI and SacII (750bp). b) NheI/PstI digestion of transformed clones. Lane M was 1kb+ DNA ladder. Expected products sizes are 3875bp and 1974bp. (This experiment was conducted once, n=1)

3.2.Verification of vector function

The PGK-TAG-2A-CER region of pB-PGK-TAG-CER clone M20 and D5 were sequenced. Chromatograms of both clones did not show mutations that caused amino acid substitution or early termination. Once sequences were confirmed, clones were purified using EndoFree Plasmid Maxi Kit (Qiagen, catalogue number: 12362) and verified by HindIII digestion to avoid cross-contamination (appendix figure 8.1.1-1).

To detect translation products of SV40T and CER, DNA of pB-PGK-CER clone M20 was electroporated into OP9 cells using Neon™ electroporation machine (Life

Technologies, catalogue number: MPK5000). Optimization condition 14 (1200V 20ms, two pulses) from Neon™'s manual was used, because it was one of the best performing conditions in early pilot studies done by Dr. Jordi Senserrich (personal communication). 1-2x10^6 cells were electroporated using a 100µL electroporation tip. These cells were cultured for 4 days to allow them time to recover from electroporation and express both proteins. Subsequently cells were seeded (1:6) to gelatin coated coverslips and stained with antibodies against SV40T (BD Pharmingen, catalogue number: 554149, clone PAb 101) and Cerulean (Life Technologies, catalogue number: A21311). An anti-GFP antibody was used because it cross-react with Cerulean. Immunohistochemistry (IHC) staining showed strong expression of SV40T and CER in OP9 cells transfected with pB-PGK-TAG-CER clone M20 and pCyL043 (figure 3.2-1). Expression of neither protein was detected in untransfected OP9 cells.

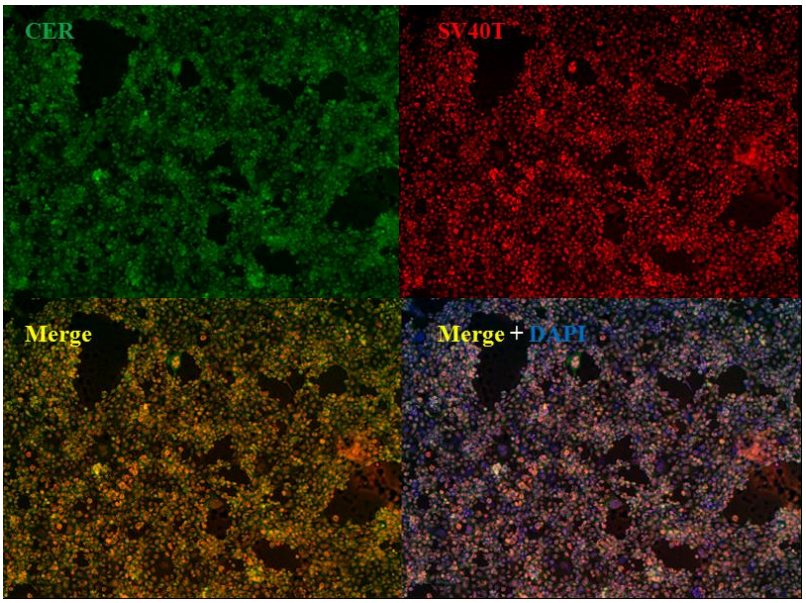

Figure 3.2-1. pB-PGK-TAG-CER clone M20 transfected OP9 cells expressed SV40T and CER proteins. Green channel was used to detect Cerulean expression with Alexa-488 conjugated anti GFP antibody recognizing Cerulean. Red channel was used to detect SV40T protein with Alexa-568 goat anti mouse antibody (Life Technologies, catalogue number A11004) recognizing SV40T positive cells labelled by mouse anti SV40T antibody. Bottom right picture was green channel and red channel merged with DAPI (Blue). Negative control pictures were shown in appendix figure 8.1.1-2. (This experiment is conducted once, n=1)

3.3.Functional test of the immortalization system

After successful confirmation of Cerulean protein expression by immune-histo-chemistry (IHC) staining, functionality of CER protein was tested. Olympus IX51 and Motic AE31 microscope failed to detect above background signal of Cerulean florescence in both FITC and CFP channels (data not shown).

Therefore, CER fluorescence was analysed using flow cytometry and confocal microscopy. Flow cytometry data showed a significant shift in V_525/50 channel (CER) in 293T cells transfected with pB-PGK-TAG-CER clone M20, but no shift in untransfected 293T cells (figure 3.3-1). This shift was continuous, without forming two separate cell populations. No shift in B_530/30 channel was observed which was used to detect FITC or GFP. On the other hand, pB-PGK-TAG-CER clone D5 showed a considerably smaller shift in CER channel, suggesting mutations might

exist outside sequenced regions that affect fluorescence generation. Thus, clone D5 was excluded in further experiments.

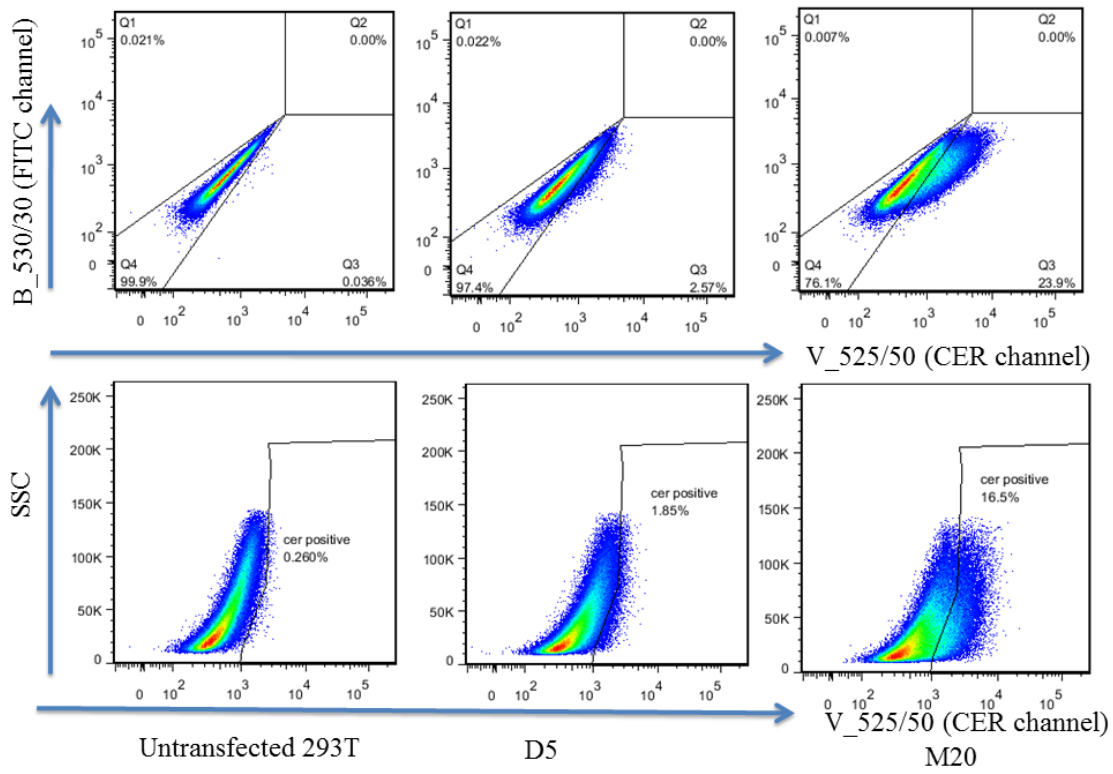

Figure 3.3-1. pB-PGK-TAG-CER transfected 293T cells showed continuous shift in V_525/50 channel but not B_530/30 channel. Left column was flow cytometry plots of untransfected 293T cells control. Gatings used in this experiment were based on them. Middle column was plots of 293T cells transfected with pB-PGK-TAG-CER clone D5, only a weak shift in V_525/50 (Cerulean) channel was detected. Right column was plots of 293T cells transfected with pB-PGK-TAG-CER clone M20. A strong shift in CER channel is detected and such shift was continuous. In cells transfected with both clones, no shift in B_530/30 channel used by FITC and GFP is detected. (This experiment is conducted once, n=1)

Next, E11.5 ventral aorta (AoV) cells were transfected with pB-PGK-TAG-CER clone M20 and pCyL043 plasmid and analysed by confocal microscopy. Untransfected AoV cells were used as negative control. Propidium Iodide (PI) staining was used to label dead cell. Merged picture of bright field, CER (465nm-550nm) and PI (560nm-760nm) showed that M20 transfected cells had strong fluorescence with emission spectra similar to CER, and such fluorescence did

not co-localize with PI staining (figure 3.3-2, a), indicated it was specific for live cells. Fluorescence intensity of pB-PGK-TAG-CER clone M20 transfected cells and untransfected control cells were compared at CER peak emission range (465-495nm) or outside CER emission range (555-585nm). Images taken at peak emission wavelength of transfected sample showed strong emission while images taken outside emission range showed no emission, such observation suggested transfected cells express fluorescence similar to CER (figure 3.3-2, a, b). As a comparison, untransfected control had almost no emission in and out Cerulean wavelength range (figure 3.3-2, a, b). Combined results from IHC, FACS and confocal microscopy firmly indicate cells transfected with pB-PGK-TAG-CER clone M20 express functional Cerulean fluorescence protein.

a)

b)

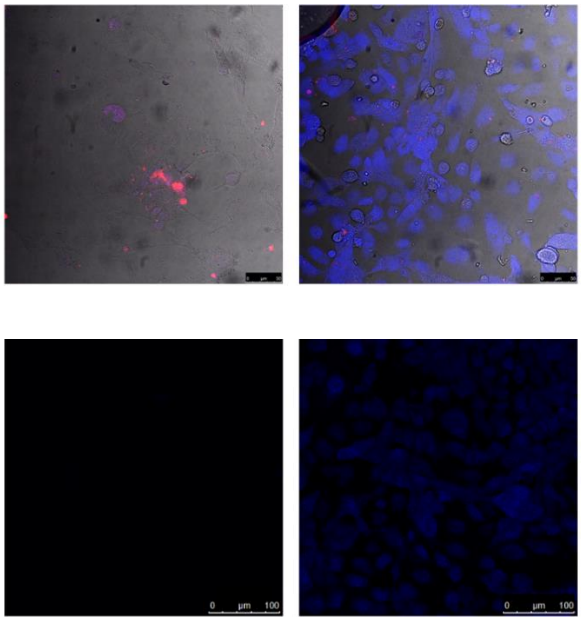

Figure 3.3-2. pB-PGK-TAG-CER transfected cells had similar fluorescence property as Cerulean. Right side pictures were primary cells transfected with pB-PGK-TAG-CER clone M20. These cells were isolated from ventral aorta of E11.5 embryos. Left side pictures were untransfected control from same source. a) Merged picture of bright field, PI staining (red) and CER (blue). These pictures indicated blue emission is not from dead (PI positive) cells. b) Fluorescence signal near peak CER emission (465-495nm). Image of cells outside of CER emission spectrum could be seen at figure 8.1.1-3. All pictures were taken with 40x oil objective. (This experiment was conducted once, n=1)

After testing Cerulean activity, SV40T antigen activity was functionally tested. Cells were harvested from AGM region of E11.5 BL6XBL6 embryos. 10^6 primary cells were electroporated with pB-PGK-TAG-CER vector and pB-PGK-CER control vector respectively. Equal amount of pCyL043 helper plasmid was added to electroporation mixture. Flow cytometry analysis at four days post electroporation showed that the transfection efficiency of pB-PGK-CER was not lower compared to efficiency of the pB-PGK-TAG-CER vector (figure 3.3-3, b). Transfected cells were seeded in 6 well plate wells, and then passaged side by side when pB-PGK-TAG-CER transfected cells reach full confluence. During every passage, cell numbers in both cultures were counted. Based on cell counting, growth curves of cells transfected with respective vectors was established (figure 3.3-3, a). Growth curve clearly shown that pB-PGK-TAG-CER transfected primary cells maintained exponential growth while pB-PGK-CER transfected control cells had a slight expansion at passage 1, then stopped growing. Because pB-PGK-CER vector shared the same pB-PGK-M9 backbone but did not induce exponential expansion of transfected cells, such exponential growth observed in pB-PGK-TAG-CER transfected cells must be result of SV40 T antigen. Taken together, the data clearly confirmed immortalization activity of pB-PGK-TAG-CER vector was dependent upon the expression of the SV40T antigen.

In summary, a functional *piggyBac* based immortalization vector was constructed. Its SV40T and CER components were verified at DNA sequence level and functionally tested. During vector validation process, basic protocols for cell culture, transfection and detection of Cerulean fluorescence were established. The work described in this chapter laid a solid foundation for further experiments.

a)

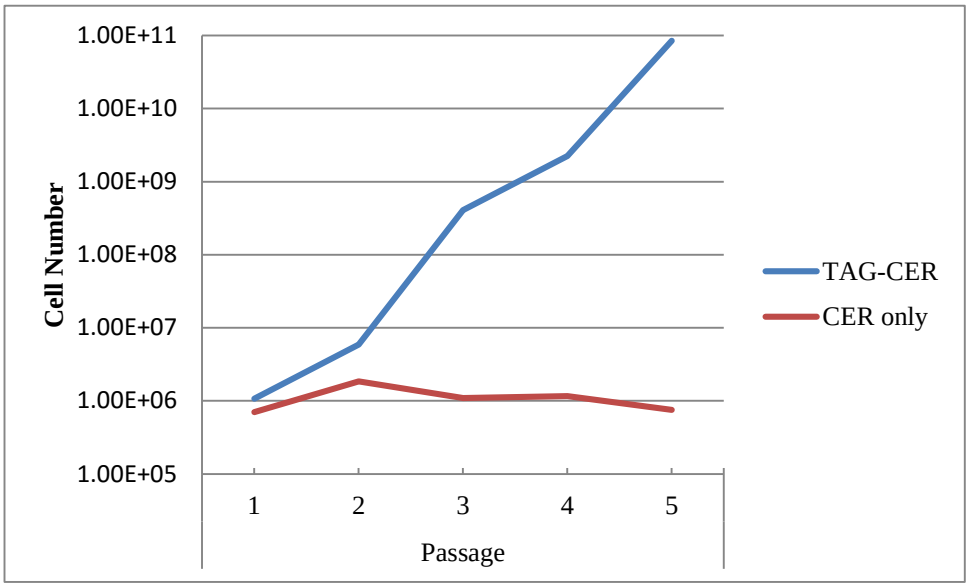

b)

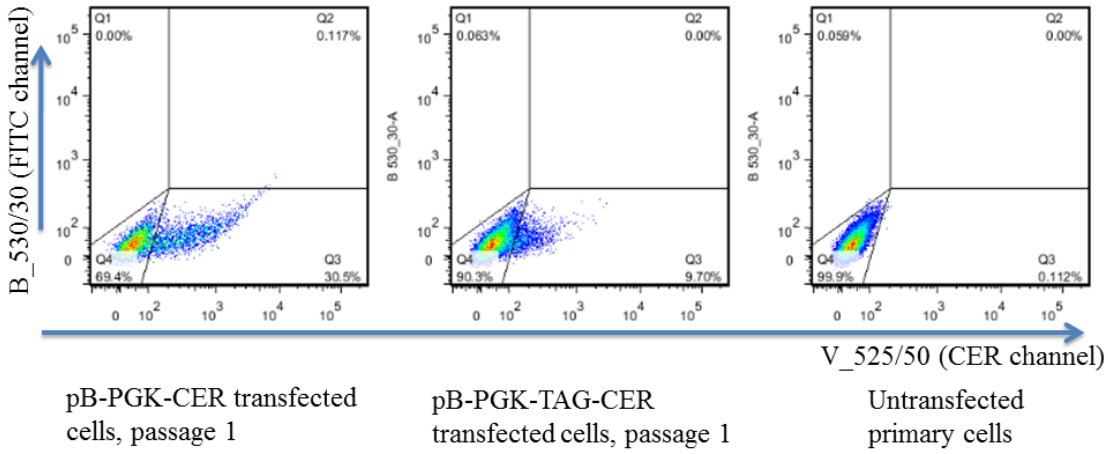

Figure 3.3-3. pB-PGK-TAG-CER vector transfected primary cells maintained exponential growth for five passages. a) pB-PGK-TAG-CER (TAG-CER) transfected cells maintained exponential growth while pB-PGK-CER (CER only) transfected primary cells ceased growth shortly after culture. b) Flow cytometry analysis of transfected primary cells 4 days after transfection. Note CER positivity rate was higher in pB-PGK-CER transfect cells compared to pB-PGK-TAG-CER transfected cells. This observation suggested observed growth difference was nod due to favourable transfection efficiency of pB-PGK-TAG-CER plasmid. (This experiment was conducted once, n=1)

4. Chapter 4: Derivation of cell lines from haematopoietic sites of mouse embryos

In this chapter, I described experiments aimed at deriving immortalized cell lines from diverse backgrounds. Such as primary cells bear different surface marker combinations of E11.5 AGM regions or primary cells from early embryos. To achieve this aim, experiments were conducted in the following ways:

- Optimizations of transfection protocol. That included finding an optimal parameter combination for E11.5 AGM derived primary cells and developed procedure to electroporate small amount of cells.
- Derived cell lines from sub-dissect AGM, included from dorsal wall of ventral aorta, where HSCs were thought to first emerge.
- Immortalized cells with different surface marker expression, including CD123, CD106, Flt3, membrane bound-SCF, VE-Cadherin.
- Derived cell lines from haematopoietic sites of a range of developmental stages (E8, E11.5)
- Established cell freezing and thawing protocol and monitored marker expression of derived lines

All in all, a method to derive cell line from small population was derived. 33 cell lines were derived from E11.5 AGM and 15 cell lines were derived from earlier embryos. Preliminary experiments showed that CD106 expression was maintained in lines tested while CD123 positive and negative cells tended to express CD123 at similar levels, caused expression level to be "blurred".

4.1. Optimization of transfection protocols

To derive cell lines from primary AGM cell, an effective transfection protocol was required. First, parameter of electroporating primary AGM cells was established. The Neon™ electroporation system used in this study was the second generation, it used capillary electroporation chamber. Such capillary chamber generated smoother electric field and required less cell number. Manual of Amaxa Nucleofector™ did not suggest sample contains less than $2X10^5$ cells. On the other hand, manual of Neon™ machine stated minimum cell number was as low as $1X10^4$ cells. However, preliminary experiments showed that some populations of interests in pooled

primary AGM samples had few thousands (10^3) cells, that translated to less than 100 target cells per AGM, thus transfection protocol was optimized to suite small cell numbers well below manufacture's recommendation. In optimization experiments, rare GFP positive cells were detected 24 hours post transfection in culture of 200 primary cells transfected with the pEGFP-N1 plasmid (figure 4.1-1). However, these rare GFP^+ cells disappeared when viewed a week post transfection. Such observation indicated that the Neon™ System could transfect as few as 200 cells, but those transfected cells failed to grow *in vitro*. More experiments were needed to enhance survival of transfected cell.

a) b)

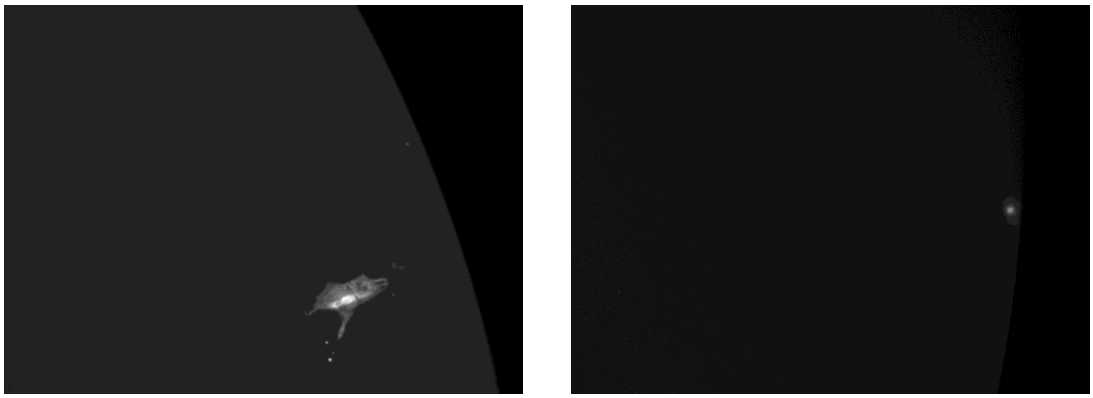

Figure 4.1-1. Single GFP^+ cells generated from 200 input cells electroporated with pEGFP-N1 plasmid with 1350V 20ms 1pulse, 24 hours after transfection. Both images were taken in GFP channel of IX51 inverted microscope a) GFP^+ cell transfected without centrifugation after transfection. b) GFP^+ cell transfected with centrifuged for 5 minutes at 1420rpm.

To find the optimal parameter combinations for transfecting embryonic primary cells, an approach based on linear programming (optimization) was adopted (Murty 1983). In all optimization experiment, primary cells were harvested from AGM region of BL6XBL6 embryo. Two initial survey experiments were conducted to explore cell survival rate of different parameter combinations, these combinations that generate viable cells collectively formed feasible combination set. This set of parameter combinations generally defined the scope of operation of electroporation system that could yield surviving cells, thus was also called "operational envelope"

in engineering. In these survey experiments, it was determined that pEGFP-N1 plasmid could be utilized to label transfected cells. Such labelling did not selectively expansion of transfected population, thus was better compared to pB-PGK-TAG-CER for optimization experiments.

Initial survey experiments discovered some rich “spots”, they were combinations of parameters that displayed favourable transfection efficiency or cell survival rate. In next phase of experiments parameter combinations near those favourable spots were examined. I hoped to find local optimal parameter combinations. Based on linear programming theory, optimal parameter combinations often appear at edge of operational envelope, hence favourable spots near edge of envelope were tested with special attention. All in all, this study covered electroporation conditions ranging from 0V (negative control) to 1700V, pulse width from 10ms to 40ms, pulse number from 0 to 3. Parameter combinations explored in this study is shown in figure 4.1-2.

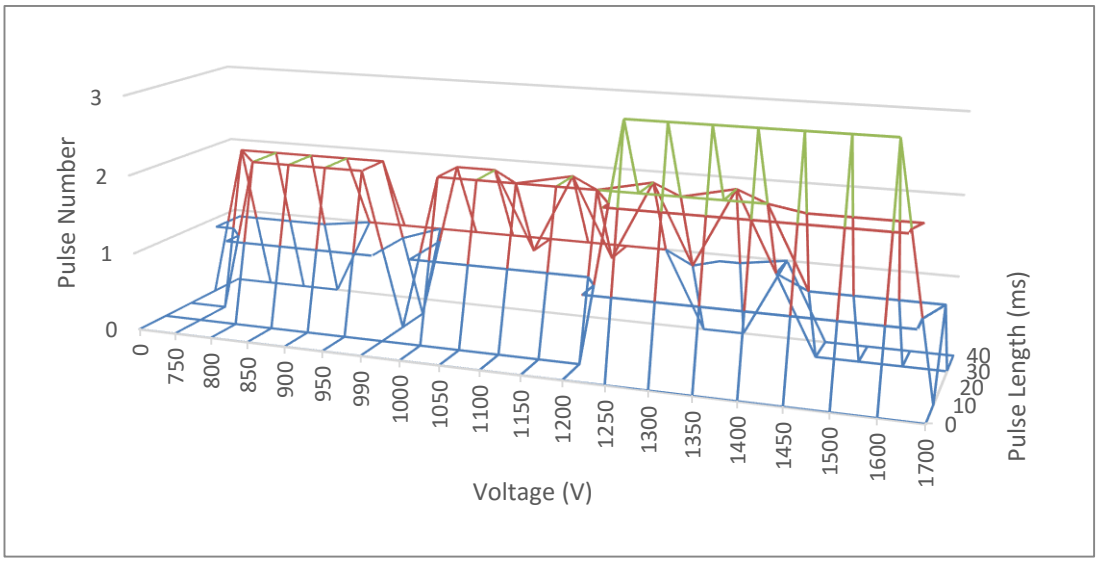

Figure 4.1-2. Electroporation conditions covered in this study. Each point on the polygon shown above represent a specific parameter combination for electroporation. Vertexes of the polygon were tested, some points on surface of polygon or inside polygon were also tested.

To improve accuracy of measurement, cell counting beads were used to measure number of survived cells. Protocol was adjusted to prevent sparks during electroporation that were damaging to primary cells. Input cell number was

increased to improve reproducibility of experiment. Mature blood cells were gated out in flow cytometry analysis with mix of lineage markers (CD45, Ter119, CD11b, Ly6G) while pro-HSCs were gated out with CD41 antibody. Remaining population of non-haematopoietic cells were analysed for transfection efficiency in either mesenchymal related population (CD105 and CD51) or endothelial related population (CD123 and VE-Cadherin). Such analysis was aimed at to discover any potential transfection bias toward specific cellular populations.

Data points of optimization were grouped based on length of electroporation (in millisecond) and number of pulses applied to primary cells. For each pulse length/pulse number pair, cell survival or transfection efficiency was plotted against voltage. It was observable that percentages of transfected cells were more consistent between replications while cell yields measured in absolute number were more variable (appendix figure 8.2.1-1 and 8.2.1-2). This kind of variation was considered to be introduced during electroporation.

Resulting graphs show several clear trends: firstly, as voltage increases, cell survival rate held steady until a certain drop-off voltage. After that voltage, cell survival (measured by percentage of $7AAD^-$ live cell) decreased linearly as voltage increases. Drop-off point for single 20ms pulse was near 1350V, for single 30ms pulse was near 1250V; for 20ms two pulses was near 1100V; for 30ms two pulses was near 900V. Drop-off voltage for 20ms 2 pulses was 200V lower compared to 20ms single pulse. Drop-off voltage for 30ms 2 pulses was 250V lower compared to 30ms single pulses. Thus wider and repeated pulses generally pushed the drop off voltage lower. On the other hand, as voltage increases, transfection efficiency tended to increase until a peak point. After that point, transfection efficiency dropped down, usually accompanied by a decrease in cell survival. Taking together cell survival and transfection efficiency, conditions with a single 20ms pulse generated high transfection efficiency while retained good cell survival.

Thus, conditions of 20ms single pulse group and adjacent conditions were analysed in more detail. No observable efficiency bias was observed (appendix figure 8.2.1-3). Based on aggregated data, conditions with 20ms 1 pulse appeared to be the best for the purposes of this project. In different voltage conditions, 1350V was the best. Comparison was also made of all conditions with 1350V voltage (figure 4.1-4). Although 1350V 30ms 1 pulse had slightly higher transfection efficiency, cell yield was lower compared to 1350V 20ms 1 pulse condition (figure 4.1-4, b).

Thus, 1350V 20ms single pulse was chosen as the electroporation condition for future experiments. For this conditions, overall cell survival and transfection efficiency were satisfactory (figure 4.1-3 and 4.1-4a and appendix figure 8.2.1-4). Moreover, E11.5 AGM primary cells bear all marker combinations tested could be effectively transfected using this condition (figure 4.1-4, c).

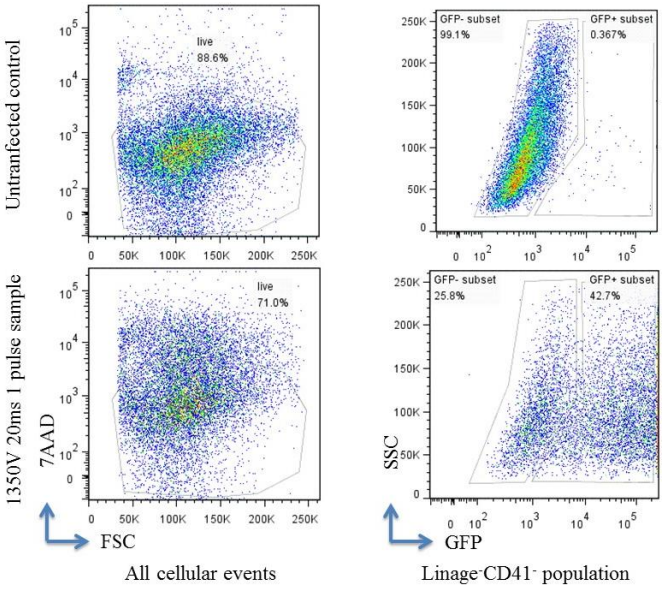

Figure 4.1-3. Flow cytometry plots showed 1350V 20ms 1 pulse condition (lower panel) retained enough survival cells (left) and a good portion of survived cells was GFP positive (right).

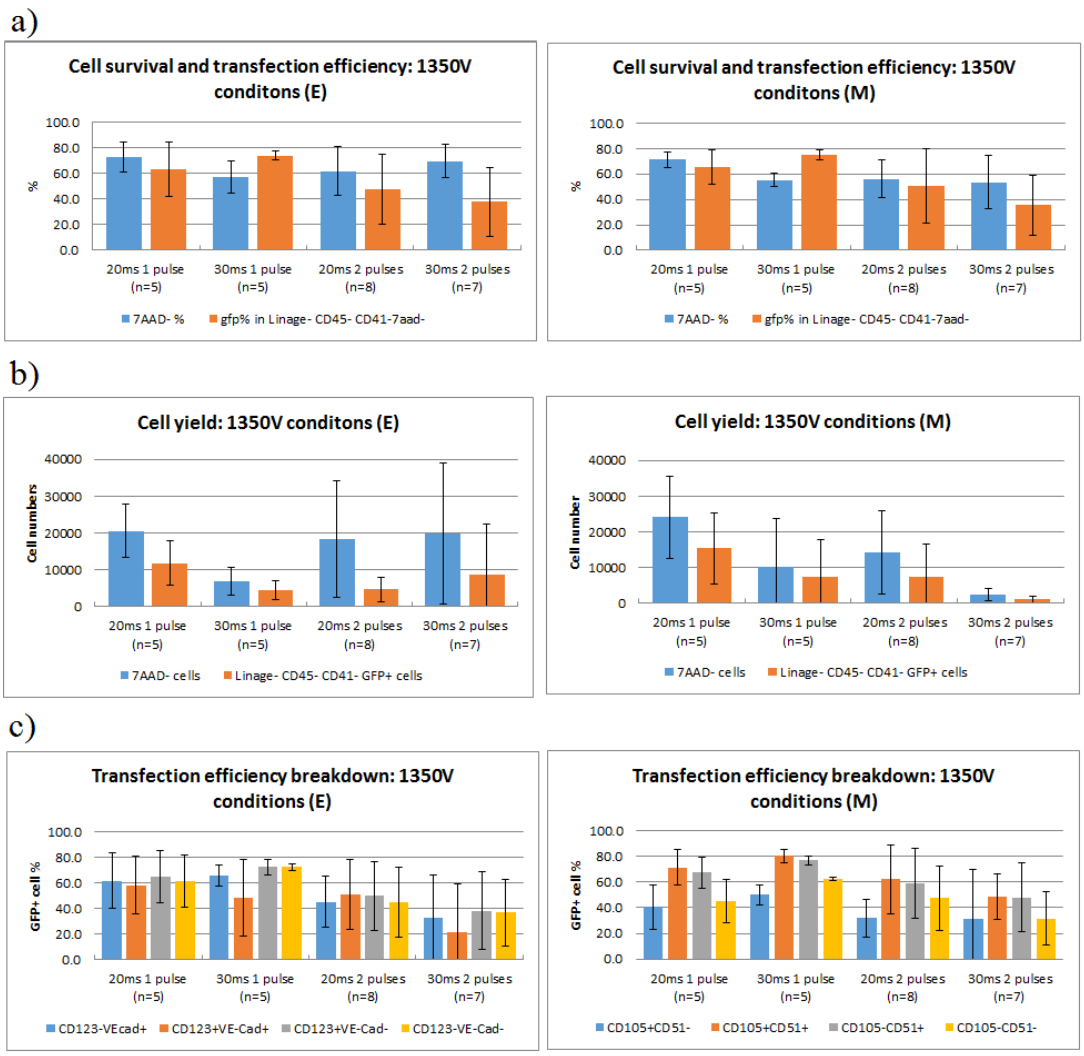

Figure 4.1-4. 1350V 20ms 1 pulse was the best condition examined. Performance of the optimal series of electroporation conditions with 1350V voltage. 20ms 1 pulse condition gave best cells yield in the series and good transfection efficiency. a) Cell survival and transfection efficiency of different conditions. Percentage of viable cell was calculated by dividing number of 7AAD$^-$ cell by number of all cellular events. b) Over all cell yield of different conditions. c) Breakdown of transfection efficiency in different subpopulations. Error bars indicated standard derivation, calculated using STDEV.S formula in Microsoft™ Office 2010.

4.2.Cell lines established from E11.5 embryos

A total of 33 cell lines were generated from 6 experiments with primary E11.5 aortic cells. Each experiment focused on a different set of ancestral cell surface marker combinations. Experiment flow was illustrated in figure 4.2-1. In six experiments

carried out, one was done with primary cells harvested from whole aorta while other experiments were done with sub-dissected ventral half of aorta. Selection of surface marker was based on combination of unpublished data and educated guess. Surface marker used in this study include CD123. CD106, membrane bound SCF, VE-Cadherin, and Flt3. Their functions in HSC maturation were discussed in section 7.2

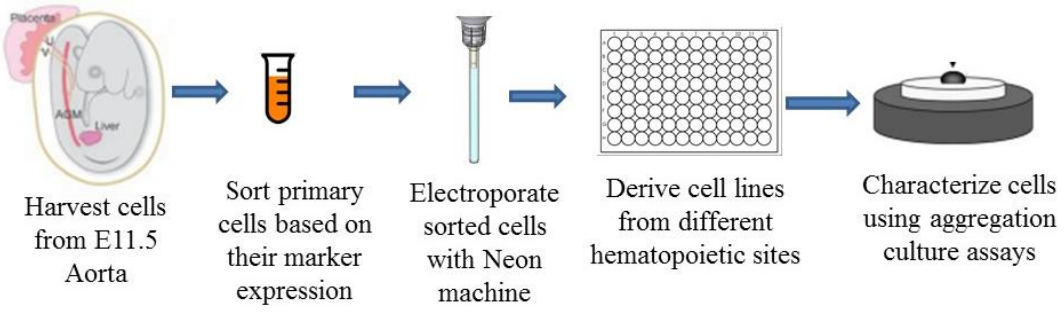

Figure 4.2-1. Experimental scheme to derive cell lines from E11.5 embryos. Either ventral aortas or whole aortas were dissected from E11.5 embryos. Dissociated cells were sorted using FACSAria II sorter. Each sorted populations was electroporated independently, and plated into different wells to establish cell lines. Established lines were tested using aggregation culture assays. Detail of cell line characterization was described in chapter 5 and 6. The picture of E11.5 embryo was reproduced with permission from Dzierzak and Speck (2008)

8 of cell lines derived were from bulk culture (each well contained one fourth of original population) and 25 of them were from low density cultures (each well received up to 50 cells, assumed cell survival rate of 10% and transfection successful rate of 90% (table 4.2-1).

Experiment No.	Cell source	Population 1			Population 2			Population 3			Population 4		
		Markers	Bulk line No	LD line No	Markers	Bulk line No	LD line No	Markers	Bulk line No	LD line No	Markers	Bulk line No	LD line No
Exp 1	Ventral arota	CD123-CD106-	1	2	CD123+CD106-	0	0	CD123+CD106-	1	1	CD123+CD106+	0	0
Exp 2	Ventral arota	CD123-CD106-	0	0	CD123+CD106-	0	0	CD123+CD106-	0	0	CD123+CD106+	0	1
Exp 3	Arota	CD123-mSCF-	0	7	CD123+mSCF-	0	1	CD123+mSCF-	0	0	CD123+mSCF+	0	0
Exp 4	Ventral arota	VE-Cad-mSCF-	1	1	VE-Cad-mSCF+	1	1	VE-Cad-mSCF+	0	1	VE-Cad+mSCF+	0	0
Exp 5	Ventral arota	Flt3-mSCF-	0	2	Flt3+mSCF-	0	2	Flt3+mSCF-	0	0	Flt3+mSCF+	0	0
Exp 6	Ventral arota	VE-Cad-Flt3-	1	3	VE-Cad-Flt3+	1	0	VE-Cad-Flt3+	2	3	VE-Cad+Flt3+	0	0

Table 4.2-1. Multiple cell lines were generated from experiments with E11.5 Aortic primary cells. In each experiment, four different populations are sorted and electroporated separately. Selection criteria of each population and number of cell lines derived from them were listed in the table. Meaning of "Bulk lines" and "Low Density" (LD) lines were described above. VE-Cad was short for VE-Cadherin and mSCF mean membrane-bound SCF.

During cell sorting, cellular events were selected based on FSC-A and SSC-A signals, then duplets were excluded based on FSC-A and FSC-H signals. Then cells positive for 7AAD, lineage, CD45 and CD41 were gated out using corresponding FMO (Fluorescence minus one) controls (appendix figure 8.2.2-1). Then gates to separate positive and negative cells were set using corresponding FMO controls (appendix figure 8.2.2-1). FACS plots for sorting samples from each experiment were shown in figure 4.2-2.

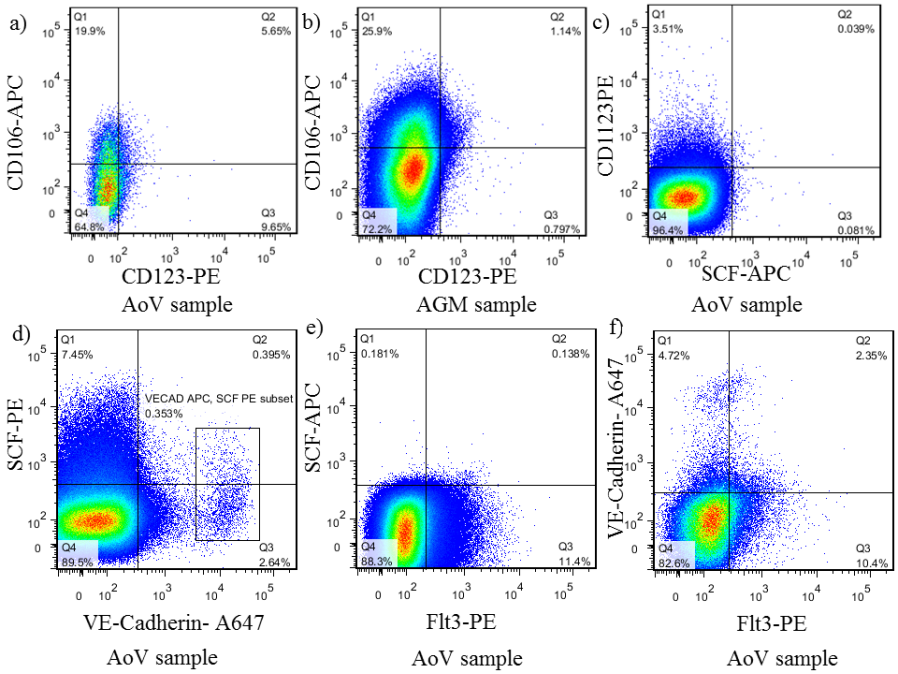

Figure 4.2-2 FACS plot of Lineage$^-$CD45$^-$CD41$^-$ population of AoV/AGM samples. Gating of different populations shown here was based on FMO controls (figure 9.7.2-2). In actual sorting experiments, some space was left between gates to enhance purity. (n=6 independent experiments performed)

It was observed that the expression level of CD123 was very low in this study (figure 4.2-2). This made separation of CD123$^+$ cells from CD123$^-$ background population difficult. A retrospective literature search showed that that murine embryonic AGM cells and cells from AGM explant contains CD123 positive cells (figure 4.2-3)(Robin, Ottersbach et al. 2006, Robin and Durand 2010), and a small population of rare CD123^{high} cells was detectable by flow cytometry. This was not observed in our study. I thought such difference could be explained by difference of

cell harvesting protocol. The Trypsin used in my study might be harmful for the CD123 molecule. Such explanation suggested that collagenase used by Robin *et al.* should be used to dissociate primary tissues in future studies to better distinguish $CD123^{high}$ cells.

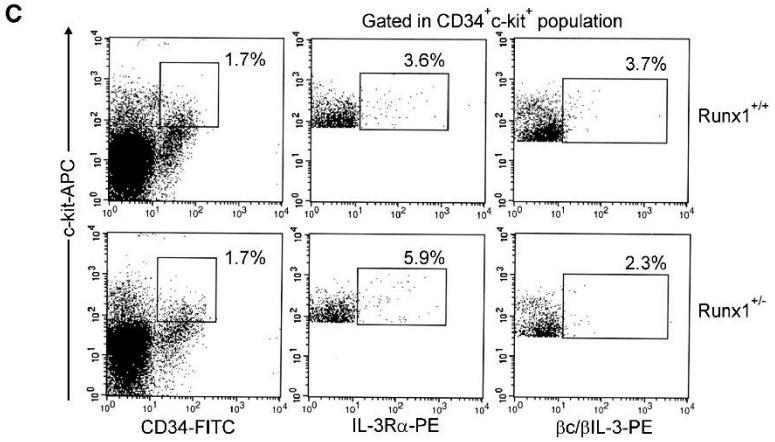

Figure 4.2-3. $CD123^{high}$ could be detected form 3 days explant culture of E11.5 AGM. The AGM explant was dissociated using Collagenase. Note the CD123 (Il3Ra) high population. Reproduced with permission from Robin, Ottersbach et al. (2006).

It was also noticed that membrane bound SCF (mSCF) expression was very weak, except in sorting experiments with SCF and VE-Cadherin. In that experiment, a population (about 8%) of SCF high cells were observed in $CD45^{-}CD41^{-}Lineage^{-}$ ventral aorta (AoV) cells. This was not due to unspecific binding of streptavidin-PE because the FMO control without biotin-SCF did not contain similar populations (appendix figure 8.2.2-3). Such above background signal of mSCF expression was not detected in another experiment with bio-SCF/strep-APC and Flt3-PE; although latterly more $CD45^{-}CD41^{-}Lineage^{-}$ AoV cells (670,782 cells) were detected compared to that observed in SCF/VE-Cadherin experiment (494,142 cells). The fact that membrane bound form of SCF was only detected once during experiments might be explained by trypsin used to make single cell suspension. Retrospective literature search indicates that SCF protein was susceptible to tryptic digestion (Lu, Clogston et al. 1991, Fan, Ding et al. 2012). It was very lucky that in one experiment involved mSCF, the trypsin did not fully

work and retained the SCF^{high} population. In further studies, the cell harvesting procedure to detect mSCF could be optimized. And/or the antibody used in Lodish's study could be used to better detect mSCF expression (Chou and Lodish 2010).

Above examples highlighted the challenge of sorting out rare cells. Constant experimentation of different cell harvesting procedures and different antibodies was needed. Standard Operating Procedures (SOP) were needed to make result of different experiments comparable. On the other hand, collecting more cell was another way to increase chance of deriving cell lines from rare primary cells. This was done in the second experiment with CD123 and CD106 staining (Experiment 2). It was aimed to generate cell lines from $CD123^+$ populations. With more embryos dissected and improved cell handling, one line (ID: P12-027 G7) was successfully generated from $CD123^+CD106^+$ primary cells. That line was tested in more detail in next chapter. This highlighted that deriving cell lines from small population could be a probabilistic event; repeat experiment multiple times might improve the chances of deriving additional cell lines from rare populations.

Next, bulk cultures from experiment 4 (marker tested: VE-Cadherin and Flt3) were sub-cloned at passage 1, each cell were seeded at 1-2 cells/well density. Out of four marker combinations tested, only population bearing marker $VE\text{-}Cadherin^+Flt3^+$ did not generate viable lines, suggested such culture contained multiple interdependent cell types. Thus it might be better to keep using bulk culture to keep the interdependent populations alive.

4.3.Cell lines established from earlier embryos (E8.5-E10.5)

Experiments were also conducted to derive cell lines from embryos of earlier developmental time points. Beside E10.5 embryos at different stage, E8.5 embryo was also used as source for cell line derivation. One aim was to explore whether E8 embryos harbored the ability to mature pro-HSC into definitive HSCs. Another aim was to test the immortalization system of primary cells on early embryos.

Cell lines from E8.5 pre-somatic stage embryo, and E10.5 30sp 32sp 34sp embryos were established. One embryos of each stage was used. AGM of E10.5 embryo of different stages were dissected separately using similar method as E11.5 embryos. The whole E8.5 embryo was dissociated. Harvested primary cells were electroporated directly without sorting. Subsequently, cells were cultured in the same way as cell lines generated from E11.5 embryos. In total, 15 cell lines were generated (table 4.3-1). 14 were from bulk culture and only one low density line was generated. This could be due to early primary cells being more fragile and having lower survival rate compared to E11.5 cells.

Embryonic day	Somatic stage	Bulk culture lines derived	Low density lines derived
E8.5	pre-somatic stage	1	0
E10.5	30sp	4	1
E10.5	32sp	3	0
E10.5	34sp	2	0
E10.5	36sp	4	0

Table 4.3-1. Number of cell lines generated from early developmental points. One embryo from each stage was used to generate cell lines.

During culture, pictures of AGM and earlier-embryo derived cell lines were taken. Those cell lines displayed distinct morphologies (see figure 4.3-1). No correlation between cell morphology and cell function was observed. And all cell lines were passaged 20 times without significant change of growth rate, suggested they did not experience crisis.

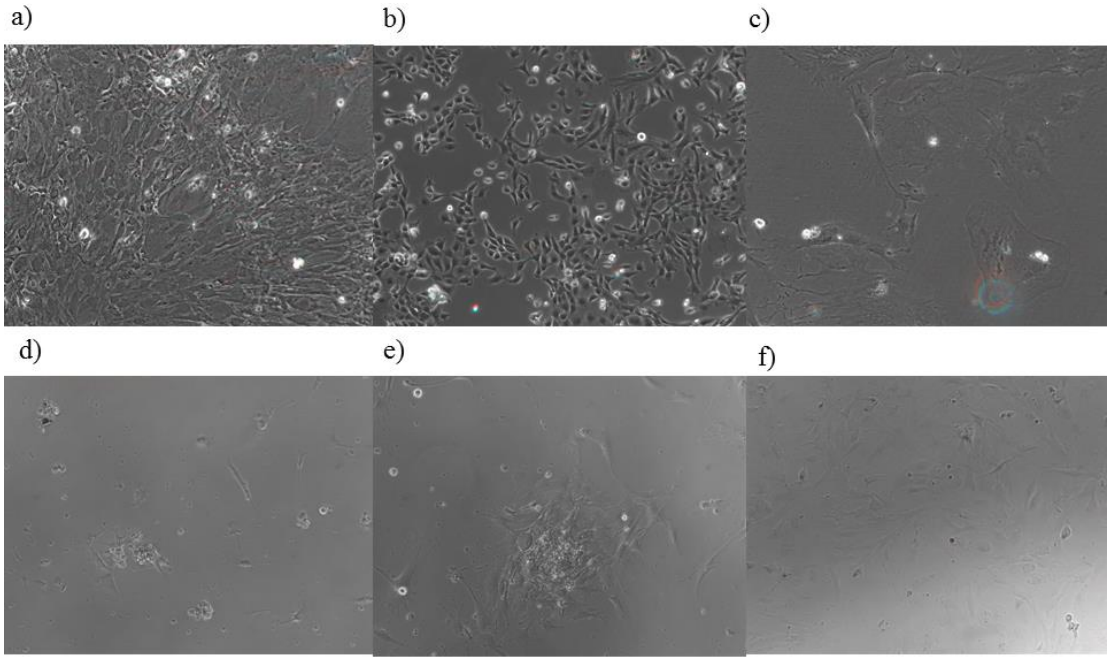

Figure 4.3-1. Cell morphologies of different AGM derived cell lines, images were taken with 10x objective in bright field. a) Cell line Q32, $CD123^{-}CD106^{+}$ low density (LD) culture, passage2. b) Cell line Q41, $CD123^{-}CD106^{-}$ LD culture, Passage 12. c) Cell line P12-004 B4, $CD123^{-}SCF^{-}$ LD culture, passage 2. d) Cell line P12-004 D5 $CD123^{+}SCF^{-}$ LD culture, passage 1. e) Cell line P12-006 A5, VE-$Cadherin^{-}SCF^{-}$ LD culture, passage 1. f) Cell line P12-006 F11, VE-$Cadherin^{+}SCF^{-}$ low density culture, passage 2.

To investigate whether cell lines maintained surface marker profile of their ancestral population, cell lines generated in a CD123/CD106 preliminary experiment were passaged for two months and stained using same antibody as initial sorting and analysed with flow cytometry (figure 4.3-2). Compared with their primary cell ancestors, CD106 expression was maintained, while CD123 experiment was somehow blurred. Part of culture derived from $CD123^{+}CD106^{+}$ population became $CD123^{-}$ and $CD123^{-}CD106^{+}$ primary cells had given progenies that were $CD123^{+}$. This suggested cell lines might adapt to culture conditions in plastics and change their surface marker expression. How such adaption affects cell line's ability to mature HSC specification was one interesting direction for further studies.

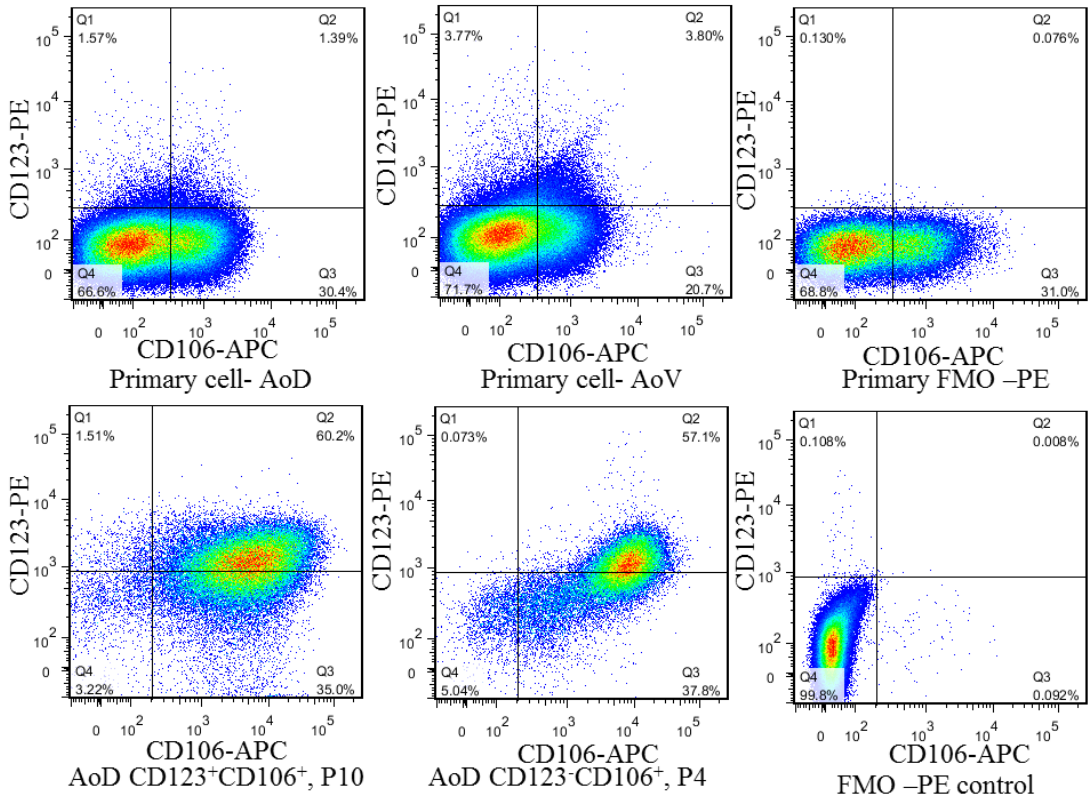

Figure 4.3-2. Comparison of marker expression level of primary cells during sorting and cell lines established thereafter. Plots showed here were 7AAD$^-$Lin$^-$CD45$^-$CD41$^-$VE-Cadherin$^-$ population gated using similar strategy shown in 9.7.2-1. Upper panel showed primary AoD (dorsal aorta) and AoV (ventral aorta) from E11.5 BL6 embryos. Gates for CD123 and CD106 were set against FMO controls. After electroporation, cell lines were derived from CD123$^+$CD106$^+$ and CD123$^-$CD106$^+$ bulk culture well of AoD samples. Two months after electroporation, two daughter lines were analysed using same staining and gating strategy (lower panel); CD123 gating was based on FMO-PE control.

5. Chapter 5: Characterization of cell lines derived from AGM or early embryos

Previous studies involved stromal cell lines mostly focused on testing derived lines' capacity to support the HSC or HPC (Xu, Tsuji et al. 1998, Oostendorp, Harvey et al. 2002). Most studies did not test derived cell lines in aggregation culture system. Such system was critical for maturation of pre-HSC or even pro-HSC (Rybtsov, Batsivari et al. 2014). To fill such obvious gap of knowledge, cell lines derived in this study were characterized using the robust aggregation system developed by Medvinsky, Taoudi et al. (2008). This rigorous assay tested one cell line's capacity to mature pro-HSCs into dHSCs. Cell lines derived from E8 embryo and E11.5 AGM region had been tested. Those lines from E11.5 AGM were derived from cells expressed CD123, CD106, Flt3 and VE-Cadherin. Derived cell lines were tested in the following ways:

- Cell lines were aggregated with E11.5 AGM cells for 4 days and were subjected to CFC-U assay. This assay estimated cell line's ability to induce Haematopoietic Progenitor Cells (HPCs).
- Selected cell lines were subjected to the more rigorous test of the E9.5 pro-HSC maturation assay. Such assay focused on the capacity of cell lines to mature pro-HSCs. In that assay, primary cells from the caudal part of E9.5 embryos were dissected and aggregated with cell lines subjected to test and cultured for 7 days. Resultant cultures were subjected to transplantation assay, CFU-C assay and flow cytometry analysis.
- At last, gene expression of supportive and non-supportive lines was compared by qPCR in order to elucidate the molecular signature of pro-HSC maturation niche. Details about qPCR were discussed in chapter 7.

Data described in this chapter showed that stromal line I derived could promote generation of various types of haematopoietic colonies. Some cell lines could promote the maturation of pro-HSC even without help of growth factors. This was superior comparted to OP9 cells. Donor derived cells could give rise to both myeloid and lymphoid cells six months past transplantation. Secondary engraftment from

aggregate culture was detected, suggesting stromal line promoted maturation of *bona fide* HSCs.

5.1. Cell lines were able to maintain and expand E11.5 AGM-derived haematopoietic progenitors

The cell lines derived in chapter 4 were tested for their ability to induce haematopoietic progenitor cells (HPC) from primary E11.5 AGM cells. HPCs presented in end of E11.5 4 day culture comes from three different sources: 1. progenitors presented in E11.5 AGM and maintained/expanded during culture. 2. Progenitors differentiated from HSCs presented in E11.5 AGM. 3. Progenitors differentiated from *de novo* matured HSC from pre-HSCs in E11.5 AGM. Previous data generated in our lab indicated that the OP9 cell line derived from mouse bone marrow (Nakano, Kodama et al. 1994) could potently maintain and expand those haematopoietic progenitors during 4 days of culture in this aggregation system (Taoudi, Gonneau et al. 2008) (Dr Stanislav Rybtsov, personal communication). By comparing cell lines derived in this study and OP9 in similar settings, the capacity of supporting HPC by these newly derived cell lines could be evaluate. Special attention was paid to cell lines that were either highly effective in expanding haematopoietic progenitors, or could not support haematopoietic progenitors at all.

A total of 8 CFU-C experiments were carried out to test 14 newly derived cell lines. Each cell line was tested in up to three biological replicates in different experiments. Experiments were carried out in 4 batches, each batch contained two experiments. They were conducted “back to back”, shared feeder cells and reagents.

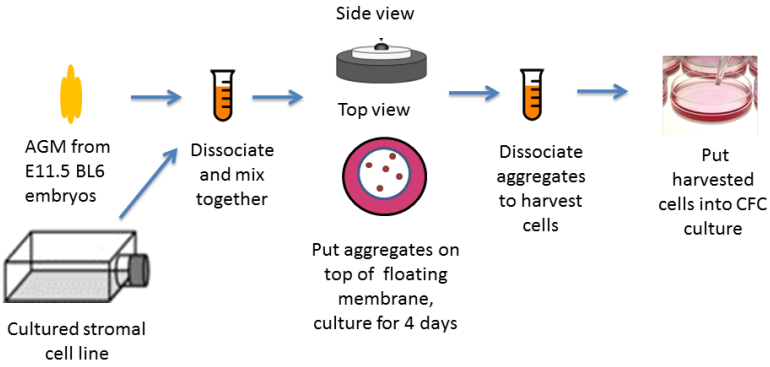

Figure 5.1-1. Procedure of E11.5 4 day culture assay. AGM of E11.5 embryos were dissociated and mixed with stromal cells. Next they were aggregated and deployed onto membranes. Each membrane had 3-5 aggregates. In each experiment, each stromal line had three membranes, one floated on medium with external growth factor supplement, one floated on medium without growth factor added, the third membrane floated on medium with growth factor but the membrane held blank aggregate with stromal cells only.

Cultures contained primary E11.5 AGM cells aggregated with OP9 were included as positive control in each experiment. An analysis of experimental consistency showed that readings from OP9 controls was quite consistent between experiments of the same batch (appendix figure 8.3-1). But some differences between batches were observed. This might be caused by the switching of animal unit during experiments. Mouse from different providers might behave differently between experiments.

Stromal cells aggregated with themselves only were named as blank culture. They were the negative controls in this study. They were used to estimate rate of spontaneously haematopoietic colonies generation. In this study, rate of spontaneously generation of haematopoietic colonies was extremely low, less than 1 per 100 cultures. Blank cultures were also observed to learn the size of shape of stromal cell clusters that grown in methylcellulose culture. That information was used to distinguish between outgrowth of stromal cells and real haematopoietic colonies.

CFU-C reading from replicates of aggregates with cell lines derived in this study displayed considerable variation similar to OP9 controls (figure 5.1-2). However,

CFU-C assay proved these cell lines could support generation of multiple types of haematopoietic colonies, included granulocyte colonies, macrophage colonies, erythrocyte colonies, mast cells, granulocyte-macrophage colonies, GEMM mixed colonies, megakaryocyte colonies. Representative pictures were shown in figure 5.1-3. Generally, more colonies were generated when growth factor is added to culture medium.

Moreover, cell lines derived in this study generated CFU-C readings in a wide range, from only very few colonies (line P12-009 E10 and P12-009 F10) to had comparable number of colonies with OP9 positive controls (line P12-015 B4). Surprisingly, later experiments showed that both CFU-non-supportive line P12-009 E10 and CFU rich line P12-015 B4 could mature E9.5 pro-HSC, suggesting CFU assay with 4 day aggregation assay of E11.5 primary AGM cells might not serve as a good indicator for pro-HSC maturation capacity.

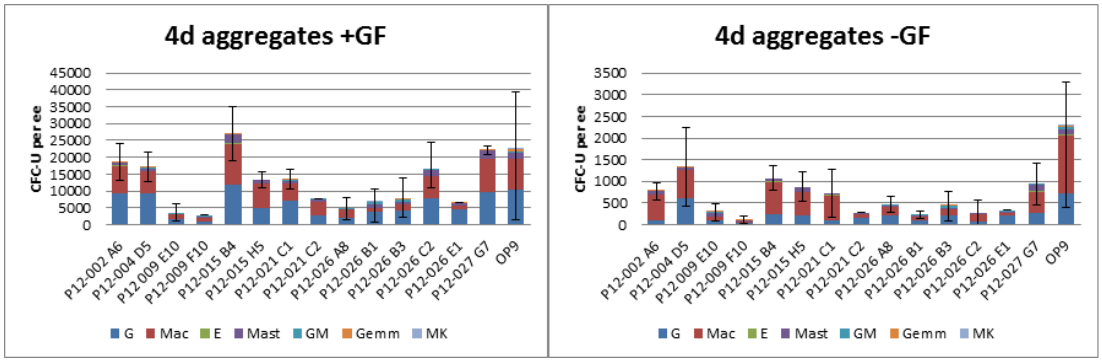

Figure 5.1-2. CFU-C colonies generated for 14 cell lines in 4 day aggregation assays. Each cell line was labelled by its name. CFU-C readouts already converted into CFU-C per embryo equivalent. Cell line P12-021 C2 and P12-026 E1 had infections and only have one viable readout, other samples had at 2-3 biological replicates. Error bars showed range of reading.

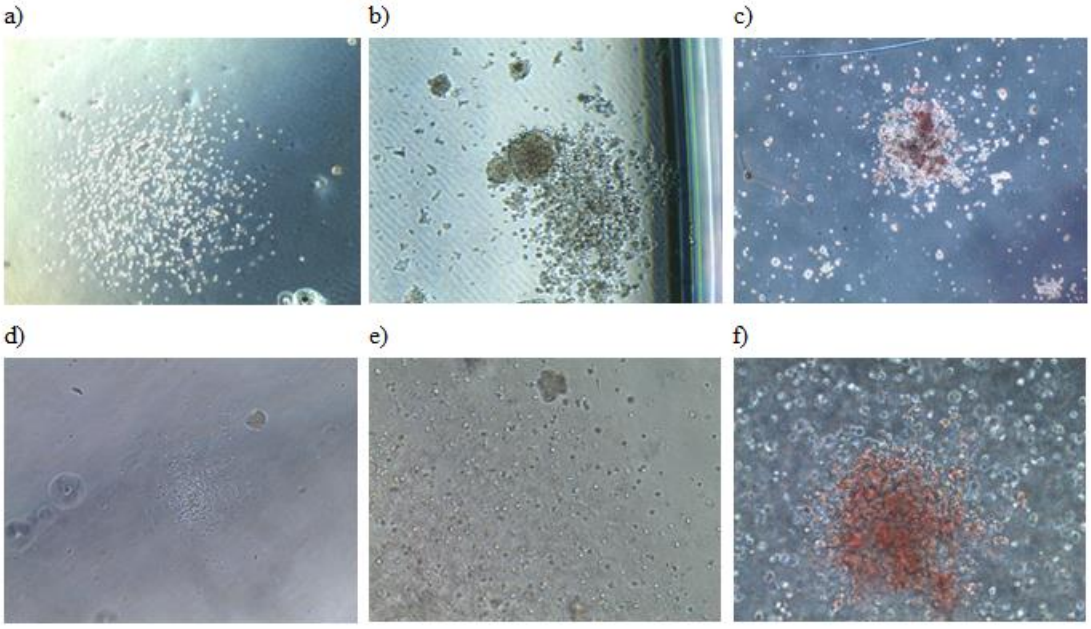

Figure 5.1-3. Haematopoietic colonies generated in CFU-C assays. a) Granulocyte colony generated by aggregating primary cells with line P12-026 E1 with growth factors. b) Macrophage colony generated by aggregating primary cells with line P12-026 A8 with growth factors. c) Erythrocyte colony (BFU-E) generated by aggregating primary cells with line P12-026 C2 cells with growth factors. d) Mast colony generated by aggregating primary cells with line P12-026 E1 with growth factors. e) GM colony generated by aggregating primary cells with line P12-026 E1 with growth factors. f) GEMM colony generated by aggregating primary cells with line P12-026 E1 with growth factors.

5.2. Cell lines were able to support maturation of pro-HSC from E9.5 embryos

Previously Dr Stanislav Rybtsov modified our E11.5 AGM region aggregation system so that OP9 cells could mature E9.5 haematopoietic precursors (pro-HSCs) into transplantable definitive HSCs (dHSCs) with the help of growth factors SCF, IL3 and Flt3l (Rybtsov, Batsivari et al. 2014). In that system no transplantable HSC could be generated without help of these growth factors. Therefore it was of interest to test cell lines derived in this study in a similar setting. Could they promote development of dHSCs from pro-HSC cells, both in the presence or absence of growth factors? (The lines tested in this study were listed in table 5.2-1).

Source	Marker/stage	Cell line name	Cell line type	Engrafted/total	Average donor contribution of engrafted mice
E11.5 AoV	VE-Cad-Flt3+	P12-026 C2	BK	3/11	45.83%
E11.5 AoV	CD123-CD106-	P12-002 A6	LD	6/21	45.53%
E11.5 AoV	Flt3+SCF-	P12-009 E10	LD	5/16	44.46%
E10.5 AGM	30sp stage	P12-021 C1	BK	2/12	42.85%
E8	Persomitic stage	P12-015 B4	BK	3/10	19.60%
E11.5 AoV	VE-Cad+Flt3-	P12-026 E3	LD	1/5	11.80%
E11.5 AoV	CD123+CD106+	P12-027 G7	LD	2/11	11.25%
P12-026 E1 Bulk	VE-Cad+Flt3-	P12-034 H12	Clonal	0/4	N/A
E11.5 Arota	CD123+SCF-	P12-004 D5	LD	0/5	N/A
E10.5 AGM	36sp stage	P12-015 H5	BK	0/5	N/A
E10.5 AGM	30sp stage	P12-021 C2	BK	0/8	N/A
OP9 postivc control				6/24	32.12%

Table 5.2-1. List of 11 cell lines tested in E9.5 HSC maturation assay. Every line listed was tested both with and without growth factors. In "source" column AoV stand for Ventral Aorta. "Marker/stage" denoted source of stromal cell used in aggregation. "Cell line name" column listed name of cell lines used. Cell line names were combination of plate and well number of original well the line was derived. For example, line P12-015 B4 come from plate P12-015, well B4. In "Cell line type" column, BK stand for Bulk culture, LD stand for low density culture. "Engrafted/total" column indicated number of mice engrafted (>5% donor contribution) and total number of mice survived for at least 6 weeks. Note cell line P12-034 H12 was derived by sub-clone line P12-026 E1 (bulk, source population: VE-Cad$^+$Flt3$^-$). (In total, 108 mice injected with aggregate contained experimental cell lines survived until 6 weeks. 22 of them were engrafted. 6 out of 24 of recipients received positive control aggregate were engrafted)

In the E9.5 pro-HSC maturation assay, caudal halves of E9.5 embryos (25-29 somite pairs, CD45.2 homozygous) were dissected and dissociated to single cells, which were aggregated with stromal cell lines or OP9 with the method used in section 5.1. Experimental flow was described in figure 5.2-1. In brief, each aggregate contained 1ee of E9.5 primary cells and 10^5 stromal cells. Two kinds of culture were set up, one with Flt3l, SCF and Il3 growth factors supplement ("+GF conditions") and one without growth factor supplement ("-GF conditions"). The next day, all cultures were carefully fed with fresh medium. Six days later, the cultures were harvested, making total culture time seven days. After harvest, the majority of cells were transplanted via tail vein. Each condition had three irradiated recipients (CD45.1 homozygous). Each irradiated recipient received harvest from about 1 aggregate

alongside with 10^5 carrier cells (CD45.1/CD45.2 heterozygous). Remaining cells were subjected to CFU-C assay and flow cytometry analysis like in section 5.1.

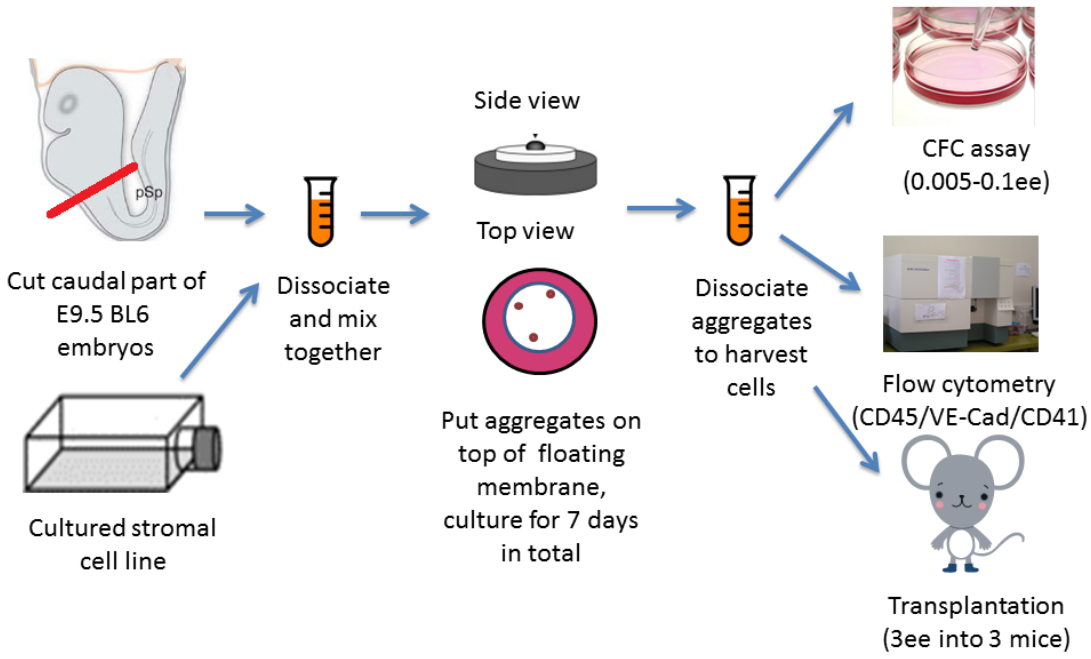

Figure 5.2-1. Procedure of E9.5 pro-HSC maturation assays. Caudal parts of E9.5 embryo were cut out between and forelimbs, they were dissociated and aggregated with stromal cells and cultured on floating membranes for 7 days. Then aggregates were harvested. Harvested cells were subjected to CFC-U, flow cytometry and transplantation assay. In one experiment, each cell line had two membranes, one with growth factor supplement and one without growth factor supplement.

Contribution of E9.5 cells to irradiated recipients was analyzed as shown in figure 5.2-2. In brief, all mice survived were analysed for donor chimerism of peripheral blood six weeks post transplantation. Donor, stromal, carrier and recipient derived cells were distinguished by their CD45 expression profile (figure 5.2-2). Recipients with more than 5% donor derived cells were considered as engrafted. Selected engrafted recipients were examined for multilineage engraftment in peripheral blood six months post transplantation. Next, one mouse form each transplantation experiment was selected and culled. Peripheral blood, bone marrow, spleen and thymus from these culled mice were dissected and dissociated. Processed samples were stained and analysed on flow cytometer. B cell, T cell and myeloid were distinguished by their respective markers.

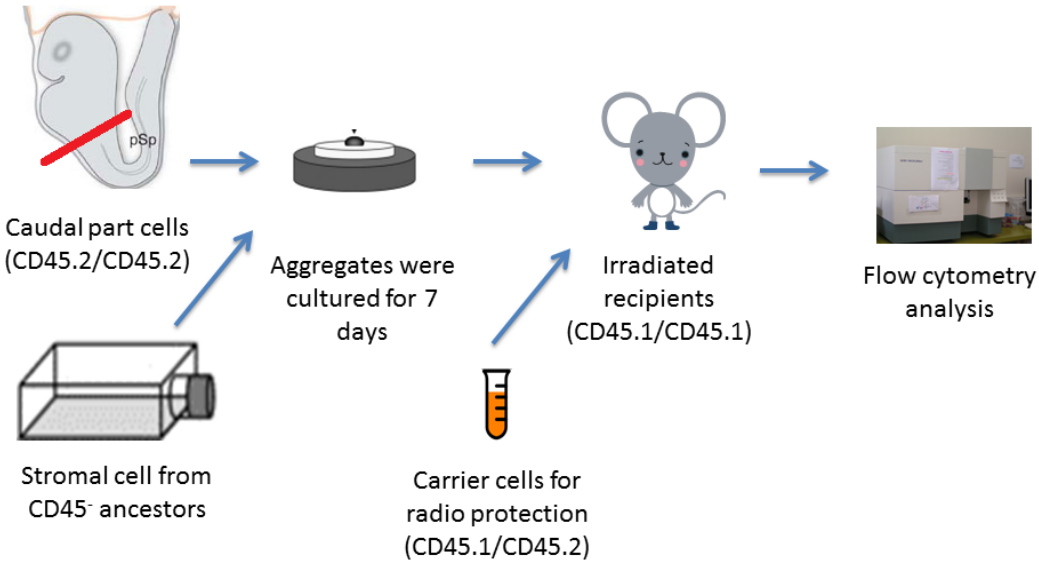

Figure 5.2-2. Experimental flow to characterize donor engraftment in recipient mice. Source of cells were distinguished by their CD45 surface marker subtype during flow cytometry analysis. Donor cells were CD45.2 homozygous. Stromal cells were derived from sorted CD45$^-$ ancestral population. Recipients were CD45.1 homozygous. Carrier cells used to radio protect recipients were harvested from bone marrow of CD45.1/CD45.2 heterozygous mice.

Experiments were performed in batches of two using the same material. Experiment with more than one mice engrafted was considered as successfully transplanted. However, it was found that the first experiment performed in a batch usually was not successful. That was, all recipients in experiments 1, 3, 5, 8 did not contain donor derived cells; even OP9 positive controls failed to engraft. On the other hand experiments 2,4,7,9 were successful, indicated by multiple engrafted mice. Only batch 4 was an exception, as mice from both experiments 6 and 7 were successful.

It was a very puzzling observation considering the fact that both experiments in one batch were conducted using same feeder cells and shared same reagent. Moreover, CFU-C assay and flow cytometry analysis at the end of aggregation culture did not show significant differences between pair of experiments in the same batch (appendix figure 8.3-2). Additionally, in experiment 6 and 7, feeder cells that were in over-confluent and culture that just reached confluence were compared. No difference was observed between experiments that generated engraftment and

experiments that did not. A detailed examination of experimental procedures revealed the length of time spend during super confluence was critical to successful engraftment of donor derived cells. In experiment 1, 3, 5 and 8 cultures stated in over confluent condition for 2-3 days. On the other hand, most culture in experiment 2,4,6,7 and 9 did not reach or just reached over confluent condition. The over confluent culture in experiment 6 and 7 stayed in confluence less than 1 day long. It seemed that cultures stayed in over-confluent condition for more than 1 days lost their ability to mature pro-HSCs. Further research was needed to determine the mechanism behind it.

Out of 11 cell lines tested, 7 were able to support maturation of E9.5 pro-HSCs to HSC (figure 5.2-3). The percentage of donor engraftment generated differed between experiments. The forth experiment, named as SRYZH4, was the best performing. Transplantation results were shown with experiment numbers in figure 5.2-3 a) and b), aggregated transplantation results were shown in figure 5.2-3 c). The average engraftment for all recipients (excluding positive and negative controls) in "–GF" conditions was 8.04% while average engraftment for all recipients excluding controls in "+GF" condition was 11.34%. Even in experiments that were successful, some lines that performed good in previous experiments failed to engraft completely. Such observation highly suggest the probabilistic nature of E9.5 pro-HSC maturation aggregation system. Average donor contribution of engrafted mice of each line was listed in table 5.2-1.

Representative flow cytometry plots of engrafted mice were shown in figure 5.2-4 with single stain controls. In each sample, contribution of donor, recipient and carrier cell in recipient peripheral blood was varied (appendix figure 8.3-3). Results showed that engraftment from cultures with growth factors supplement yielded more engraftment compared to cultures without growth factors. OP9 cells were found to be the most stable cell line supporting generation of engraftable HSC. I found that 5 cell lines supported generation of engraftable HSCs when aggregated with E9.5

pro-HSCs in the absence of growth factors ("-GF" conditions). In particular, embryonic cells aggregated with lines P12-002 A6, P12-009 E10 and P12-021 C1 generated more than 20% donor engraftment in "–GF" conditions (appendix figure 8.3-3). This was better than E9.5 caudal part/OP9 aggregates which did not give engraftment when cultured with growth factors. As seen in table 5.2-1, cell lines that were able to mature E9.5 pro-HSCs came from diverse background. They also came from different embryonic stages, including E8, E10.5 and E11.5 embryos. E11.5 cell lines derived from various surface marker combinations were able to mature precursors of HSCs, including $CD123^{-}CD106^{-}$, $CD123^{+}CD106^{+}$, $Flt3^{+}SCF^{-}$, $VE\text{-}Cad^{+}Flt3^{-}$ and $VE\text{-}Cad^{-}Flt3^{+}$. These observations suggested that niche cells which could mature E9.5 pro-HSCs into definitive HSCs might existed at multiple developmental time points and expressed different surface markers.

a)

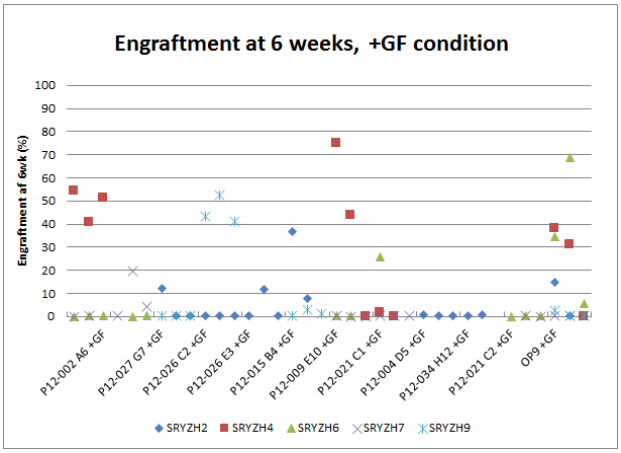

b)

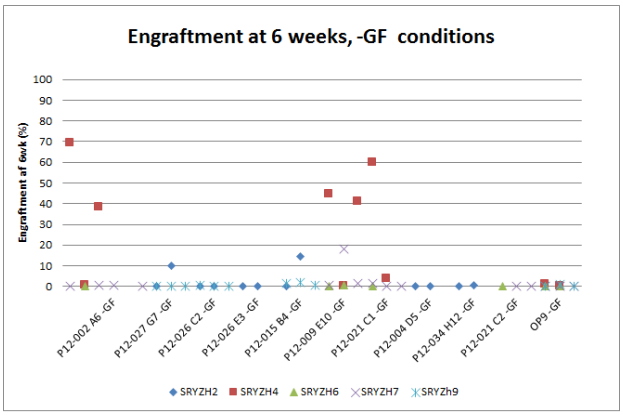

c)

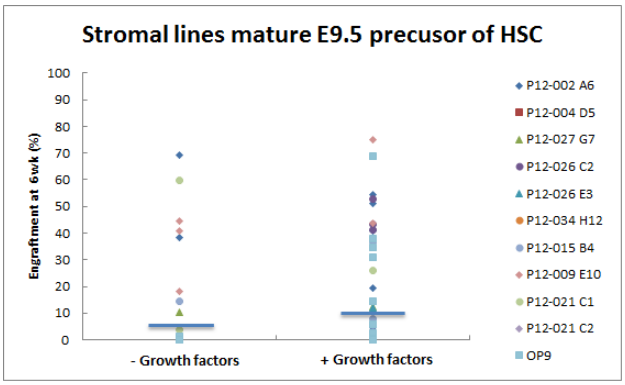

Figure 5.2-3. Peripheral blood of transplanted recipients contained donor derived cells, six weeks after transplantation. Eleven cell lines were tested alongside with OP9 positive control. Seven of these lines promoted donor engraftment, four did not. a) Performance of cell lines with growth factors, each experiment was labelled with their names. Each dot represented one mouse. b) Performance of cell lines without growth factors. The labels were in the same layout as panel a. c) Combined results of all experiment, grouped by cell line name. 22 mice were engrafted out of 108 transplanted in five experiments.

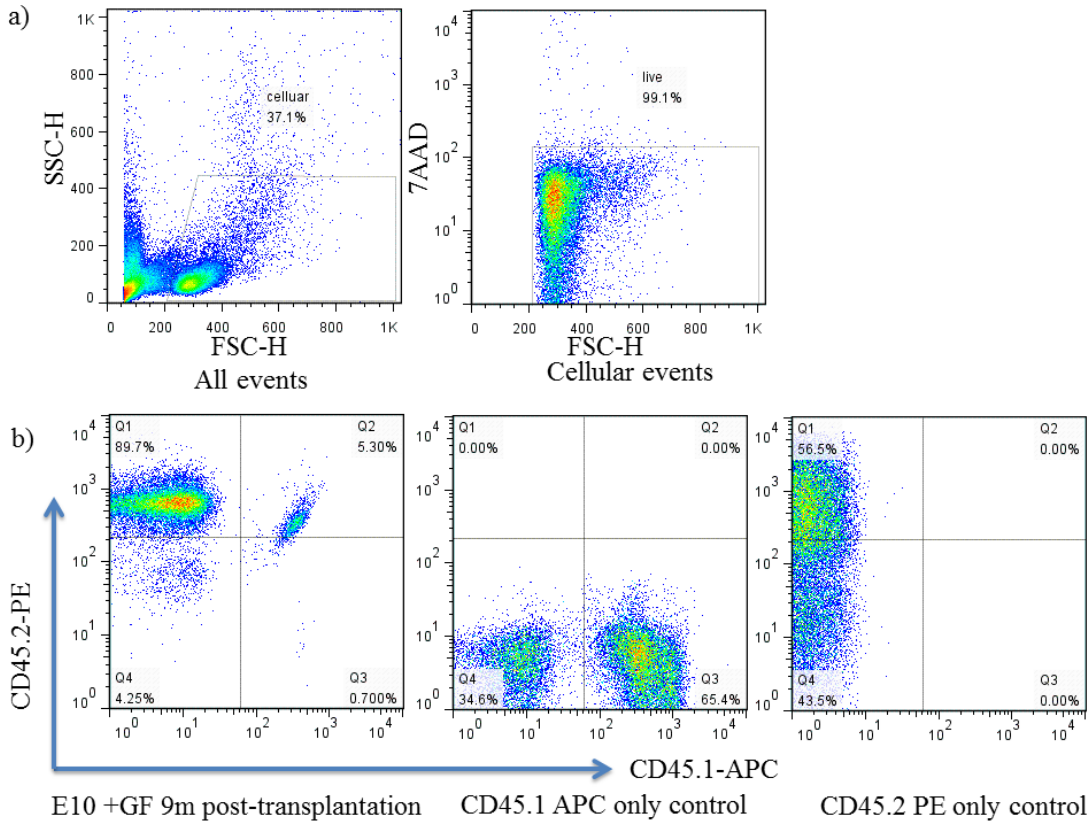

Figure 5.2-4. Peripheral blood sample of engrafted recipients contained CD45.2 homozygous cells of donor origin. This sample was taken 9 months post transplantation. a) Gating strategy to select blood cells (left) and to gate out dead cells (right). b) Left, flow plot of peripheral blood of engrafted recipient. This mouse was injected with E9.5 primary cells aggregated with cell line P12-009 E10, +GF condition. Centre, CD45.1-APC single stain control sample. Right, CD45.2-PE single stain control sample. To view all 108 flow plots for 5 different experiments, please see appendix figure 8.3-3.

To characterize donor engraftment obtained, selected engrafted recipients were further analysed. According to lab protocol, peripheral blood samples were taken from recipient mice again 6 months after transplantation. Compared engraftment rates at 6 weeks and 6 months, engraftments in some recipients did increase (Figure 5.2-5). Experiment SRYZH4 contained most mice where engraftment increased over time.

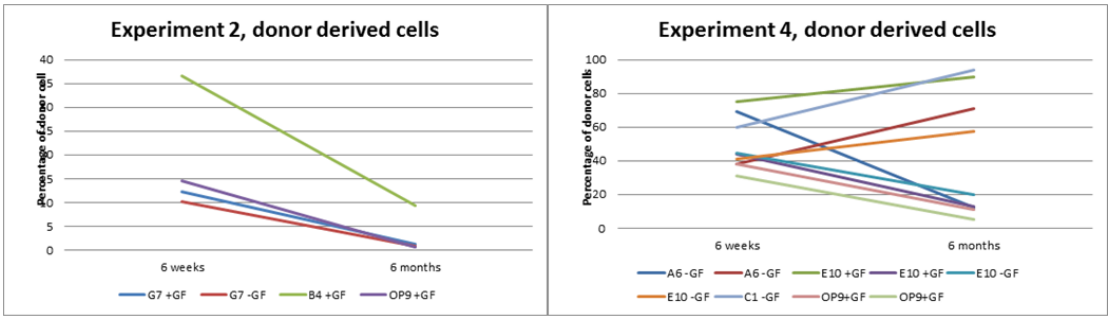

Figure 5.2-5. Percentage of CD45.2 donor chimerism changed after transplantation. Donor cell percentages were measured as percentage of CD45.2 homozygous cells in all 7AAD$^-$ cellular events.

After confirming that donor derived cells was retained after 6 months, blood samples of these mice were analysed for multilineage engraftment. The gating strategy and flow cytometry plot for FMO controls were shown in appendix figure 8.3-4. After excluded recipient and carrier cells, donor derived cells were analysed for B220 and CD3e expression to detect B cell and T cells respectively. Myeloid cells were characterized by Mac-1 (macrophage) and Gr-1 (granulocyte) expression. It was noticed that some cell lines supported generation of HSCs that could achieve multilineage repopulation (B cell, T cell and myeloid cells) while other cell lines tested did not (figure 5.2-6). No correlation between ancestral markers or development stage and multi-lineage engraftment was observed. The cellular identity of donor derived haematopoietic-maker-negative engraftment of P12-021 C1-GF aggregated culture showed in figure 5.2-6 had not yet been determined. Further experiments were needed to establish their identity. More efforts were needed to investigate those donor derived cells without B cell, T cell and myeloid markers.

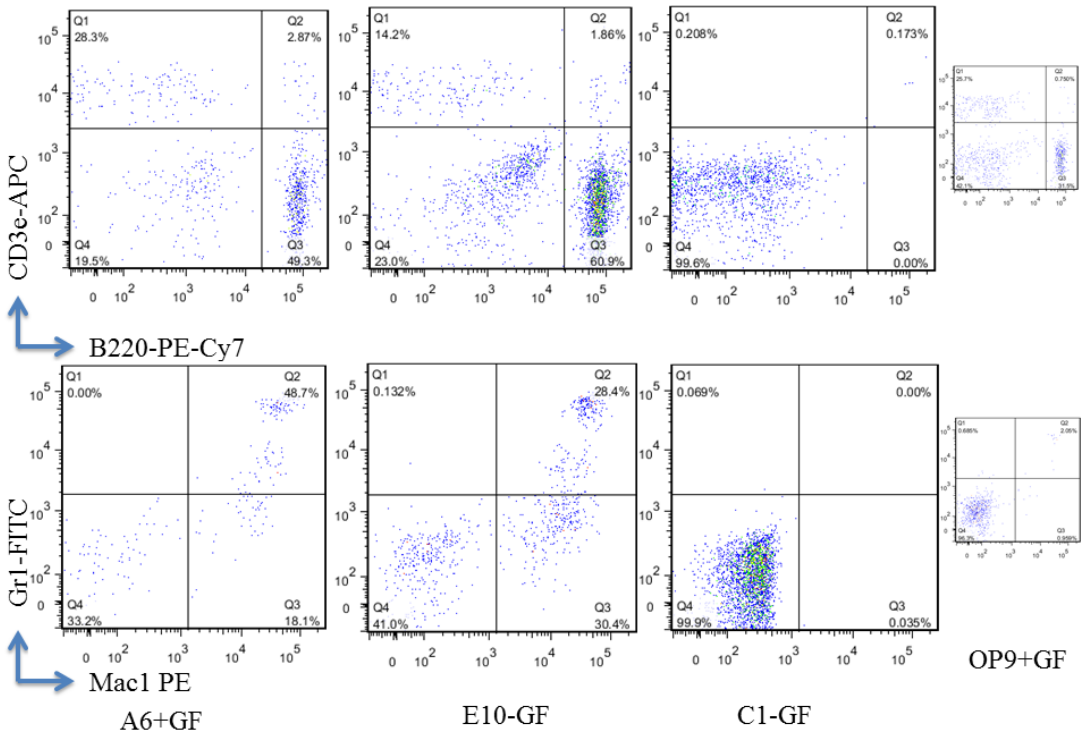

Figure 5.2-6. Multilineage flow cytometry analysis of selected mice after 6 months. "A6 +GF" plots were from aggregates contained the P12-002 A6 low density line (passage 30) with growth factors supplement. Engraftment at 6 weeks was 54.3% and at 6 months was 38.1%. "E10 –GF" plots were from aggregates contained the P12-009 E10 low density line (passage 32) without growth factors supplement. Engraftment at 6 weeks was 40.8% and at 6 months was 33.5%. "C1 -GF" plots were from aggregates contained the P12-021 C1 bulk line (passage 23) without growth factors supplement. Engraftment at 6 weeks was 59.8% and at 6 months was 59.3%. "OP9 +GF" plots were from aggregates contained OP9 positive control cell (passage 30) with growth factors supplement. Engraftment at 6 weeks was 38% and at 6 months was 19.6%. All mice were from experiment SRYZH4. Gating strategy and FMO controls were listed in appendix figure 8.3-4. All plots for multilineage engraftment were included in supplementary files. In total, 24 mice were analysed.

Finally, four mice were culled to check multilineage engraftment in blood, bone marrow, spleen and thymus. One mouse was selected from each of those four experiments that yielded engraftment (table 5.2-2). The mouse from experiment 2 (mouse ID: SRYZH 216) was negative control. That mouse was engrafted at 6 weeks post transplantation but engraftment dropped below 5% 6 months after transplantation. The other three mice had engraftments either very high (70.7%),

high (52.4%) or modest (24.3%) 6 months after transplantation. Gating strategy and FMO controls were shown in appendix figure 8.3-5. Profiles of donor derived cells differed between different recipients and organs. The mouse that received primary cells aggregated with cell line P12-002 A6 was the best performing with both lymphoid and myeloid donor contribution detected in multiple tissues (figure 5.2-7, brown bar, appendix figure 8.3-6). Significant numbers of $CD4^+CD8^+$ and CD4 single positive cells were present in thymus, although number of CD4 single positive cells was low. The mouse received 026-C6 aggregate also contained both lymphoid and myeloid donor contribution in multiple tissues. However, less cells were detected compared to A6 recipient, this observation was in line with the fact that C2 engraftment level at 6 months was 46.4% lower compared to A6 recipient. The mouse received P12-021 C1 aggregate performed worst; this recipient had very few donor derived cells in bone marrow, spleen and thymus. There was significant donor contribution in blood, but the majority of $CD45.1^-$ donor derived cells did not have B cell, T cell, macrophages and granulocytes markers. The identity of these blood circulating non-haematopoietic cells required further study. Moreover, mechanism behind such cell line specific contribution observed in this experiment was worth further investigation.

Aggregated cell line	Marker	Type	Passage	Growth factors	Engraftment at 6 weeks	Engraftment at 6 months
P12-027 G7	CD123+CD106+	LD	9	with	12.30%	1.30%
P12-002 A6	CD123-CD106-	LD	30	without	38.30%	70.70%
P12-021 C1	E10.5 30sp	Bulk	44	with	25.90%	52.40%
P12-026 C2	Flt3+VE-Cad-	Bulk	10	with	41.30%	24.30%

Table 5.2-2. List of mice tested for multilineage engraftment in multiple organs. Engraftments are measured by percentage of CD45.2 homo cells in all live cells of blood sample. P12-027 G7 mouse is used as a negative control.

Contributions of donor derived cells to B cell, T cell and myeloid cell lineages were shown in figure 5.2-7, with original flow cytometry plot shown in appendix figure 8.3-6. Above background (mouse 2 1 6 was negative control) contribution to most lineages was detected. Original flow cytometry plots were shown in appendix figure 8.3-6. Donor contribution to specific lineages of specific recipient was positively

correlated with overall contribution of that recipient, as shown in table 5.2-2 and figure 5.2-7. No obvious bias of contribution toward certain lineages was detected.

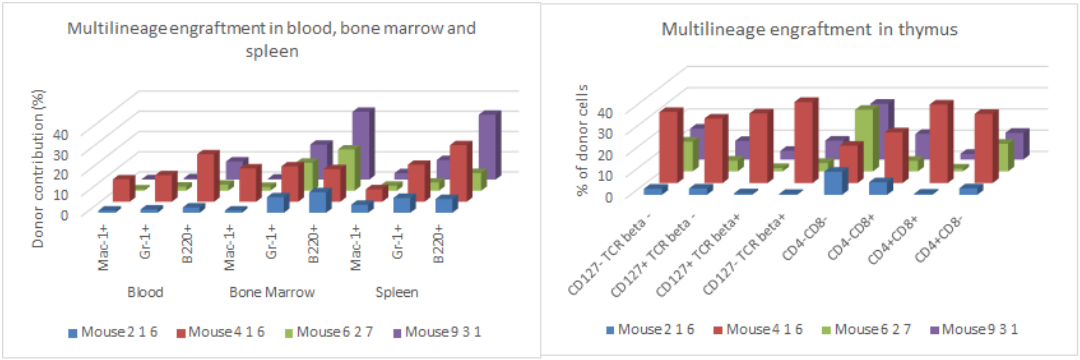

Figure 5.2-7. Donor derived cells contributed to B, T and myeloid cell lineages. Such multilineage contribution was detectable in multiple organs. Donor contribution was measured as percentage of CD45.1$^-$Ter119$^-$ cells to total Ter119$^-$ live cells in that specific cell compartment. Sample were taken at least six months after transplantation. Mouse 2 1 6 received cells aggregated with line P12-027 G7, +GF condition, it was the negative control. Mouse 4 1 6 received aggregate of P12-002 A6, -GF condition. Mouse 6 2 7 received aggregate of P12-021 C1, +GF condition. Mouse 9 3 1 received aggregate P12-026 C2, +GF condition Gating strategy was shown in appendix 8.3-5. Original flow plots were included in supplementary files. (n=4)

Secondary transplantation experiments were carried out. A mouse which received E9.5 caudal parts aggregated with cell line P12-021 C1 with growth factors supplement was used. Its donor chimerism at 6 weeks was 25.9% and donor chimerism at 6 months was 52.4%. 7 weeks after secondary transplantation, two secondary recipients had 3.28% and 1.11% of donor derived cells in circulating blood (figure 5.2-8) respectively. Secondary engraftment data confirmed the fact that E9.5 primary caudal part cells could produce *bona fide* HSC after aggregation with newly derived cell lines. However, the majority of blood cells in the secondary recipient came from carrier cells in first transplantation (10^5 bone marrow cells per recipient), although in the primary recipient used for secondary transplantation, their contribution in peripheral blood were roughly the same. This observation also

suggested E9.5 that derived cells were being out competed by carrier cells. How to increase its competitiveness remained an interesting direction for further studies.

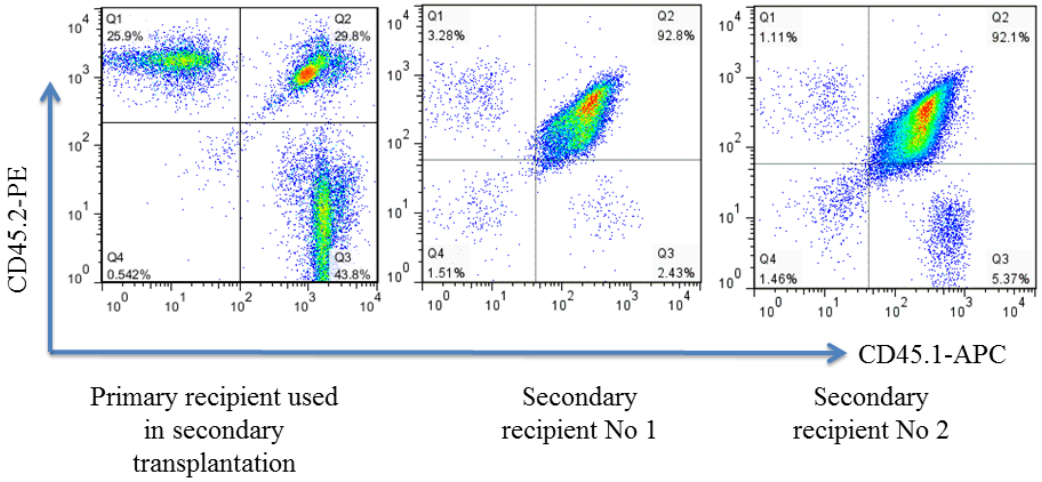

Figure 5.2-8. Secondary recipients contained low level donor contribution 7 weeks after transplantation. Left plot was the peripheral blood sample of primary recipient used for secondary transplantation. Middle and right picture were secondary recipient. Each secondary recipient received cell amount equivalent to one third of one femurs bone. Note that donor derived cells were CD45.2 homozygous, carrier cells were CD45.1 homozygous and recipient cells were CD45.1/CD45.2 heterozygous. (n=2).

To detect whether immortalized stromal cells were able to engraft in primary recipients, blood samples were taken from three mice six months after transplantation and had their genomic DNA were isolated. CER fragments were amplified alongside with Myo. It was used as an internal control, reaction parameters were listed in appendix table 8.2-1. PCR result suggested no CER DNA was detectable in recipients' peripheral blood (figure 5.2-9). Such data suggested stromal cells were cleared from recipients by immune system after transplantation.

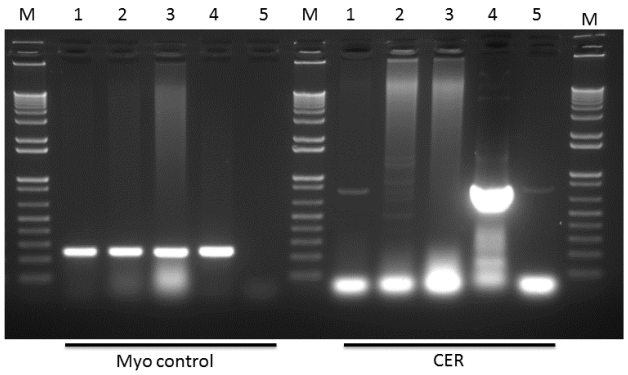

Figure 5.2-9. No genomic DNA containing CER sequence could be detected from blood sample by PCR. Two lane M were 1Kb+ ladder. Left panel was Myo internal control sample, right was CER sample. Lane 1 of both panels were gDNA isolated from blood of mouse SRYZH 6 3 8. Lane 2 of both panels were gDNA from mouse SRYZH 9 2 9. Lane 3 of both panels were gDNA from mouse SRYZH 9 2 10. Lane 4 of both panels were positive control, verified gDNA isolation from mouse ear sample was used as a positive control template for Myo. CER plasmid was used as a positive control template for CER. Lane 5 of both panels were no template negative control.

Taken together, data presented in this chapter demonstrated that cell lines derived in this study could support production of HPCs as well as HSCs. HSCs produced could achieve long term multilineage haematopoietic engraftment in multiple organs of primary recipients. Such haematopoietic maturation capacity could be observed with cell lines derived from populations expressing several different combinations of markers and from haematopoietic related sites of different developmental stages. Donor derived cells from engrafted primary recipient could engraft secondary recipients, although at low levels. More interestingly, cell line P12-002 A6, P12-027 G7, P12-015 B4, P12-009 E10 and P12-021 C1 could mature HSCs without the help of externally added growth factors; this was superior compared to OP9 cells. All these data demonstrated that immortalized cell lines derived from haematopoietic sites could promote maturation of pro-HSCs into definitive HSC. The environment that support haematopoietic maturation existed in multiple time points and was not confined to specific surface marker profile.

6. Chapter 6: Gene expression in AoV cells (RT-qPCR)

A set of reverse transcription quantitative PCR (RT-qPCR) experiments was carried out to compare the transcriptional profiles of cell lines that could mature pro-HSCs into dHSC and those that could not. A set of preliminary experiments was conducted to determine reliability and reproducibility of qPCR platform used by characterizing its systematic errors and random errors. To better control the quality of experiment, MIQE standard was adhered (Bustin, Benes et al. 2009).

Later, 9 cell lines derived in this project and OP9 control were tested for expression of haematopoietic genes. Expression information was extracted and compared with data generated in Nagao, Ohta et al. (2008).

In summary, in this chapter, the following was achieved:

- Establishment of a reliable qPCR experimental platform that compatible with MIQE standard
- Used such platform to determine expression level of key haematopoietic genes in 9 cell lines.
- Analysis of expression data and comparison of results with Nagao *et al.*'s result.

6.1. QPCR primer design

64 haematopoietic related genes were selected based on the literature, microarray data generated in our laboratory and on advice from various members of our group (appendix table 8.4-1). Primer pairs against 13 of these genes passed validation, their sequence were listed in table 6.1-1. Most remaining primer pairs failed to amplify when tested with cDNA from OP9 and cell line P12-009 E10, P12-021 C1, P12-015 B4. It was not clear if such failure can be attributed to these primer pairs tested or tested cell lines just didn't express corresponding transcripts at all.

Primer pair Tbp E6/7 was used as reference gene. Primers were designed for Ubiquitin C (Ubc), which was used as reference in Prof Berthold Göttgens's recent publication (Moignard, Macaulay et al. 2013).

It was discovered in primer verification experiments that amplification efficiency will fluctuate more than 0.1 between runs, even when the same preparation of cDNA and primer-probe mix were used (appendix table 8.4-5). It was more related to the

ratio of mixing of primer-probe-mix and cDNA solution. So a standard curve was set up for each primer pair used in every run to compensate for such fluctuations.

Primer Pair	Gene	5' Primer sequence	5' Tm	3'Primer sequence	3' Tm	Amplicon size (nt)	UPL probe #
Il3ra E3/4	CD123	gaagggcagggacatcttt	59	agagggagagcgactggaat	60	71	26
Flt3l E6/7	FLt3 ligand	aggcctgccagaatttctct	60	tagggctatgggactccttg	59	89	25
Bmp4 E3/4b	Bmp4	gatctttaccggctccagtct	59	cctgggatgttctccagatg	60	143	101
Itgav E14/15	Cd51	ggtgtggatcgagctgtctt	60	caaggccagcatttacagtg	59	61	21
Cdh2 E14/15	N-cadherin	ggtggaggagaagaagaccag	60	ggcatcaggctccacagtat	60	72	67
Inhba E2/3	inhibin beta a	atcatcacctttgccgagtc	60	tcactgccttccttggaaat	59	71	72
Tgfb1 E2/3	TGFbeta1	tggagcaacatgtggaactc	59	cagcagccggttaccaag	60	71	72
Vcam1 E6/7	VCAM1	tggtgaaatggaatctgaacc	59	cccagatggtggtttcctt	59	86	34
Jag1 E23/24	Jagged1	gaggcgtcctctgaaaaaca	60	acccaagccactgttaagaca	59	72	6
Wnt4 E2/3	wnt4	actggactccctccctgtct	60	tgcccttgtcactgcaaa	59	109	62
Kitl E1/2	SCF	agcgctgcctttccttatg	60	ccttggttttgacaagaggatt	59	95	68
Nes E2/3	Nestin	tcccttagtctggaagtggcta	60	ggtgtctgcaagcgagagtt	60	68	67
Tbp E6/7	TBP	ggggagctgtgatgtgaagt	60	ccaggaaataattctggctca	59	93	97

Table 6.1-1. Sequence of 13 primer pairs used. Melting temperature data were calculated using Roche's UPL assay design centre.

6.2. qPCR Characterization of cell lines

cDNA isolated from 9 cell lines derived in this project plus OP9 positive control were tested (table 6.2-1). OP9 was chosen because it was the best haematopoietic promoting cell line I have on hand. Out of those 10 lines, 7 could mature E9.5 pro-HSCs into definitive HSC while 3 lines could not. Sample information was listed in table below.

Cell line	Typle	Source	Passage	Engraftment	cDNA concentration (ng/μL)
P12-002 A6	Low density	E11.5 AoV	15	Yes	125
P12-004 D5	Low density	E11.5 Aorta	13	Yes	125
P12-009 E10	Low density	E11.5 AoV	10	Yes	200
P12-015 B4	Bulk	E8 presomitic tissue	22	Yes	125
P12-015 H5	Low density	E10.5 36sp AGM	17	No	125
P12-021 C1	Bulk	E10.5 32sp AGM	22	Yes	125
P12-021 C2	Bulk	E10.5 32sp AGM	17	No	68.06
P12-026 C2	Bulk	E11.5 AoV	13	No	125
P12-027 G7	Low density	E11.5 AGM	6	Yes	125
OP9		Adult mouse bone marrow	33	Yes	125

Table 6.2-1. List of cell lines subjected to RT-qPCR experiment. Note "Yes" in Engraftment column indicated that E9.5 caudal parts cells co-aggregated with that cell line generated more that 5% donor chimerism at 6 weeks. Engraftment data was taken from experiments SRYZH 2, 4, 6, 7 and 9.

Expression levels normalized to Tbp were shown in table 6.2-2. Raw Crossing points reading for all transcripts were in appendix table 8.4-3. Amplification efficiencies were in acceptable range and compensated using standard curve. No significant elevated standard error was observed during experiments.

	Supportive							Non-supportive		
	P12-002 A6	P12-009 E10	P12-026 C2	P12-027 G7	P12-015 B4	P12-021 C1	OP9	P12-004 D5	P12-021 C2	P12-015 H5
Itgav	13.55	72.00	12.55	4.79	9.13	11.88	3.10	1.75	12.04	16.91
Vcam1	41.64	600.49	17.39	35.75	50.56	8.40	2.69	16.34	6.23	55.33
Inhba	18.13	4.96	22.16	1.08	3.63	13.00	1.45	1.00	16.11	6.68
Tgfb1	5.43	79.34	5.66	2.46	7.94	4.23	1.39	1.45	9.06	6.73
Bmp4	4.72	13.27	2.23	1.17	2.04	0.19	0.67	0.68	0.70	4.11
Cdh2	3.94	5.10	5.06	0.33	0.64	4.08	0.51	0.11	3.68	5.46
Jag1	1.96	3.58	2.75	0.14	0.44	0.76	2.14	0.07	0.67	0.75
Nes	2.36	12.47	3.41	0.11	0.28	0.42	ND	0.05	1.16	1.15
Kitl	0.55	2.95	0.05	0.38	0.47	0.24	0.13	0.38	0.27	0.98
Il3ra	0.31	0.22	0.16	0.02	0.03	0.06	0.10	0.01	0.13	0.11
Flt3l	0.03	0.09	0.08	0.01	0.02	0.00	0.04	0.01	0.01	0.04
Wnt4	0.03	0.54	0.28	0.00	0.17	0.50	0.30	0.01	0.30	0.23
Tbp	1	1	1	1	1	1	1	1	1	1

Table 6.2-2. Relative expression level of 13 transcripts used in 10 cell lines. Expression level was normalized to Tbp, the housekeeping gene. ND was not determined. (n=3)

The box and whisker plot below (figure 6.2-3) showed a varied expression profile across different primer pairs. Detailed examination of data from cell line E10 showed Cp readings of most transcripts were higher compared to other lines, suggested cell line P12-009 E10 had less mRNA in total RNA content. One explanation could be that E10 cell line had more ribosomal RNA, which was consistent with its faster replication speed.

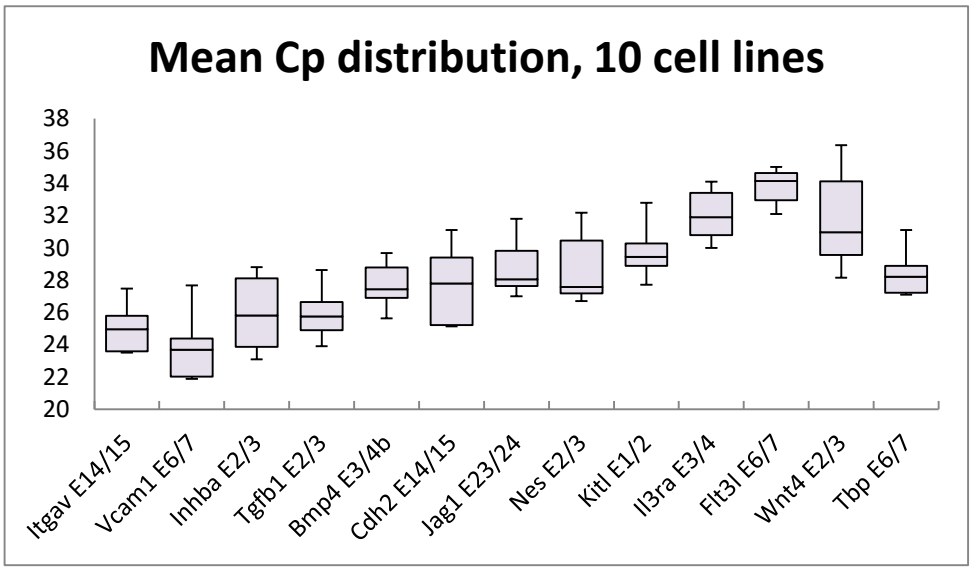

Figure 6.2-3. Box and whisker plot showed distributions of Cp in all 10 cell lines. Upper and lower whiskers indicated maximum and minimum Cp respectively. Beside Tbp E6/7, primer pairs were sorted according to their max Cp value.

Reference primer pair Tbp E6/7 gave relatively stable readings in most cell lines. Different expression level of reference gene could be caused by difference of mRNA

percentage in total RNA content. Further experiments were needed to monitor the stability of Tbp expression in various cell lines of different passages. It was important to determine the frequency that outliers appear, if Tbp expression was not as stable as it seemed to be, alternative reference genes like Ubc could be used (Moignard, Macaulay et al. 2013).

To better compare expression values across different cell lines, Crossing points (Cp) were converted to relative expression values and were normalized against Tbp expression value (Table 6-2.2). A two tailed student t-test was applied to all normalized expression values. Result (data not shown) showed no different could be detected between average expression of cell lines that could mature pro-HSCs and those that could not. There were no difference between supportive and non-supportive clones at individual transcript level neither. Thus I focused on expression variability between different cell lines. Based on coefficient of variation of normalized expression of 10 cell lines (appendix figure 8.4-2), 6 out of 13 transcripts had a coefficient of variation bigger than 100%, suggesting these transcripts were differently regulated between cell lines. The high variable group included Itgav, Vcam1, Tgfb1, Bmp4, Nes, Kitl. On the other hand, expression of Inhba, Cdh2, Jag1, Il3ra. Flt3l and Wnt4 was less variable.

In 2008, Kenji Nagao *et al.* (Nagao, Ohta et al. 2008) analysed sub-clones of cell lines derived from E10.5 mouse AGM by Nakahata's group (Xu, Tsuji et al. 1998). Nagao and colleagues performed sub-cloning of those AGM derived lines. One of the sub-clones analysed, AGM-S3-A9, could support haematopoietic progenitor expansion during co-culture, and could maintain HSC activity in murine BM LSK cells. Another sub-clone, AGM-S3-A7, of same origin failed to do so. They compared expression profiles of those two sub-clones and OP9 positive control cell line generated using the Affymetrix® MG-U74 microarray platform. I extracted their microarray data from NCBI's GEO resource (dataset: GSE11891, GEO

Accession: GPL81) and compared its expression value with qPCR data collected in this project.

Reference gene used in this study was used to normalize expression level extracted from Nagao's experiment. In my data, average Tbp expression of supportive cell lines in qPCR experiment were 1.47 fold higher compared to expression of Tbp in OP9, and average Tbp expression in non-supportive cell lines was 2.88 times higher than Tbp expression in OP9. That was comparable with Nagao et al.'s result (1.35 fold higher for supportive cell line and 0.98 fold for non-supportive cell line). However, expression differences of many genes between feeder lines derived in this project and OP9 control were significantly higher. In the most extreme case, in OP9 cells, Nes expression level was barely detectable, with only 1 out of 6 replicates have a Cp of 38.54, but Nes Cp in stromal lines derived in this project are generally around 28, indicating at least 1024 (2^{10}) fold expression difference. After exclusion of Nes, on average transcripts of interest in haematopoietic-supportive lines had normalized expression 8.63 fold higher compared to OP9. Non-supportive lines had normalized expression 3.42 times higher. Such large differences were not observed in Nagao *et al.*'s microarray experiments. In their data, after excluding Nes, normalized fold change of average expression level between supportive clone and OP9 was 1.40, between non-supportive clone and OP9 was 1.39. I checked all expression values in their assay (figure 6.2-5). In their data, overall distribution of expression values was similar between two sub-clones and OP9, indicating the lack of expression difference in 13 genes selected was not biased, but a representation of overall trend.

It was unclear which distribution their data had, but it was unlikely this data was normally distributed since frequency of expression values was not symmetrical. Such difference could be explained by qPCR platforms had larger liner detection range. Microarrays had very high throughput compared to qPCR method, but their probe sets sometimes could be over saturated by excessive transcript binding and

underestimate transcript content. That oversaturation might cause the chip reader fail to recognize higher expression values.

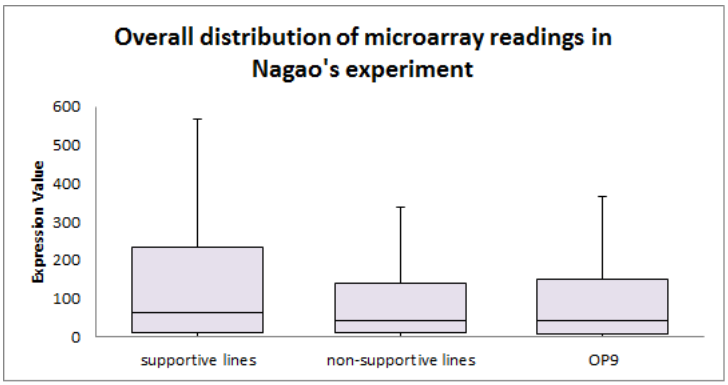

Figure 6.2-5. Overall distribution of expression values of two sub-clones and OP9 extracted from Nagao *et al.*'s data. Distribution figures shown here were based on raw readings directly exported from GEO2R "value distribution" page.

Correlation analysis was conducted between each pair of transcripts. Five transcripts showed highly correlated expression patterns, with correlation higher than 0.93. They were Itgav, Vcam1, Tgfb1, Bmp4, Nes and Kitl. Their normalized expression levels in cell lines derived in this study were higher compared to expression level in OP9 positive control. On average, supportive cell lines expressed Itgav 6.67 fold higher than OP9; expressed Vcam1 46.65 fold higher; expressed Tgfb1 12.55 fold higher; expressed Bmp4 5.85 fold higher; expressed Nes 2188.6 fold higher and expressed Kitl 5.76 fold higher. On average, non-supportive lines expressed Itgav 3.31 fold higher than OP9; expressed Vcam1 9.64 fold higher; expressed Tgfb1 4.12 fold higher, expressed Bmp4 2.72 fold higher, expressed Nes 544.35 fold higher and expressed Kitl 4.07 fold higher.

In Nagao et al.'s experiment, expression level of these transcripts were more varied. Itgav expression level was 28% less than OP9 in supportive clone and was 17% less in non-supportive clone. Vcam1 expression level was 31% more than OP9 in supportive clone and was 23% less in non-supportive clone. Tgfb1 expression level was 112% more than OP9 in supportive clone and was 14% more in non-supportive clone. Bmp4 expression level was 75% more than OP9 in supportive clone and was

5% less in non-supportive clone. Nes expression level was 143% more than OP9 in supportive clone and was 117% more in non-supportive clone. Kitl expression level was 12% more than OP9 in supportive clone and was 66% less in non-supportive clone (see figure 6.2-6). The fact that these genes with diverse haematopoietic-related function highly correlated expression profile suggested that they were tightly regulated by the same set of "core" transcriptional regulators which might define the identity of HSC maturation niche.

	Itgav	Vcam1	Inhba	Tgfb1	Bmp4	Cdh2	Jag1	Nes	Kitl	Il3ra	Flt3l	Wnt4
Itgav	1.00											
Vcam1	0.98	1.00										
Inhba	0.00	-0.19	1.00									
Tgfb1	0.98	0.99	-0.12	1.00								
Bmp4	0.95	0.95	-0.04	0.93	1.00							
Cdh2	0.55	0.36	0.68	0.40	0.50	1.00						
Jag1	0.68	0.64	0.33	0.65	0.70	0.53	1.00					
Nes	0.97	0.95	0.09	0.96	0.95	0.54	0.79	1.00				
Kitl	0.96	0.97	-0.23	0.96	0.96	0.40	0.54	0.90	1.00			
Il3ra	0.50	0.40	0.59	0.42	0.60	0.64	0.72	0.58	0.39	1.00		
Flt3l	0.71	0.66	0.24	0.67	0.73	0.59	0.90	0.80	0.60	0.55	1.00	
Wnt4	0.61	0.51	0.19	0.58	0.40	0.56	0.53	0.54	0.45	0.16	0.48	1

Table 6.2-3. Correlation matrix of normalized expression value of different transcripts in 10 cell lines. Highlighted primer pairs had correlation higher than 0.9. Correlation matrix was generated using Excel 2013's data analysis tool.

Itgav (CD51, Integrin alpha V) was a cell adhesion molecule involved in HSC niche interaction. It was showed that most human Nestin^{+} cells were also positive for PDGFα and Itgav. Those PDGFα^{+}CD51^{+} cells could support haematopoietic progenitor cell expansion (Pinho, Lacombe et al. 2013). Plus Itgav (CD51) expression was observed in intra-aortic haematopoietic clusters in E10.5 AGM (Boisset, Clapes et al. 2013). It was also reported that Itgav induced Tgfb1 activation was critical for the normal development of retinal vascular endothelial cells (Arnold, Ferrero et al. 2012).

Vcam1 was a cell adhesion molecule that bind to Integrin α4β1 complex. It was involved in HSC-niche interaction by modulating HSC homing and mobilization (Simmons, Masinovsky et al. 1992) (Papayannopoulou, Craddock et al. 1995). Literature search did not reveal anything meaningful discussing co-regulation mechanism between Vcam1 and its co-regulated peers.

Bmp4 was another critical secreted factor showed pattern of co-regulation. It was a potent mesodermal inducer and promotes haematopoietic specification (Sadlon, Lewis et al. 2004). Furthermore, literature indicated Bmp4 was selectively expressed in the stroma cells below intra-aortic haematopoietic clusters, polarized to the ventral wall of dorsal aorta (Marshall, Kinnon et al. 2000), suggested Bmp4 might had indispensable roles in HSC maturation after mesodermal stage (Durand, Robin et al. 2007). It was observed that some Nestin positive MSCs isolated from bone marrow could secret Bmp4 when co-cultured with neurospheres derived cells (Wislet-Gendebien, Bruyere et al. 2004). It would be interesting to see if Nestin positive cells in AGM expressed Bmp4. They might be a critical part of haematopoietic maturation niche.

Tgfb1 was a powerful regulator of cell cycle (for review, see Hu and Zuckerman (2001)). Bai *et al.* showed that in pluripotent stem cell differentiation models, TGF beta signalling could promote mesodermal formation at early stage but was inhibitory to formation of $CD34^{+}CD31^{+}VE\text{-}Cad^{+}$ progenitors. This finding suggested a stage specific role of TGF beta signalling in early haematopoietic development (Bai, Xie et al. 2013). Data from co-culture assays suggested Tgfb1 was beneficial to haematopoietic maturation while data from pluripotent cell differentiation assay did not support such idea. However, Bai *et al.* did not conduct any transplantation experiment, only tested haematopoietic progenitor content with CFU assays. As a result, differentiated cells they produced might not represent real haematopoietic stem cells.

Another very interesting molecule of the co-regulated group was Nes. Nes (Nestin) was a cell cycle related protein. Beside its co-regulation events with Itgav and Bmp4 described above, Nestin positive cells had other important haematopoietic functions. Mirko *et al.* showed that the $Nestin^{+}$ perivascular cells support human HSPCs (Corselli, Chin et al. 2013). Simon *et al.* showed $Nestin^{+}$ cells were a critical

component of mouse bone marrow niche for haematopoietic stem cells (Mendez-Ferrer, Michurina et al. 2010).

The last member of co-regulation group was Kitl, its common name was SCF (stem cell factor). Since primer pair used in this study could not distinguish solvable form and membrane bound form of SCF, SCF was considered as a secreted molecule. SCF was a critical regulator that controls haematopoietic cell survival. Kitl locus was also known as steel locus (SI). Complete knocking-out of SCF production leaded to anaemia and embryonic lethality (Ding, Saunders et al. 2012). SCF was also a critical cytokine for the aggregation system used in this study. The fact that cell lines derived in this project expressed SCF at a higher concentration might imply that the SCF was widely expressed at haematopoiesis locations during embryonic development. This was confirmed by Nagao's supportive clone. Their non-supportive clone expressed less SCF compared to OP9. Culture adoption and sub-cloning might contributed to the loss of SCF expression and ability to support haematopoietic expansion of that specific clone.

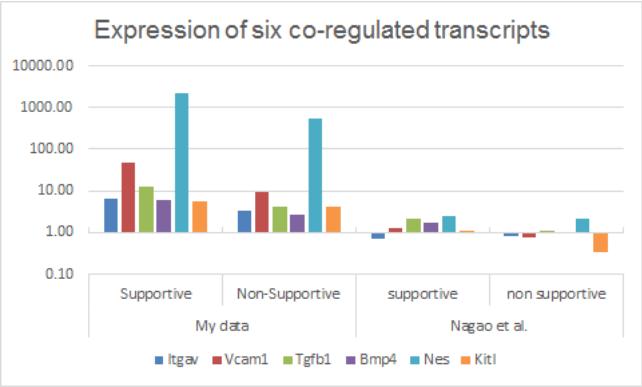

Figure 6.2-6. Expression of six co-regulated transcripts in stromal lines. All expression values were normalized to Tbp expression first, then normalized to expression in OP9 cell lines. Readings from Nagao's microarray were directly taken from GEO2R without further normalization or quality control measures. Probeset ID for Itgav was 98366_at; for Vcam1 was 92559_at; for Tgfb1 was 101918_at; for Bmp4 was 93455_s_at; for Nes was 103549_at; for Kitl was 99577_at. Note y axis was log scale.

In this study, expression level of five haematopoietic related cytokines and receptors were investigated, they were: Cdh2, Jag1, Il3ra, Flt3l, Wnt4 (figure 6.2-7). In this study, Cdh2 expression level in supportive lines was 6.25 fold higher than OP9 and in non-supportive clones was 6.09 fold higher. Jag1 expression was 25% less than OP9 in supportive lines and was 77% less in non-supportive lines. Il3ra expression was 38% higher than OP9 in supportive lines and 11% less in non-supportive lines. Flt3l expression was 5% lower than OP9 in supportive lines and 45% lower in non-supportive lines. Wnt4 expression was 14% lower than OP9 in supportive lines and 39% lower in non-supportive lines.

In Nagao et al.'s experiment, Cdh2 expression level in supportive lines was 16% lower than OP9 and in non-supportive clones was 37% lower. Jag1 expression was 74% less than OP9 in supportive lines and was 76% less in non-supportive lines. Il3ra expression was 47% higher than OP9 in supportive lines and 12% higher in non-supportive lines. Flt3l expression was 149% higher than OP9 in supportive lines and 97% higher in non-supportive lines. Wnt4 expression was 2% lower than OP9 in supportive lines and 5.43 fold higher in non-supportive lines.

Cdh2 (N-Cadherin) was an adhesion molecule that was involved in stem cell niche interaction (Arai, Hosokawa et al. 2012). Recent research measured the force generated by N-Cadherin based stem cell-niche interaction model (Burk, Monzel et al. 2015).

Jag1 was the ligand of Notch1. Notch was critical to normal embryonic haematopoietic development (Bigas, D'Altri et al. 2012). Both qPCR data and Nagao *et al.*'s microarray data showed stromal cell lines had less Jag1 compared to OP9 controls. One explanation could be OP9 was very good at inducing Notch signalling, and lines derived in this study could be enhanced by overexpressing Jag1. The other explanation could be cell lines promote maturation of pro-HSCs without strong activation of Notch signalling. If the later explanation was true, it would be interesting to study the Notch independent interaction of pro-HSC and surrounding

niche. Jag1 expression was also positively correlated with Flt3l expression, literature search revealed nothing discussing such co-regulation event.

Il3ra (Interleukin 3 receptor alpha) was the specific subunit of interleukin 3 receptor. It was known that IL3 signalling was critical in aggregation system used in this project, and IL3 did not directly function at pro-HSC but works through surrounding niche. So it was speculated that at least some compartment of HSC maturation niche expresses Il3ra.

Another factor investigated was Flt3l. It was ligand for Flt3, a tyrosine kinase. Flt3 was expressed at human LT-HSC (Kikushige, Yoshimoto et al. 2008) and mouse ST-HSCs (Christensen and Weissman 2001). Previous work conducted in our lab indicated Flt3l was a powerful haematopoiesis promoting cytokine in aggregation system. It would be very interesting to continue screening all the cell lines derived in this project and compare haematopoietic stem cell maturation ability between Flt3l high lines and lines that expressed less Flt3l.

Wnt4 was another secreted factor investigated in this study. Wnt4 was picked up by educated guess. Wnt signalling was required for haematopoietic specification of endothelial cells (Ruiz-Herguido, Guiu et al. 2012).

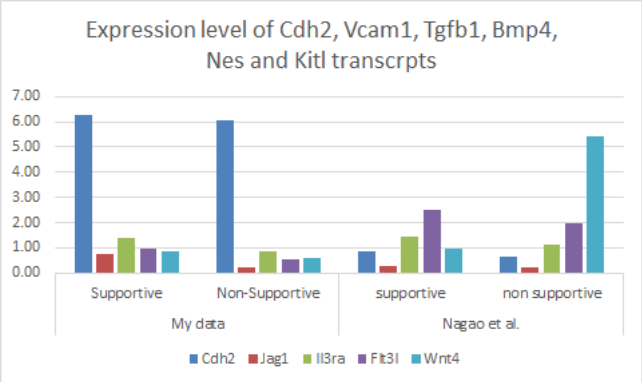

Figure 6.2-7. Expression of Cdh2, Jag1, Il3ra, Flt3l and Jag1 in stromal lines. Readings from Nagao's microarray were directly taken from GEO2R without further normalization or quality control measures. Probeset ID for Cdh2 was 102852_at; for Jag1 was 116304_at; for Il3ra was 92955_at; for Flt3l was 102929_s_at; for Wnt4 was 103238_at. All expression values were normalized to Tbp expression first, then normalized to expression in OP9 cell lines.

At last, Inhba was investigated in this study. In this study, normalized expression of Inhba in supportive lines were 7.22 fold higher than OP9, in non-supportive lines it was 5.45 fold higher. In Nagao's experiment, normalized expression of Inhba in supportive clone was 2.35 fold higher than OP9 and 83% higher in non-supportive clone. Inhba (Inhibin beta-a) was the homolog of human INHBA gene. The human INHBA gene was a subunit of inhibin complex which antagonize Activin activity. Cerdan *et al*. showed that Activin A promoted expansion of mesodermal fate in human embryonic stem cells and stimulate early haematopoietic development (Cerdan, McIntyre et al. 2012). How Inhba involved in pro-HSC maturation was open to further studies.

After analysing each transcript, normalized expression of each transcript in different cell lines and percentage of engraftment from E9.5 pro-HSC maturation assay were compared. Only expression of Jag1 shows weak correlation (0.84) with engraftment level in with growth factors conditions and overall engraftment (0.85) (appendix table 8.4-7). Further investigation was needed to find a marker of haematopoietic maturation ability.

At last, a correlation analysis between each stromal cell lines and OP9 were conducted (table 6.2-4). It was observed that cell lines P12-009 E10, P12-027-G7, P12-015 B4, P12-004 D5, P12-015 H5 were highly correlated (correlation bigger than 0.95). These cell lines came from different developmental stages, some could support pro-HSC maturation and some could not. A follow up RNA-seq study would better determine the significance of such correlation.

	P12-002 A6	P12-009 E10	P12-026 C2	P12-027 G7	P12-015 B4	P12-021 C1	OP9	P12-004 D5	P12-021 C2	P12-015 H5
P12-002 A6	1.00									
P12-009 E10	0.90	1.00								
P12-026 C2	0.83	0.52	1.00							
P12-027 G7	0.92	1.00	0.54	1.00						
P12-015 B4	0.93	1.00	0.58	1.00	1.00					
P12-021 C1	0.70	0.38	0.94	0.40	0.45	1.00				
OP9	0.69	0.56	0.68	0.57	0.61	0.73	1.00			
P12-004 D5	0.92	1.00	0.55	1.00	1.00	0.40	0.55	1.00		
P12-021 C2	0.54	0.21	0.88	0.21	0.28	0.95	0.63	0.22	1.00	
P12-015 H5	0.95	0.98	0.64	0.98	0.99	0.54	0.66	0.98	0.35	1.00

Table 6.2-4. Correlation coefficient of normalized expression in 10 cell lines. Highlighted cell lines have correlation higher than 0.95. Correlation matrix was generated using Excel 2013's data analysis tool.

7. Chapter 7: Discussion

In this chapter, different aspects of this study were discussed. Section 7.1 discussed about the construction of immortalization vector and directions of further improvements. Section 7.2 discussed about designing immortalization protocol, cell line derivation and generation of new cell lines. Section 7.3 discussed characterization of cell lines. Section 7.4 was focused at qPCR assay. At last in section 7.5, I gave a new model of haematopoietic specification using multi-ordered stochastic Markov model.

In section 1.3.2, some previous works were reviewed. This project was aimed at to address some caveats of previous studies. For example, cell lines from wild type AGM tissue were derived using a stronger immortalization factor to avoid going through crisis. A *piggyBac* based immortalization system replaced viral immortalization system used in some previous studies (Seandel, Butler et al. 2008). Fluorescence marker was introduced into immortalization vector to mark transfected cells. Plus, newly derived cell lines were compared with OP9 cells (Nakano, Kodama et al. 1994)to determine if they better capture the maturation capacity of maturing pro-HSCs.

In summary, in this study the concept of deriving stage or marker specific cell lines with haematopoietic maturation capacity was verified. Cell lines derived in this study had better haematopoietic maturation capacity compares with OP9. To further fulfil the potential of this immortalization system, more improvements could be made to accommodate derivation of cell lines from populations of extremely low cell number. The immortalization vector could be improved to better label transfected cells. Also transfection parameters could be explored further to improve efficiency and survival. Experimental protocols to derive cell lines could also be optimized to promote survival of very low cell numbers. Sorting protocol and antibodies used could be optimized to better separate positive and negative cell populations. Moreover, the E9.5 aggregation culture system should also be

stabilized. To discover mechanism of stem cell niche interaction, high throughput systems like Fluidigm and RNAseq systems were needed. It would allow high throughput screening of additional haematopoietic genes.

7.1. Discussion about vector establishment

The vector constructed in this study was aimed at improve some caveats of previous studies. Previous work done by Oostendorp, Medvinsky et al. (2002) were forced to employ constitutive expressed immortalization factor and didn't achieve direct immortalization without going through crisis. I wanted to improve that by achieving direct immortalization. In this study, I used the SV40T immortalization factor that was stronger compared to tsA58. SV40T was chosen as the immortalization factor because it was used to directly immortalize murine cells in previous studies (Pipas 2009). To fine adjust expression of SV40T and prevent over-alteration of the transcriptome by SV40T during immortalization, the powerful CAG promoter originally on *piggyBac* backbone was replaced with weaker PGK promoter. This change was aimed at lower SV40T expression to prevent possible over-alteration of haematopoietic related transcription program. The DNA sequence corresponding to SV40T intron was retained to stabilize its RNA expression.

The tsA58 immortalization system used in Oostendorp's study was easy to use and expression of immortalization vector was reversible, this was advantageous compared to some of the later works with viral delivery systems (Seandel, Butler et al. 2008). My immortalization system was also designed to be easy to use. The *piggyBac* system I employed avoided the tedious work of viral particle generation and did not contain infectious material. Others also shown that *piggyBac* transposons could be excised from genome (Wang, Lin et al. 2008) (Woltjen, Michael et al. 2009). This property should allow the immortalization factor to be turned off. It would be very interesting to test this capacity in future experiments.

Pervious study conducted by Oostendorp and Rafii did not label immortalized cells. This made distinguish feeder cell and primary cell in co-culture very difficult, especially when primary cells and immortalized cells were from the same origin. To separate them, I introduced a Cerulean fluorescent label into the immortalization vector (Sarkar, Koushik et al. 2009). Cerulean had an excitation/emission profile that did not interfere with detection of FITC and PE and had the brightest fluorescence in this range, made it an excellent candidate marker to use in experiment involved multicolour flow cytometry analysis. T2A, one member of 2A self-cleaving peptide family (Kim, Lee et al. 2011), was used to fuse SV40T and CER together. Using the 2A polypeptide to drive expression of multiple proteins had two advantages. First, it was shorter compared to IRES, thus was easier to manipulate and reduced overall plasmid size. Second, because CER and SV40T were fused together in the same open reading frame, expression of CER confirmed that SV40T coding region was successfully translated. However, later experiments confirmed that expression of CER was not strong enough to label all transfected cells. The silencing of CER could be caused by positional effect. Or T2A might reduce CER protein production level. To counter this problem, a stronger and more silencing-resistant marker might be required.

During this study, it was noticed that in culture, sometimes stromal cells grow drastically and consumed a lot media. It would be much better if growth of stromal cells in culture could be inhibited. One way to achieve it was to introduce a chemically inducible suicidal gene into the immortalization vector, like iCasp9 system (Ramos, Asgari et al. 2010).

It would be easy to replace components of the PGK-SV40T-2A-CER cassette. The immortalization vector constructed in this study was designed with a modular concept, with accurate maps of all molecules generated during vector construction at single nucleotide resolution. With all mapped intermediate vector on hand, it would be very easy to replace CER with more efficient labels. A panel of *piggyBac* based

vector each had different immortalization factor/label combination could be established since the pB-PGK backbone was modified to contain SalI and NcoI restriction sites. Another possible modification was to move Cerulean fluorescence marker forward of SV40T antigen and use a stronger promoter. In this setting, expression of CER would be significantly increased, and SV40T expression might also increase. To go one step further, the SV40T and Cerulean could be controlled under independent promoters, enabling fine adjustment of their expression.

Finally, because electroporation did not involve receptor-envelope recognition, the vector I used was organism neutral. It could be applied towards cells from any species that could be immortalized with SV40T. One only needed to adjust electroporation parameter to apply the system to new species.

7.2. Discussion about cell line generation

Previous works by Xu, Tsuji et al. (1998) and Oostendorp, Medvinsky et al. (2002) established cell lines from AGM region of E11.5 and E10.5 embryos. They demonstrated cell lines derived from AGM region could support HSC and/or progenitors. In this study, I pushed a little further to investigate if cell lines derived from earlier developmental time points could mature pro-HSC. I tried to sub-dissect E11.5 AGM region and establish cell lines from primary cells having different surface marker combinations. Such study would reveal dynamic of interactions between different populations in AGM region.

To achieve this goal, I developed a protocol to sub-dissect AGM region into HSC-rich ventral aorta (AoV) and HSC-depleted dorsal aorta (AoD) and establish cell lines separately. After successfully derived cell lines from dorsal and ventral aorta, I tried to sort sub-dissected cells and establish lines from sorted populations. Preliminary experiments carried out using primary cells from E11.5 ventral aorta showed some cell populations of interest contain only about 1000 cells.

Primary cell loss during transfection was minimized to increase cell recovery. I used 1.5mL electrically neutral tube instead of 5mL polystyrene tubes. Such electrical neutral tubes greatly reduced number of cells lost due to them stuck to the tube wall. By adjust tube holder and parameter of sorter, I achieved better aiming of drop stream and greatly reduced number of centrifuging and liquid transfer steps. These improvements yielded some success; I generated cell lines from populations with only a few thousand cells.

The bottleneck of transfecting cell populations with even smaller number was cell survival. I successfully transfected a population of only 200 cells with pEGFP-N1 plasmid, judged by observing GFP^+ cells next day. But the lone survivors failed to grow. Further improvements were need to focus on reduce cell loss and enhance cell survival. One potential way of improving cell survival was to shorten length of pulse. Experiments done in this study did not fully explored the survivability of all experimental conditions. Based on trends with 30ms and 20ms conditions, conditions with 10ms length and slightly higher voltages (higher than 1350V) could have better survivability without compromising transfection efficiency.

Plus, samples with low cell number might require lower voltages compared to samples with plenty of cells, so a special experiment could be conducted to find optimal electroporation parameter for populations with less than 10^5 cells. Amount of plasmid applied to sample with small numbers could also be reduced. A quick chart of electroporation parameters and plasmid amount suitable for different sample size could help researchers determine optimal condition to transfect different samples.

Fluorochromes and antibodies used for flow cytometry could be adjusted to enhance separation of positive and negative populations, this would enhance recovery rate of cell populations with weak expression of surface markers.

To enhance cell survival after transfection, several methods could be used. First, Matrigel® could be used to coat wells of 96 well plate to better facilitate cell

attachment. It might provide extra cellular matrix that was needed for cell survival. Also, untransfected primary cells from stage-matched EGFP embryos could be used as a source of feeder cell. These cells can provide the much needed niche for transfected cells to grow. After a few passages, primary cells will reach crisis and cease to growth, leaving only immortalized cells in culture.

In this study, cell lines bear different markers were derived. The markers used to sort primary cells were: Il3ra (CD123), Vcam1 (CD106), membrane bound SCF, VE-Cadherin and Flt3. They were chosen based on educated guess. Il3ra (Interleukin 3 receptor alpha) was the specific subunit of interleukin 3 receptor. It was known that IL3 signalling was critical in aggregation system used in this project, and IL3 had positive effect on HSC emergence in AGM region (Robin, Ottersbach et al. 2006). So it was speculated that at least some compartment of HSC maturation niche expresses Il3ra. However, in this study, the expression level of Il3ra detected in ventral aorta cells was very weak. One possible explanation was that the collagenase/dispase solution used in this study was too strong and digested CD123 molecule on cell surface. Gentler dissociation methods like Accutase or just collagenase itself might be beneficial for detecting Il3ra positive cells.

Vcam1 was a cell adhesion molecule that binds to Integrin α4β1 complex. It was involved in HSC-niche interaction by modulating HSC homing and mobilization (Simmons, Masinovsky et al. 1992) (Papayannopoulou, Craddock et al. 1995). During my study, $Vcam1^+$ populations was detected in AoV cells and quite a few cell lines were generated from $Vcam1^+$ primary cells.

SCF was a critical regulator that control haematopoietic cell survival. Kitl locus was also known as steel locus (SI). It produced cytokine that bind to c-kit receptor. Complete knocking out SCF productions lead to anaemia and embryonic lethality (Alexander 2000-). Membrane bound SCF was critical for normal haematopoiesis. SCF was also a critical cytokine within aggregation system used in this study. In this study, membrane-bound SCF expression was also very weak, expect in the

experiment involved VE-Cadherin and membrane-bound SCF. Because the FMO "–SCF" control behaved normally in that experiment, the most likely reason of detecting SCF expression in the VE-Cadherin/SCF experiment was the signal was real. It could be that in other experiments, the membrane-bound SCF proteins were destroyed, caused a loss of SCF signal. In the VE-Cadherin/SCF experiment, the dissociation solution somehow worked less effectively, leaving some membrane-bounded protein intact. In the future, weaker dissociation solutions could be used to retain the membrane-bound SCF proteins. Less secondary antibodies could also be used to prevent over amplification of fluorescence signals.

The fourth marker tested was VE-Cadherin. It was demonstrated that HSCs emerged from VE-Cadherin positive pre-HSC stages (Rybtsov, Sobiesiak et al. 2011). Thus the VE-Cadherin positive endothelial lining in dorsal aorta must contained some permissive niche to allow maturation of pro-HSCs into pre-HSCs and definitive HSCs. In this study, successful separation of VE-Cadherin positive and negative primary cells was achieved. Cell lines were derived from both populations.

The last marker tested was Flt3. It was expressed at human LT-HSC (Kikushige, Yoshimoto et al. 2008) and mouse ST-HSCs (Christensen and Weissman 2001). And my data indicated Flt3l was a powerful haematopoiesis promoting cytokine in aggregation system used in this project. It was hoped that Flt3 might be used as a marker to enrich niche related cells. In this study, cell lines were derived from both Flt3 positive and Flt3 negative cells. However, no enrichment of pro-HSC maturation capacity was detected yet. More experiments were needed to determine whether Flt3 could be used as a marker of pro-HSC maturation capacity.

Data gathered in this study indicated that the idea of establishing cell lines from sorted primary cells was achievable. This achievement was of better than previous studies. However, I screened markers mentioned above. They did not enrich pro-HSC maturation capacity. This finding suggested additional markers and more cell lines were needed to be screened.

7.3. Discussion about cell line characterization

One of the disadvantages of previous studies was that most studies only characterized cell lines using flat co-culture method. In this study, I decided to use the more robust 3D liquid gas interface aggregation system (Taoudi, Gonneau et al. 2008). The aggregation system we used not only could support growth and expansion of HPCs and HSCs *in vitro*, it also can mature pro-HSCs into definitive HSCs. That was seldom achieved previously. Two assays were uses in this study based on the aggregation system. (1) A four days E11.5 aggregation assay was used to demonstrate cell lines can produce haematopoietic progenitor cells from E11.5 embryos. (2) Cells from caudal half of E9.5 embryos were aggregated to stromal cells in E9.5 pro-HSC maturation assay to demonstrate that these lines could mature pro-HSCs from of E9.5 mouse embryos.

The four days E11.5 aggregation system was known to support maintenance of haematopoietic progenitors *ex vivo*. In this system, OP9 cell line could potently expand progenitors in aggregation culture, thus was used as positive control. The results gathered in this study indicated that some cell lines derived in this project could support production of haematopoietic progenitors from primary cells of E11.5 embryos. All kinds of colonies were generated, including GEMM (Granulocyte, Erythrocyte, Monocyte, Megakaryocyte) colonies. And the number of colonies varies between different lines, ranged from very low to comparable to OP9 positive controls. However, it was discovered that results of four days E11.5 aggregation assays were not correlated with E9.5 pro-HSC maturation assay. This suggested improvement of E11.5 assay was needed. Experimental protocol needed to be streamlined, animal source and husbandry procedure should be stable. Change of animal housing like happened during this study should be avoided at all cost. Dissection and sample handling could be improved to minimize contamination and sunk of membranes that caused data loss. To prevent stromal cells interfere

colony-counting in CFU-C assays, stromal cells could be killed by suicidal gene introduced within an improved immortalization vector.

The other assay employed, the E9.5 pro-HSC maturation assay, was aimed at to determine if cell lines derived in this study could mature pro-HSCs presented in caudal half of E9.5 embryos. Dr Stanislav Rybtsov made necessary improvement to culture system. He demonstrated that by extending culture time to seven days and adding SCF, Flt3L and Il3, such culture system could mature pro-HSCs into definitive HSC (Rybtsov, Batsivari et al. 2014). However, no engraftment was observed when aggregating E9.5 primary cells with OP9 without presence of growth factors. The results gathered in this study indicated that some cell lines derived in this study could mature pro-HSCs into definitive HSCs. The functions of HSCs derived were verified via multilineage assay and secondary transplantation. A few of the lines could achieve primary engraftment without help of growth factors. This was an advance compared to previous studies.

It was noticed that cell lines that were capable of maturing pro-HSCs were derived from diverse developmental stage and populations each carried different marker combinations. This finding suggested cells capable of functioning as developing haematopoietic niche existed at multiple time points and bear different markers. Another interesting observation made with the E9.5 pro-HSC maturation assay was stromal cells stayed in over-confluence culture for more than one day failed to promote pro-HSC maturation. Such maturation capacity could only be regained by a period of free growth. During culture, the capacity of mature pro-HSC seemed to be periodically lost and regained, thus “oscillating”.

Such finding challenged the notion that HSC were matured by some rare niche cells with in. If such rare cell existed, transplantation result should be “all or nothing”. That was cell lines with haematopoietic maturation potential should mature HSC every time while lines without such potential should never matured pro-HSC to definitive HSC. That was not true. The high failure rate of experiments of

maturation of E9.5 pro-HSC suggested pro-HSC maturation niche was not “all or nothing”, or put it in a more scientific way, the pro-HSC maturation niche was not “deterministic”. One interesting question arise from this observation, that if haematopoietic maturation niche was not deterministic, how was such potential regulated?

To investigate these derived cell lines further, several improvements were needed. Beside improvements to aggregation system mentioned two paragraphs above, several improvements were needed for E9.5 pro-HSC assay. The pro-HSCs and definitive HSCs were more fragile compared to progenitors, thus E9.5 pro-HSC assay was more time sensitive compared to E11.5 four day aggregation assay. Dissection, sample processing, culture harvesting and transplantation all needed to be sped up. Because the pro-HSC maturation niche was dynamic, time of cells spend in free growth needed to be carefully monitored, especially when cell lines grew at different speed. Another way to better capture the dynamic pro-HSC niche was to use primary cells from Runx1 +23 enhancer reporter transgenic mice (23GFP mice), the Runx1 +23 enhancer could label cells going through EHT (Swiers, Baumann et al. 2013). With 23GFP cells, one could detect maturing pro-HSC in. In this way, capacity of pro-HSC maturation could be visualized by GFP activity. Stromal cells near GFP^+ cells should have pro-HSC maturation capacity, they could be easily sampled. With such improvements, cell lines derived in this study could be better studied. The mechanism behind their pro-HSC maturation capacity could be revealed.

7.4. Discussion about qPCR

A RT-qPCR assay was carried out to probe haematopoietic related gene expression. In this study, qPCR was used to determine expression level of key haematopoietic genes in derived cell lines. List of haematopoietic related transcripts were determined by educated guess. Then a RT-qPCR system was established to

determine expression level of transcript of interest. MIQE standard was used to help design RT-qPCR experiment. Current qPCR experimental platform was robust. In follow up research, RNA-Seq might replace qPCR. It could increase the throughput of gene expression study. With more genes and cell lines tested, additional co-regulation events could be revealed and novel regulatory mechanisms could be estimated.

Current RT-qPCR results showed some interesting correlation of haematopoietic genes. Data discussed in section 6.2 shown a cluster of co-regulation. Its members included Itgav, Vcam1, Tgfb1, Bmp4, Nes and Kitl. Such co-regulation was interesting, suggested they were regulated by same set of regulators during haematopoietic development. However, with only limited data on hand, it was hard to accurately determine possible master regulators just based on promoter sequences alone. More events of co-regulation were needed to enhance accuracy of regulatory mechanism prediction. However no correlation between expressions of haematopoietic genes with phenotype was detected (percentage of engraftment). To further investigate expression profile of haematopoietic related genes, current RT-qPCR protocol should be improved.

7.5. Interpretation of results using multi-ordered stochastic Markov model

In this project, several cell lines with haematopoietic maturation capacity were established from mouse embryos of different developmental stage and had ancestors bearing different surface markers. The unique “first time failure” phenomena suggesting pro-HSC maturation capacity was oscillating and was related to free growth of stromal cells. How I could fit such findings into the wider picture of definitive HSC maturation was worth discussing.

HSCs were no strangers to oscillation. For example, Gata2, one critical haematopoietic transcription factors was oscillating in adult haematopoietic cells (Koga, Yamaguchi et al. 2007) and in developing aorta (Prof. Elaine Dzierzak’s

personal communication). To model the developing aorta, Variable-ordered Markov Random Field model could be applied. It abstracted every cell in developing aorta as a node in field. Each cell interacted with other cells nearby through cell to cell interactions. They also secreted signaling molecules to ECM, created a disseminating wave of signal that gradually spread from one cell to another. Such signaling wave could be reinforced or antagonized by neighboring cells. Thus, diffusion of signaling molecules could be treated as a gradual process that advances from one cell to next. Systems with properties were named as cellular automaton.

Initially, every cell had similar transcriptional state (starting state). At the next time point, every cell updated its cell state based on previous state and the signals it received from its neighbors. After they updated their cell states, each cell sent out signals to their neighbors according to transcriptional program of the new state. This goes on and on, gradually, different cells started to acquire drastically different identity and behave differently.

Russian mathematician Andrey Markov and others developed mathematical tool to describe such systems. To honor his contribution, it was named as Markov Random Field (Kindermann, Snell et al. 1980). In such field, the conditional probability distribution of future state of every node only depended upon its present state. In 1983, scientist introduced memory of past events into Markov Random field to makes it Variable-order Markov models (Rissanen 1983). Theoretical biologist already used it to describe firing and interactions of complex neuronal systems (ZIPPO 2010). I though similar model could also be applied to simulate of embryonic development events like ones occurred in the developing haematopoietic niche.

In stochastic model like Variable-ordered Markov Random Field, outcome of development was naturally variable because the stochastic nature of both external signaling and its internal procession. It was hard to determine developmental path of individual cells, but a probability distribution of different cell types ensured in most

of times, enough cells of each type were produced to meet the embryo's demand. Or in a mathematical word, an expectation of number of specific cell lineage at certain developmental time point could be established, like in E11.5 mouse embryos, only one definitive HSC was expected to exist per AGM (Kumaravelu, Hook et al. 2002, Taoudi, Gonneau et al. 2008).

One property of stochastic model was that some embryos at left most part of distribution would not have enough cells to survive. That means the naturally, some embryos would not generate enough haematopoietic cell and/or HSCs during embryonic development. That might contribute to natural abortion observed in embryonic development. On the other hand, if one embryo developed too many definitive HSCs in AGM region, there were simply not enough niches in fetal liver for all of them to colonize it. Without fetal liver niche, excessive HSC would differentiate or die and ultimately disappear. To assure robustness of developmental program, powerful attractor states existed so cells divide and acquire new identity (cell states) of desired types. These attractor states had high frequency in entire distribution and could ensure enough cells for most lineages needed.

Under stochastic paradigm, cell state was more important than ontogeny. This view was reinforced by successful reprogramming of various cell lineages using Yamanaka strategy (Takahashi, Tanabe et al. 2007). Reprogramming of differentiated cells to vastly different identity suggested that memory of past differentiation steps could be overcame if correct transcriptional program was established. To prohibit trans-differentiation or reverse-differentiation in normal embryonic development, cell memory served as a ratchet to restrict cell state change toward undesired directions. *In vivo*, lineage selection of a cell was strongly influenced by its neighbors. But after *in vitro* isolation, cellular memory and fate selection could be changed by expression of transcriptional program from other lineages (Kim, Flaßkamp et al. 2014) or remodeling of DNA methylation and histone modification patterns (Hou, Li et al. 2013).

Such property was of great use to study specification of HSC during embryonic development. One possible way to establish HSC cell identity with aggregation culture was to erase cell memory of endothelial cells. If that worked, they should be more responsive to cues produced by haematopoietic promoting cell lines. This could be achieved by adding epigenetic remodeler like 5-Azacytidine or 3-deazaneplanocin A to aggregation culture medium. In normal *in vivo* development, most endothelial cells in aortic linings were committed to endothelial fate. This was critical for normal function of the aortic wall. However in aggregation culture those non-haematopoietic endothelial fated cells were wasted. “Unlocking” these cells should enhance production of transplantable HSCs.

In stochastic model, at beginning all cells in p-SP region were similar. Purely by chance, some cells turned on haematopoietic related program and started to secret haematopoietic promoting morphogens. Such secretion was regulated by positive feedback loops, thus such haematopoietic maturation signaling was amplified from cell to cell and formed a traveling wave that reflected in p-SP and AGM region. After a while, these travelling waves slowed down and became stationary. Haematopoietic clusters were formed at peak of such stationary waves. Frequency of haematopoietic cluster and spacing between each cluster was determined by rate of diffusion of participating morphogens through tissue (transformation matrix) and shape of aortic wall. Because stem cell precursors were developing simultaneously alongside surrounding endothelial cells, synchronization was critical to successful wave formation. Similarly, in *in vitro* culture feeder (stromal) lines must be able to grow alongside with precursors of HSC and transduce haematopoietic signaling in-between in order to maintain and expand such haematopoietic waves.

To maintain haematopoietic waves in aggregation culture, the phase of development between feeder cells and stem cell precursors needed to be matched. It was observed that embryonic HSCs had different cell cycle rates compared to their mature counterparts (Pietras, Warr et al. 2011). Embryonic HSCs cycled faster, matching

cycling time of their neighbors. It might be postulated the haemogenic endothelial cells that were in the same phase as surrounding cells had better chance of developing into definitive HSCs. Cells out of synchrony might be just naturally eliminated.

The unique “first time failure” phenomena observed in this study might of extra importance. In two back to back experiments, most first experiment failed to generate engraftable HSCs, while latter experiment is usually good. Such difference was not related to over-confluence. But it was likely relates to time spent after reaching confluence. I postulated that cells might turn off embryonic development related genes induced by rapid growth after reaching confluence; these embryonic related gene regulatory networks might only be switched back on after sustained growth. Thus cells that had been expanding were more responsive to haematopoietic signal. They were more “primed” to interact with pro-HSCs in aggregation culture. After a while in confluence, inhibition of growth turned off some embryonic haematopoietic development related transcriptional programs. In such condition, cells lost their capacity to promote maturation of pro-HSCs.

To investigate effect of cell cycle in aggregation culture, cell’s growth rate could be studied with Fucci reporter mice. Fucci reporter mice by Abe et al. (Abe, Sakaue-Sawano et al. 2013) contained two fluorescence labeled cell cycle proteins that could label cells at different stage of cell cycle with different colors. To advance a step further, one could use single cell digital qPCR assay to detect genes that were cycling in stromal cells. Digital qPCR had the advantage of absolute quantification, thus avoided problem of determining amplification efficiency of individual template (White, VanInsberghe et al. 2011). Understanding of such oscillating gene regulatory network was especially important for describing phases of stromal cell. By matching stromal cell’s cycle with primary cells in aggregates, probability of successful HSC maturation might be greatly increased.

Polarization of HSC specification to the ventral wall of the dorsal aorta also suggested that signals to promote HSC maturation did not just come from inside aorta. External signaling also plays a role in HSC specification. To enhance HSC specification in our aggregation system, stromal cell lines used in aggregation assay could be transfected to express such signals. One possible way was to express ventralizing signal of E10.5 to E11.5 embryo in stromal cells. This might enhance definitive HSC generation in aggregate system.

The most important feature of the stochastic model was that it enables direct study of formation of haematopoietic wave in aorta explant or aggregation culture. Before generation of stationary haematopoietic wave and formation of haematopoietic cluster, there should be local random drift in signaling. Then traveling waves inside aorta should form. With fluorescence reporter and time lapse imaging device, local drift and traveling waves could be visualized. One way to visualize waves in HSC specification was to take advantage of inherent property of cellular automaton- every cell was equal; they received signals and passed it on to generate a wave of haematopoietic morphogens. So stromal lines could be transfected with fluorescence reporter knocked into promoter of various morphogens. Or they could be transfected with reporter driven by promoters that could be activated by specific morphogens. Such compound reporter cell lines could be aggregated with untransfected primary cell to detect morphogen waves in aggregates. Fluorescence intensity of each cell could be determined using fluorescence microscopy. With time lapse imaging, a time series of images can be generated. Then various cells inside aggregates could be sampled to generate a time series of light intensity (correlate to intensity of cell signaling). A filter, either by wavelet analysis or Fourier transform, could be applied to filter out local noises that did not grow to larger coherent structure. Background removed time series could be subjected to Fourier transform to distinguish major components in frequency spectrum. Components that appear multiple times in multiple locations could be considered as main components of haematopoietic

maturation wave. By doing this, morphogens that affected haematopoietic clusters formation in aggregates could be identified; they were likely to be responsible for haematopoietic cluster formation. And parameters of morphogen gradient generation and wave formation could also be determined.

Besides determining parameters of individual morphogen wave, haematopoietic specification wave could also be determined by fluorescence reporter driven by haematopoietic promoters, like Runx1, Kit, or Sca-1. Pattern generated by haematopoietic wave should match pattern observed in aorta wall (figure 7.5-1, a). After filtering out local fluctuations, haematopoietic wave function could be derived. It could determine the probability of a specific cell in AGM region to become a haematopoietic cell.

Wave function was the mathematical language to describe the haematopoietic specification wave. With wave function, computer simulation of haematopoietic cluster formation could be achieved. Haematopoietic wave could be decomposed as a combination of effect of single haematopoietic factor/signaling (figure 7.5-1, b). This could be done with Fourier Transform using wave function of individual haematopoietic signaling as “base” frequency in frequency domain (figure 7.5-1, c). Fourier transform could help quantify contribution of each haematopoietic signaling to overall generation of haematopoietic clusters (figure 7.5-1, d).

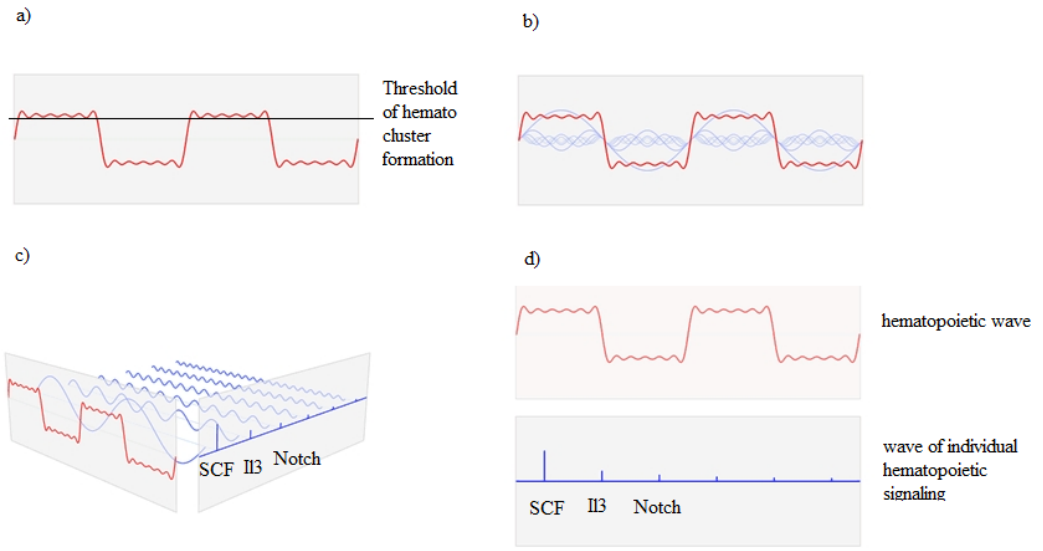

Figure 7.5-1. A hypothetical case of Fourier transform of haematopoietic waves. a) Haematopoietic wave was devised based on oscillating expression of key haematopoietic transcriptional factor and location of haematopoietic clusters in tissue wall. b) Haematopoietic wave was combined effect of many individual signaling. c) Fourier transform of haematopoietic wave in frequency domain detect its main frequency components. d) Based on frequency, main signaling in haematopoietic wave was determined. Note signaling molecules mentioned here was just to explain the case. They did not correspond to real events in haematopoietic field. Image modified from http://en.wikipedia.org/wiki/Fourier_transform#mediaviewer/File:Fourier_transform_time_and_frequency_domains_%28small%29.gif **under creative common license, original author: Lucas V. Barbosa.**

More interestingly, haematopoietic wave function also enabled manipulation of the shape and size of haematopoietic wave in tissue of given shape and size, thus manipulate the shape and size of haematopoietic clusters that contained definitive HSC. Manipulation could be achieved by changing shape or size of aggregates, or by careful modifying feeder cell's ability to produce certain haematopoietic molecule and how they respond to them. With such a capacity, it may be possible to massively generate HSC from 3D aggregate or even 2D flat culture.

To summarize, it had long been observed that during embryonic development, complex patterns arose from almost homogenous tissue via collective behavior of many cells. Behavior of such a collection of cells could be described using

Variable-order Markov Random Fields. Data gathered in this project suggested haematopoietic specification was not restrained by limited availability of niche. And the “first time failure” phenomena observed in E9.5 aggregation experiment suggested that haematopoietic specification was a stochastic process. Alan Turing proved that complex mosaic pattern could arise from 3D tubular Markov field with even just 2 to 3 signaling molecules (Turing 1952). Such mosaic patterns were formed by waves of signaling that travel inside the developing niche that gradually become stationary. Thus I postulated that the complex pattern of haematopoietic cluster arose in developing dorsal aorta by waves of few simple haematopoietic signaling molecules that become stationary.

In summary, a novel immortalization system was established in this study. With it, cell lines were derived from multiple embryonic stages or bear different cell surface marker combinations. Derived cell lines displayed haematopoietic promotion capacity that enables maturation of dHSCs from pro-HSCs. Such capacity was not restrained to specific marker combination or time point tested, suggested HSC maturation was not restrained by availability of niche. The “first time failure” phenomena observed in experiment suggested HSC maturation process was stochastic and depending of cooperation of both pro-HSC and surrounding cells. It was proposed that such cooperation depended on synchronization of phase between precursor of stem cell and their neighbor. They formed wave of haematopoietic signaling and induced haematopoietic cluster formation. Immortalization system developed and cell lines derived in this study could help detecting such haematopoietic waves and investigate the HSC maturation process *in vitro*.

8. Appendix

8.1.Establishment of immortalization system

8.1.1. Generation of vectors

Item	Tube (unit: µL)				
	A	B	C	D	E
pB-PGK-M9 digested by NcoI/SalI	4	4	4	4	4
pCR-BluntII-TAG8 digested by NcoI/XmaI	0	4	0	4	8
pCR-BluntII-CER1 digested by XmaI/XhoI	0	0	2	1	1
18MΩ water	9	5	7	4	0
10X T4 DNA ligase buffer	1.5	1.5	1.5	1.5	1.5
NEB T4 DNA ligase	0.5	0.5	0.5	0.5	0.5
Total	15	15	15	15	15

Table 8.1.1-1. Triple ligation of pB-PGK backbone, TAG and CER fragments. Tube A, B,C were negative controls. Tube E had higher TAG concentrations. For plate D,E a total of 80 clones were screened (40 each).

a) b)

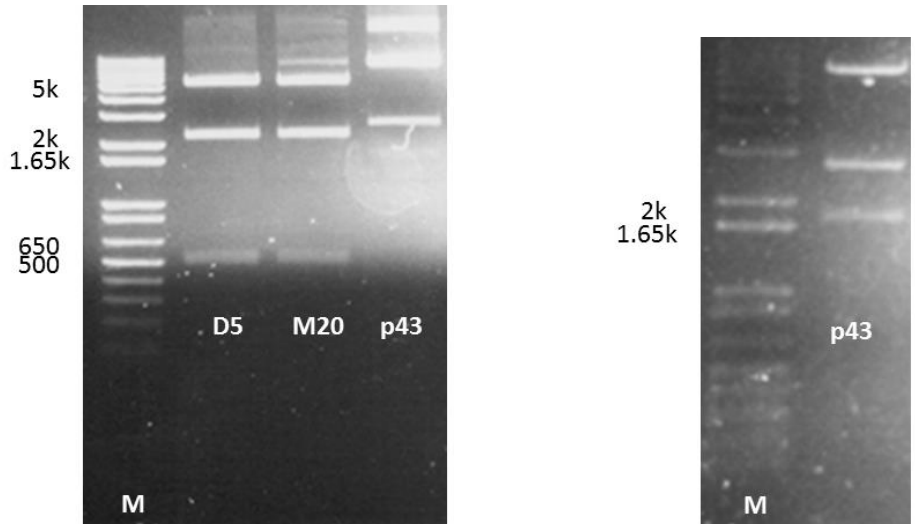

Figure 8.1.1-1. Digestion of pB-PGK-TAG-CER and pCyL043 plasmid after maxiprep. a) HindIII digestion of three maxiprep products. Note clone D5 and M20 had correct bands. Lane p43 was HindIII digested pCyL043 plasmid, it had distinct digestion products. This ruled out possibility of cross contamination. b) BamHI/NotI digestion of pCyL043 plasmid (Lane p43), released the 1791bp DNA encoding *piggyBac* transposase. Lane M in both figures were 1kb plus DNA ladder.

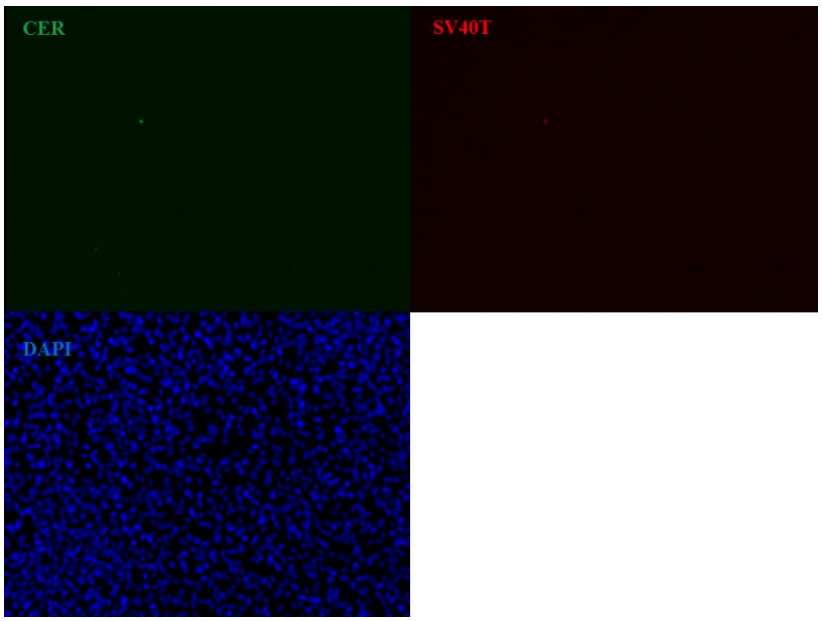

Figure 8.1.1-2. Immunostaining of untransfected OP9 negative controls, showed Cerulean staining (Green) SV40T (Red) and DAPI (Blue). Green channel was Alexa-488 conjugated anti GFP antibody recognizing Cerulean, Red channel was Alexa-568 goat anti mouse antibody recognizing SV40T positive cells labelled by mouse anti SV40T antibody. Pictures here were taken with similar parameters as corresponding ones in figure 3.2-1.

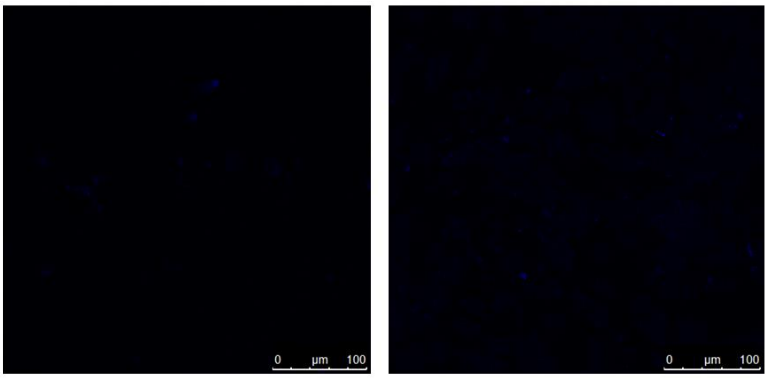

Figure 8.1.1-3. Spectrum property of transfected cells. These negative control pictures were taken with same parameter of those in figure 3.3-2. They showed fluorescence signal outside peak CER emission (555-585nm) of untransfected control (left) and M20 transfected cells (right), 40x oil objective.

8.2.Establishment of cell lines

8.2.1. Establishing transfection parameters

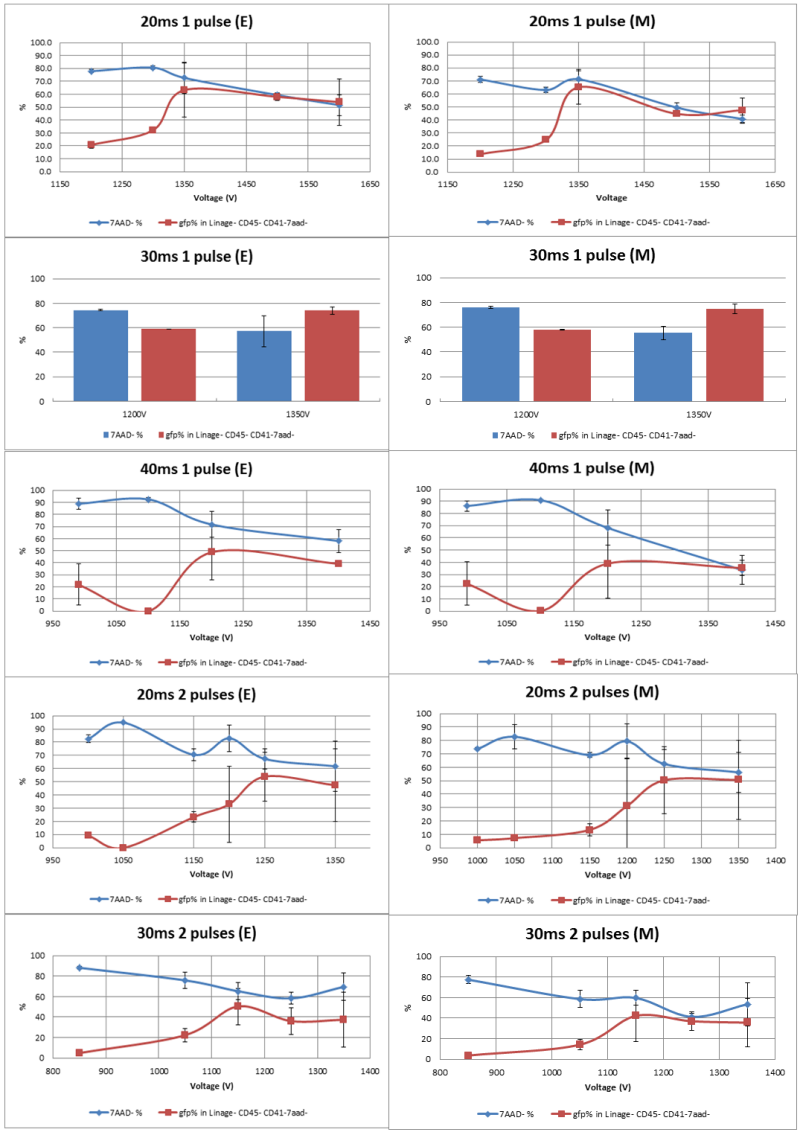

Figure 8.2.1-1. Cell survival and transfection efficiency measured as percentage of parent population in optimization experiments. Primary AGM cells from E11.5 BL6XBL6 embryos were used. "7AAD- %" was percentage of 7AAD negative cells in all cellular events. "GFP% in Lineage- CD45- CD41- 7AAD- " was percentage of GFP positive cells in all Lineage$^-$CD45$^-$CD41$^-$7AAD$^-$ cells Figures labelled with "E" displayed data gathered from samples stained with antibodies against endothelial markers, and figures labelled with "M" displayed data gathered from samples stained with antibodies against mesenchymal markers. Error bars showed standard derivation calculated by STDEV.S formula in Excel 2010. (Different conditions were experimented from one to three times.)

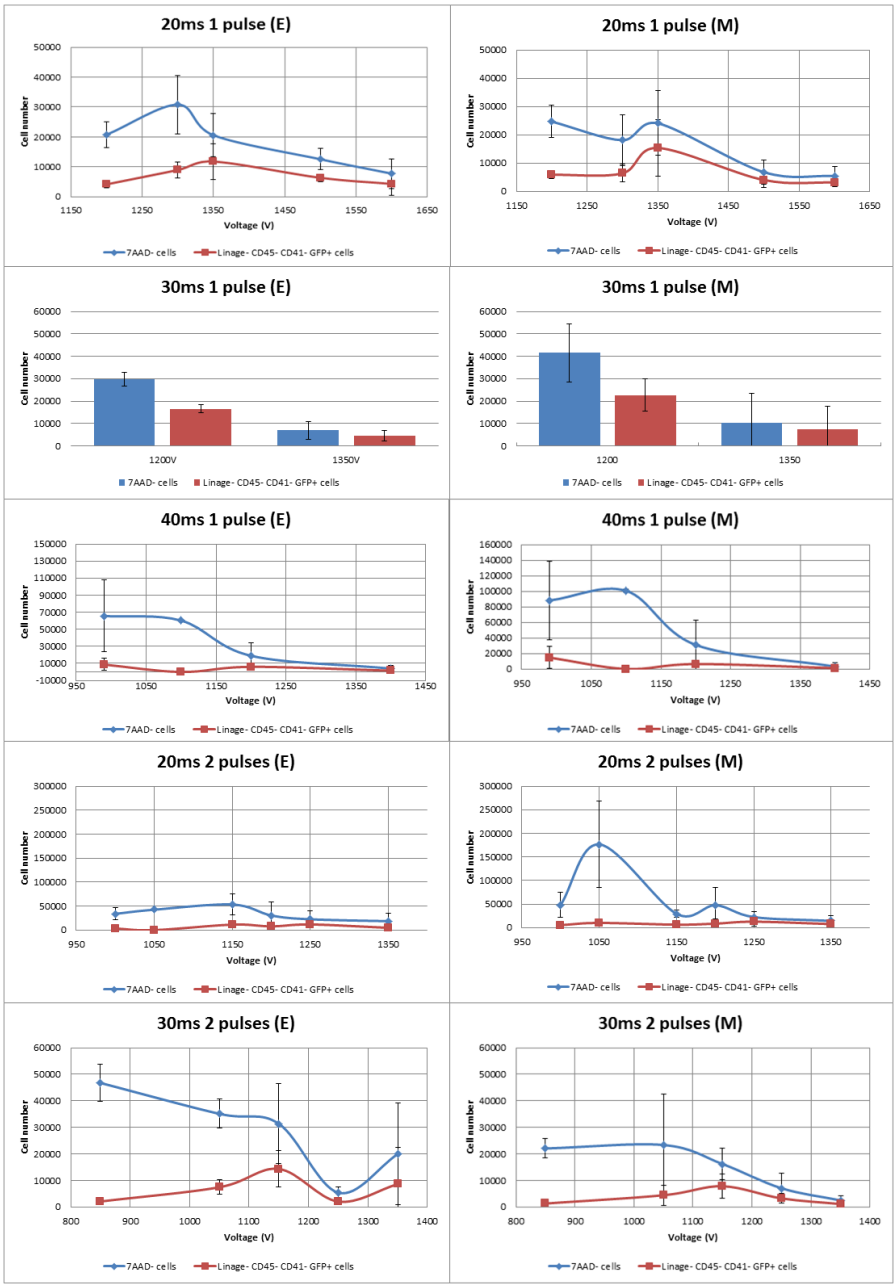

Figure 8.2.1-2. Cell survival and transfection efficiency measured as cell yield in optimization experiments. Primary AGM cells from E11.5 BL6XBL6 embryos were used. "7AAD$^-$ cells" was total number of 7AAD negative cells calculated using counting beads and normalized to 100000 input cells. "Lineage$^-$CD45$^-$CD41$^-$7AAD$^-$ GFP$^+$ cells" was total number of Lineage$^-$CD45$^-$CD41$^-$7AAD$^-$GFP$^+$ cells calculated using similar methods. Figures labelled with "E" displayed data gathered from samples stained with antibodies against endothelial markers, and figures labelled with "M" displayed data gathered from samples stained with antibodies against mesenchymal markers. Error bars showed standard derivation calculated by STDEV.S formula in Excel 2010. (Different conditions were experimented from one to three times.)

a)

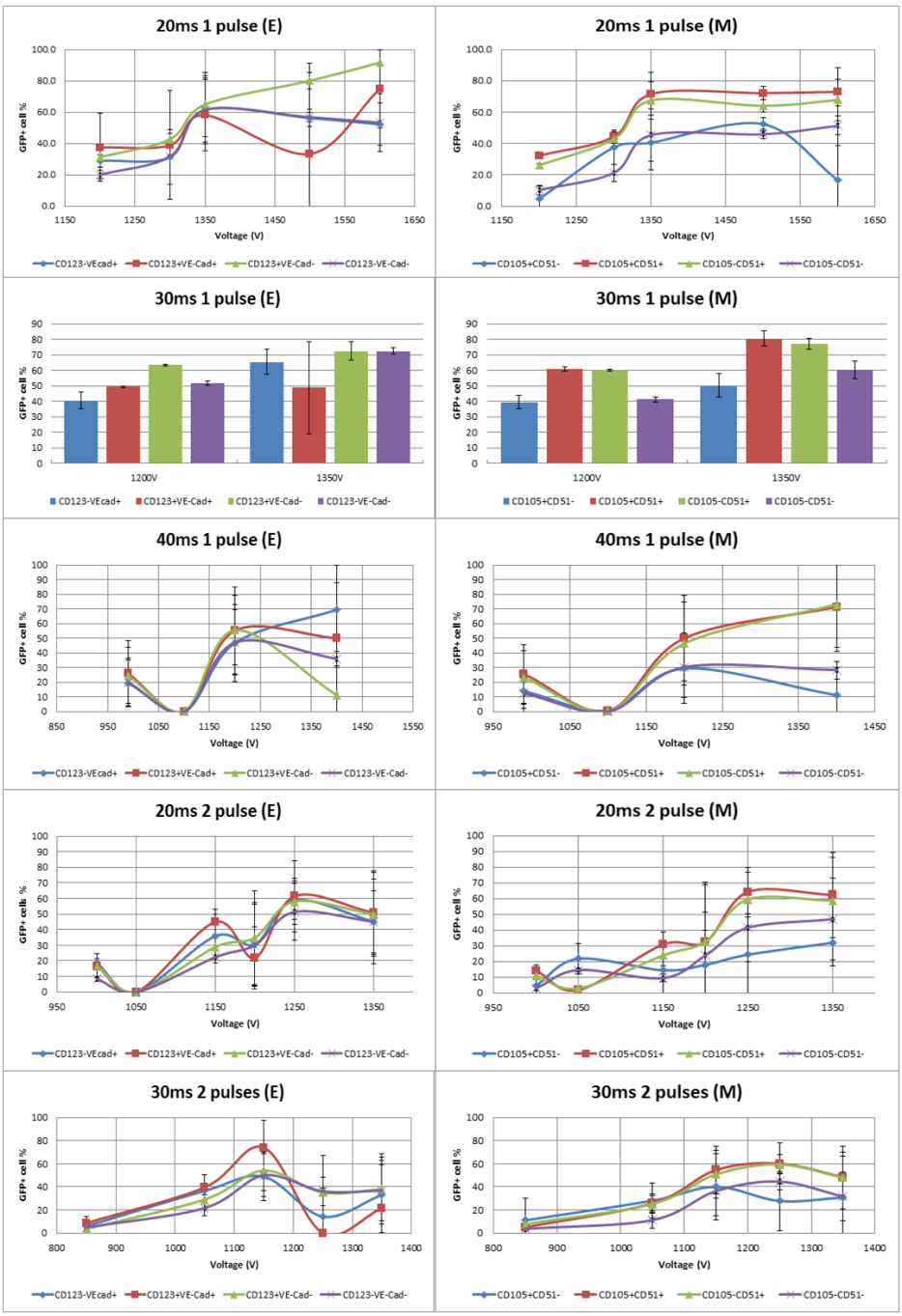
20ms 1 pulse (E)
20ms 1 pulse (M)
30ms 1 pulse (E)
30ms 1 pulse (M)
40ms 1 pulse (E)
40ms 1 pulse (M)
20ms 2 pulse (E)
20ms 2 pulse (M)
30ms 2 pulses (E)
30ms 2 pulses (M)
GFP+ cell %
Voltage (V)
1200V
1350V
CD123-VEcad+
CD123+VE-Cad+
CD123+VE-Cad-
CD123-VE-Cad-
CD105+CD51-
CD105+CD51+
CD105-CD51+
CD105-CD51-

b)

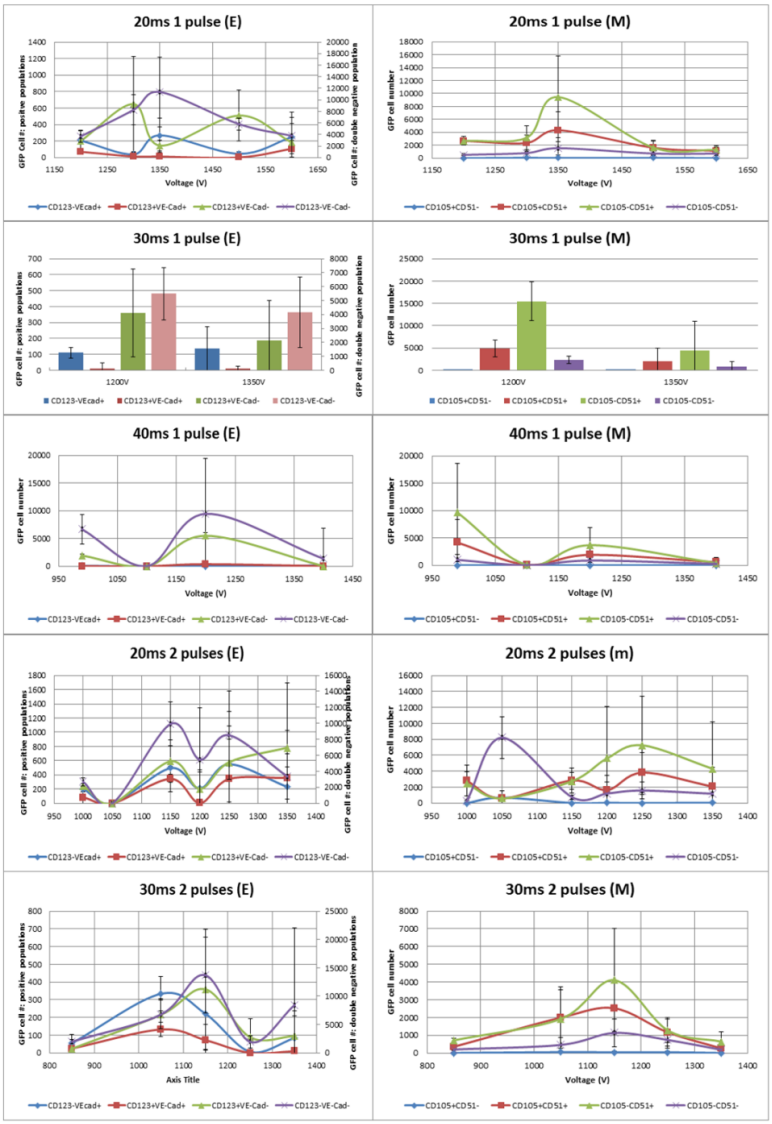

Figure 8.2.1-3 Marker specific transfection yield of optimization experiments. Primary AGM cells from E11.5 BL6XBL6 embryos were used. Figures labelled with "E" displayed data gathered from samples stained with antibodies against endothelial markers, and figures labelled with "M" displayed data gathered from samples stained with antibodies against mesenchymal markers. a) Cell survival and transfection efficiency measured as percentage of parental populations. b) Cell survival and transfection efficiency measured as cell yield. Number of GFP$^+$ cells was calculated using counting beads and normalized to 100000 input cells. Note for endothelial staining, most cells were VE-Cad$^-$CD123$^-$, so these double negative populations were plotted on secondary Y axis. Error bars showed standard derivation calculated by STDEV.S formula in Excel 2010. Each condition was replicated from 2 to 8 times.

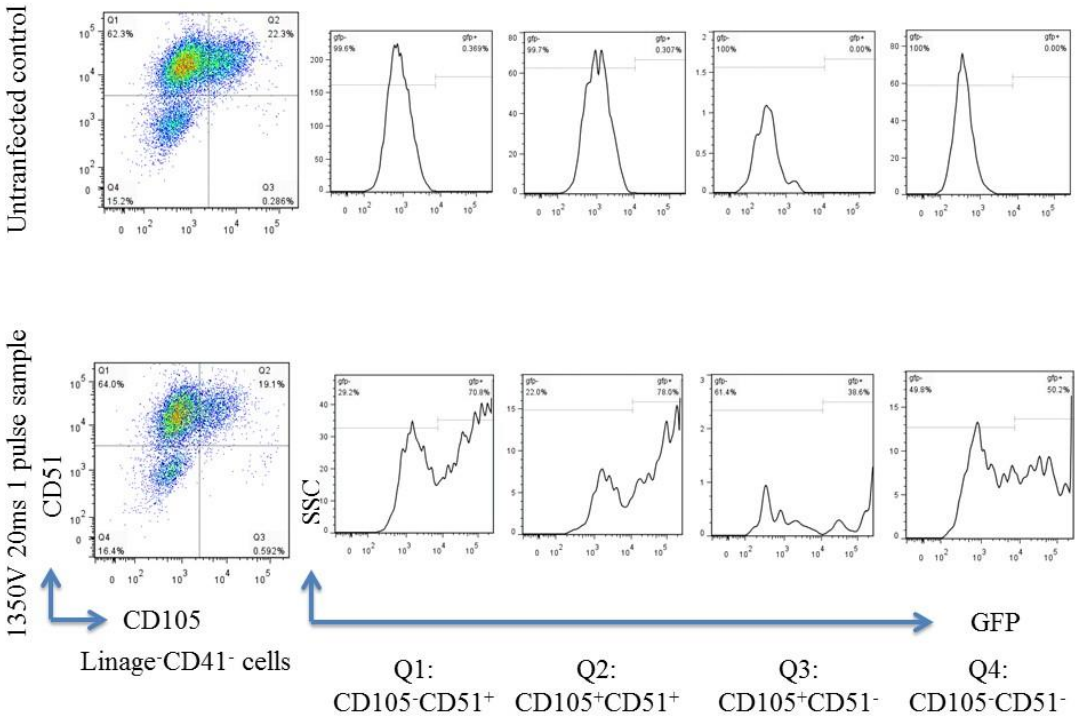

Figure 8.2.1-4 Transfection efficiency was not biased to specific cell compartment. Left plot was CD105 and CD51 expression of Lineage^{-}CD51^{-} population, right four plots were GFP expression of each quadrant of left plot.

8.2.2. Establishing feeder cell lines from mouse Embryos

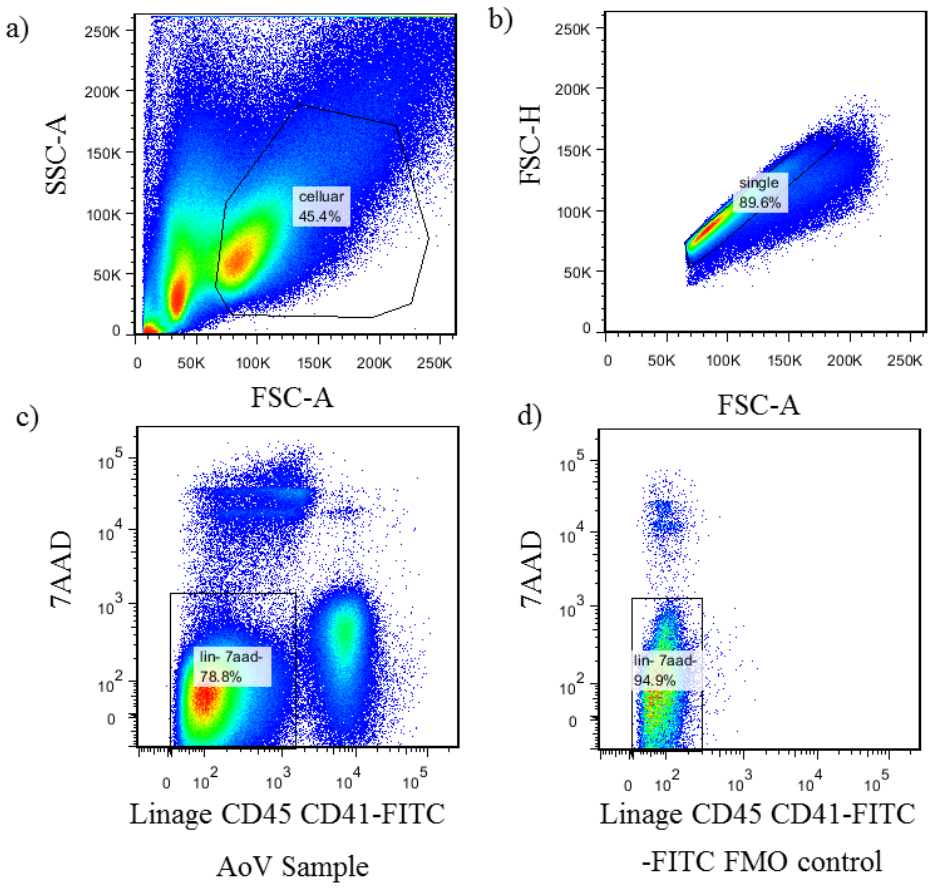

Figure 8.2.2-1. Gating strategy used to sort E11.5 primary cells. Experiment showed here was ventral aorta samples stained with CD123 and mSCF. Lineage, CD45, CD41 were stained by biotinylated antibody and labelled with streptavidin-FITC antibody. a) All events were displayed on SSC-FSC plot and only events with size and shape similar to a cell were selected. b) Single cells were selected based on FSC-H and FSC-A signal. c) FACS plot showed ventral aorta sample with 7AAD and FITC channel, only 7AAD$^-$ (live) and FITC$^-$ (CD45$^-$,CD41$^-$, Ter119$^-$,Mac-1$^-$, Gr1$^-$ cells were selected for further studies. d) Similar FACS plot showed FMO –FITC control made AGM derived primary cells from same litter. In this controls, all other antibodies were same with AoV sample, but Lineage, CD45 CD41 antibodies were not stained.

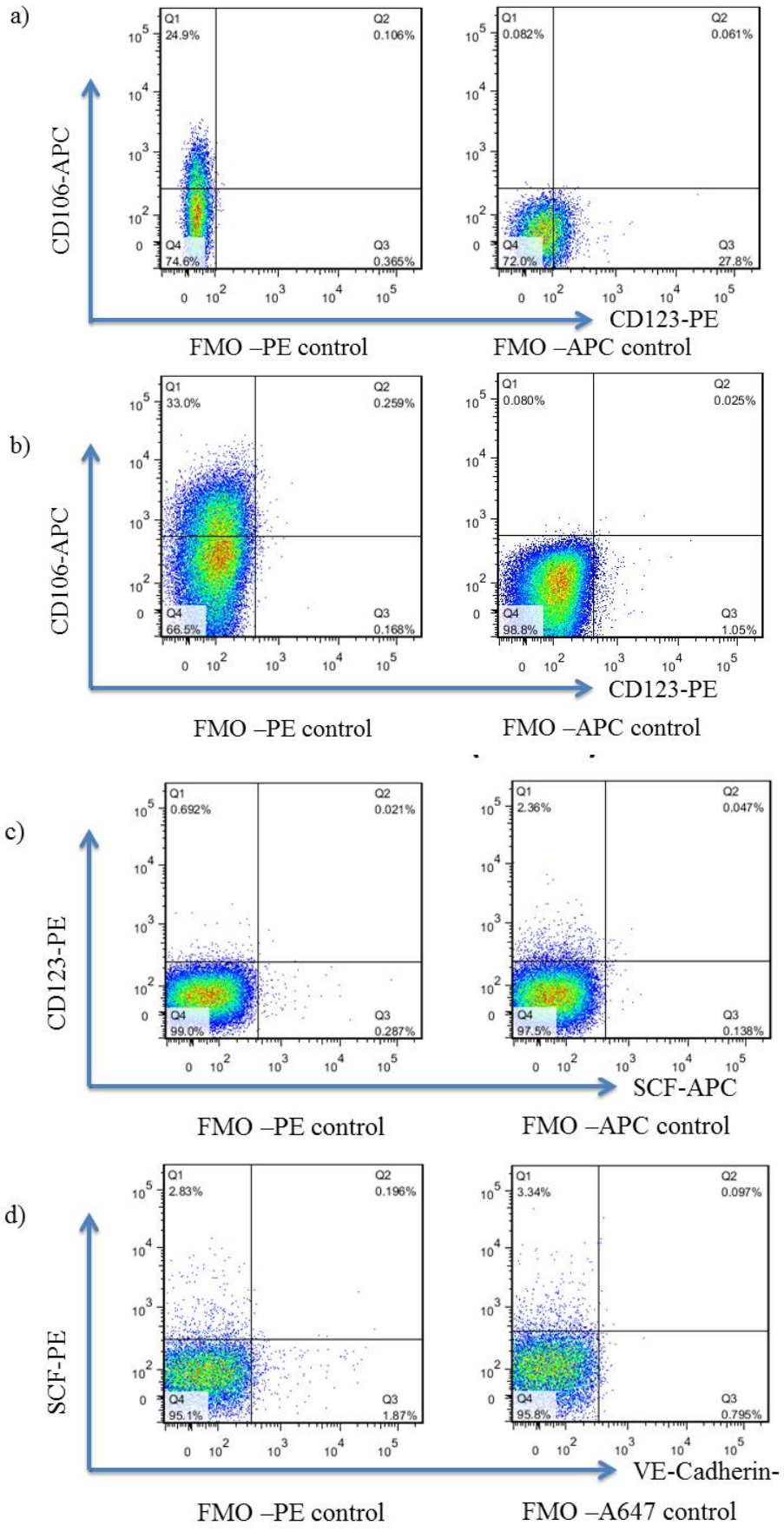
a)
CD106-APC
CD123-PE
Q1 24.9%
Q2 0.106%
Q4 74.6%
Q3 0.365%
Q1 0.082%
Q2 0.061%
Q4 72.0%
Q3 27.8%
FMO –PE control
FMO –APC control
b)
CD106-APC
CD123-PE
Q1 33.0%
Q2 0.259%
Q4 66.5%
Q3 0.168%
Q1 0.080%
Q2 0.025%
Q4 98.8%
Q3 1.05%
FMO –PE control
FMO –APC control
c)
CD123-PE
SCF-APC
Q1 0.692%
Q2 0.021%
Q4 99.0%
Q3 0.287%
Q1 2.36%
Q2 0.047%
Q4 97.5%
Q3 0.138%
FMO –PE control
FMO –APC control
d)
SCF-PE
VE-Cadherin-
Q1 2.83%
Q2 0.196%
Q4 95.1%
Q3 1.87%
Q1 3.34%
Q2 0.097%
Q4 95.8%
Q3 0.795%
FMO –PE control
FMO –A647 control

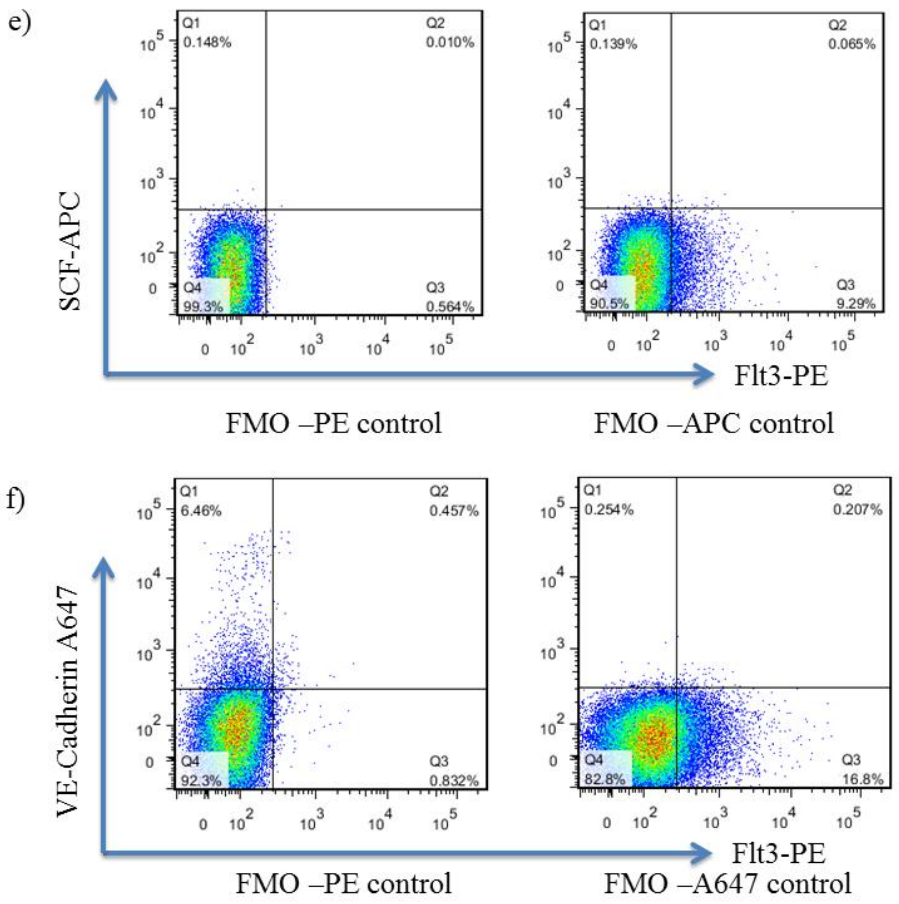

Figure 8.2.2-2. FACS plot of FMO –PE and FMO –APC controls used to set gates for marker of interest. a) P12-001/002 experiment with CD123 and CD106. b) P12-027 experiment with CD123 and CD106. c) P12-003/004 experiment with CD123 and SCF. d) P12-006/007 experiment with VE-Cadherin and SCF. Note the FMO –SCF control had 2.83% of SCF positive cells, higher than FMO-SCF control in panel e). e) P12-008/009 experiment with Flt3 and SCF. f) P12-016 experiment with VE-Cadherin and Flt3.

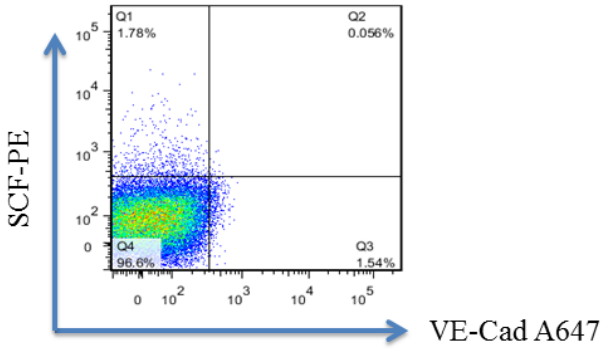

Figure 8.2.2-3. FMO –PE control of VE-Cadherin SCF sorting.

8.3.Characterization of AoV Cell lines

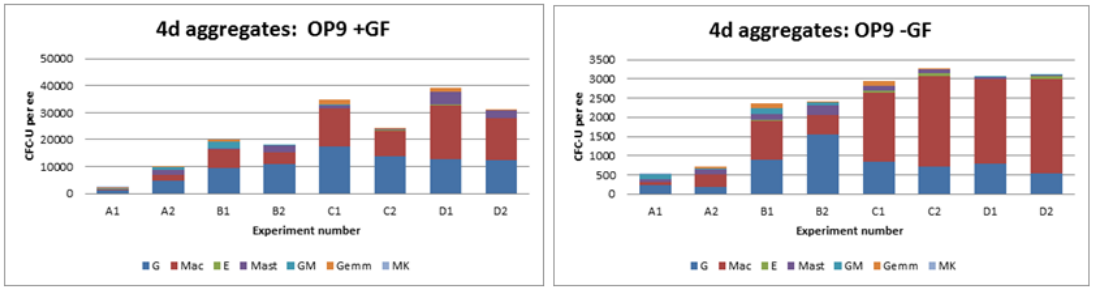

Figure 8.3-1. Colonies generated from OP9 positive controls in 8 different experiments. In each experiment, 300-500K feeder cells were aggregated with 0.6-1 embryo equivalent (ee) E11.5 AGM derived primary cells and cultured for 4 days without feeding. Then for "with growth factor" conditions, 0.01ee of cultured cells were distributed to two dishes, for "without growth factor" conditions, 0.1ee of cultured cells were distributed to two dishes. 7 days later, colonies in both dishes were counted and calculated into CFC-U per ee and averaged.

a)

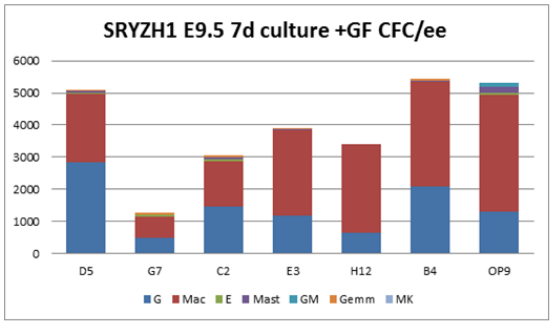
SRYZH1 E9.5 7d culture +GF CFC/ee
6000
5000
4000
3000
2000
1000
0
D5 G7 C2 E3 H12 B4 OP9
G Mac E Mast GM Gemm MK

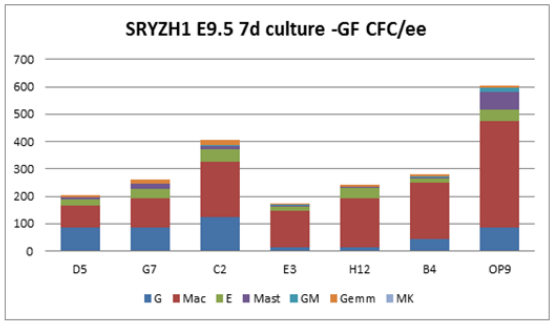
SRYZH1 E9.5 7d culture -GF CFC/ee
700
600
500
400
300
200
100
0
D5 G7 C2 E3 H12 B4 OP9
G Mac E Mast GM Gemm MK

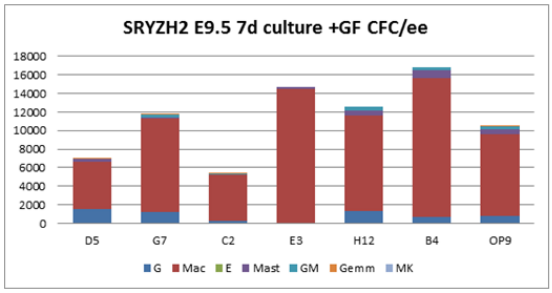
SRYZH2 E9.5 7d culture +GF CFC/ee
18000
16000
14000
12000
10000
8000
6000
4000
2000
0
D5 G7 C2 E3 H12 B4 OP9
G Mac E Mast GM Gemm MK

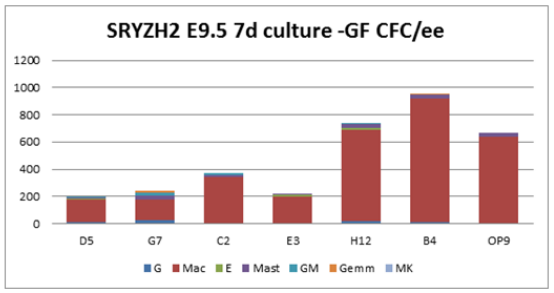
SRYZH2 E9.5 7d culture -GF CFC/ee
1200
1000
800
600
400
200
0
D5 G7 C2 E3 H12 B4 OP9
G Mac E Mast GM Gemm MK

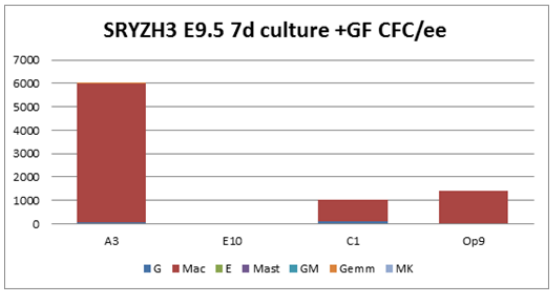
SRYZH3 E9.5 7d culture +GF CFC/ee
7000
6000
5000
4000
3000
2000
1000
0
A3 E10 C1 Op9
G Mac E Mast GM Gemm MK

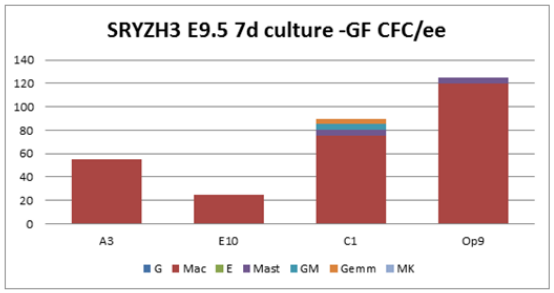
SRYZH3 E9.5 7d culture -GF CFC/ee
140
120
100
80
60
40
20
0
A3 E10 C1 Op9
G Mac E Mast GM Gemm MK

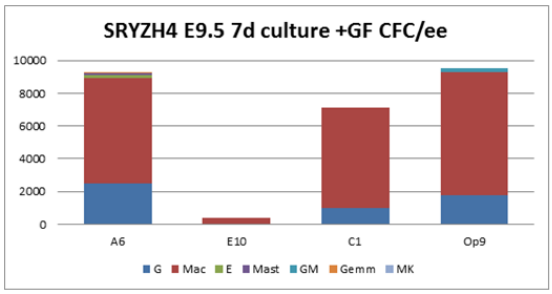
SRYZH4 E9.5 7d culture +GF CFC/ee
10000
8000
6000
4000
2000
0
A6 E10 C1 Op9
G Mac E Mast GM Gemm MK

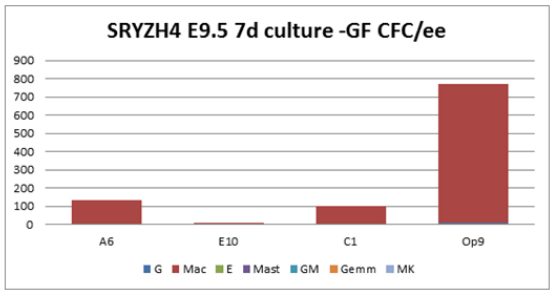
SRYZH4 E9.5 7d culture -GF CFC/ee
900
800
700
600
500
400
300
200
100
0
A6 E10 C1 Op9
G Mac E Mast GM Gemm MK

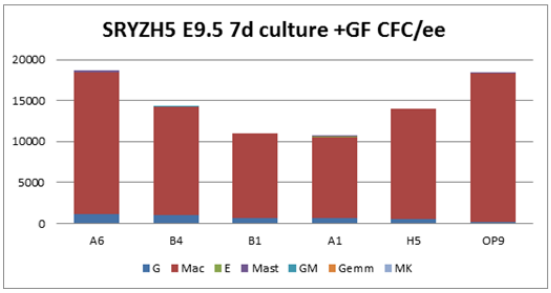
SRYZH5 E9.5 7d culture +GF CFC/ee
20000
15000
10000
5000
0
A6
B4
B1
A1
H5
OP9
G Mac E Mast GM Gemm MK

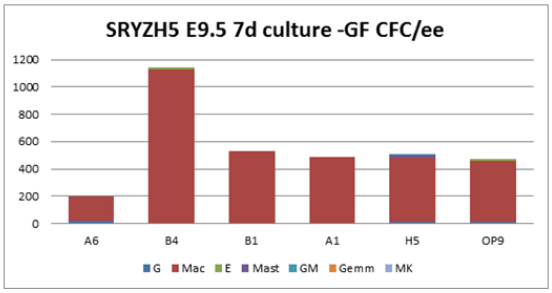
SRYZH5 E9.5 7d culture -GF CFC/ee
1200
1000
800
600
400
200
0
A6
B4
B1
A1
H5
OP9
G Mac E Mast GM Gemm MK

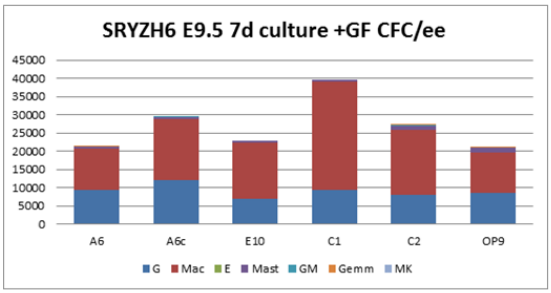
SRYZH6 E9.5 7d culture +GF CFC/ee
45000
40000
35000
30000
25000
20000
15000
10000
5000
0
A6
A6c
E10
C1
C2
OP9
G Mac E Mast GM Gemm MK

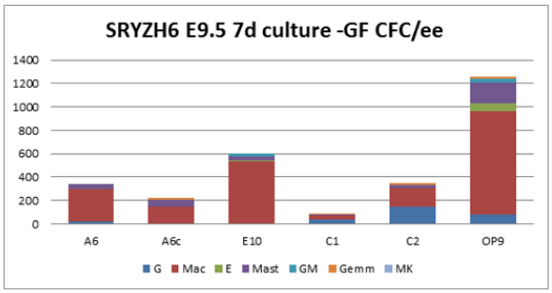
SRYZH6 E9.5 7d culture -GF CFC/ee
1400
1200
1000
800
600
400
200
0
A6
A6c
E10
C1
C2
OP9
G Mac E Mast GM Gemm MK

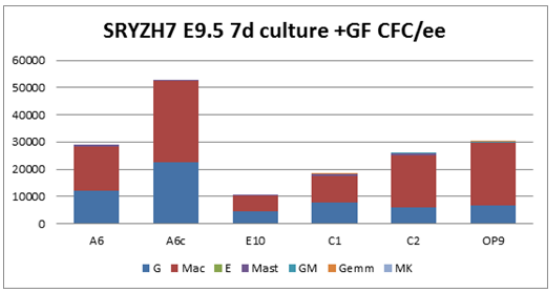
SRYZH7 E9.5 7d culture +GF CFC/ee
60000
50000
40000
30000
20000
10000
0
A6
A6c
E10
C1
C2
OP9
G Mac E Mast GM Gemm MK

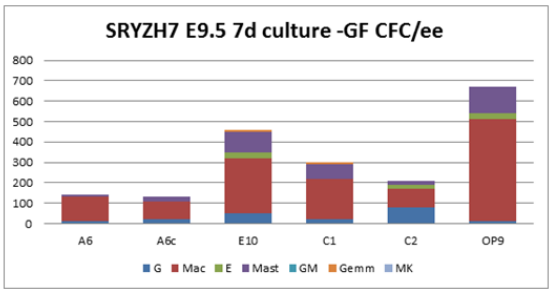
SRYZH7 E9.5 7d culture -GF CFC/ee
800
700
600
500
400
300
200
100
0
A6
A6c
E10
C1
C2
OP9
G Mac E Mast GM Gemm MK

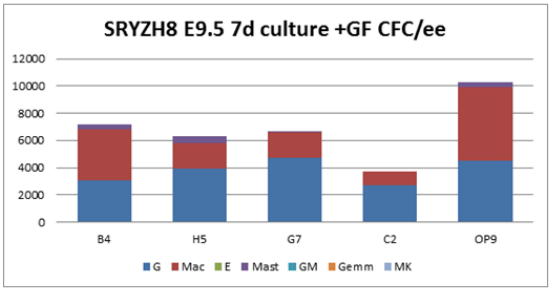
SRYZH8 E9.5 7d culture +GF CFC/ee
12000
10000
8000
6000
4000
2000
0
B4
H5
G7
C2
OP9
G Mac E Mast GM Gemm MK

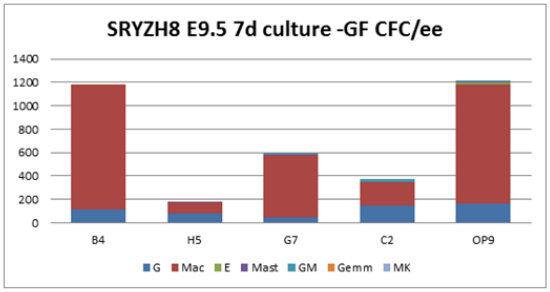
SRYZH8 E9.5 7d culture -GF CFC/ee
1400
1200
1000
800
600
400
200
0
B4
H5
G7
C2
OP9
G Mac E Mast GM Gemm MK

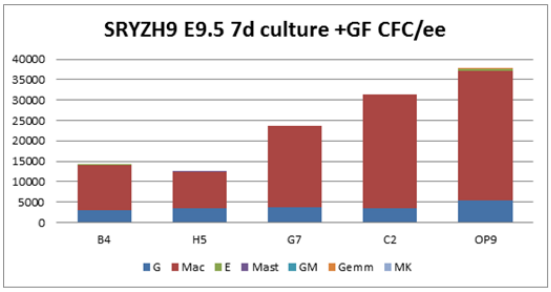
SRYZH9 E9.5 7d culture +GF CFC/ee
40000
35000
30000
25000
20000
15000
10000
5000
0
B4
H5
G7
C2
OP9
G Mac E Mast GM Gemm MK

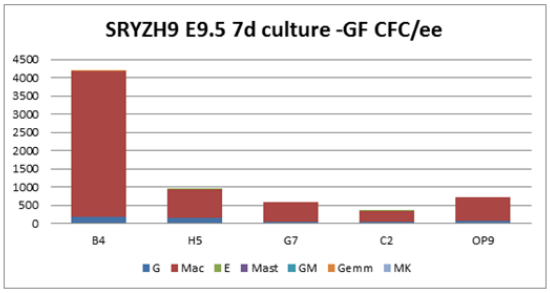
SRYZH9 E9.5 7d culture -GF CFC/ee
4500
4000
3500
3000
2500
2000
1500
1000
500
0
B4
H5
G7
C2
OP9
G Mac E Mast GM Gemm MK

b)

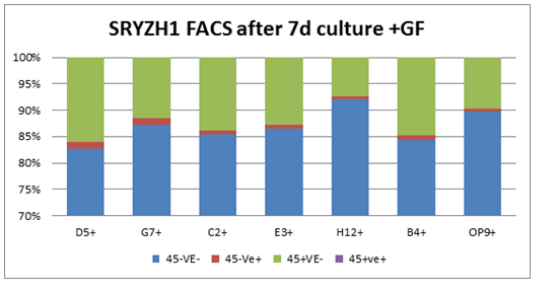
SRYZH1 FACS after 7d culture +GF
100%
95%
90%
85%
80%
75%
70%
D5+
G7+
C2+
E3+
H12+
B4+
OP9+
45-VE-
45-Ve+
45+VE-
45+ve+

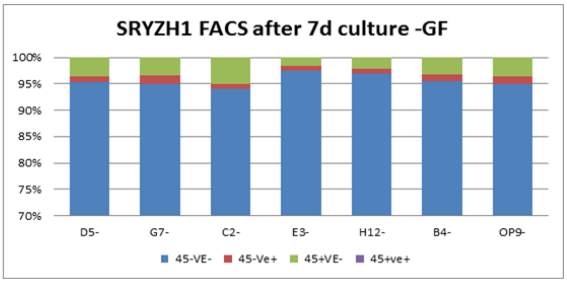
SRYZH1 FACS after 7d culture -GF
100%
95%
90%
85%
80%
75%
70%
D5-
G7-
C2-
E3-
H12-
B4-
OP9-
45-VE-
45-Ve+
45+VE-
45+ve+

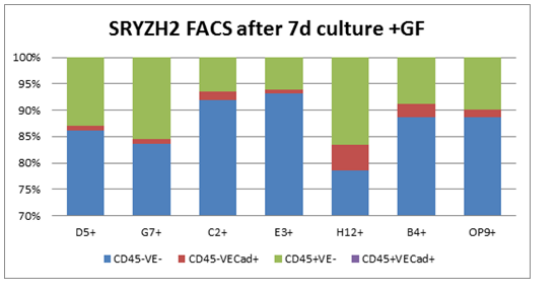
SRYZH2 FACS after 7d culture +GF
100%
95%
90%
85%
80%
75%
70%
D5+
G7+
C2+
E3+
H12+
B4+
OP9+
CD45-VE-
CD45-VECad+
CD45+VE-
CD45+VECad+

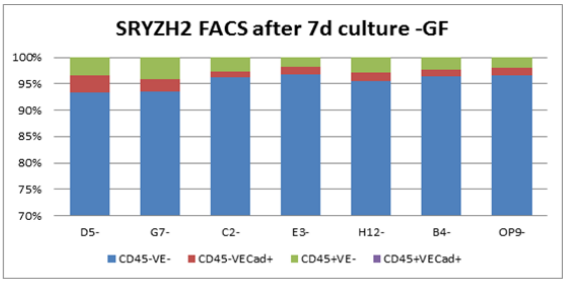
SRYZH2 FACS after 7d culture -GF
100%
95%
90%
85%
80%
75%
70%
D5-
G7-
C2-
E3-
H12-
B4-
OP9-
CD45-VE-
CD45-VECad+
CD45+VE-
CD45+VECad+

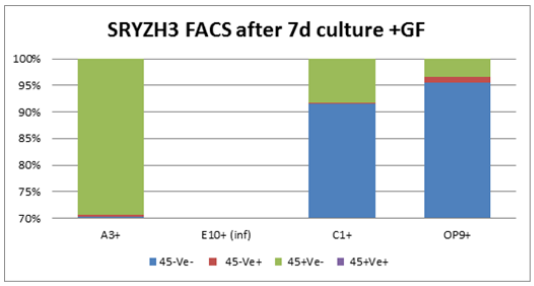
SRYZH3 FACS after 7d culture +GF
100%
95%
90%
85%
80%
75%
70%
A3+
E10+ (inf)
C1+
OP9+
45-Ve-
45-Ve+
45+Ve-
45+Ve+

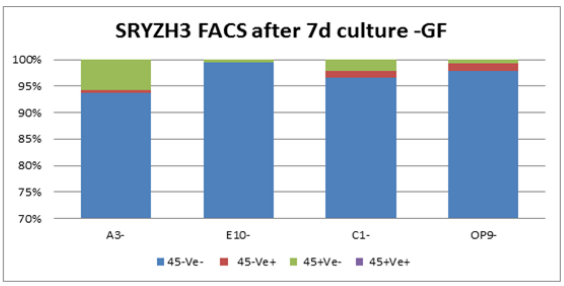
SRYZH3 FACS after 7d culture -GF
100%
95%
90%
85%
80%
75%
70%
A3-
E10-
C1-
OP9-
45-Ve-
45-Ve+
45+Ve-
45+Ve+

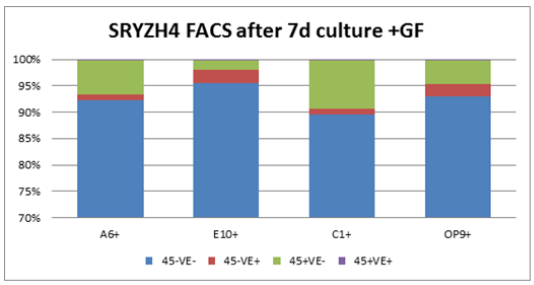
SRYZH4 FACS after 7d culture +GF
100%
95%
90%
85%
80%
75%
70%
A6+
E10+
C1+
OP9+
45-VE-
45-VE+
45+VE-
45+VE+

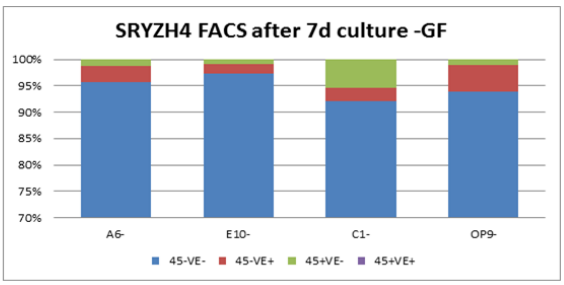
SRYZH4 FACS after 7d culture -GF
100%
95%
90%
85%
80%
75%
70%
A6-
E10-
C1-
OP9-
45-VE-
45-VE+
45+VE-
45+VE+

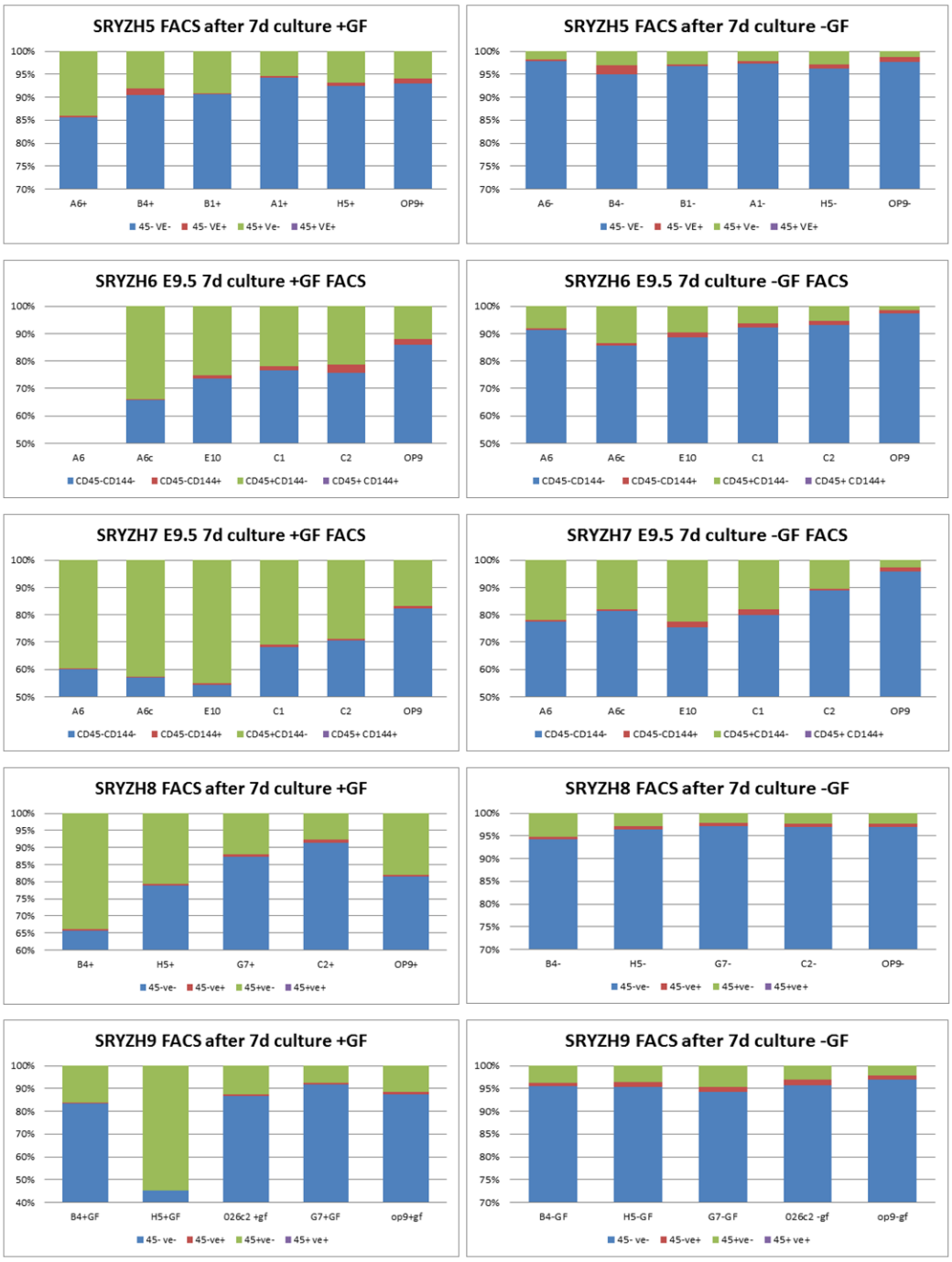

Figure 8.3-2. Flow cytometry and CFU-C analysis results of aggregates after 7 days of culture. a) CFU-C readings from culture after 7 days of culture. For +GF conditions, 0.01ee of cells were used in CFU assays, for –GF conditions, 0.1ee of cells were used. b). Results of flow analysis of aggregates after 7 days of culture. Note SRYZH was the surfix of name ofmy experiments. Note following membranes were sunk or infected during culture. E3+GF in SRYZH1; E3+GF, H12+GF,B4+GF,OP9+GF in SRYZH2; E10+GF, A3+GF in SRYZH3; A1-GF in SRYZH5.

a) SRYZH2

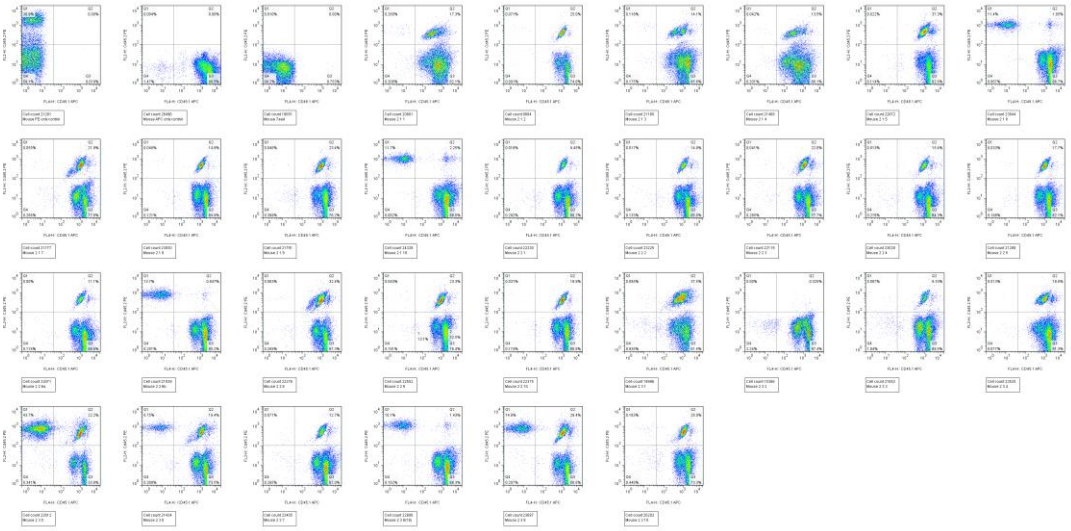

b) SRYZH4

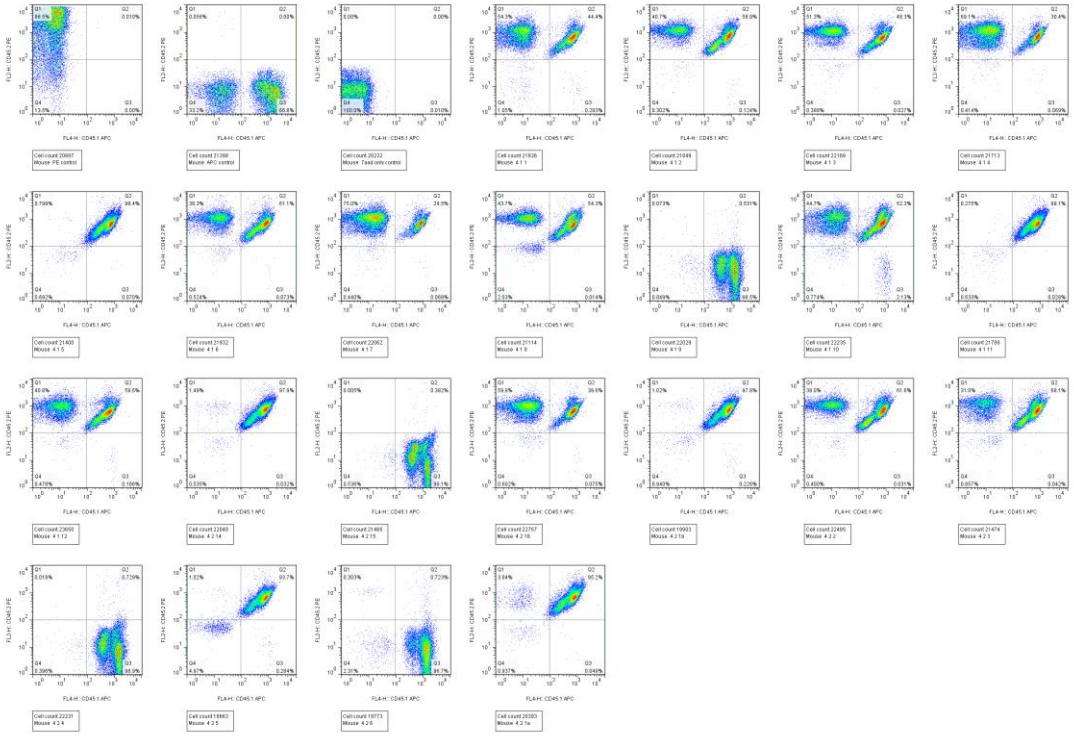

c) SRYZH6

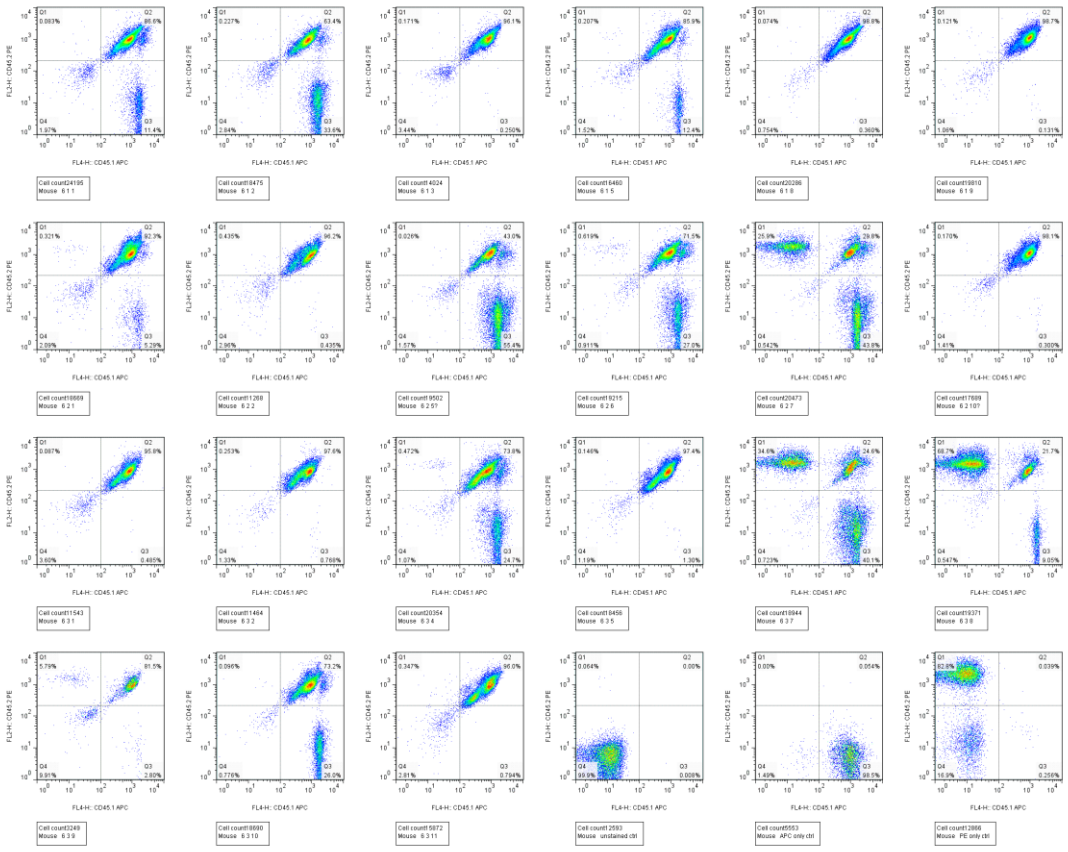

d) SRYZH7

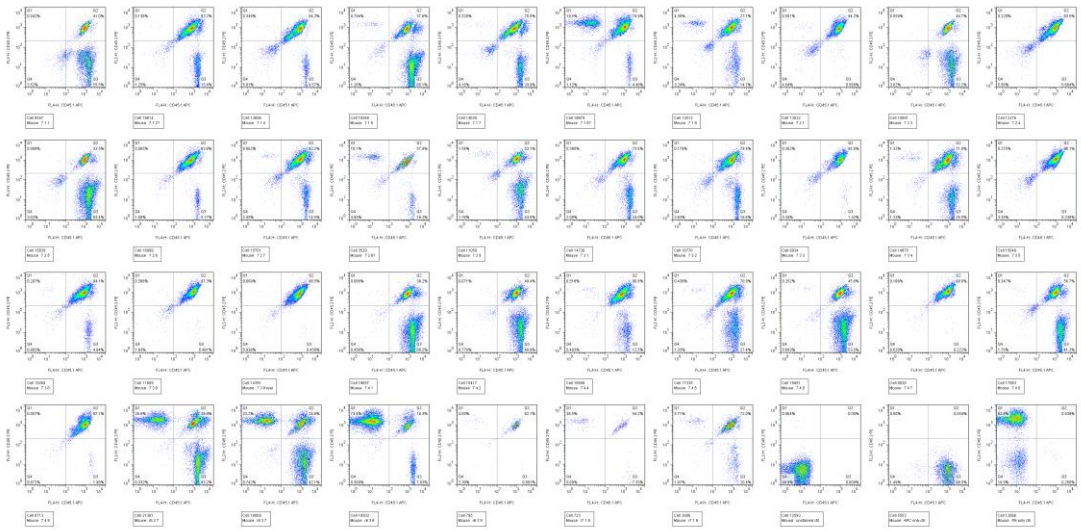

e) SRYZH9

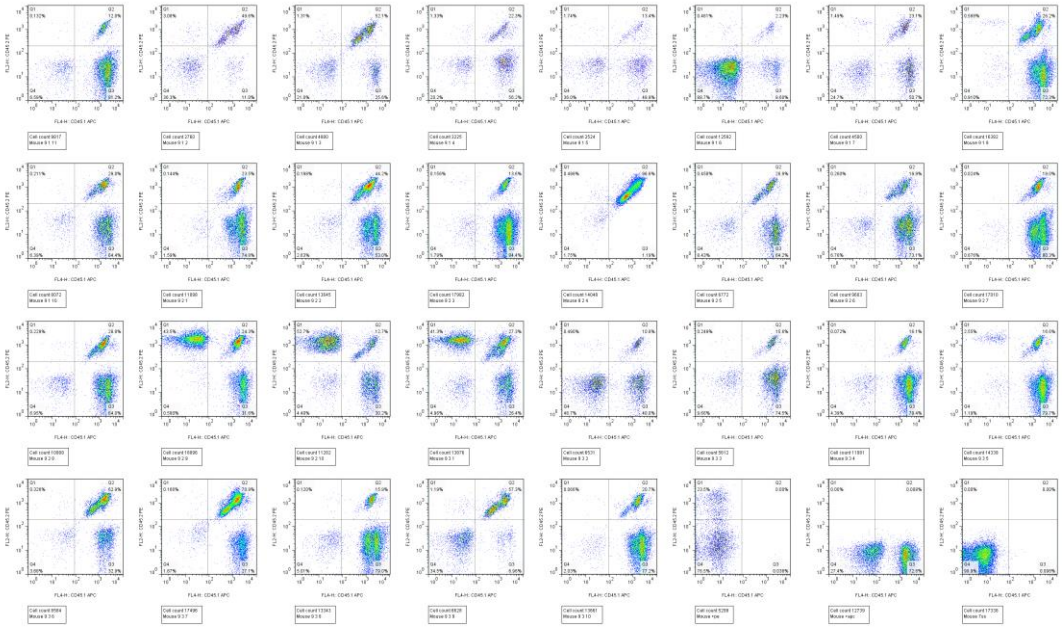

Figure 8.3-3. Flow cytometry plots of all recipients survived until 6 weeks post transplantation. That included 108 recipients received experimental aggregates and 24 recipients received positive control aggregates. Those aggregates were transplanted in 5 different experiments belonged to 4 batches (SRYZH6 and SRYZH7 belonged to the same batch). Each experiment had its own OP9 control mice. For every bleeding, three separate blood samples were prepared for two single stain controls and unstained negative control. Each plot in this figure was labelled with original earmark number, they were explained in injection record files (see supplementary electronical files).

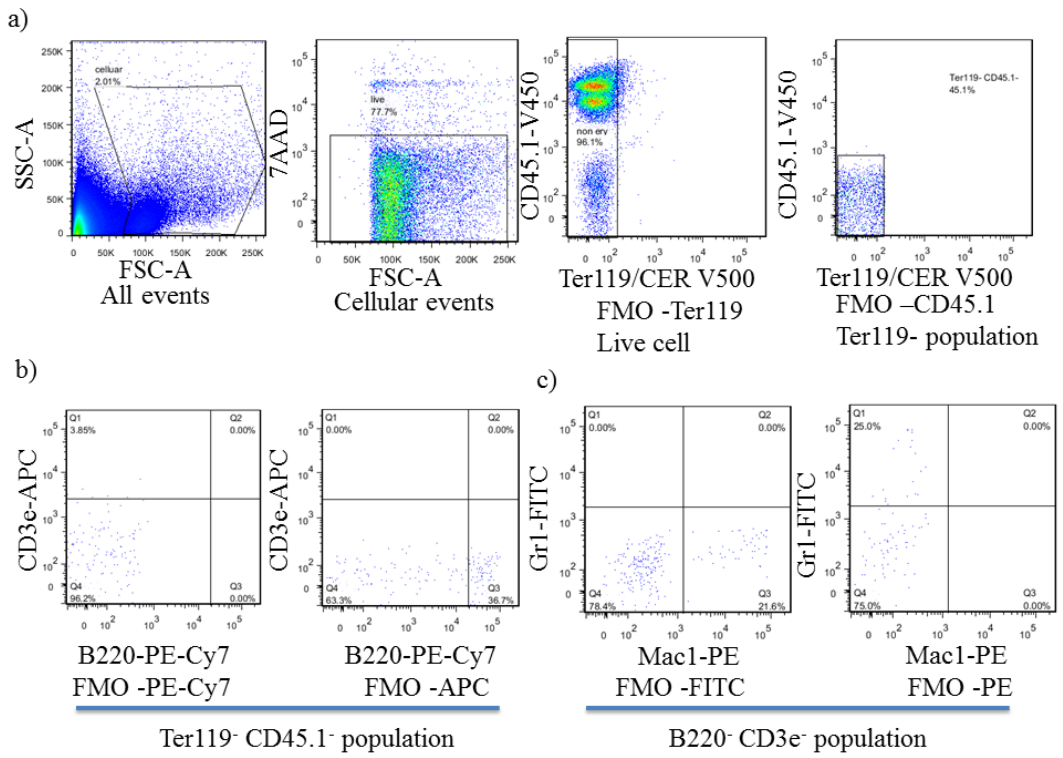

Figure 8.3-4. Gating and FMO controls of multilineage FACS analysis. Panel a) showed gating to remove debris, dead cell, Ter110^{+} cells, CD45.1^{+} recipient and carrier cells in a stepwise manner (left to right). Panel b) showed FMO controls to set gate for B220 and CD3e in Ter119^{-}CD45^{-} population from panel a. Panel c) showed FMO controls to set gate for Mac1 and Gr1 in B220^{-}CD3e^{-} population from panel b.

a)

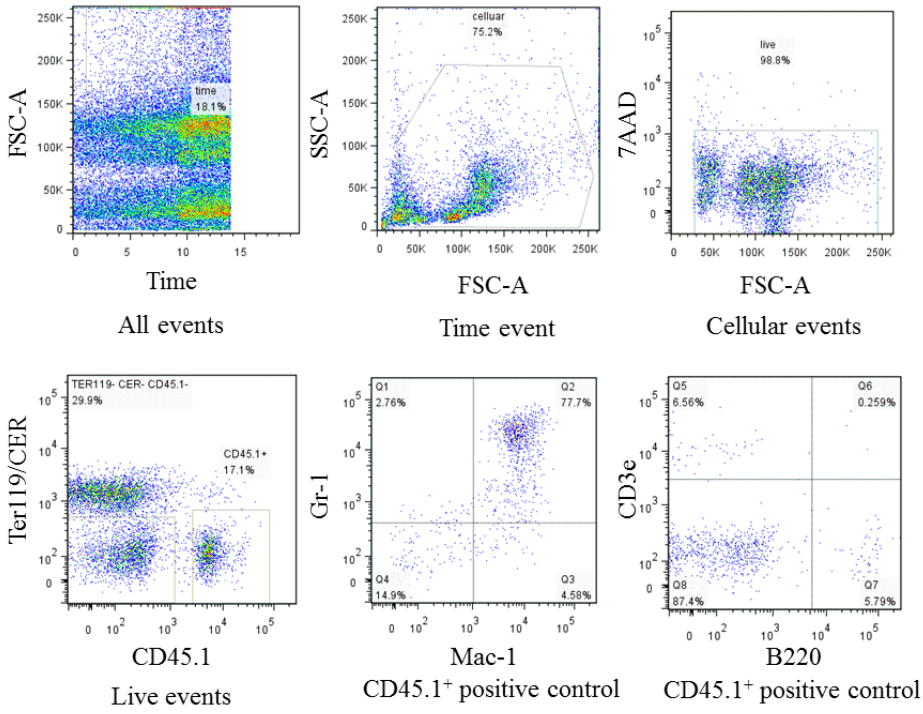
FSC-A
Time
time
18.1%
All events
SSC-A
FSC-A
cellular
75.2%
Time event
7AAD
FSC-A
live
98.8%
Cellular events
Ter119/CER
CD45.1
TER119- CER- CD45.1-
29.9%
CD45.1+
17.1%
Live events
Gr-1
Mac-1
Q1
2.76%
Q2
77.7%
Q4
14.9%
Q3
4.58%
CD45.1+ positive control
CD3e
B220
Q5
6.56%
Q6
0.259%
Q8
87.4%
Q7
5.79%
CD45.1+ positive control

b)

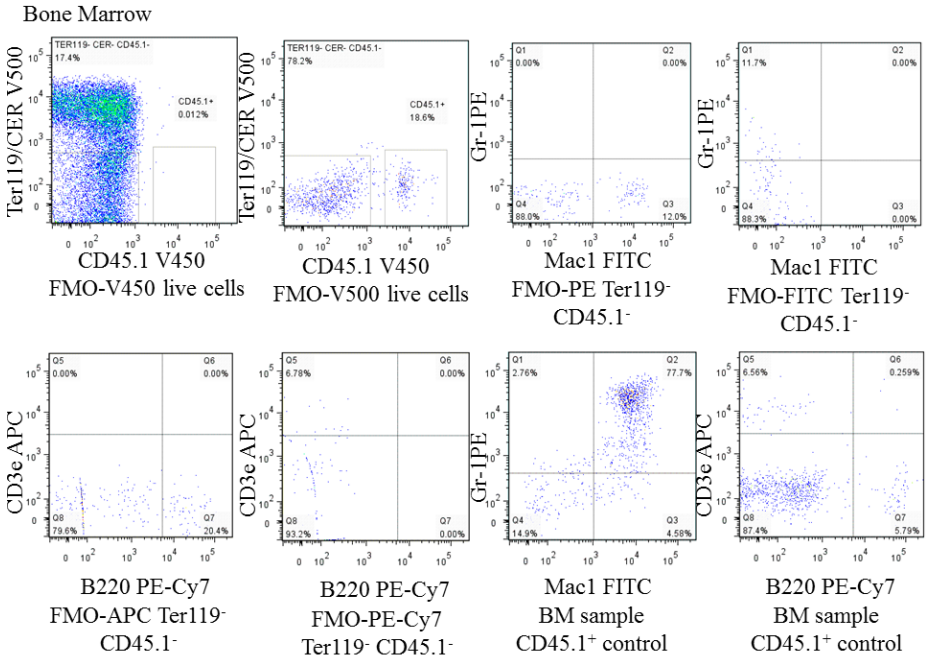
Bone Marrow
Ter119/CER V500
CD45.1 V450
TER119- CER- CD45.1-
17.4%
CD45.1+
0.012%
FMO-V450 live cells
TER119- CER- CD45.1-
78.2%
CD45.1+
18.6%
FMO-V500 live cells
Gr-1PE
Mac1 FITC
Q1
0.00%
Q2
0.00%
Q4
88.0%
Q3
12.0%
FMO-PE Ter119- CD45.1-
Q1
11.7%
Q2
0.00%
Q4
88.3%
Q3
0.00%
FMO-FITC Ter119- CD45.1-
CD3e APC
B220 PE-Cy7
Q5
0.00%
Q6
0.00%
Q8
79.6%
Q7
20.4%
FMO-APC Ter119- CD45.1-
Q5
6.78%
Q6
0.00%
Q8
93.2%
Q7
0.00%
FMO-PE-Cy7 Ter119- CD45.1-
Q1
2.76%
Q2
77.7%
Q4
14.9%
Q3
4.58%
BM sample CD45.1+ control
Q5
6.56%
Q6
0.259%
Q8
87.4%
Q7
5.79%
BM sample CD45.1+ control

c)

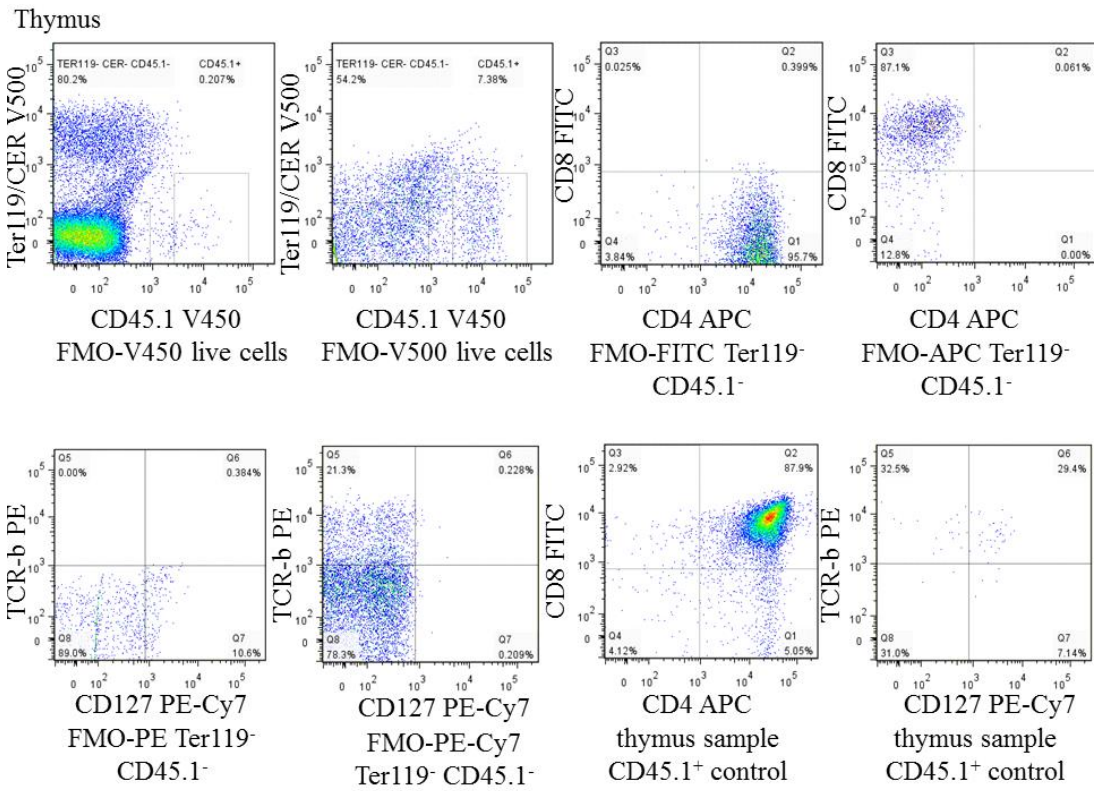

Figure 8.3-5. Gating and FMO for multi-organ multilineage analysis. a) Gating strategy for multilineage analysis. All sample groups shared similar gating strategy. The sample shown was from bone marrow. b) FMO control sets for bone marrow/blood/spleen. c) FMO control sets for thymus. Note bone marrow, blood and spleen samples shared same set of antibodies, while thymus used another set of antibodies, so two sets of FMO controls were used in this analysis.

Blood

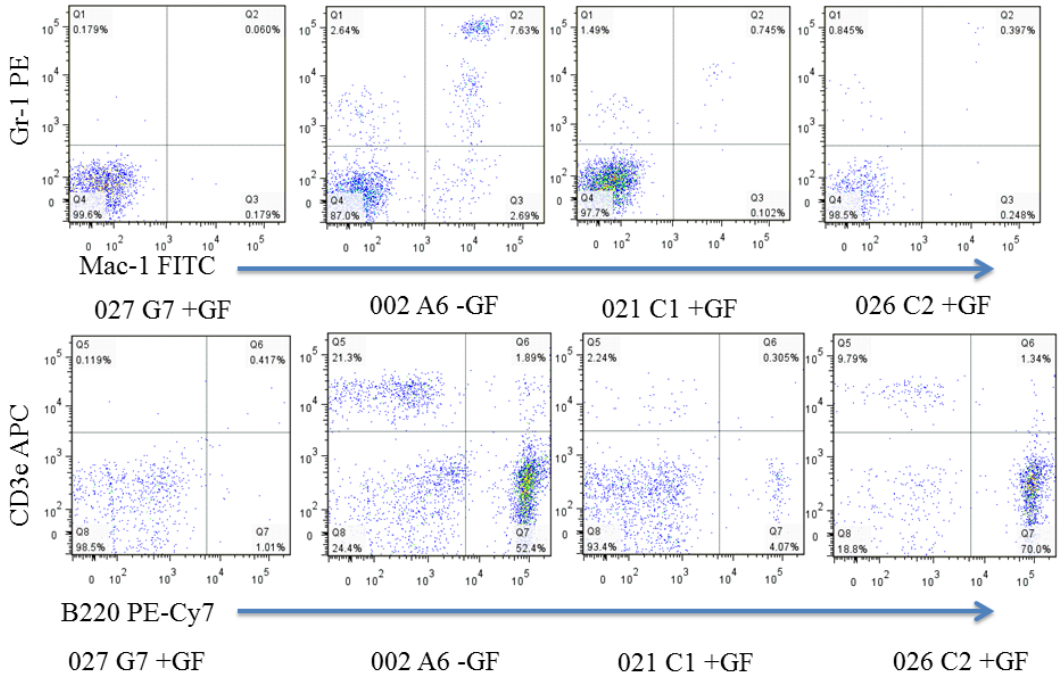

Bone Marrow

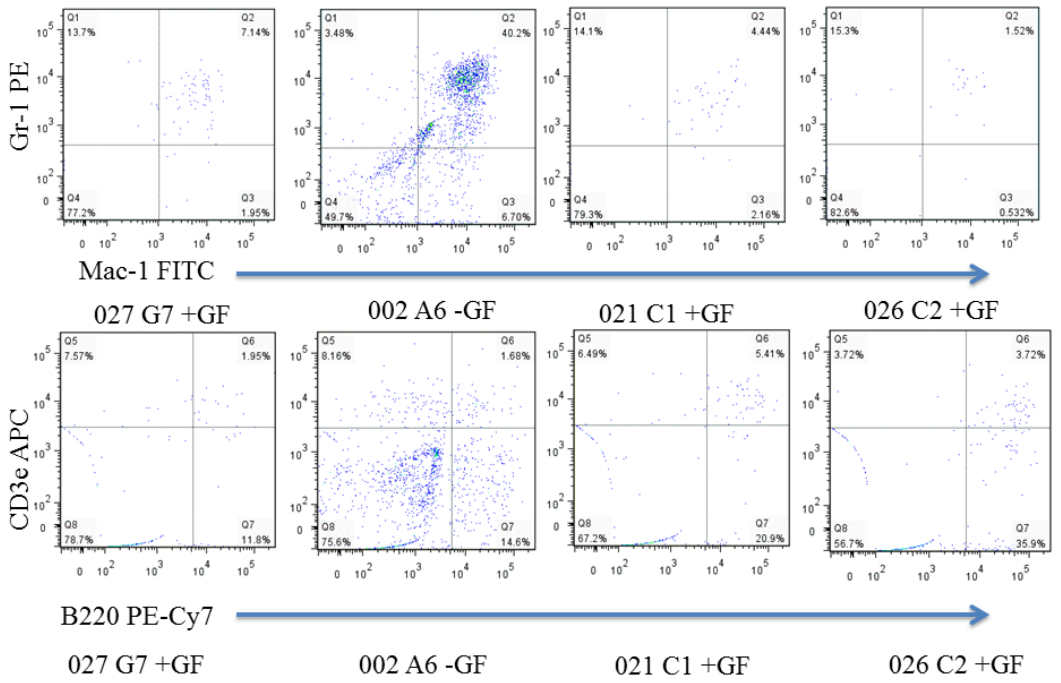

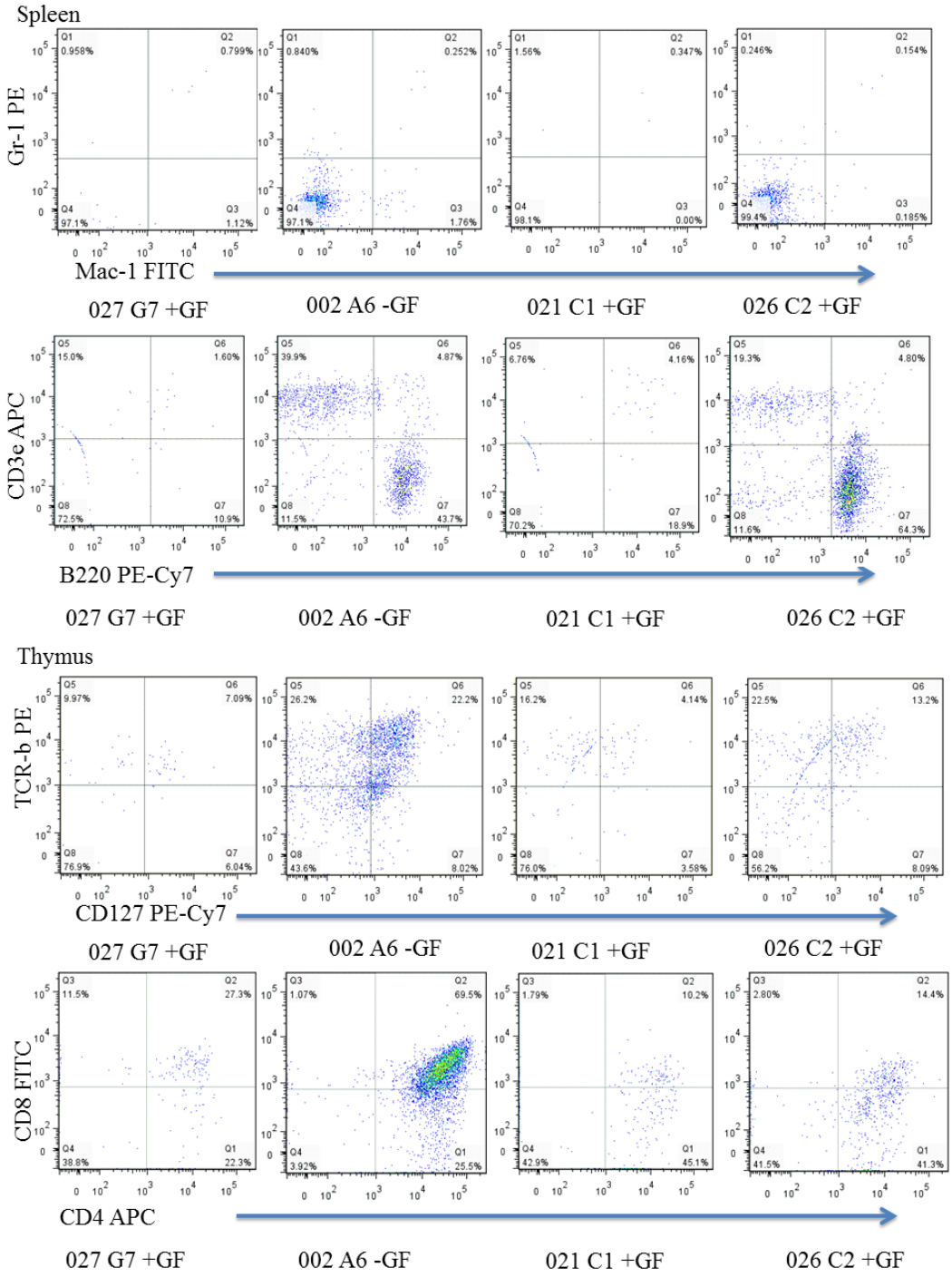

Figure 8.3-6. Flow cytometry plots of engraftments in multiple organs. Four mice were analysed for multilineage engraftments. A P12-027 G7 + GF mouse from SRYZH2 experiment was negative control. Blood, Bone marrow and spleen samples were stained with antibodies against Gr-1 PE, Mac-1 FITC, CD3e APC and B220 PE-Cy7. On the other hand, thymus samples were analysed with TCR-b PE, CD127 PE-Cy7, CD8 FITC and CD4 APC antibodies. All plots were representing Ter119^{-}CD45.1^{-} populations. FMO controls were shown in figure 9.8.2-3.

a) Reaction system

Item	Concentration	Volume (μL)
18MΩ water	n/a	9.4
10X Cl buffer	10X	2
Solution Q	10X	4
dNTP	10mM each	0.4
Forward Primer	100nM	0.5
Reverse Primer	100nM	0.5
Taq DNA polymerase	5u/μL	0.2
Blood gDNA	Individual labelled	5
Total		22

b) PCR parameter

Cycle	Step	Temperature(℃)	Time
1	Pre-Denature	95	5min
35	Denature	94	30s
	Annealing	58	30s
	Extension	72	60s
1	Final extension	72	10min
	Cool off	4	Hold

Table 8.3-1. PCR system used to detect CER fragment in gDNA isolated from recipient mice. a) Components of reaction system used, b) parameter of PCR used. gDNA concentration for mouse SRYZH6-3-8 was 23.6ng/μL, for SRYZH9-2-9 is 203.7 ng/μL and for SRYZH9-2-10 was 342.3ng/μL.

8.4. qPCR

The quality of qPCR reaction were reported here. In both plates, PPM Flt3l E6/7 did not generate good standard curves. The abundance of Flt3l transcript in total cDNA was low, that caused wells with low cDNA concentration had different amplification efficiency or failed to amplify all together. Besides that, each plate had two PPMs yielded slightly higher amplification efficiency between 2.1 and 2.15. The quality of cDNA slightly varied between different cell lines. Most cell lines had around 2 PPMs yielded standard error higher than 0.2. However, cDNA from 002 A6, 009 E10 and 015 B4 showed less consistency between replicates. Some even happens in low Cp wells, indicated problem more than just low cDNA concentration. Based on

previous experience, such inconsistencies were probably caused by trace contamination introduced during RNA extraction and reverse transcription.

Common Name	MGI symbol	# of pair designed	Transcript ID	Common Name	MGI symbol	# of pair designed	Transcript ID
Angiopoetin 2	Angpt2	1	NM_007426.3	Il6	Il6	4	NM_031168.1
Angiopoetin like 1	Angptl1	3	NM_028333.2	IL7	Il7	3	NM_008371.4
Angiopoetin like 3	Angptl3	3	NM_013913.3	Inhibin beta a	Inhba	1	NM_008380.1
BMP4	Bmp4	3	NM_007554.2	Insulinoma-associated 1	Insm1	1	NM_016889.3
N-cadherin	Cdh2	2	NM_007664.4	Jagged2	Jag2	2	NM_010588.2
G-CSF	Csf3	3	NM_009971.1	SCF	Kitl	1	NM_013598.2
Chemokine (C-X-C motif) ligand 13	Cxcl13	1	NM_018866.2	Madcam1	Madcam1	2	NM_013591.2
Desert hedgehog	Dhh	0	NM_007857.4	NEL-like 1 (chicken)	Nell1	1	NM_001037906.2
Dlk2	Dlk2	2	NM_207666.2	NOV	Nov	1	NM_010930.4
DLL1	Dll1	2	NM_007865.3	E-selectin/CD62	Sele	2	NM_011345.2
DLL3	Dll3	2	NM_007866.2	Sonic hedgehog	Shh	0	NM_009170.3
Dll4	Dll4	2	NM_019454.3	TGFbeta1	Tgfb1	1	NM_011577.1
Epiregulin	Ereg	3	NM_007950.2	TGFbeta3	Tgfb3	3	NM_009368.3
Fgf11	Fgf11	1	NM_010198.1	CD90	Thy1	2	NM_009382.3
bFGF	Fgf2	2	NM_008006.2	TPO	Tpo	5	NM_009417.2
Fgf9	Fgf9	1	NM_013518.3	Vascular endothelial growth factor C	vegfc	1	NM_009506.2
Flt3	Flt3	3	NM_010229.2	Wif1	Wif1	3	NM_011915.2
FLT3 (CD135)	Flt3	2	NM_010229.2	Wnt1	Wnt1	3	NM_021279.4
FLt3 ligand	Flt3l	4	NM_013520.3	Wnt10b	Wnt10b	3	NM_011718.2
Growth differentiation factor 10	Gdf10	1	NM_145741.2	Wnt11	Wnt11	3	NM_009519.2
Glial cell line derived neurotrophic factor	Gdnf	1	NM_010275.2	Wnt16	Wnt16	3	NM_053116.4
ICAM-1	Icam1	1	NM_010493.2	Wnt4	Wnt4	1	NM_009523.2
IGF binding ptr2	Igfbp2	1	NM_008342.2	Tbp	Tbp	1	NM_013684.3
Indian Hedgehog	Ihh	0	NM_010544.2	Ubiquitin C	Ubc	1	NM_019639.4
IL3	Il3	1	NM_010556.4				

Table 8.4-1. All genes selected for qPCR primer design and their target transcripts.

Primer pair name	5' primer sequence	3'primer sequence	UPL probe #	Primer pair name	5' primer sequence	3'primer sequence	UPL probe #
Angpt2 E5/6	cacactgaccttccccaact	cccacgtccatgtcacagta	82	Il3 E4/5	tacatctgcgaatgactctgc	ggctgaggtggtctagaggtt	94
Angptl1 E3/4	gatggctctgtcaatttcttca	gatggctctgtcaatttcttca	48	Il6 E3/4	gctaccaaactggatataatcagga	gctaccaaactggatataatcagga	6
Angptl3 E3/4	cctcttcaactgaacgaaacag	tctgttataaacggcagagcag	4	Il7 E1/2	cgcagaccatgttccatgt	tctttaatgtggcactcagatgat	27
Bmp4 E3/4	gaggagtttccatcacgaaga	gaggagtttccatcacgaaga	89	Inhba E2/3	atcatcacctttgccgagtc	tcactgccttccttggaaat	72
Cdh2 E13/14	gccatcatcgctatccttct	ccgtttcatccatcaccacaaa	18	Insm1 E1	ggtttgctctgcctaccaat	tcacccaaaacaacccgta	108
Csf3 E2/3	gctgctggagcagttgtg	gggatccccagagagtgg	17	Jag2 E2/4	cgtcattccctttcagttcg	cctcatctggagtggtgtca	95
Cxcl13 E1/2	tgaggctcagcacagcaa	atgggcttccagaatacgg	63	Kitl E1/2	agcgctgcctttccttatg	ccttggttttgacaagaggatt	68
Dhh E2/3	cacgtatcggtcaaagctgat	gtagttccctcagccccttc	75	Madcam1 E3/4	tgctgacccatagaaaggagat	gctcagcagaggtcgtgtt	21
Dhh E1/2	accgcctgatgacagagc	tcgtagtggagtgaatcctgtg	49	Nell1 E18/19	cagcagtgccgatgtctg	cagctcaaactagggcaagc	34
Dlk2 E4/5	ggggtggtgagtaccactgt	cctggttgtcctggcact	100	Nov E3/4	agtggacctgtggctcaga	tcaactcctacggtggcttc	11
Dll1 E4/5b	gaaggttgctctgtgtttctgc	ccctggcagacagattgg	7	Sele E7/8	caaatcccagtctgcaaagc	acatttcatgttgccctgct	47
Dll3 E4/5	gggggcagctgtagtgaa	acatcgaagcccgtagaatc	106	Shh E1/2	ccaattacaaccccgacatc	gcatttaacttgtctttgcacct	32
Dll4 E3/4	cggaaaccttctcactcaac	ttggatgatgatttggctga	72	Tgfb1 E2/3	tggagcaacatgtggaactc	cagcagccggttaccaag	72
Ereg E1/2	ttgacgctgctttgtctagg	ggatcacggttgtgctgat	96	Tgfb3 E5/6	ccctggacaccaattactgc	tcaatataaaggggcgtaca	25
Fgf11 E1/2	ctttgccagaaacagctcct	gcctttgagctgaggctct	56	Thy1 E2/3	aactcttggcaccatgaacc	tcgggacacctgcaagac	15
Fgf2 E1/2	cggctctactgcaagaacg	tgcttggagttgtagtttgacg	4	Tpo E8/9	gtaggggcactgcaccag	catcaggacccaggattttg	9
Fgf9 E1/2	tgcaggactggatttcatttag	ccaggcccactgctatactg	60	Vegfc E4/5	cagacaagttcattcaattattagacg	catgtcttgttagctgcctga	53
Flt3 E9/10	gcctcatttccttgtgaacag	tgatcgcaaaatttagatatgctg	88	Wif1 E9/10	ggcagacactgcaataagagg	ttaagtgaaggcgtgtgtcg	40
Flt3 E22/23	tggagcagccattctatgc	ccgcttccttgagtcaaaag	18	Wnt1 E1/2	acagtagtggccgatggtg	cttggaatccgtcaacaggt	25
Flt3l E7/8	cctaggatgcgagccttgt	tgttttggttcccaactcg	102	Wnt10b E3/4	ttcacgagtgtcagcacca	aaagcactctcacggaaacc	70
Gdf10 E1/2	aagtacaaccgaagaggtgctc	gcttttggtcgatcatttcc	52	Wnt11 E3/4	caggatcccaagccaataaa	tccagggaggcacgtaga	94
Gdnf E1/2	tccaactgggggtctacg	gacatcccataacttcatcttagagtc	70	Wnt16 E3/4	catgaatctacacaacaacgaagc	ttttccagcaggttttcaca	92
Icam1 E1/2	cccacgctacctctgctc	gatggatacctgagcatcacc	81	Wnt4 E2/3	actggactcccctcctgtct	tgcccttgtcactgcaaa	62
Igfbp2 E2/3	gcgggtacctgtgaaaagag	cctcagagtggtcgtcatca	62	Tbp E6/7	gggagctgtgatgtgaagt	ccaggaaatattctggctca	97
Ihh E2/3	tgcattgctctgtcaagtctg	gctccccgttctctaggc	83	Ubc E2/2	gaccagcagaggctgatctt	cctctgaggcgaaggactaa	11

Table 8.4-2. All qPCR primer pair designed in this study. These primer pairs were only compatible with Roche's UPL technology with corresponding probes listed above.

	Supportive							Non-supportive		
	P12-002 A6	P12-009 E10	P12-026 C2	P12-027 G7	P12-015 B4	P12-021 C1	OP9	P12-004 D5	P12-021 C2	P12-015 H5
Itgav E14/15	25.06	24.94	24.82	24.98	25.35	23.59	27.48	27.16	23.51	23.6
Vcam1 E6/7	23.44	21.88	24.35	22.08	22.88	24.09	27.68	23.94	24.46	21.89
Inhba E2/3	24.64	28.8	24	27.13	26.68	23.46	28.57	27.97	23.09	24.94
Tgfb1 E2/3	26.38	24.8	25.97	25.94	25.55	25.08	28.63	27.43	23.92	24.93
Bmp4 E3/4b	26.58	27.38	27.31	27.01	27.51	29.56	29.68	28.53	27.61	25.64
Cdh2 E14/15	26.84	28.76	26.13	28.86	29.18	25.13	30.08	31.1	25.22	25.23
Jag1 E23/24	27.85	29.27	27.01	30.06	29.74	27.56	28.01	31.8	27.67	28.1
Nes E2/3	27.58	27.47	26.7	30.49	30.4	28.42	ND	32.18	26.88	27.48
Kitl E1/2	29.69	29.55	32.78	28.63	29.63	29.24	32.01	29.35	28.97	27.71
Il3ra E3/4	30.49	33.28	31.13	32.66	33.8	31.3	32.48	34.1	29.99	30.89
Flt3l E6/7	33.95	34.55	32.1	34.34	34.44	34.86	33.74	35.01	33.2	32.16
Wnt4 E2/3	34.07	32.01	30.29	36.35	31.08	28.15	30.87	34.23	28.85	29.79
Tbp E6/7	28.82	31.11	28.47	27.24	28.54	27.16	29.11	27.97	27.1	27.68

Table 8.4-1. Mean crossing points of each transcript in cell lines tested. Related plate IDs were 01167992, 01167961 and 01167962. ND is not determined. (n=3)

a)

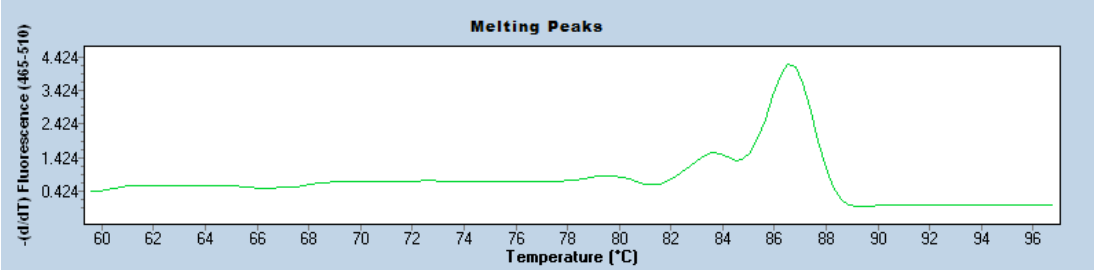

b)

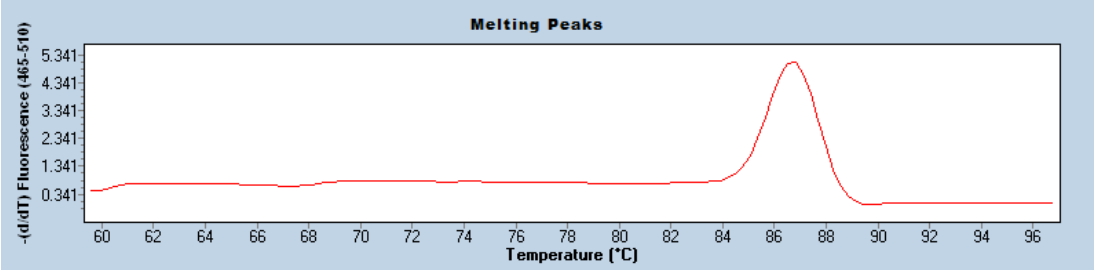

Figure 8.4-1. Melting curves generated from primer pair Flt3l E6/7. Panel a showed melting curve from 4ng replicate well 1. This well contained non-specific product. Panel b showed melting curve from 4ng replicate well 2. This well contained only one amplification product.

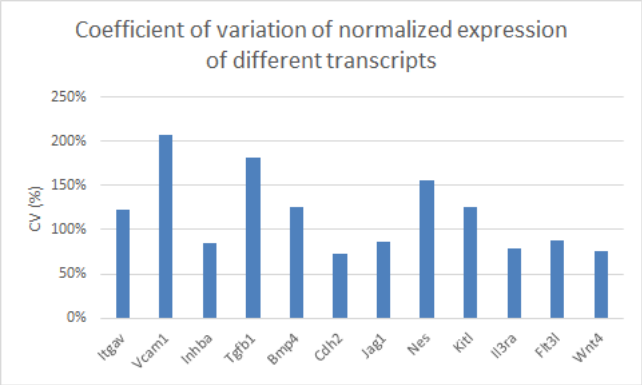

Figure 8.4-2. Coefficient of variation of normalized expression for each transcript in 10 cell lines. Standard derivations were calculated using STDEV.P function in Excel 2013, averages were calculated using Average function in Excel 2013, coefficient of variations were calculated using formula CV=Stdev/average.

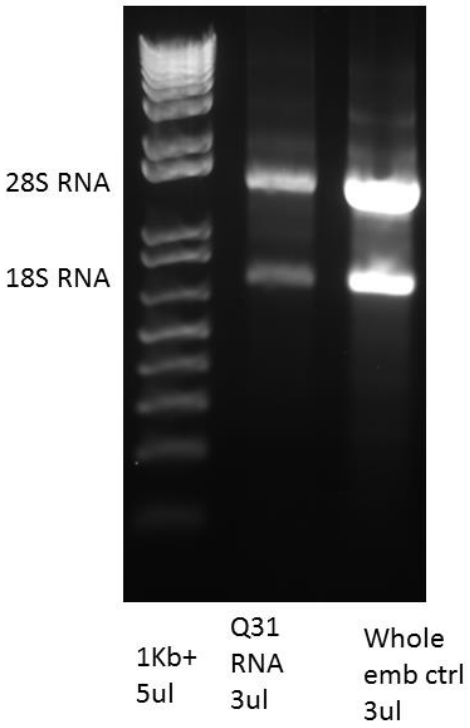

Figure 8.4-3. Native agarose electrophoresis of extracted RNA sample. Left lane was 50ng 1KB+ DNA ladder to determine the amount of RNA isolated. Middle lane was RNA isolated from 10^6 cells of line P11-100 Q31 passage 22. Right lane was Positive control isolated from several E11.5 embryos. Note the 28S and 18S RNA were the most abundant fraction of all.

	Itgav	Vcam1	Inhba	Tgfb1	Bmp4	Cdh2	Jag1	Nes	Kitl	Il3ra	Flt3l	Wnt4	Add gf	Minus gf	All
Itgav	1.00														
Vcam1	0.98	1.00													
Inhba	0.00	-0.19	1.00												
Tgfb1	0.98	0.99	-0.12	1.00											
Bmp4	0.95	0.95	-0.04	0.93	1.00										
Cdh2	0.55	0.36	0.68	0.40	0.50	1.00									
Jag1	0.68	0.64	0.33	0.65	0.70	0.53	1.00								
Nes	0.97	0.95	0.09	0.96	0.95	0.54	0.79	1.00							
Kitl	0.96	0.97	-0.23	0.96	0.96	0.40	0.54	0.90	1.00						
Il3ra	0.50	0.40	0.59	0.42	0.60	0.64	0.72	0.58	0.39	1.00					
Flt3l	0.71	0.66	0.24	0.67	0.73	0.59	0.90	0.80	0.60	0.55	1.00				
Wnt4	0.61	0.51	0.19	0.58	0.40	0.56	0.53	0.54	0.45	0.16	0.48	1.00			
Add gf	0.31	0.29	0.39	0.29	0.36	0.27	0.84	0.46	0.14	0.52	0.74	0.27	1.00		
Minus gf	0.58	0.55	0.21	0.54	0.60	0.37	0.43	0.55	0.53	0.59	0.17	0.33	0.27	1.00	
All	0.50	0.47	0.39	0.47	0.55	0.38	0.85	0.60	0.35	0.67	0.64	0.38	0.89	0.67	1.00

Table 8.4-4. Correlation between expression level of single transcript in feeder cells and cell lines ability to promote maturation of E9.5 precursor measured by average engraftment after 6 weeks. Note "all" was weighted average of +GF and –GF conditions.

8.5. Discussion

8.5.1. Chaos and stochastic progress related background information

HSC specification was a complex dynamic process involves multiple cell populations. Most dynamic processes fitted into two categories: chaos or stochastic (Smith 2007). Both systems could contain complex regulatory networks where a slight perturbation of input could lead to drastically altered outcomes. However, there was one important distinction: chaos was deterministic while stochastic system was random. That was, if input A was feed into a chaotic system, it would always generate result B, while slightly modified input A' would generate a drastically different result Z. Repetition of putting input A into such system always got result B, while A' always got result Z. Early development of *C. elegans* was perhaps one of the most recognized chaotic systems in biology. A map could be drawn to show the fate of every cell generated from zygotes to adulthood (Sulston, Schierenberg et al. 1983). The sequence of events happen in embryonic development was determined. However, a slight perturbation, like disruption of a gene or killing a specific cell in early development could cause drastic and yet reproducible changes. On the other hand, a stochastic system was random; repeating the same experiment would generate different results each time. After many repetitions, a distribution appeared

indicating how likely each outcome was going to happen in one experiment (Expectation).

Of course, the boundary between stochastic system and chaotic system was arbitrary. With more knowledge about behavior of system under study and more computing power, it became possible to simulate stochastic systems which could be analyzed as chaotic. Analysis of atmosphere was a typical case of such change. About 200 years ago, weather forecast was primary based on probability of past events, thus was purely stochastic. At that time numerical (deterministic) forecasting was almost impossible. However, with the advancement of atmospheric modeling and computing, now atmosphere system could be simulated as chaotic (at least in the short term) and the accuracy of numerical forecasting was greatly improved.

Current paradigm of developmental biology was mostly deterministic. An ultimate goal of many researchers was trying to determine ontogeny of various adult cell type by generate fate maps all the way up to zygote, or at least to totipotent inner cell mass (ICM). This paradigm was proven on lower animal and yielded many important insights on embryonic development of higher animals. However, this paradigm had some shortcomings when applied to more complex species. It had difficulty explain variation of embryonic development. For example, E11.5 AGM roughly contained only one definitive HSC. If definitive HSC generation was deterministic, some kind of HSC suppression mechanism must existed to maintain correct number of definitive HSC in AGM region by killing off excessive definitive HSCs. But such mechanism was yet discovered although it could be easily revealed by knock-out screening.

On the other hand, stochastic model could explain observed variation of embryonic development. In stochastic model, there is no roadmap of development exist. Generation of cell numbers of different types follow respective distribution. Rare embryos that did not have enough cells generated simply died. Embryos had too

much dHSC would have no problem in development because those extra HSCs would differentiate due to lack of niche.

The stochastic nature of embryonic development was introduced by “cellular automaton”. That is, every cell decided its action based on its state of its gene regulatory network (or in a mathematical word, cell state) and signals received from neighboring cells. So the state of embryo could be described using Markov Random Field.

9. Bibliography

Abe, T., et al. (2013). "Visualization of cell cycle in mouse embryos with Fucci2 reporter directed by Rosa26 promoter." Development **140**(1): 237-246.

Adamo, L., et al. (2009). "Biomechanical forces promote embryonic haematopoiesis." Nature **459**(7250): 1131-1135.

Adolfsson, J., et al. (2005). "Identification of Flt3+ Lympho-Myeloid Stem Cells Lacking Erythro-Megakaryocytic Potential: A Revised Road Map for Adult Blood Lineage Commitment." Cell **121**(2): 295-306.

Ahuja, D., et al. (2005). "SV40 large T antigen targets multiple cellular pathways to elicit cellular transformation." Oncogene **24**(52): 7729-7745.

Akashi, K., et al. (2000). "A clonogenic common myeloid progenitor that gives rise to all myeloid lineages." Nature **404**(6774): 193-197.

Alexander, W. S. (2000-). "Cytokine Action in Hematopoietic Stem Cell Regulation." Madame Curie Bioscience Database [Internet]. Retrieved 2013-08-03, 2013, from http://www.ncbi.nlm.nih.gov/books/NBK6511/.

Arai, F., et al. (2012). "Role of N-cadherin in the regulation of hematopoietic stem cells in the bone marrow niche." Ann N Y Acad Sci **1266**: 72-77.

Arnold, T. D., et al. (2012). "Defective retinal vascular endothelial cell development as a consequence of impaired integrin alphaVbeta8-mediated activation of transforming growth factor-beta." J Neurosci **32**(4): 1197-1206.

Bai, H., et al. (2013). "The Balance of Positive and Negative Effects of TGF-beta Signaling Regulates the Development of Hematopoietic and Endothelial Progenitors in Human Pluripotent Stem Cells." Stem Cells Dev.

Bertrand, J. Y., et al. (2010). "Haematopoietic stem cells derive directly from aortic endothelium during development." Nature **464**(7285): 108-111.

Bigas, A., et al. (2012). "The Notch pathway in hematopoietic stem cells." Curr Top Microbiol Immunol **360**: 1-18.

Bigas, A., et al. (2013). "Notch and Wnt signaling in the emergence of hematopoietic stem cells." Blood Cells, Molecules, and Diseases **51**(4): 264-270.

Bloor, A. J., et al. (2002). "The role of the stem cell leukemia (SCL) gene in hematopoietic and endothelial lineage specification." J Hematother Stem Cell Res **11**(2): 195-206.

Boisset, J.-C., et al. (2010). "In vivo imaging of haematopoietic cells emerging from the mouse aortic endothelium." Nature **464**(7285): 116-120.

Boisset, J. C., et al. (2013). "Integrin alphaIIb (CD41) plays a role in the maintenance of hematopoietic stem cell activity in the mouse embryonic aorta." Biol Open **2**(5): 525-532.

Buckley, S. M., et al. (2011). "Maintenance of HSC by Wnt5a secreting AGM-derived stromal cell line." Exp Hematol **39**(1): 114-123.e111-115.

Burk, A. S., et al. (2015). "Quantifying adhesion mechanisms and dynamics of human hematopoietic stem and progenitor cells." Sci Rep **5**: 9370.
Burns, C. E., et al. (2005). "Hematopoietic stem cell fate is established by the Notch–Runx pathway." Genes Dev **19**(19): 2331-2342.
Bustin, S. A., et al. (2009). "The MIQE guidelines: minimum information for publication of quantitative real-time PCR experiments." Clin Chem **55**(4): 611-622.
Caprioli, A., et al. (1998). "Blood-borne seeding by hematopoietic and endothelial precursors from the allantois." Proc Natl Acad Sci U S A **95**(4): 1641-1646.
Carmeliet, P., et al. (1996). "Abnormal blood vessel development and lethality in embryos lacking a single VEGF allele." Nature **380**(6573): 435-439.
Cary, L. C., et al. (1989). "Transposon mutagenesis of baculoviruses: analysis of Trichoplusia ni transposon IFP2 insertions within the FP-locus of nuclear polyhedrosis viruses." Virology **172**(1): 156-169.
Cattelino, A., et al. (2003). "The conditional inactivation of the β-catenin gene in endothelial cells causes a defective vascular pattern and increased vascular fragility." The Journal of Cell Biology **162**(6): 1111-1122.
Cedar, H. and Y. Bergman (2011). "Epigenetics of haematopoietic cell development." Nat Rev Immunol **11**(7): 478-488.
Cerdan, C., et al. (2012). "Activin A promotes hematopoietic fated mesoderm development through upregulation of brachyury in human embryonic stem cells." Stem Cells Dev **21**(15): 2866-2877.
Chadwick, K., et al. (2003). "Cytokines and BMP-4 promote hematopoietic differentiation of human embryonic stem cells." Blood **102**(3): 906-915.
Charbord, P., et al. (2002). "Comparative study of stromal cell lines derived from embryonic, fetal, and postnatal mouse blood-forming tissues." Exp Hematol **30**(10): 1202-1210.
Chen, M. J., et al. (2009). "Runx1 is required for the endothelial to haematopoietic cell transition but not thereafter." Nature **457**(7231): 887-891.
Chickarmane, V., et al. (2009). "Computational Modeling of the Hematopoietic Erythroid-Myeloid Switch Reveals Insights into Cooperativity, Priming, and Irreversibility." PLoS Comput Biol **5**(1): e1000268.
Choi, K.-D., et al. (2012). "Identification of the Hemogenic Endothelial Progenitor and Its Direct Precursor in Human Pluripotent Stem Cell Differentiation Cultures." Cell Reports **2**(3): 553-567.
Choi, K., et al. (1998). "A common precursor for hematopoietic and endothelial cells." Development **125**(4): 725-732.
Chou, S. and H. F. Lodish (2010). "Fetal liver hepatic progenitors are supportive stromal cells for hematopoietic stem cells." Proceedings of the National Academy of Sciences **107**(17): 7799-7804.
Christensen, J. L. and I. L. Weissman (2001). "Flk-2 is a marker in hematopoietic stem cell differentiation: a simple method to isolate long-term stem cells." Proc Natl Acad Sci U S A **98**(25): 14541-14546.
Christensen, J. L., et al. (2004). "Circulation and Chemotaxis of Fetal Hematopoietic Stem Cells." PLoS Biol **2**(3): e75.
Collins, L. S. and K. Dorshkind (1987). "A stromal cell line from myeloid long-term bone marrow cultures can support myelopoiesis and B lymphopoiesis." J Immunol **138**(4): 1082-1087.

Corselli, M., et al. (2013). "Perivascular support of human hematopoietic stem/progenitor cells." Blood **121**(15): 2891-2901.
Cumano, A., et al. (2001). "Intraembryonic, but Not Yolk Sac Hematopoietic Precursors, Isolated before Circulation, Provide Long-Term Multilineage Reconstitution." Immunity **15**(3): 477-485.
de Bruijn, M. F. and N. A. Speck (2004). "Core-binding factors in hematopoiesis and immune function." Oncogene **23**(24): 4238-4248.
de Bruijn, M. F. T. R., et al. (2002). "Hematopoietic Stem Cells Localize to the Endothelial Cell Layer in the Midgestation Mouse Aorta." Immunity **16**(5): 673-683.
de Bruijn, M. F. T. R., et al. (2000). "Definitive hematopoietic stem cells first develop within the major arterial regions of the mouse embryo." The EMBO Journal **19**(11): 2465-2474.
Detrich, H. W., 3rd, et al. (1995). "Intraembryonic hematopoietic cell migration during vertebrate development." Proc Natl Acad Sci U S A **92**(23): 10713-10717.
Dieterlen-Lievre, F. (1975). "On the origin of haemopoietic stem cells in the avian embryo: an experimental approach." J Embryol Exp Morphol **33**(3): 607-619.
Dieterlen-Lievre, F., et al. (2010). "Allantois and placenta as developmental sources of hematopoietic stem cells." Int J Dev Biol **54**(6-7): 1079-1087.
Dieterlen-Lievre, F. and C. Martin (1981). "Diffuse intraembryonic hemopoiesis in normal and chimeric avian development." Dev Biol **88**(1): 180-191.
Ding, L. and S. J. Morrison (2013). "Haematopoietic stem cells and early lymphoid progenitors occupy distinct bone marrow niches." Nature **495**(7440): 231-235.
Ding, L., et al. (2012). "Endothelial and perivascular cells maintain haematopoietic stem cells." Nature **481**(7382): 457-462.
Durand, C., et al. (2007). "Embryonic stromal clones reveal developmental regulators of definitive hematopoietic stem cells." Proceedings of the National Academy of Sciences **104**(52): 20838-20843.
Dzierzak, E. and N. A. Speck (2008). "Of lineage and legacy: the development of mammalian hematopoietic stem cells." Nat Immunol **9**(2): 129-136.
Eilken, H. M., et al. (2009). "Continuous single-cell imaging of blood generation from haemogenic endothelium." Nature **457**(7231): 896-900.
Endoh, M. O. M. O. S. N. S. i. (2002). "SCL/tal‐1‐dependent process determines a competence to select the definitive hematopoietic lineage prior to endothelial differentiation." The EMBO Journal **21**(24): 6700-6708.
Ernst, P., et al. (2004). "Definitive Hematopoiesis Requires the Mixed-Lineage Leukemia Gene." Developmental Cell **6**(3): 437-443.
Fan, J., et al. (2012). "A novel monoclonal antibody of human stem cell factor inhibits umbilical cord blood stem cell ex vivo expansion." Journal of Hematology & Oncology **5**: 73-73.
Ferkowicz, M. J. and M. C. Yoder (2005). "Blood island formation: longstanding observations and modern interpretations." Exp Hematol **33**(9): 1041-1047.
Ferrara, N., et al. (1996). "Heterozygous embryonic lethality induced by targeted inactivation of the VEGF gene." Nature **380**(6573): 439-442.
Fidanza, V., et al. (1996). "Double knockout of the ALL-1 gene blocks hematopoietic differentiation in vitro." Cancer Res **56**(6): 1179-1183.
Fitch, S. R., et al. (2012). "Signaling from the sympathetic nervous system regulates hematopoietic stem cell emergence during embryogenesis." Cell Stem Cell **11**(4): 554-566.

Francoise-Lievre, F. (2005). "Commitment of hematopoietic stem cells in avian and mammalian embryos: an ongoing story." Int J Dev Biol **49**(2-3): 125-130.
Fraser, M. (2002). "Welcome to the piggyBac website." Retrieved 08/04, 2013, from http://piggybac.bio.nd.edu/.
Fraser, M. J., et al. (1995). "Assay for movement of Lepidopteran transposon IFP2 in insect cells using a baculovirus genome as a target DNA." Virology **211**(2): 397-407.
Fujiwara, Y., et al. (1996). "Arrested development of embryonic red cell precursors in mouse embryos lacking transcription factor GATA-1." Proc Natl Acad Sci U S A **93**(22): 12355-12358.
Gadue, P., et al. (2006). "Wnt and TGF-β signaling are required for the induction of an in vitro model of primitive streak formation using embryonic stem cells." Proceedings of the National Academy of Sciences **103**(45): 16806-16811.
Gartner, S. and H. S. Kaplan (1980). "Long-term culture of human bone marrow cells." Proc Natl Acad Sci U S A **77**(8): 4756-4759.
Gordon-Keylock, S., et al. (2013). "Mouse extraembryonic arterial vessels harbor precursors capable of maturing into definitive HSCs." Blood **122**(14): 2338-2345.
Goss, C. M. (1928). "Experimental removal of the blood island of Amblystoma punctatum embryos." Journal of Experimental Zoology **52**(1): 45-63.
Hartenstein, V. (2006). "Blood cells and blood cell development in the animal kingdom." Annu Rev Cell Dev Biol **22**: 677-712.
Hirschi, K. K. (2012). "Hemogenic endothelium during development and beyond." Blood **119**(21): 4823-4827.
Hoogenkamp, M., et al. (2007). "The Pu.1 Locus Is Differentially Regulated at the Level of Chromatin Structure and Noncoding Transcription by Alternate Mechanisms at Distinct Developmental Stages of Hematopoiesis." Molecular and Cellular Biology **27**(21): 7425-7438.
Horn, C. and E. A. Wimmer (2000). "A versatile vector set for animal transgenesis." Development Genes and Evolution **210**(12): 630-637.
Hou, P., et al. (2013). "Pluripotent Stem Cells Induced from Mouse Somatic Cells by Small-Molecule Compounds." Science **341**(6146): 651-654.
Hu, X. and K. S. Zuckerman (2001). "Transforming growth factor: signal transduction pathways, cell cycle mediation, and effects on hematopoiesis." J Hematother Stem Cell Res **10**(1): 67-74.
Huang, G., et al. (2008). "PU.1 is a major downstream target of AML1 (RUNX1) in adult mouse hematopoiesis." Nat Genet **40**(1): 51-60.
Huber, T. L., et al. (2004). "Haemangioblast commitment is initiated in the primitive streak of the mouse embryo." Nature **432**(7017): 625-630.
Irion, S., et al. (2010). "Temporal specification of blood progenitors from mouse embryonic stem cells and induced pluripotent stem cells." Development **137**(17): 2829-2839.
Ishikawa, T., et al. (2001). "Mouse Wnt receptor gene Fzd5 is essential for yolk sac and placental angiogenesis." Development **128**(1): 25-33.
Issaad, C., et al. (1993). "A murine stromal cell line allows the proliferation of very primitive human CD34++/CD38- progenitor cells in long-term cultures and semisolid assays." Blood **81**(11): 2916-2924.
Ivanovs, A., et al. (2014). "Identification of the niche and phenotype of the first human hematopoietic stem cells." Stem Cell Reports **2**(4): 449-456.

Ivanovs, A., et al. (2011). "Highly potent human hematopoietic stem cells first emerge in the intraembryonic aorta-gonad-mesonephros region." J Exp Med **208**(12): 2417-2427.
Jackson, S. A., et al. (2010). "Differentiating Embryonic Stem Cells Pass through 'Temporal Windows' That Mark Responsiveness to Exogenous and Paracrine Mesendoderm Inducing Signals." PLoS ONE **5**(5): e10706.
Jones, C. M., et al. (1996). "Bone morphogenetic protein-4 (BMP-4) acts during gastrula stages to cause ventralization of Xenopus embryos." Development **122**(5): 1545-1554.
Jordan, C. T., et al. (1990). "Cellular and developmental properties of fetal hematopoietic stem cells." Cell **61**(6): 953-963.
Kennedy, M., et al. (2012). "T Lymphocyte Potential Marks the Emergence of Definitive Hematopoietic Progenitors in Human Pluripotent Stem Cell Differentiation Cultures." Cell Reports **2**(6): 1722-1735.
Kiel, M. J. and S. J. Morrison (2008). "Uncertainty in the niches that maintain haematopoietic stem cells." Nat Rev Immunol **8**(4): 290-301.
Kiel, M. J., et al. (2005). "SLAM family receptors distinguish hematopoietic stem and progenitor cells and reveal endothelial niches for stem cells." Cell **121**(7): 1109-1121.
Kikushige, Y., et al. (2008). "Human Flt3 is expressed at the hematopoietic stem cell and the granulocyte/macrophage progenitor stages to maintain cell survival." J Immunol **180**(11): 7358-7367.
Kim, J. H., et al. (2011). "High Cleavage Efficiency of a 2A Peptide Derived from Porcine Teschovirus-1 in Human Cell Lines, Zebrafish and Mice." PLoS ONE **6**(4): e18556.
Kim, P. G., et al. (2013). "Signaling axis involving Hedgehog, Notch, and Scl promotes the embryonic endothelial-to-hematopoietic transition." Proceedings of the National Academy of Sciences **110**(2): E141–E150.
Kim, S. M., et al. (2014). "Direct conversion of mouse fibroblasts into induced neural stem cells." Nat. Protocols **9**(4): 871-881.
Kindermann, R., et al. (1980). Markov Random Fields and Their Applications, American Mathematical Society.
Kissa, K. and P. Herbomel (2010). "Blood stem cells emerge from aortic endothelium by a novel type of cell transition." Nature **464**(7285): 112-115.
Kitajima, K., et al. (2005). "Redirecting differentiation of hematopoietic progenitors by a transcription factor, GATA-2." Blood **107**(5): 1857-1863.
Kitajima, K., et al. (2006). "Multipotential differentiation ability of GATA-1-null erythroid-committed cells." Genes Dev **20**(6): 654-659.
Koga, S., et al. (2007). "Cell-cycle–dependent oscillation of GATA2 expression in hematopoietic cells." Blood **109**(10): 4200-4208.
Kondo, M., et al. (1997). "Identification of clonogenic common lymphoid progenitors in mouse bone marrow." Cell **91**(5): 661-672.
Kozak, M. (1987). "An analysis of 5'-noncoding sequences from 699 vertebrate messenger RNAs." Nucleic Acids Res **15**(20): 8125-8148.
Krassowska, A., et al. (2006). "Promotion of haematopoietic activity in embryonic stem cells by the aorta-gonad-mesonephros microenvironment." Exp Cell Res **312**(18): 3595-3603.

Kumano, G., et al. (1999). "Spatial and temporal properties of ventral blood island induction in Xenopus laevis." Development **126**(23): 5327-5337.
Kumano, K., et al. (2003). "Notch1 but Not Notch2 Is Essential for Generating Hematopoietic Stem Cells from Endothelial Cells." Immunity **18**(5): 699-711.
Kumaravelu, P., et al. (2002). "Quantitative developmental anatomy of definitive haematopoietic stem cells/long-term repopulating units (HSC/RUs): role of the aorta-gonad-mesonephros (AGM) region and the yolk sac in colonisation of the mouse embryonic liver." Development **129**(21): 4891-4899.
Kusadasi, N., et al. (2002). "Stromal cells from murine embryonic aorta-gonad-mesonephros region, liver and gut mesentery expand human umbilical cord blood-derived CAFC(week6) in extended long-term cultures." Leukemia **16**(9): 1782-1790.
Kyba, M., et al. (2003). "Enhanced hematopoietic differentiation of embryonic stem cells conditionally expressing Stat5." Proc Natl Acad Sci U S A **100 Suppl 1**: 11904-11910.
Lécuyer, E. and T. Hoang (2004). "SCL: From the origin of hematopoiesis to stem cells and leukemia." Exp Hematol **32**(1): 11-24.
Lacaud, G., et al. (2002). Runx1 is essential for hematopoietic commitment at the hemangioblast stage of development in vitro.
Lancrin, C., et al. (2009). "The haemangioblast generates haematopoietic cells through a haemogenic endothelium stage." Nature **457**(7231): 892-895.
Larsson, J. and S. Karlsson (2005). "The role of Smad signaling in hematopoiesis." Oncogene **24**(37): 5676-5692.
Ledran, M. H., et al. (2008). "Efficient hematopoietic differentiation of human embryonic stem cells on stromal cells derived from hematopoietic niches." Cell Stem Cell **3**(1): 85-98.
Lee, D., et al. (2008). "ER71 Acts Downstream of BMP, Notch, and Wnt Signaling in Blood and Vessel Progenitor Specification." Cell Stem Cell **2**(5): 497-507.
Lee, H. J., et al. (2013). "Biomechanical force in blood development: Extrinsic physical cues drive pro-hematopoietic signaling." Differentiation **86**(3): 92-103.
Lengerke, C., et al. (2008). "BMP and Wnt Specify Hematopoietic Fate by Activation of the Cdx-Hox Pathway." Cell Stem Cell **2**(1): 72-82.
Li, Z., et al. (2012). "Mouse embryonic head as a site for hematopoietic stem cell development." Cell Stem Cell **11**(5): 663-675.
Li, Z., et al. (2013). "Simple piggyBac transposon-based mammalian cell expression system for inducible protein production." Proceedings of the National Academy of Sciences **110**(13): 5004-5009.
Ling, K.-W., et al. (2004). "GATA-2 Plays Two Functionally Distinct Roles during the Ontogeny of Hematopoietic Stem Cells." J Exp Med **200**(7): 871-882.
Liu, F., et al. (2012). "ER71 specifies Flk-1+ hemangiogenic mesoderm by inhibiting cardiac mesoderm and Wnt signaling." Blood **119**(14): 3295-3305.
Lo Celso, C., et al. (2009). "Live-animal tracking of individual haematopoietic stem/progenitor cells in their niche." Nature **457**(7225): 92-96.
Lu, H. S., et al. (1991). "Amino acid sequence and post-translational modification of stem cell factor isolated from buffalo rat liver cell-conditioned medium." J Biol Chem **266**(13): 8102-8107.

Lu, S.-J., et al. (2010). Directed Differentiation of Red Blood Cells from Human Embryonic Stem Cells. Cellular Programming and Reprogramming. S. Ding, Humana Press. **636:** 105-121.
Lugus, J. J., et al. (2009). "Both primitive and definitive blood cells are derived from Flk-1+ mesoderm." Blood **113**(3): 563-566.
Lugus, J. J. P. C. M. Y. D. C. K. (2008). "Both primitive and definitive blood cells are derived from Flk-1+ mesoderm." Blood **113**(3): 563-566.
Lustig, A. J. (1999). "Crisis intervention: The role of telomerase." Proc Natl Acad Sci U S A **96**(7): 3339-3341.
Lux, C. T., et al. (2008). "All primitive and definitive hematopoietic progenitor cells emerging before E10 in the mouse embryo are products of the yolk sac." Blood **111**(7): 3435-3438.
MaÉNo, M., et al. (1985). "The Localization of Precursor Cells for Larval and Adult Hemopoietic Cells of Xenopus Laevis in two Regions of Embryos." Development, Growth & Differentiation **27**(2): 137-148.
Marshall, C. J., et al. (2000). "Polarized expression of bone morphogenetic protein-4 in the human aorta-gonad-mesonephros region." Blood **96**(4): 1591-1593.
Masaki Takeuchi, A. M. (2000). Hematopoiesis in Fetal Liver. Madame Curie Report. J. Kelle. Austin Texas, Landes Bioscience.
Matsunari, H., et al. (2013). "Blastocyst complementation generates exogenic pancreas in vivo in apancreatic cloned pigs." Proceedings of the National Academy of Sciences.
Matsuoka, S., et al. (2001). "Generation of definitive hematopoietic stem cells from murine early yolk sac and paraaortic splanchnopleures by aorta-gonad-mesonephros region–derived stromal cells." Blood **98**(1): 6-12.
Mead, P. E., et al. (1998). "SCL specifies hematopoietic mesoderm in Xenopus embryos." Development **125**(14): 2611-2620.
Medvinsky, A. and E. Dzierzak (1996). "Definitive hematopoiesis is autonomously initiated by the AGM region." Cell **86**(6): 897-906.
Medvinsky, A., et al. (2011). "Embryonic origin of the adult hematopoietic system: advances and questions." Development **138**(6): 1017-1031.
Medvinsky, A., et al. (2008). "Analysis and manipulation of hematopoietic progenitor and stem cells from murine embryonic tissues." Curr Protoc Stem Cell Biol **Chapter 2**: Unit 2A 6.
Medvinsky, A. L., et al. (1993). "An early pre-liver intraembryonic source of CFU-S in the developing mouse." Nature **364**(6432): 64-67.
Mendez-Ferrer, S., et al. (2010). "Mesenchymal and haematopoietic stem cells form a unique bone marrow niche." Nature **466**(7308): 829-834.
Migliaccio, G., et al. (1986). "Human embryonic hemopoiesis. Kinetics of progenitors and precursors underlying the yolk sac----liver transition." The Journal of Clinical Investigation **78**(1): 51-60.
Mikkola, H. K. and S. H. Orkin (2006). "The journey of developing hematopoietic stem cells." Development **133**(19): 3733-3744.
Minegishi, N., et al. (1999). "The mouse GATA-2 gene is expressed in the para-aortic splanchnopleura and aorta-gonads and mesonephros region." Blood **93**(12): 4196-4207.
Moignard, V., et al. (2013). "Characterization of transcriptional networks in blood stem and progenitor cells using high-throughput single-cell gene expression analysis." Nat Cell Biol **15**(4): 363-372.

Monteiro, R., et al. (2011). "The gata1/pu.1 lineage fate paradigm varies between blood populations and is modulated by tif1γ." The EMBO Journal **30**(6): 1093-1103.
Moore, M. A. and J. J. Owen (1965). "Chromosome marker studies on the development of the haemopoietic system in the chick embryo." Nature **208**(5014): 956 passim.
Moore, M. A. and J. J. Owen (1967). "Chromosome marker studies in the irradiated chick embryo." Nature **215**(5105): 1081-1082.
Moriguchi, T. and M. Yamamoto (2014). "A regulatory network governing Gata1 and Gata2 gene transcription orchestrates erythroid lineage differentiation." Int J Hematol.
Morrison, S. J., et al. (1995). "The purification and characterization of fetal liver hematopoietic stem cells." Proceedings of the National Academy of Sciences **92**(22): 10302-10306.
Mukouyama, Y.-s., et al. (2005). "Peripheral nerve-derived VEGF promotes arterial differentiation via neuropilin 1-mediated positive feedback." Development **132**(5): 941-952.
Muller, A. M., et al. (1994). "Development of hematopoietic stem cell activity in the mouse embryo." Immunity **1**(4): 291-301.
Murty, K. G. (1983). Linear programming, Wiley.
Nagao, K., et al. (2008). "Expression profile analysis of aorta-gonad-mesonephros region-derived stromal cells reveals genes that regulate hematopoiesis." Biochem Biophys Res Commun **377**(1): 205-209.
Nakagawa, M., et al. (2006). AML1/Runx1 rescues Notch1-null mutation-induced deficiency of para-aortic splanchnopleural hematopoiesis.
Nakajima-Takagi, Y., et al. (2012). "Role of SOX17 in hematopoietic development from human embryonic stem cells." Blood **121**(3): 447-458.
Nakano, T., et al. (1994). "Generation of lymphohematopoietic cells from embryonic stem cells in culture." Science **265**(5175): 1098-1101.
Nishikawa, S. I., et al. (1998). "Progressive lineage analysis by cell sorting and culture identifies FLK1+VE-cadherin+ cells at a diverging point of endothelial and hemopoietic lineages." Development **125**(9): 1747-1757.
Nobuhisa, I., et al. (2014). "Sox17-Mediated Maintenance of Fetal Intra-Aortic Hematopoietic Cell Clusters." Molecular and Cellular Biology **34**(11): 1976-1990.
Nobuhisa, I., et al. (2003). "Regulation of Hematopoietic Development in the Aorta-Gonad-Mesonephros Region Mediated by Lnk Adaptor Protein." Molecular and Cellular Biology **23**(23): 8486-8494.
Normile, D. (2013). "Stem cell research. Chimeric embryos may soon get their day in the sun." Science **340**(6140): 1509-1510.
North, T. E., et al. (2009). "Hematopoietic Stem Cell Development Is Dependent on Blood Flow." Cell **137**(4): 736-748.
Nostro, M. C., et al. (2008). "Wnt, Activin, and BMP Signaling Regulate Distinct Stages in the Developmental Pathway from Embryonic Stem Cells to Blood." Cell Stem Cell **2**(1): 60-71.
Novotny, E., et al. (2009). "In vitro hematopoietic differentiation of mouse embryonic stem cells requires the tumor suppressor menin and is mediated by Hoxa9." Mechanisms of Development **126**(7): 517-522.
Ogawa, M., et al. (1991). "Expression and function of c-kit in hemopoietic progenitor cells." J Exp Med **174**(1): 63-71.

Ohneda, O., et al. (1998). "Hematopoietic stem cell maintenance and differentiation are supported by embryonic aorta-gonad-mesonephros region-derived endothelium." Blood **92**(3): 908-919.
Olivier, E., et al. (2012). "Novel, High-Yield Red Blood Cell Production Methods from CD34-Positive Cells Derived from Human Embryonic Stem, Yolk Sac, Fetal Liver, Cord Blood, and Peripheral Blood." Stem Cells Translational Medicine **1**(8): 604-614.
Oostendorp, R. A., et al. (2005). "Generation of murine stromal cell lines: models for the microenvironment of the embryonic mouse aorta-gonads-mesonephros region." Methods Mol Biol **290**: 163-172.
Oostendorp, R. A., et al. (2002). "Stromal cell lines from mouse aorta-gonads-mesonephros subregions are potent supporters of hematopoietic stem cell activity." Blood **99**(4): 1183-1189.
Oostendorp, R. A., et al. (2002). "Embryonal subregion-derived stromal cell lines from novel temperature-sensitive SV40 T antigen transgenic mice support hematopoiesis." J Cell Sci **115**(Pt 10): 2099-2108.
Oostendorp, R. A., et al. (2005). "Long-term maintenance of hematopoietic stem cells does not require contact with embryo-derived stromal cells in cocultures." Stem Cells **23**(6): 842-851.
Osawa, M., et al. (1996). "Long-term lymphohematopoietic reconstitution by a single CD34-low/negative hematopoietic stem cell." Science **273**(5272): 242-245.
Ottersbach, K. and E. Dzierzak (2010). "The placenta as a haematopoietic organ." Int J Dev Biol **54**(6-7): 1099-1106.
Paik, E. J. and L. I. Zon (2010). "Hematopoietic development in the zebrafish." Int J Dev Biol **54**(6-7): 1127-1137.
Palis, J., et al. (1995). "Initiation of hematopoiesis and vasculogenesis in murine yolk sac explants." Blood **86**(1): 156-163.
Palis, J., et al. (1999). "Development of erythroid and myeloid progenitors in the yolk sac and embryo proper of the mouse." Development **126**(22): 5073-5084.
Papayannopoulou, T., et al. (1995). "The VLA4/VCAM-1 adhesion pathway defines contrasting mechanisms of lodgement of transplanted murine hemopoietic progenitors between bone marrow and spleen." Proceedings of the National Academy of Sciences **92**(21): 9647-9651.
Peeters, M., et al. (2009). "Ventral embryonic tissues and Hedgehog proteins induce early AGM hematopoietic stem cell development." Development **136**(15): 2613-2621.
Pevny, L., et al. (1995). "Development of hematopoietic cells lacking transcription factor GATA-1." Development **121**(1): 163-172.
Pick, M., et al. (2007). "Differentiation of human embryonic stem cells in serum-free medium reveals distinct roles for bone morphogenetic protein 4, vascular endothelial growth factor, stem cell factor, and fibroblast growth factor 2 in hematopoiesis." Stem Cells **25**(9): 2206-2214.
Pietras, E. M., et al. (2011). "Cell cycle regulation in hematopoietic stem cells." J Cell Biol **195**(5): 709-720.
Pinho, S., et al. (2013). "PDGFRalpha and CD51 mark human Nestin+ sphere-forming mesenchymal stem cells capable of hematopoietic progenitor cell expansion." J Exp Med **210**(7): 1351-1367.
Pipas, J. M. (2009). "SV40: Cell transformation and tumorigenesis." Virology **384**(2): 294-303.
Porcher, C., et al. (1996). "The T Cell Leukemia Oncoprotein SCL/tal-1 Is Essential for Development of All Hematopoietic Lineages." Cell **86**(1): 47-57.

Purpura, K. A., et al. (2008). "Analysis of the temporal and concentration-dependent effects of BMP-4, VEGF, and TPO on development of embryonic stem cell–derived mesoderm and blood progenitors in a defined, serum-free media." Exp Hematol **36**(9): 1186-1198.
Rafii, S., et al. (2012). "Human ESC-derived hemogenic endothelial cells undergo distinct waves of endothelial to hematopoietic transition." Blood **121**(5): 770-780.
Ramos, C. A., et al. (2010). "An inducible caspase 9 suicide gene to improve the safety of mesenchymal stromal cell therapies." Stem Cells **28**(6): 1107-1115.
Rasmussen, T. L., et al. (2012). "VEGF/Flk1 Signaling Cascade Transactivates <italic>Etv2</italic> Gene Expression." PLoS ONE **7**(11): e50103.
Riddell, J., et al. (2014). "Reprogramming Committed Murine Blood Cells to Induced Hematopoietic Stem Cells with Defined Factors." Cell **157**(3): 549-564.
Rissanen, J. (1983). "A universal data compression system." Information Theory, IEEE Transactions on **29**(5): 656-664.
Robb, L., et al. (1996). "The scl gene product is required for the generation of all hematopoietic lineages in the adult mouse." Embo j **15**(16): 4123-4129.
Robert-Moreno, À., et al. (2005). "RBPjκ-dependent Notch function regulates Gata2 and is essential for the formation of intra-embryonic hematopoietic cells." Development **132**(5): 1117-1126.
Robin, C. and C. Durand (2010). "The roles of BMP and IL-3 signaling pathways in the control of hematopoietic stem cells in the mouse embryo." Int J Dev Biol **54**(6-7): 1189-1200.
Robin, C., et al. (2006). "An Unexpected Role for IL-3 in the Embryonic Development of Hematopoietic Stem Cells." Developmental Cell **11**(2): 171-180.
Ruiz-Herguido, C., et al. (2012). "Hematopoietic stem cell development requires transient Wnt/beta-catenin activity." J Exp Med **209**(8): 1457-1468.
Ruiz-Herguido, C., et al. (2012). "Hematopoietic stem cell development requires transient Wnt/beta-catenin activity." J Exp Med **209**(8): 1457-1468.
Rybtsov, S., et al. (2014). "Tracing the origin of the HSC hierarchy reveals a SCF dependent, IL-3 independent

CD43- embryonic precursor." Stem Cell Reports.
Rybtsov, S., et al. (2011). "Hierarchical organization and early hematopoietic specification of the developing HSC lineage in the AGM region." J Exp Med **208**(6): 1305-1315.
Sánchez, M.-J., et al. (2001). "Selective rescue of early haematopoietic progenitors in Scl–/– mice by expressing Scl under the control of a stem cell enhancer." Development **128**(23): 4815-4827.
Sabin, F. R. (2002). "Preliminary note on the differentiation of angioblasts and the method by which they produce blood-vessels, blood-plasma and red blood-cells as seen in the living chick. 1917." J Hematother Stem Cell Res **11**(1): 5-7.
Sadlon, T. J., et al. (2004). "BMP4: Its Role in Development of the Hematopoietic System and Potential as a Hematopoietic Growth Factor." Stem Cells **22**(4): 457-474.
Saga, Y., et al. (1996). "MesP1: a novel basic helix-loop-helix protein expressed in the nascent mesodermal cells during mouse gastrulation." Development **122**(9): 2769-2778.
Samokhvalov, I. M., et al. (2006). "Multifunctional reversible knockout/reporter system enabling fully functional reconstitution of the AML1/Runx1 locus and rescue of hematopoiesis." genesis **44**(3): 115-121.

Sanchez, M. J., et al. (1996). "Characterization of the first definitive hematopoietic stem cells in the AGM and liver of the mouse embryo." Immunity **5**(6): 513-525.
Sarkar, P., et al. (2009). "Photophysical properties of Cerulean and Venus fluorescent proteins." Journal of Biomedical Optics **14**(3): 034047-034047-034049.
Sasaki, K. and Y. Sonoda (2000). "Histometrical and Three-Dimensional Analyses of Liver Hematopoiesis in the Mouse Embryo." Archives of Histology and Cytology **63**(2): 137-146.
Sasaki, T., et al. (2010). "Regulation of hematopoietic cell clusters in the placental niche through SCF/Kit signaling in embryonic mouse." Development **137**(23): 3941-3952.
Seandel, M., et al. (2008). "Generation of a functional and durable vascular niche by the adenoviral E4ORF1 gene." Proceedings of the National Academy of Sciences **105**(49): 19288-19293.
Shalaby, F., et al. (1997). "A Requirement for Flk1 in Primitive and Definitive Hematopoiesis and Vasculogenesis." Cell **89**(6): 981-990.
Shen, M. M. (2007). "Nodal signaling: developmental roles and regulation." Development **134**(6): 1023-1034.
Simmons, P. J., et al. (1992). "Vascular cell adhesion molecule-1 expressed by bone marrow stromal cells mediates the binding of hematopoietic progenitor cells." Blood **80**(2): 388-395.
Smith, L. (2007). Chaos: A Very Short Introduction, OUP Oxford.
Society, A. C. (2011). Global cancer facts & figures 2nd edition. Atlanta, Ga, Atlanta, Ga. : American Cancer Society, c2011.**:** 60.
Spangrude, G. J., et al. (1988). "Purification and characterization of mouse hematopoietic stem cells." Science **241**(4861): 58-62.
Sroczynska, P. L. C. K. V. L. G. (2009). "The differential activities of Runx1 promoters define milestones during embryonic hematopoiesis." Blood **114**(26): 5279-5289.
Sturgeon, C. M., et al. (2014). "Wnt signaling controls the specification of definitive and primitive hematopoiesis from human pluripotent stem cells." Nat Biotechnol **32**(6): 554-561.
Suárez-Álvarez, B., et al. (2012). Mobilization and Homing of Hematopoietic Stem Cells. Stem Cell Transplantation. C. López-Larrea, A. López-Vázquez and B. Suárez-Álvarez, Springer US. **741:** 152-170.
Sulston, J. E., et al. (1983). "The embryonic cell lineage of the nematode Caenorhabditis elegans." Dev Biol **100**(1): 64-119.
Sumi, T., et al. (2008). "Defining early lineage specification of human embryonic stem cells by the orchestrated balance of canonical Wnt/β-catenin, Activin/Nodal and BMP signaling." Development **135**(17): 2969-2979.
Suzuki, N., et al. (2013). "Generation of engraftable hematopoietic stem cells from induced pluripotent stem cells by way of teratoma formation." Mol Ther **21**(7): 1424-1431.
Swiers, G., et al. (2013). "Early dynamic fate changes in haemogenic endothelium characterized at the single-cell level." Nat Commun **4**.
Swiers, G., et al. (2006). "Genetic regulatory networks programming hematopoietic stem cells and erythroid lineage specification." Dev Biol **294**(2): 525-540.
Szabo, E., et al. (2010). "Direct conversion of human fibroblasts to multilineage blood progenitors." Nature **468**(7323): 521-526.

Tagoh, H., et al. (2002). "Transcription factor complex formation and chromatin fine structure alterations at the murine c-fms (CSF-1 receptor) locus during maturation of myeloid precursor cells." Genes Dev **16**(13): 1721-1737.
Takahashi, K., et al. (2007). "Induction of pluripotent stem cells from adult human fibroblasts by defined factors." Cell **131**(5): 861-872.
Takahashi, K. and S. Yamanaka (2006). "Induction of pluripotent stem cells from mouse embryonic and adult fibroblast cultures by defined factors." Cell **126**(4): 663-676.
Takubo, K., et al. (2010). "Regulation of the HIF-1α Level Is Essential for Hematopoietic Stem Cells." Cell Stem Cell **7**(3): 391-402.
Taoudi, S., et al. (2008). "Extensive hematopoietic stem cell generation in the AGM region via maturation of VE-cadherin+CD45+ pre-definitive HSCs." Cell Stem Cell **3**(1): 99-108.
Tavian, M., et al. (1996). "Aorta-associated CD34+ hematopoietic cells in the early human embryo." Blood **87**(1): 67-72.
Tavian, M., et al. (1999). "Emergence of intraembryonic hematopoietic precursors in the pre-liver human embryo." Development **126**(4): 793-803.
Tavian, M. and B. Peault (2005). "Embryonic development of the human hematopoietic system." Int J Dev Biol **49**(2-3): 243-250.
Tsai, F.-Y., et al. (1994). "An early haematopoietic defect in mice lacking the transcription factor GATA-2." Nature **371**(6494): 221-226.
Tsai, F.-Y. and S. H. Orkin (1997). "Transcription Factor GATA-2 Is Required for Proliferation/Survival of Early Hematopoietic Cells and Mast Cell Formation, But Not for Erythroid and Myeloid Terminal Differentiation." Blood **89**(10): 3636-3643.
Tsai, S. F., et al. (1991). "Functional analysis and in vivo footprinting implicate the erythroid transcription factor GATA-1 as a positive regulator of its own promoter." Genes Dev **5**(6): 919-931.
Tsapogas, P., et al. (2014). "In vivo evidence for an instructive role of fms-like tyrosine kinase-3 (FLT3) ligand in hematopoietic development." Haematologica **99**(4): 638-646.
Turing, A. M. (1952). "The chemical basis of morphogenesis." Philosophical Transactions of the Royal Society of London. Series B, Biological Sciences **237**(641): 37-72.
Turpen, J. B. (1998). "Induction and early development of the hematopoietic and immune systems in Xenopus." Dev Comp Immunol **22**(3): 265-278.
Ueno, H. and I. L. Weissman (2006). "Clonal Analysis of Mouse Development Reveals a Polyclonal Origin for Yolk Sac Blood Islands." Developmental Cell **11**(4): 519-533.
Ueno, H. and I. L. Weissman (2010). "The origin and fate of yolk sac hematopoiesis: application of chimera analyses to developmental studies." Int J Dev Biol **54**(6-7): 1019-1031.
Vieira, J. M., et al. (2010). "VEGF receptor signaling in vertebrate development." Organogenesis **6**(2): 97-106.
Visvader, J. E., et al. (1998). "Unsuspected role for the T-cell leukemia protein SCL/tal-1 in vascular development." Genes Dev **12**(4): 473-479.
Voges, M., et al. (2010). "CEACAM1 recognition by bacterial pathogens is species-specific." BMC Microbiology **10**(1): 117.
Wang, L., et al. (2004). "Endothelial and Hematopoietic Cell Fate of Human Embryonic Stem Cells Originates from Primitive Endothelium with Hemangioblastic Properties." Immunity **21**(1): 31-41.

Wang, W., et al. (2008). "Chromosomal transposition of PiggyBac in mouse embryonic stem cells." Proc Natl Acad Sci U S A **105**(27): 9290-9295.
Weisel, K. C., et al. (2006). "Stromal cell lines from the aorta-gonado-mesonephros region are potent supporters of murine and human hematopoiesis." Exp Hematol **34**(11): 1505-1516.
Weisel, K. C. and M. A. Moore (2005). "Genetic and functional characterization of isolated stromal cell lines from the aorta-gonado-mesonephros region." Ann N Y Acad Sci **1044**: 51-59.
White, A. K., et al. (2011). "High-throughput microfluidic single-cell RT-qPCR." Proceedings of the National Academy of Sciences **108**(34): 13999-14004.
Wilkinson, R. N., et al. (2009). "Hedgehog and Bmp Polarize Hematopoietic Stem Cell Emergence in the Zebrafish Dorsal Aorta." Developmental Cell **16**(6): 909-916.
Wilson, A. and A. Trumpp (2006). "Bone-marrow haematopoietic-stem-cell niches." Nat Rev Immunol **6**(2): 93-106.
Wineman, J., et al. (1996). "Functional heterogeneity of the hematopoietic microenvironment: rare stromal elements maintain long-term repopulating stem cells." Blood **87**(10): 4082-4090.
Winnier, G., et al. (1995). "Bone morphogenetic protein-4 is required for mesoderm formation and patterning in the mouse." Genes Dev **9**(17): 2105-2116.
Wislet-Gendebien, S., et al. (2004). "Nestin-positive mesenchymal stem cells favour the astroglial lineage in neural progenitors and stem cells by releasing active BMP4." BMC Neurosci **5**: 33.
Woltjen, K., et al. (2009). "piggyBac transposition reprograms fibroblasts to induced pluripotent stem cells." Nature **458**(7239): 766-770.
Xu, M. J., et al. (1998). "Stimulation of mouse and human primitive hematopoiesis by murine embryonic aorta-gonad-mesonephros-derived stromal cell lines." Blood **92**(6): 2032-2040.
Yoder, M. C. and K. Hiatt (1997). "Engraftment of Embryonic Hematopoietic Cells in Conditioned Newborn Recipients." Blood **89**(6): 2176-2183.
Yoder, M. C., et al. (1997). "In vivo repopulating hematopoietic stem cells are present in the murine yolk sac at day 9.0 postcoitus." Proceedings of the National Academy of Sciences **94**(13): 6776-6780.
Yokomizo, T. and E. Dzierzak (2010). "Three-dimensional cartography of hematopoietic clusters in the vasculature of whole mouse embryos." Development **137**(21): 3651-3661.
ZIPPO, A. G. (2010). NEURONAL ENSEMBLE MODELING AND ANALYSIS WITH VARIABLE ORDER MARKOV MODELS.
Zovein, A. C., et al. (2008). "Fate Tracing Reveals the Endothelial Origin of Hematopoietic Stem Cells." Cell Stem Cell **3**(6): 625-636.